

# Protein Expression and Glycosylation in CHO Cells

by

Inn Huam Yvonne Yuk

B.S. Chemistry  
California Institute of Technology, 1996

SUBMITTED TO THE DEPARTMENT OF CHEMICAL ENGINEERING  
IN PARTIAL FULFILLMENT OF THE REQUIREMENTS FOR THE DEGREE OF

DOCTOR OF PHILOSOPHY IN CHEMICAL ENGINEERING  
at the  
MASSACHUSETTS INSTITUTE OF TECHNOLOGY

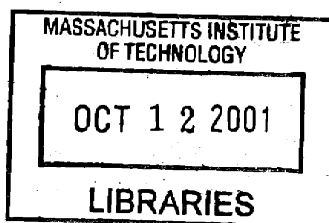
SEPTEMBER 2001

© 2001 Massachusetts Institute of Technology. All Rights Reserved.

Signature of Author: \_\_\_\_\_  
Department of Chemical Engineering  
August 8, 2001

Certified by: \_\_\_\_\_  
Daniel I. C. Wang  
Institute Professor  
Thesis Supervisor

Accepted by: \_\_\_\_\_  
Daniel Blankshtein  
Professor of Chemical Engineering  
Chairman, Committee for Graduate Students



ARCHIVES

SECRET

NOV 11 1950



# Protein Expression and Glycosylation in CHO Cells

by

Inn Huam Yvonne Yuk

Submitted to the Department of Chemical Engineering on August 8, 2001  
In Partial Fulfillment of the Requirements for the Degree of  
Doctor of Philosophy in Chemical Engineering

## ABSTRACT

A successful mammalian cell culture process depends on sufficient expression and correct glycosylation of the recombinant product. Low product titer and inconsistent protein glycosylation constitute two major problems frequently encountered in biopharmaceutical production. Using Chinese Hamster Ovary (CHO) cells expressing recombinant human interferon-gamma (IFN- $\gamma$ ) as the model system, this thesis investigated strategies that can potentially enhance heterologous protein expression or control the extent of protein glycosylation.

There has been considerable interest in developing culture strategies to improve productivity in mammalian cell lines by limiting the cellular growth rate. An initial investigation demonstrated the difficulty in obtaining growth-arrested cells that are robust and productive. In the following study, a method to rapidly generate and isolate CHO cells that exhibit enhanced potential for use in proliferation-controlled bioprocesses was developed. By combining bicistronic retroviral technology with an appropriate selection strategy, a subpopulation was isolated from a heterogeneous cell population. To evaluate the effectiveness of this screening process, the performance of this selected subpopulation was compared with that of the original population under identical growth-arresting conditions. Important differences were observed: by contrast to the original population, the selected cells maintained consistently high viabilities and continued to stably express recombinant proteins after being growth-arrested for two weeks.

Asparagine-linked (N-linked) glycosylation can significantly impact critical properties of human therapeutic proteins. An essential step in N-linked glycosylation is the transfer of an oligosaccharide from dolichol phosphate (Dol-P) to a potential glycosylation site on a polypeptide. Variability in the success of this reaction affects the extent of glycosylation on proteins. Radiolabeling studies showed that over the course of CHO batch culture, glycosylation precursor concentrations remained within a two-fold range, and overall protein glycosylation increased by 15-25%. Given the key role of Dol-P in glycosylation, its availability was postulated to limit glycosylation by controlling the abundance of glycosylation precursors. To test this hypothesis, the impact of Dol-P feeding on CHO cells was investigated. Although exogenous Dol-P was incorporated by CHO cells and processed into glycosylation precursors in a dose-dependent manner, Dol-P supplementation had no marked effects on the level of glycosylation precursors or on the extent of glycosylation.

Thesis Supervisor: Daniel I. C. Wang  
Title: Institute Professor



## ACKNOWLEDGEMENTS

Numerous people have contributed to this work. It would be impossible to list all of them here. Key contributions came from my thesis advisor, Professor Daniel Wang, my thesis committee members---Professors Linda Griffith, Doug Lauffenburger, and Harvey Lodish---and my research collaborator, Dr. Stefan Wildt, a former post-doc in Professor Greg Stephanopoulos' group.

First, I thank Professor Wang. There would be no thesis to write without Professor Wang's generous support and sincere, perceptive advice. In trusting me to work independently, Professor Wang has given me confidence in my own abilities. I am especially grateful for Professor Wang's no-nonsense attitude and responsible ways.

Next, I thank my thesis committee. Their support at critical times has been instrumental in helping me reach this point. There have been times when I was pleasantly surprised and greatly encouraged by their genuine concern for me. My family is indebted to Professor Lodish: he has directly contributed two MIT PhDs to the Yuk family. I am grateful to Professors Griffith and Lauffenburger for their wise counsel and encouragement.

Professor Lodish has made the work here possible---with his direct and indirect help. I thank Drs. Jonathan Bogan and Xuedong Liu from the Lodish lab for providing the bicistronic retroviral vectors used in the protein expression work and helpful discussions. I thank Professors Hirschberg and Robbins at Boston University for their encouragement to proceed with the glycosylation work.

I thank Dr. Stefan Wildt for his friendship and collaboration. Stefan made Chapter 3 of this thesis possible. It has been an enriching experience working with Stefan: I am grateful for the long discussions, laughs and encouragement.....booaaarrgghh! Thank you also to Dunja and Leon for the hospitality of the Wildt family.

I have learned much from both Professor Wang and his former students. In alphabetical order, I thank Brian Follstad for quietly taking care of the whole lab, Joydeep Goswami for showing us why he also has an MBA, Sherry Gu for "luring" me into the group, Araba Lamouse-Smith for her sensibility, Steve Meier for being the best officemate ever, Gregg Nyberg for helping me get started, and Jifeng Zhang for teaching me how to use the MS and HPLC. I am particularly grateful to Steve for his wit and advice. I also thank Robert Balcarcel for entertaining conversations and encouragement. I wish they all hadn't graduated so soon after I joined the group! Thank you also to the more recent members of the group---Steve Fox, Daniel Kamei, Hiro Kusunose, Henry Lam, Wensheng Xu, and Yin Jin---for their friendship and considerate ways.

Thank you to friends in the BPEC headquarters---Lorraine Cable, Audrey Childs, Sara Puffer, Darlene Ray and Lisa Resnick---for their patient help despite my constant intrusion. Thank you to Dan Darling for his ready smile and many assistances. I am also grateful for the efficiency and friendliness of Janet Fisher, Elaine Aufiero, Suzanne

Easterly, Annie Fowler and Maria Nargi. John Langrill deserves special mention for his computing expertise and fine humor.

Thank you also to BPECers of building 16: Adam Capitano for being the most friendly non-inhabitant, Jean-Francois Hamel for keeping us safe in the lab, Klaudyne Hong for mental strength and Bettina Knorr for Teutonic strength, Dena Janigian for her irrepressible spirit, Mark Powers for being the esteemed Dr. Powers. I also thank Carolyn Baker, Anand Sivaraman and Artemis Kalezi for their excellent company during those early and late hours in lab.

I am grateful to the Howard Hughes Medical Institute for a predoctoral fellowship that has supported me through this entire time at MIT. I also thank NSF for funding BPEC, where the work was performed.

Although most of my time at MIT was spent at work, quality time with friends outside the lab is greatly appreciated. Special thanks to Gloria Tsuen, Haiyan Zhang, Ken Lau, and Leslie Loo for helping me through the early years with their prayers and friendship. Thank you to Christine Su for being the best roommate at MIT. Special thanks also to Miranda Yap, Maria Klapa and Javier Femenia for your encouragement in the later years---I wish I had known them earlier. Thank you to Kurt Yanagimachi and Mike Leison for their friendship and help in NJ and Ashdown, respectively. A big thank you to long-time pal Tiffany Lee---I'm glad I've known her for so long. Thank you also to friends in the Bay area for the incentive to be back on the West Coast.

Mrs. Charles Cowman's Streams in the Desert and Dr. Charles Stanley's In Touch magazine provided much encouragement through the past few years. I am grateful for the many lessons God has taught me, because they have strengthened my faith in Him. As David proclaimed in Psalm 23, "Yea, though I walk through the valley of the shadow of death, I will fear no evil; for You are with me; Your rod and Your staff, they comfort me." The greatest blessings from my time at MIT have been the opportunities to witness and experience the grace of God. Thank you to Park Street Church, friends in the Graduate Christian Fellowship and Ashdown Monday night Bible study. Special thanks to Jane Brock, Michael Kistler, Yann Schrodi, John Sogade, Beata Tao and Derrick Tate for their prayers and encouragement in the early years.

Finally, I thank my family for their love and understanding. Thank you to Mommy for her faithful prayers---which have transformed and continue to transform me---all these years. Thank you to Pappy, for his patience and his faith in me. I am grateful to my brother for his good example. Thank you to Eugene, for his responsible ways---manifested clearly in taking care of the wedding---and his prayers. BBMIH! I am grateful to my parents for their unwavering support and constant encouragement, and I look forward to spending quality time with them in the near future.

# TABLE OF CONTENTS

<b>ABSTRACT</b> .....	<b>3</b>
<b>ACKNOWLEDGEMENTS</b> .....	<b>5</b>
<b>TABLE OF CONTENTS</b> .....	<b>7</b>
<b>LIST OF FIGURES AND TABLES</b> .....	<b>11</b>
<b>1. INTRODUCTION TO THESIS</b> .....	<b>17</b>
<b>1.1 BACKGROUND</b> .....	<b>17</b>
1.1.1 <i>Mammalian Cell Culture</i> .....	<b>17</b>
1.1.2 <i>Apoptosis</i> .....	<b>19</b>
1.1.3 <i>Population Heterogeneity</i> .....	<b>20</b>
1.1.4 <i>N-linked Glycosylation</i> .....	<b>23</b>
1.1.5 <i>Model System</i> .....	<b>26</b>
<b>1.2 MOTIVATION</b> .....	<b>28</b>
<b>1.3 THESIS OBJECTIVES</b> .....	<b>30</b>
<b>1.4 THESIS ORGANIZATION</b> .....	<b>30</b>
<b>2. INITIAL INVESTIGATION INTO PROTEIN PRODUCTION FROM GROWTH-ARRESTED CELLS</b> .....	<b>33</b>
<b>2.1 ABSTRACT</b> .....	<b>33</b>
<b>2.2 INTRODUCTION</b> .....	<b>34</b>
<b>2.3 MATERIALS AND METHODS</b> .....	<b>38</b>
2.3.1 <i>Cell line</i> .....	<b>38</b>
2.3.2 <i>Culture Medium and Maintenance</i> .....	<b>39</b>
2.3.3 <i>Cell Enumeration</i> .....	<b>39</b>
2.3.4 <i>Flow Cytometry</i> .....	<b>40</b>
2.3.5 <i>Determination of IFN-<math>\gamma</math> Glycosylation and Concentration</i> .....	<b>40</b>
2.3.6 <i>Serum-containing and Serum-free Experiments</i> .....	<b>41</b>
<b>2.4 RESULTS</b> .....	<b>42</b>
2.4.1 <i>Serum-containing and Serum-free Culture</i> .....	<b>42</b>
2.4.2 <i>Culture Viabilities</i> .....	<b>43</b>
2.4.3 <i>Cell Densities</i> .....	<b>45</b>
2.4.4 <i>Cell Cycle Analyses</i> .....	<b>48</b>
2.4.5 <i>IFN-<math>\gamma</math> Production</i> .....	<b>49</b>
2.4.6 <i>IFN-<math>\gamma</math> Glycosylation Site Occupancy</i> .....	<b>52</b>
<b>2.5 DISCUSSION</b> .....	<b>55</b>

<b>3. AN EFFECTIVE SCREEN FOR GROWTH-ARRESTED RECOMBINANT PROTEIN PRODUCERS .....</b>	<b>61</b>
3.1 ABSTRACT.....	61
3.2 INTRODUCTION.....	62
3.3 MATERIALS AND METHODS .....	67
3.3.1 <i>Plasmid Constructions</i> .....	67
3.3.2 <i>Cell Lines and Culture</i> .....	67
3.3.3 <i>Retrovirus Production</i> .....	68
3.3.4 <i>Infection</i> .....	69
3.3.5 <i>GFP Fluorescence Measurements</i> .....	69
3.3.6 <i>IFN-<math>\gamma</math> Concentration Determination</i> .....	71
3.3.7 <i>Cell Density and Viability Measurements</i> .....	71
3.4 RESULTS .....	71
3.4.1 <i>Generation of Bicistronic Ecotropic Retroviruses</i> .....	71
3.4.2 <i>Selection Strategy</i> .....	72
3.4.3 <i>Comparison of Serum-Free Culture Characteristics</i> .....	73
3.4.3.1 Cell Viabilities .....	73
3.4.3.2 Cell Densities.....	76
3.4.3.3 Percent of Cells Producing GFP .....	78
3.4.3.4 Mean GFP Fluorescence Intensity .....	80
3.4.3.5 Overlay of calibrated FACS data.....	82
3.4.3.6 Coexpression of IFN- $\gamma$ and GFP .....	82
3.5 DISCUSSION .....	85
<b>4. RELATIVE LLO AND GLYCOSYLATION LEVELS IN CHO CELLS OVER THE COURSE OF BATCH CULTURE.....</b>	<b>95</b>
4.1 ABSTRACT.....	95
4.2 INTRODUCTION.....	96
4.3 MATERIALS AND METHODS .....	103
4.3.1 <i>Cell Line</i> .....	103
4.3.2 <i>Cell Culture</i> .....	103
4.3.3 <i>Serum-Free Media: RPMI-SFM and CHO-S-SFM II</i> .....	104
4.3.4 <i>Radiolabeled RPMI-SFM Batch Cultures</i> .....	105
4.3.5 <i>Radiolabeled CHO-S-SFM II Batch Cultures</i> .....	105
4.3.6 <i>Determination of Cell Numbers and Viability</i> .....	106
4.3.7 <i>Determination of Glucose and Lactate Concentrations</i> .....	106
4.3.8 <i>Isolation of Lipid-linked Oligosaccharides (LLOs) and Cellular Proteins</i> 106	
4.3.9 <i>Extraction of Secreted Proteins</i> .....	108
4.3.10 <i>Determination of Radioactivity</i> .....	108
4.3.11 <i>Cell Cycle Analyses</i> .....	109



4.4 RESULTS .....	109
4.4.1 <i>Radiolabeled RPMI-SFM Batch Cultures</i> .....	109
4.4.1.1 Cell Density and Viability .....	110
4.4.1.2 Glucose and Lactate Concentrations .....	112
4.4.1.3 Relative LLO Levels over Culture Time.....	112
4.4.1.4 Relative Glycosylation Levels over Culture Time.....	113
4.4.2 <i>Radiolabeled CHO-S-SFM II Batch Cultures</i> .....	118
4.4.2.1 Cell Density and Viability .....	121
4.4.2.2 Glucose and Lactate Concentrations .....	121
4.4.2.3 Cell Cycle Distributions .....	121
4.4.2.4 Relative LLO Levels over Culture Time.....	124
4.4.2.5 Relative Glycosylation Levels over Culture Time.....	127
4.5 DISCUSSION .....	129
<b>5. EFFECTS OF DOLICHOL PHOSPHATE SUPPLEMENTATION ON CHO BATCH CULTURES.....</b>	<b>135</b>
5.1 ABSTRACT.....	135
5.2 INTRODUCTION.....	136
5.3 MATERIALS AND METHODS .....	144
5.3.1 <i>CHO Cell Line and Culture</i> .....	144
5.3.2 <i>Dol-P Supplementation</i> .....	144
5.3.4 <i>Determination of Cell Density, Viability and Mode of Cell Death</i> .....	145
5.3.4 <i>Analyses of IFN-<math>\gamma</math> Glycosylation and Concentration</i> .....	145
5.3.5 <i>Cell Cycle Analyses</i> .....	146
5.3.6 <i>Determination of Glucose and Lactate Concentrations</i> .....	146
5.3.7 <i>LLO and Cellular Protein Extractions</i> .....	147
5.3.8 <i>Radioactivity Measurements</i> .....	147
5.3.9 <i>Uptake and Incorporation of exogenous <math>^3\text{H}</math> Dol-P into LLO by CHO cells</i> .....	147
5.3.10 <i>Distribution of <math>^3\text{H}</math> Dol-P in CHO cells and Impact of Dol-P on IFN-<math>\gamma</math> Glycosylation</i> .....	148
5.3.11 <i>Effects of Dol-P supplementation on Cell Cycle, Growth and Viability of CHO cells</i> .....	150
5.3.12 <i>Impact of Dol-P Supplementation on LLO and Cellular Glycosylation Levels</i> .....	150
5.3.12.1 RPMI-SFM Cultures .....	150
5.3.12.2 CHO-S-SFM II Cultures.....	151
5.3.13 <i>IFN-<math>\gamma</math> Glycosylation Time Profile Studies</i> .....	151

5.4 RESULTS .....	152
5.4.1 <i>Uptake and Incorporation of Exogenous <sup>3</sup>H Dol-P into LLO by CHO cells</i> .....	152
5.4.2 <i>Distribution of <sup>3</sup>H Dol-P in CHO cells and Impact of Dol-P on IFN-<math>\gamma</math> Glycosylation</i> .....	155
5.4.3 <i>Effects of Dol-P supplementation on Cell Cycle, Growth and Viability of CHO cells</i> .....	162
5.4.4 <i>Impact of Dol-P Supplementation on LLO and Cellular Glycosylation Levels</i> .....	163
5.4.4.1 RPMI-SFM Cultures .....	165
5.4.4.2 CHO-S-SFM II Cultures.....	168
5.4.5 <i>IFN-<math>\gamma</math> Glycosylation Time Profile Studies</i> .....	168
5.5 DISCUSSION .....	176
<b>6. SUMMARY AND RECOMMENDATIONS FOR FUTURE WORK .....</b>	<b>183</b>
6.1 SUMMARY .....	183
6.1.1 <i>Protein Expression in CHO cells</i> .....	183
6.1.2 <i>Protein Glycosylation in CHO batch cultures</i> .....	185
6.2 RECOMMENDATIONS FOR FUTURE WORK.....	187
6.2.1 <i>Protein Expression in CHO cells</i> .....	187
6.2.2 <i>Protein Glycosylation in CHO batch cultures</i> .....	189
<b>ABBREVIATIONS .....</b>	<b>191</b>
<b>REFERENCES.....</b>	<b>193</b>

## LIST OF FIGURES AND TABLES

### Chapter 2: Initial Investigation into Protein Production from Growth-arrested Cells

---

<b>Figure 2-1</b> .....	<b>35</b>
Schematic illustrating the basic concept behind the controlled proliferation bioprocess.	
<b>Figure 2-2</b> .....	<b>44</b>
Viabilities of $\gamma$ -CHO cells cultured under 4 different conditions are plotted over time.	
<b>Figure 2-3</b> .....	<b>47</b>
Viable cell densities of cultures in presence (A), and absence (B) of 5% serum.	
<b>Figure 2-4</b> .....	<b>50</b>
Cell cycle distribution of attached $\gamma$ -CHO cells grown in 5% serum-containing culture with (A), and without (B) regular exchange of fresh serum medium.	
<b>Figure 2-5</b> .....	<b>51</b>
Cell cycle distribution of attached $\gamma$ -CHO cells grown in serum-free culture with (A), and without (B) regular exchange of fresh serum-free medium.	
<b>Figure 2-6</b> .....	<b>53</b>
Specific IFN- $\gamma$ productivity of $\gamma$ -CHO cells under the following culture conditions: serum-containing culture with regular fresh 5% serum medium exchange ( $\blacktriangle$ ); serum-containing batch culture ( $\blacksquare$ ); serum-free culture with regular fresh serum-free medium exchange ( $\times$ ); serum-free batch culture ( $\circ$ ).	
<b>Figure 2-7</b> .....	<b>54</b>
Glycosylation site occupancy distribution of IFN- $\gamma$ secreted by $\gamma$ -CHO cells cultured in 5% serum-containing medium with (A), and without (B) regular exchange of fresh 5% FBS medium.	
<b>Figure 2-8</b> .....	<b>56</b>
Glycosylation site occupancy distribution of IFN- $\gamma$ secreted by $\gamma$ -CHO cells cultured in serum-free medium with (A), and without (B) regular exchange of fresh serum-free medium.	
<b>Table 2-1</b> .....	<b>37</b>
Potential advantages of controlled proliferation bioprocess for protein production over classical methods.	

## LIST OF FIGURES AND TABLES

### Chapter 3: An Effective Screen for Growth-arrested Recombinant Protein Producers

---

<b>Figure 3-1</b> .....	66
Cartoon illustrating the concept of bicistronic retroviral expression of both the secreted model therapeutic protein IFN- $\gamma$ , and the cytosolic green fluorescent protein (GFP).	
<b>Figure 3-2</b> .....	70
Schematic diagram of the pMX-IFN $\gamma$ -IRES-GFP retroviral expression vector.	
<b>Figure 3-3</b> .....	74
Flowchart of the experimental procedure. Helper cell-lines were transfected with plasmid pMX-IFN $\gamma$ -IRES-GFP (Figure 3-2).	
<b>Figure 3-4</b> .....	75
Cell viabilities over the course of serum-free culture were compared between the original population (O), and the selected subpopulation ( $\blacktriangle$ ) of cells.	
<b>Figure 3-5</b> .....	77
Cell densities over the course of serum-free culture were compared between the original population (O), and the selected subpopulation ( $\blacktriangle$ ) of cells.	
<b>Figure 3-6</b> .....	79
Percent of GFP-producing cells within the original population (O), and the selected subpopulation ( $\blacktriangle$ ) are compared over the course of serum-free culture.	
<b>Figure 3-7</b> .....	81
Mean GFP fluorescence intensities measured by FACS of the original population (O), and the selected subpopulation ( $\blacktriangle$ ) are compared over the course of serum-free culture.	
<b>Figure 3-8</b> .....	83
Calibrated FACS data of the selected subpopulation of cells taken at 0, 6 and 12 days after serum removal were overlaid onto a single plot.	
<b>Figure 3-9</b> .....	84
Coexpression of cytosolic reporter GFP ( $\boxtimes$ ) and secreted model therapeutic protein IFN- $\gamma$ ( $\blacklozenge$ ) by the selected subpopulation of cells over the course of serum-free culture.	

## LIST OF FIGURES AND TABLES

### Chapter 4: Relative LLO and Glycosylation Levels in CHO cells over the Course of Batch Culture

---

<b>Figure 4-1</b> .....	<b>99</b>
Schematic of the N-linked oligosaccharide processing pathway in the endoplasmic reticulum and Golgi compartments.	
<b>Figure 4-2</b> .....	<b>111</b>
Cell densities (A) and viabilities (B) measured in parallel RPMI-SFM batch cultures.	
<b>Figure 4-3</b> .....	<b>114</b>
Concentrations of glucose (A) and lactate (B) in RPMI-SFM over culture time.	
<b>Figure 4-4</b> .....	<b>115</b>
<sup>14</sup> C radioactivity measured in LLO extracts divided by total cell number (A), or by <sup>3</sup> H leucine radioactivity detected in cellular protein extracts (B).	
<b>Figure 4-5</b> .....	<b>117</b>
Ratio of <sup>14</sup> C to <sup>3</sup> H radioactivities measured in cellular and secreted proteins over the course of CHO batch culture.	
<b>Figure 4-6</b> .....	<b>120</b>
Cell densities (A) and viabilities (B) measured in parallel CHO-S-SFM II batch cultures.	
<b>Figure 4-7</b> .....	<b>122</b>
Glucose (A) and lactate (B) concentrations in CHO-S-SFM II over culture time.	
<b>Figure 4-8</b> .....	<b>123</b>
Cell cycle distributions of $\gamma$ -CHO batch cultures in CHO-S-SFM II.	
<b>Figure 4-9</b> .....	<b>125</b>
<sup>14</sup> C radioactivity measured in LLO extracts divided by total cell number (A), or by <sup>3</sup> H leucine radioactivity detected in cellular protein extracts (B).	
<b>Figure 4-10</b> .....	<b>126</b>
<sup>14</sup> C radioactivity measured in LLO extracts divided by viable cell number.	
<b>Figure 4-11</b> .....	<b>128</b>
Ratio of <sup>14</sup> C to <sup>3</sup> H radioactivities measured in cellular and secreted proteins over the course of CHO-S-SFM II batch culture.	

## LIST OF FIGURES AND TABLES

### Chapter 5: Effects of Dolichol Phosphate Supplementation on CHO Batch Cultures

---

<b>Figure 5-1</b> .....	140
Schematic of the N-linked glycosylation pathway in the endoplasmic reticulum.	
<b>Figure 5-2</b> .....	154
Uptake and incorporation of <sup>3</sup> H Dol-P into LLO by CHO cells.	
<b>Figure 5-3</b> .....	157
Total cell density (A), and viability (B) of four parallel batch cultures supplemented with 0 µg/ml, 12 µg/ml, 17 µg/ml and 35 µg/ml Dol-P, respectively.	
<b>Figure 5-4</b> .....	158
Distribution of <sup>3</sup> H Dol-P in cells (A), microsomes (B), and LLO (C) obtained from γ-CHO batch cultures supplemented with varying amounts of Dol-P.	
<b>Figure 5-5</b> .....	159
Viabilities of CHO batch cultures supplemented with varying amounts of Dol-P.	
<b>Figure 5-6</b> .....	160
Glycosylation site occupancy of IFN-γ accumulated in medium after 62 hours of batch culture.	
<b>Figure 5-7</b> .....	161
Glycosylation microheterogeneity of IFN-γ secreted by CHO cells after 62 hours of culture in the presence of varying amounts of supplemental Dol-P.	
<b>Figure 5-8</b> .....	164
Cell density (A) and percent of necrotic cells (B) in CHO batch cultures supplemented with varying amounts of Dol-P.	
<b>Figure 5-9</b> .....	166
Impact of Dol-P supplementation on relative LLO levels normalized to cell number (A) and <sup>3</sup> H radioactivity in cellular proteins (B).	
<b>Figure 5-10</b> .....	167
Impact of Dol-P supplementation on cellular proteins extracted at regular time intervals from RPMI-SFM CHO batch cultures.	

<b>Figure 5-11</b> .....	<b>170</b>
Impact of Dol-P supplementation on relative LLO levels normalized to cell number (A) and <sup>3</sup> H radioactivity in cellular proteins (B).	
<b>Figure 5-12</b> .....	<b>171</b>
Impact of Dol-P supplementation on cellular proteins extracted at regular time intervals from CHO-S-SFM II CHO batch cultures.	
<b>Figure 5-13</b> .....	<b>172</b>
Cell density (A) and culture viability (B) profiles of four CHO-S-SFM II batch cultures supplemented with varying amounts of Dol-P.	
<b>Figure 5-14</b> .....	<b>173</b>
Glucose (A) and lactate (B) concentrations in CHO-S-SFM II culture medium supplemented with varying amounts of Dol-P.	
<b>Figure 5-15</b> .....	<b>174</b>
Glycosylation site occupancy of IFN- $\gamma$ secreted by CHO cells over time.	
<b>Figure 5-16</b> .....	<b>175</b>
Time profiles of viable cell density (A) and concentration of IFN- $\gamma$ accumulated in culture medium (B).	
<b>Figure 5-17</b> .....	<b>180</b>
Regulatory influences on the first step in the dolichol pathway (adapted from Kean et al., 1999).	





## **1. Introduction to Thesis**

### **1.1 BACKGROUND**

Advances in recombinant DNA technology have revolutionized the treatment of human diseases. Since 1982, when human insulin produced in recombinant *Escherichia coli* was approved for use in the United States, numerous recombinant pharmaceutical products have been successfully introduced into the drug market. Today, sales of recombinant protein therapeutics produced by bacteria, yeast and animal cells generate billions of dollars for the biopharmaceutical industry.

Productivity is often a key determinant in evaluating the feasibility of a recombinant protein production process. The selection of robust, high-producing cell lines is a critical early step in optimizing mammalian cell culture processes. However, as record numbers of mammalian cell culture products enter clinical trials, it is evident that considerations of product quality and consistency are as important as product yield. Compared to mammalian cells, bacteria and yeast have higher growth rates, are easier to manipulate, and can produce larger quantities of recombinant proteins at lower costs. Despite the advantages associated with these lower organisms, mammalian cells are often favored for therapeutic protein production on account of their ability to correctly fold and post-translationally modify proteins (Datar et al., 1993).

#### **1.1.1 Mammalian Cell Culture**

A major obstacle in mammalian cell culture is the high cost of producing and purifying secreted recombinant protein from the culture medium. Difficulties in achieving and maintaining high cell concentrations, high specific productivities, and consistently high

viabilities conspire to lower the product yield from mammalian cell culture processes. Loss of viable cells in biopharmaceutical manufacturing can also result in product degradation---at both the oligosaccharide and polypeptide levels---by the glycosidases and proteases released upon cell lysis (Gramer and Goochee, 1993).

The sensitivity of the fragile mammalian cells to the culture environment causes many problems. Cell damage due to hydrodynamic effects (Hu and Peshwa, 1991) and sparging (Meier et al., 1999) in bioreactors are known to cause cell death. Culture performance is also dependent on dissolved oxygen concentration (Ozturk and Palsson, 1990), temperature (Jenkins and Hovey, 1993), pH and nutrient concentrations (Miller et al., 2000). By altering the reactor system and operating conditions, cell viabilities and densities can be enhanced (Avgerinos et al., 1990; Batt et al., 1990; Hu and Peshwa, 1991).

To generate higher quantities of therapeutic protein products, biochemical engineering research has focused on developing techniques to increase viable cell densities in mammalian cell cultures. In addition to progress in bioreactor designs, improvements in the design of medium and feeding strategies have also been made (Glacken et al., 1986; Jo et al, 1993; Zhou et al., 1995). In particular, researchers from this laboratory developed a stoichiometric nutrient feeding approach that resulted in a twenty-fold enhancement in product concentration, a substantial decrease in byproduct concentrations, and an increase in maximum viable cell density to 10 million cells/ml (Xie and Wang, 1994). Despite the success of these approaches, massive cell death still prevailed to abruptly end the culture processes.

### **1.1.2 Apoptosis**

The productivity of batch cultures of recombinant mammalian cell lines is often limited by the rapid entry of cells into the decline phase---the period of culture when cell viability falls after maximum cell density has been reached. Various studies have attributed this decline in culture viability to apoptosis, a genetically-controlled form of cell death (Al-Rubeai and Singh, 1998; Al-Rubeai and Singh, 1998; Goswami et al., 1999; Mercille and Massie et al., 1994; Zanghi et al., 1999).

The other major mode of cell death in mammalian cells is necrosis (Wyllie et al., 1980). Necrosis is a passive process and occurs primarily in response to severe extracellular insult: the plasma membrane ruptures and disintegrates as a result of violent perturbations in the environment, such as hypoxia, hypothermia, chemical toxins and physical trauma. By contrast, apoptosis is an active cellular phenomenon triggered by much milder stimuli, such as serum deprivation, nutrient and oxygen limitation. Apoptotic cell death requires metabolic energy and protein synthesis, and is typically accompanied by visible morphological changes, such as cell shrinkage, membrane blebbing, and chromatin condensation (Fesus et al., 1991). In mammals, apoptosis is a normal and necessary cellular function for homeostasis, development, and the prevention of cancerous growth. For example, apoptosis is required for the formation of fingers and toes in a developing human fetus. However, in the context of biopharmaceutical manufacturing, the apoptotic program should be obviated to prolong the productive phase of animal cells in batch cultures, and to avoid the adverse effects of serum- and protein-free medium on cells.

To reduce apoptosis in cell culture processes, three fundamental approaches have been taken (Cotter and Al-Rubeai, 1995; Mastrangelo and Betenbaugh, 1998): (1) alleviating nutrient deprivation by feeding strategies, (2) employing apoptosis-suppressing chemical additives to block key apoptosis effectors, and (3) metabolic engineering involving anti-apoptotic survival genes. For example, the overexpression of anti-apoptotic proteins such as Bcl-2 in mammalian cell lines have successfully increased the culture viability by protecting the cells from apoptotic death triggered by nutrient and growth factor limitations as well as other proapoptotic signals (Adams and Cory, 1998; Goswami et al., 1999). These results demonstrate that the genetic background of the cell line is a critical parameter in mammalian cell culture.

### **1.1.3 Population Heterogeneity**

Efforts to prevent apoptotic cell death in mammalian cell culture have generally involved either the use of cell culture strategies to eliminate apoptosis triggers from the culture environment, or the application of genetic engineering to overexpress anti-apoptotic survival genes. Despite progress in bioreactor operation strategies and metabolic engineering approaches to improve culture robustness, cell death remains a significant problem in mammalian cell culture.

Recent work from this laboratory presents an alternative strategy to improve culture viability---the selection of more robust cells based on the heterogeneous nature of a cell population. Follstad and coworkers demonstrated that the heterogeneity in mitochondrial membrane potential within a population of hybridoma cells translated into differences in susceptibility to apoptosis (Follstad et al., 2000). When they used this

heterogeneity to separate the cells into subpopulations belonging to opposite ends of the mitochondrial membrane potential spectrum, the resulting subpopulations manifested clear morphological and biochemical variances in resistance to apoptosis and continued to maintain the differences in mitochondrial membrane potential for many generations. This finding provides clear evidence for the existence of more robust subpopulations within a population of wild-type cells.

Various mechanisms can lead to population heterogeneity. The phenomenon known as “asymmetric cell division” results in sister cells differing in morphological and/or biochemical characteristics (Jan and Jan, 1998). The operative mechanism behind this developmental heterogeneity may involve intrinsic properties such as the partitioning of RNA, membrane proteins and other molecules in specific cellular regions before cellular division or asymmetry in the cell division plane with respect to the orientation of the mitotic spindle (Horvitz and Herskowitz, 1992). However, the difficulties of tracking individual cells through many rounds of cell division complicate efforts to determine the precise mechanism of asymmetric cell division (Jan and Jan, 1998).

Non-developmental mechanisms can also give rise to population heterogeneity. Single nucleotide substitutions, DNA frameshifts, genetic “hotspots”, and jumping genes can all contribute to the formation of new mutant subpopulations (Crow, 1983). Recessive mutants that form may survive even though they are not as robust as the wild-type cell line.

Cells that are genetically identical and maintained in an identical environment can still exhibit heterogeneity that is not a function of variances in the extracellular environment or cell cycle (Spudich and Koshland, 1976). A CHO320 clone expressing

IFN- $\gamma$  exhibited heterogeneity at the levels of the intracellular environment, characteristics of mitosis, and intracellular content of recombinant IFN- $\gamma$  (Coppen et al., 1995). Rat pancreatic  $\beta$ -cells varied extensively in their individual sensitivity to glucose-inducible metabolic changes *in vitro*, demonstrating intercellular functional diversity among cells characterized by specific morphological features (Pipeleers, 1992; van Schravendijk et al., 1992). Cells within clonal and subclonal populations of NIH 3T3 cultures consistently manifested significant diversity in their response to growth constraints, such as low serum concentration (Yao et al., 1990; Chow et al., 1994) and culture confluency (Yao and Rubin, 1993; Yao and Rubin, 1994). The progeny of these NIH 3T3 cells maintained the differences in adaptive response, indicating the heritable nature of the distinct traits. These researchers supported the concept of “progressive state selection” which assumes the existence of numerous metastable states within a cell population. After prolonged exposure to selective pressure, only cells in the states that are best adapted to handle the stress will eventually survive.

Differences in transcriptional state may be the cause of non-genetic population heterogeneity (Dykhuizen and Hartl, 1983). There is evidence to argue for the existence of threshold mechanisms that control the induction or repression of genes; genetic regulatory compounds operating at low concentrations can effect large fluctuations in genetic regulation and translation (McAdams and Arkin, 1999; McAdams and Arkin, 1998). While theoretical deterministic models also support the use of biological switches to convert cells between physiological states and have successfully explained population heterogeneity in a number of biological systems (Chung and Stephanopoulos, 1996), the non-unique model solutions suggest that the appearance of heterogeneity may occur by

chance. Hence, slight changes in the levels of certain factors may produce macroscopic physiological changes (Spudich and Koshland, 1976).

The above experimental and theoretical observations provide convincing evidence to contradict the assumption of population homogeneity within a cell culture. Heterogeneity within a cloned cell line needs to be considered the design and scale-up of fermentation systems for large-scale production of recombinant proteins. Culture heterogeneity also raises issues of reliability and predictability of the process and adds a level of uncertainty to process modeling. However, biochemical engineers can also view population heterogeneity from a different angle---it presents numerous opportunities for the development of novel cell culture improvement strategies.

#### **1.1.4 N-linked Glycosylation**

Many recombinant therapeutic proteins are characterized by asparagine-linked (N-linked) glycosylation, the most extensive post-translational modification performed on proteins by mammalian cells (reviewed by Kornfeld and Kornfeld, 1985).

Glycosylation imparts many desirable features to proteins (reviewed by Goochee et al., 1991). The numerous functions ascribed to protein glycosylation can be broken down into two principal categories. First, protein-linked glycans modulate biochemical attributes of proteins, such as bioactivity, folding and immunogenicity. Second, protein-linked glycans serve as determinants in molecular recognition events. For instance, specific oligosaccharide structures on the surfaces of proteins target particular enzymes to lysosomes (Dahms et al., 1989), and mediate the uptake of asialoglycoproteins by a hepatic receptor (Ashwell and Harford, 1982).

A crucial step in N-linked glycosylation is the oligosaccharyltransferase-mediated transfer of oligosaccharide from the lipid dolichol phosphate in the endoplasmic reticulum (ER) to an asparagine residue within the Asn-Xaa-Ser/Thr (where Xaa can be any amino acid except proline) consensus sequence on a polypeptide. It is generally observed, both in cultured cells and *in vitro*, that this reaction does not occur at every identical potential glycosylation site on different molecules of the same protein. This results in glycosylation site occupancy heterogeneity (also known as glycosylation “macroheterogeneity”) whereby two different protein populations---one bearing and one lacking oligosaccharide---are created for each potential glycosylation site on protein.

A structured kinetic modeling framework of this critical step in N-linked glycosylation predicted the dependence of glycosylation site occupancy on: (1) protein synthesis rate, (2) lipid-linked oligosaccharide (LLO) availability, (3) oligosaccharyltransferase activity and expression, (4) primary amino acid sequence near the potential glycosylation site, (5) polypeptide translocation rate, and (6) competition from other cotranslational events (Shelikoff et al., 1996). Based on this model, fractional site occupancy is predicted to increase under the following conditions: (1) decreased protein production, (2) increased lipid-linked oligosaccharide (LLO) concentration, (3) increased oligosaccharyltransferase activity, (4) decreased folding kinetics, (5) increased size of the glycosylation region, and (6) decreased distance of the glycosylation region from the ER membrane.

This step is followed by multiple reactions in the ER and Golgi that catalyze subsequent removal and addition of sugars to the glycoprotein. Since each of these enzyme-catalyzed reactions may or may not occur, heterogeneity is introduced at each



step along the glycosylation pathway. In this way, glycosylation inherently generates heterogeneity in the protein product.

The choice of host expression system significantly impacts the structures of N-linked oligosaccharides on glycoproteins (reviewed by Jenkins et al., 1996). The same recombinant protein can exhibit dramatically different glycosylation patterns when expressed in different types of species, tissues or cells. The variations in glycosylation are attributed to differences in the presence, concentration, kinetic characteristics, and compartmentalization of individual glycosyltransferases and glycosidases among the expression hosts.

Additional product glycosylation heterogeneity can be introduced by altering the cell culture environment (reviewed by Goochee et al., 1991). Within a specific cell culture process, glycosylation heterogeneity is affected primarily by cell culture conditions, such as dissolved oxygen tension (Kunkel et al., 2000), pH (Borys et al., 1993), ammonia (Borys et al., 1994), presence of serum (Gawlitzeck et al., 1995), lipid supplementation (Jenkins et al., 1994), glucose starvation (Elbein, 1987) and culture length (Hooker et al., 1995). Potential mechanisms that could explain these cell culture effects include the following: (1) depletion of the cellular energy state, (2) disruption of the local ER and Golgi environment, (3) interference with vesicle trafficking, and (4) modulation of glycosidase and glycosyltransferase activities (reviewed in Goochee et al., 1991). To properly interpret the effect of cell culture conditions on glycosylation, it is important to measure their impact on parameters that directly influence the glycosylation reaction. For instance, the impact of glucose concentration on the lipid-linked

oligosaccharide levels should be addressed when determining its influence on glycosylation site occupancy.

Molecules of the same protein differing in glycosylation can possess significantly different pharmacokinetic properties and biological activities (reviewed by Rademacher et al., 1988). Hence, the biopharmaceutical industry is particularly concerned about the impact of N-linked glycosylation heterogeneity on the quality of their glycoprotein products. For drug regulation purposes, glycoprotein therapeutics are often required to demonstrate consistent glycosylation patterns (Liu, 1992).

#### **1.1.5 Model System**

The Chinese Hamster Ovary (CHO) cell line is perhaps the most extensively-used mammalian cell line in the biopharmaceutical manufacturing industry. CHO cells are known among mammalian cells for their relative robustness, high growth rates, ease of genetic manipulation, high protein productivities and adaptability to protein-free culture. Among established mammalian cell lines, CHO cells generate recombinant proteins with glycosylation patterns that most closely resemble the naturally-occurring human forms (Utsumi et al., 1989). Since non-human glycosylation patterns are potentially immunoreactive (Jenkins and Curling, 1994), the ability of CHO cells to correctly glycosylate their products has further contributed to its widespread industrial use.

Glycosylation of recombinant human interferon-gamma (IFN- $\gamma$ ) produced by CHO cells has been particularly well-studied. In humans, activated T-lymphocytes and natural killer cells secrete IFN- $\gamma$  during an immune response. A member of the cytokine family, IFN- $\gamma$  has potent anti-viral, anti-proliferative and immunomodulatory activities

(Farrar and Schreiber, 1993). Human IFN- $\gamma$  cDNA has been cloned (Devos et al., 1982) and expressed in several hosts, including CHO cells (Scahill et al., 1983), *Escherichia coli* (Arakawa et al., 1985), insect cells (James et al., 1995) and transgenic mice (James et al., 1995). Among these expression systems, CHO cell-derived IFN- $\gamma$  bears the closest resemblance to the naturally occurring human form (Curling et al., 1990).

Natural IFN- $\gamma$  exists as a partially glycosylated dimer (Rinderknecht et al., 1984). Glycosylation has been implicated in facilitating the correct folding and dimerization of this protein (Sareneva et al., 1994). The oligosaccharides have been shown to protect IFN- $\gamma$  from proteolysis by elastase, cathepsin G and plasmin (Sareneva, 1995). Glycosylation also has a significant impact on the pharmacokinetic properties of a protein. CHO cell-derived IFN- $\gamma$  was cleared more slowly by perfused rabbit liver and kidney than *Escherichia coli*-derived IFN- $\gamma$  (Bocci et al., 1985). This is attributed to the higher affinity of the renal clearance system for smaller and more positively charged molecules---nonglycosylated IFN- $\gamma$  is positively charged with a mass around 34 kDa (Farrar and Schreiber, 1993), while IFN- $\gamma$  glycosylated by CHO cells are larger in size (average about 50 kDa in mass) and contain negative charges contributed by sialic acid residues attached to the ends of the glycans (Curling et al., 1990). The *in vivo* clearance rates of three different forms of IFN- $\gamma$  increased in the order: native glycosylated human IFN- $\gamma$ , nonglycosylated IFN- $\gamma$ , and recombinant insect cell-derived IFN- $\gamma$  (Sareneva et al., 1993). The high-mannose oligosaccharides associated with insect cell leads to the rapid elimination of proteins with high mannose content by mannose receptors on tissue resident macrophages (Ezekowitz and Stahl, 1988). Hence, improper glycosylation can

be even more detrimental to the circulatory half-life of a protein than lack of glycosylation.

IFN- $\gamma$  has two potential N-linked glycosylation sites as Asn 25 and Asn 97. Both natural (Rinderknecht et al., 1984) and CHO-derived human IFN- $\gamma$  (Mutsaers et al., 1986; James et al., 1995) exist in three forms differing in N-linked glycosylation status: doubly glycosylated at Asn 25 and Asn 97, singly glycosylated almost exclusively at Asn 25, and non-glycosylated. The variable site occupancy of IFN- $\gamma$  produced in CHO batch cultures has made it an excellent model system for studying the factors that control the extent of glycosylation.

## **1.2 MOTIVATION**

A successful mammalian cell culture process depends on both sufficient expression and correct glycosylation of the recombinant product. Low product titer and inconsistent protein glycosylation constitute two major problems commonly encountered in biopharmaceutical production.

Uncontrolled cell proliferation used in typical mammalian cell culture processes leads to accumulation of toxic metabolic products, nutrient deprivation, product degradation and massive cell death. There has been considerable interest in developing culture strategies that improve productivity in mammalian cell lines by limiting the cellular growth rate. Literature results have suggested that controlled cell proliferation bioprocesses can improve product yield and quality (Mazur et al., 1998; Fussenegger et al., 1997). By separating the cell culture process into a growth phase for rapid cell growth, followed by a proliferation-inhibited phase during which cells can devote their

resources towards heterologous protein production, this alternative method for manufacturing recombinant protein should increase productivity. The physiological stability associated with growth-arrested cells might also enhance consistency in product quality.

Heterogeneity in protein glycosylation presents special challenges to the development and production of a candidate therapeutic with consistent properties (Jenkins et al., 1996). An essential step in N-linked glycosylation is the *en bloc* transfer of an oligosaccharide chain from the endoplasmic reticulum membrane lipid dolichol phosphate (Dol-P) to a potential glycosylation site on a polypeptide. Glycosylation site occupancy heterogeneity results from variability in the success of this reaction at identical asparagines residues on different molecules of the same protein. This major form of protein heterogeneity is known to change with time in batch and fed-batch cultures of CHO cells (Nyberg, 1998; Castro et al., 1995; Curling et al., 1990). Various lines of evidence suggest that the intracellular amount of Dol-P controls the flux through the glycosylation pathway (Pan and Elbein, 1990; Grant and Lennarz, 1983; Carson et al., 1981). Since the lipid-linked oligosaccharide (LLO) species that functions as the oligosaccharide donor in N-linked glycosylation is formed from the sequential addition of monosaccharides to Dol-P, the extent of glycosylation may be limited by subsaturating levels of Dol-P. To understand the regulation of glycosylation throughout a culture process, it is necessary to determine the relationship between Dol-P availability, LLO levels, and the extent of protein Dol-P availability glycosylation.

### **1.3 THESIS OBJECTIVES**

Recombinant protein yield and quality are critical parameters in optimizing mammalian cell culture production processes. Using CHO cells expressing recombinant human IFN- $\gamma$  as the model system, this thesis investigated strategies that can potentially enhance heterologous protein expression or control the extent of protein glycosylation.

The major goals of this thesis are to: (1) evaluate the feasibility of using proliferation-controlled bioprocesses for recombinant protein production, (2) develop an effective method for rapidly generating and isolating cells that are optimized to produce heterologous proteins under growth-arresting conditions, (3) determine the relative abundance of lipid-linked oligosaccharides (LLOs) and the extent of glycosylation over the course of batch culture, and (4) test the hypothesis that dolichol phosphate (Dol-P) availability is a bottleneck in the glycosylation pathway.

### **1.4 THESIS ORGANIZATION**

The first chapter of the thesis introduces the research topic, discusses briefly the motivations for this work, and outlines the major objectives of the experiments. The subsequent four chapters detail the main body of experimental work performed in this thesis. Since the specific goals for the research in chapters 2, 3, 4 and 5 are unique, each of these four chapters contains its own distinct background material, description of the experimental procedures, research results and discussion of the findings. Chapter 2 describes an initial investigation into protein production from growth-arrested cells, and highlights the issues that are likely to arise in proliferation-controlled bioprocesses. Chapter 3 presents an effective strategy to rapidly generate and isolate CHO cells that are

better optimized for recombinant protein production under growth-arresting conditions. Chapter 4 documents the relative levels of glycosylation precursors and protein glycosylation in CHO cells over the course of batch culture. Chapter 5 details the effects of exogenous dolichol phosphate, the glycosyl donor, on batch cultures of CHO cells. Chapter 6, the final chapter in this thesis, summarizes the important conclusions drawn from the previous four chapters, and provides recommendations for future work.





## **2. Initial Investigation into Protein Production from Growth-arrested Cells**

### **2.1 ABSTRACT**

In view of the many potential benefits associated with protein production from growth-arrested cells, an initial investigation into the feasibility of this cytostatic bioprocess was conducted using  $\gamma$ -CHO cells. These anchorage-dependent Chinese Hamster Ovary (CHO) cells expressed human Interferon-gamma (IFN- $\gamma$ ) under the control of the SV40 early promoter. In this work, the use of serum-withdrawal as a means of cell proliferation control was evaluated. To investigate the impact of different culture conditions on product quality, IFN- $\gamma$  glycosylation site occupancy was also analyzed. Growth arrest was found to have a negligible effect on the extent of IFN- $\gamma$  glycosylation. Serum withdrawal proved to be a simple and effective means of arresting cell growth, but it also adversely impacted culture performance. After two weeks of serum withdrawal, both the cell viabilities and specific IFN- $\gamma$  productivities dropped by over 40%. Although some robust  $\gamma$ -CHO cells remained after two weeks of serum-free culture, these growth-arrested cells produced much less IFN- $\gamma$  on the average than the proliferating cells. Even if subpopulations that produce relatively higher amounts of IFN- $\gamma$  exist, there are no easy ways to isolate them. Since two major considerations for selecting recombinant protein production cell lines are robustness and high productivities, the  $\gamma$ -CHO cells were unsuitable for use in controlled proliferation bioprocesses.

## 2.2 INTRODUCTION

The commercial use of transformed mammalian cells to produce recombinant therapeutic proteins has revolutionized the treatment of human diseases. Batch cultivation is often the method of choice for large-scale recombinant protein production because it is a relatively simple yet reliable and controllable process. However, mammalian cell batch culture processes suffer from a major disadvantage: the period of highest protein production is typically limited to a short interval of the bioprocess either during exponential growth or when cells have reached their maximal cell density. Uncontrolled cell proliferation results in rapid accumulation of toxic metabolic products and nutrient deprivation in batch cultures. Continued proliferation soon results in the rapid exit of the cells from their optimal production phase and the entry into a decline phase characterized by massive cell death. This early loss of viable cells limits the yield from each production run. Furthermore, dying cells release proteases, glycosidases, and other intracellular components that degrade the product (Gramer, 1995). Delaying the onset of cell death would extend the production process and increase productivity.

There has been considerable interest in developing culture strategies that improve productivity in mammalian cell lines by limiting the cellular growth rate (Fussenegger and Bailey, 1998; Fussenegger et al., 1998; Al-Rubeai et al., 1992). An ideal cell culture process based on controlled cell proliferation can increase product titer by decoupling cell growth from heterologous protein production. As illustrated in Figure 2-1, this biphasic production method begins with a growth phase to allow for rapid cell proliferation. At the desired high cell density, growth arrest of the cells is initiated. Ideally, the cytostatic cells

remain viable for an extended time period during which they devote their resources to recombinant protein synthesis.

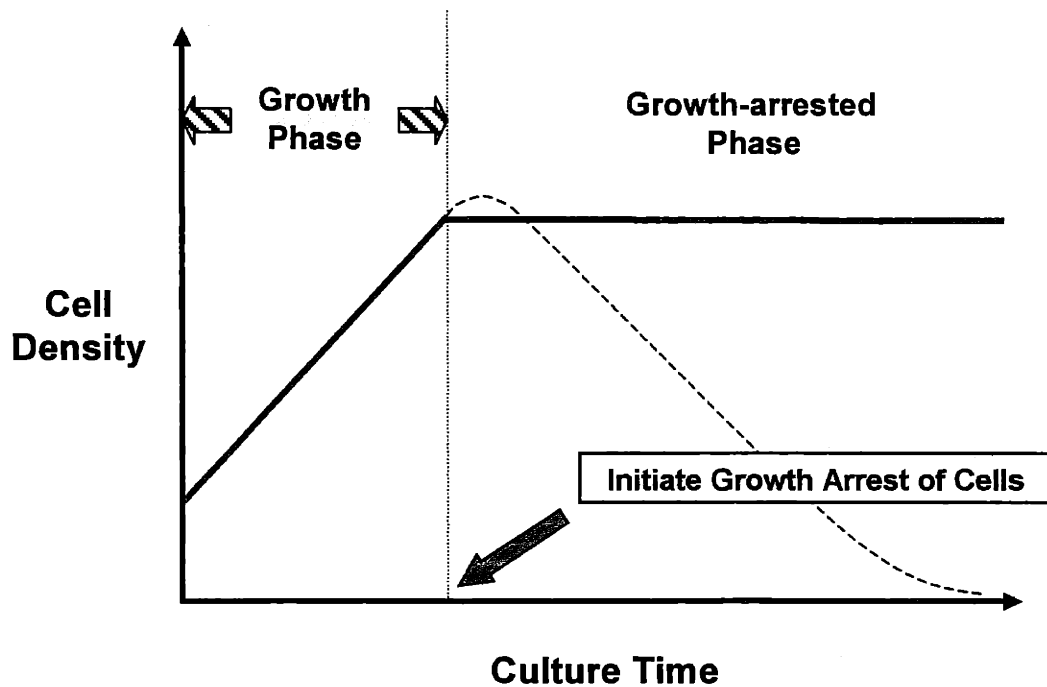


**Figure 2-1.** Schematic illustrating the basic concept behind the controlled proliferation bioprocess. In a typical culture process, after the cells reach the maximal cell density, the onset of massive cell death leads to a rapid decline in cell density (as shown by the dotted line). By contrast, in an ideal controlled proliferation bioprocess, cells are allowed to expand until they have reached their optimal cell density, which is then preserved by the induction of a sustained growth arrest (as illustrated by the solid line).

In principle, controlled cell proliferation bioprocesses have numerous advantages over classical production processes (Table 2-1). First, non-proliferative cells may be able to remain viable for longer time periods, thereby extending the production run. Second, quiescent cells should have higher specific productivity, since product formation no longer needs to compete with growth-associated metabolic processes for cellular resources. Third, the increased cellular stability and slower rates of genetic shifts expected in quiescent cells should result in higher product homogeneity. Fourth, the production costs for maintaining quiescent cells should be lower because of the slower rate of medium exhaustion.

In view of the many potential benefits associated with protein production from quiescent cells, an initial investigation into this process was conducted using a Chinese Hamster Ovary (CHO) cell line that was already available in this laboratory. The ability to produce the human Interferon-gamma protein (IFN- $\gamma$ ) lends these cells the name “ $\gamma$ -CHO”. CHO cells are known for the high stability of chromosomally integrated heterologous transgenes and their relative ease of large-scale cultivation in various modes. CHO cells have a glycosylation machinery that most resembles its human counterpart; recombinant glycoproteins produced by CHO cells show glycosylation patterns similar, if not identical, to that found in native human glycoproteins (Jenkins and Curling, 1994). In addition, various well-established, useful CHO cell mutants exist; the DUK line of CHO cells, being deficient in dihydrofolate reductase (DHFR), permits the facile selection of transformants. These favorable characteristics have made CHO cells the pre-eminent cell line used in the biopharmaceutical industry.

<b><u>Classical Batch Bioprocess for Protein Production</u></b>	<b><u>Controlled Proliferation Bioprocess for Protein Production</u></b>
◆ Cells die soon after exponential growth phase	◆ Cells may remain viable for longer time periods
◆ Product formation competes with growth-associated metabolic processes	◆ Cellular resources may be used more exclusively for product formation
◆ Protein quality is often inconsistent (e.g., glycosylation heterogeneity)	◆ Cellular stability and lower genetic drift may lead to more consistent product quality
◆ Rapidly growing cells quickly exhaust nutrients in medium	◆ Slower rate of medium exhaustion should lower production costs

**Table 2-1.** Potential advantages of controlled proliferation bioprocess for protein production over classical methods. The left-hand column lists the problems commonly associated with classical recombinant protein production processes. The right-hand column describes the theoretical strengths of recombinant protein production from growth-arrested cells.

Proliferation control of the  $\gamma$ -CHO cell line has been shown to be readily achieved by serum withdrawal (Sanfeliu et al., 2000). In serum-free medium, the  $\gamma$ -CHO cells demonstrated a considerable degree of growth control entering quiescence; a large

fraction of the cells continued to stay viable and non-proliferative for weeks under serum-free conditions. Insulin supplementation enabled the growth-arrested cells to reenter the cell cycle, but it also induced apoptosis. The presence of serum protected the cells from cell death after insulin addition.

In evaluating the potential of a particular cell line for quiescent phase protein production, four factors are critical. First, an effective means of controlling cell proliferation must exist for the cell line. Second, the cells must maintain high viabilities for extended time periods under growth-arresting conditions. Third, recombinant protein expression should be stable in the growth-arrested cells. Fourth, the protein quality should be uniformly high. For instance, consistent product glycosylation should be demonstrated before a production process can be established.

This series of experiments was performed to investigate the feasibility of using  $\gamma$ -CHO cells that are growth-arrested by serum withdrawal to produce IFN- $\gamma$ . The impact of serum withdrawal on  $\gamma$ -CHO growth, cell cycle distribution, and IFN- $\gamma$  productivity and glycosylation was studied.

## **2.3 MATERIALS AND METHODS**

### **2.3.1 Cell line**

An anchorage-dependent CHO cell line expressing human Interferon-gamma (IFN- $\gamma$ ) driven by the SV40 early promoter was obtained from Dr. Walter Fiers (Scahill et al., 1983). This recombinant cell line, referred to as  $\gamma$ -CHO, was created from a dihydrofolate reductase deficient (DHFR<sup>-</sup>) CHO cell line by cotransfecting the cells with genes for both DHFR and human IFN- $\gamma$ . Unlike the transformed cells, the parental DHFR<sup>-</sup> CHO cells

cannot synthesize their own ribonucleosides, and require the presence of external ribonucleosides for their survival. The cells were selected for growth in 0.25  $\mu$ M methotrexate, a competitive inhibitor of the DHFR enzyme. Subsequent rounds of methotrexate selection greatly amplified the DHFR gene and the adjacent IFN- $\gamma$  gene in these transformed cells. Hence, the selected cells should contain multiple copies of the IFN- $\gamma$  gene. The cells were adapted to grow in 5% serum containing medium. Frozen stocks of the cell line were prepared.

### **2.3.2 Culture Medium and Maintenance**

The basal medium used in all cultures was Iscove's Modified Dulbecco's Medium (IMDM, Gibco) supplemented with 0.25  $\mu$ M methotrexate and 20 U/ml penicillin-20  $\mu$ g/ml streptomycin. In most cases, the medium was further supplemented with 5% dialyzed fetal bovine serum (FBS). All cultures were incubated at 37°C in an environment with 95% relative humidity and 5-10% CO<sub>2</sub> overlay. Unless otherwise stated, all reagents used were purchased from Sigma.

### **2.3.3 Cell Enumeration**

Adherent cells were detached by trypsin, and resuspended in 10% FBS. Detached cells were spun down, the supernatant was removed and retained for IFN- $\gamma$  analyses, while the cell pellets were resuspended in 1 ml fresh media. Measurements using both attached and detached cells contributed towards the determination of the cell density and culture viability. Cells were diluted with isotonic solution of 0.4% trypan blue and counted using a hemacytometer and microscope. Trypan blue dye exclusion distinguishes viable cells

from dead cells: viable cells exclude the dye, but dead cells have lost their membrane integrity and are stained blue.

#### **2.3.4 Flow Cytometry**

One to two million cells from each culture flask were trypsinized, centrifuged and resuspended in 0.5 ml stain solution. This solution contained 1.5% polyethylene glycol-4000 (PEG-4000), 1.5% PEG-8000, 50 µg/ml propidium iodide, 180 units/ml RNAase, 0.1% Triton-X-1000, and 4 mM sodium citrate; the final pH of solution was adjusted to 7.2. After a 20-minute incubation at 37°C, 0.5 ml salt solution was added (1.5% PEG-4000, 1.5% PEG-8000, 50 mg/ml propidium iodide, 0.1% Triton-X-1000, 0.4 M sodium chloride, and final pH of solution was adjusted to 7.2). For the next 12 to 36 hours, the sample was stored in the dark at 4°C. Cell sorting was performed on a FACScan flow cytometer (Becton Dickinson). 30,000 events per sample were collected. Results were modeled with the ModFit Lt. v.2 analysis software (Verity Software House) to quantify the cell cycle distribution within each sample.

#### **2.3.5 Determination of IFN-γ Glycosylation and Concentration**

Glycosylation macroheterogeneity of accumulated IFN-γ was determined by the immunoprecipitation of IFN-γ from culture supernatants and analysis of the purified protein by means of micellar electrokinetic capillary chromatography (MECC), as described in detail by Nyberg et. al. (1999). Briefly, IFN-γ immunoprecipitation was achieved with immobilized IFN-γ antibodies in the form of Resolute-γ beads (Celltech). Following immunoprecipitation, the IFN-γ was directly eluted into the MECC running



buffer and analyzed using the MECC method developed by James et al. (1994). In this type of chromatography, glycoform migration time was inversely related to the extent of glycosylation; the elution order of the different forms of IFN- $\gamma$  was as follows: fully-glycosylated IFN- $\gamma$  (2-sites glycosylated) emerged first, followed by the partially-glycosylated IFN- $\gamma$  (1-site glycosylated), and finally the non-glycosylated IFN- $\gamma$ . Chromatograms obtained from the System Gold data acquisition software (Beckman Instruments) were exported to the GS370 peak integration software (Hoefer Scientific Instruments) for further analyses. This software quantified the area of the peaks corresponding to the three IFN- $\gamma$  glycoforms. In this way, the relative distribution of the three IFN- $\gamma$  glycoforms within any culture sample was determined. Concentrations of IFN- $\gamma$  were measured with an ELISA kit (Biosource International).

### **2.3.6 Serum-containing and Serum-free Experiments**

Cells with identical culture history were inoculated at  $1.5 \times 10^5$  cells/ml in 25 cm<sup>2</sup> T-flasks containing 5 ml of 5% FBS containing medium. After 2 days of incubation, the 5% FBS medium was removed from the subconfluent cultures. The cells were washed with phosphate buffered saline (PBS), and fresh medium was added to the cultures as specified. Every 48 hours, adherent cells were collected by trypsinization and counted. In certain instances, the spent medium was exchanged for fresh medium every 48 hours. Cells were also used for FACS measurements and the culture supernatant was retained for IFN- $\gamma$  analyses.

## 2.4 RESULTS

### 2.4.1 Serum-containing and Serum-free Culture

To study the impact of serum withdrawal on  $\gamma$ -CHO cells, the performance of  $\gamma$ -CHO cells grown in duplicate batch cultures containing either serum-free medium or medium supplemented with 5% serum was investigated. An additional set of experiments was performed simultaneously to separate the effects of serum withdrawal from those arising from lactate accumulation or nutrient deprivation. In these parallel cultures, possible nutrient limitations or metabolic waste accumulations were minimized by replacing the old medium with fresh medium---with or without 5% serum---every other day.

At the start of these experiments, cells that had been growing exponentially for 2 days in 5% serum were transferred into fresh medium, and subjected to four different culture conditions. The cultures differed in the presence of 5% serum, as well as in the execution of regular fresh medium exchange. In the first culture condition, cells were grown in the presence of 5% serum-containing medium; every other day, the old medium was removed, and replaced with fresh 5% serum-containing medium. In the second culture condition, cells were grown in the batch mode in 5% serum-containing medium; medium replacement strategy was not applied. In the third culture condition, cells were cultured in serum-free medium with regular fresh serum-free medium exchange. In the fourth culture condition, cells were grown in serum-free batch culture. At 48 hour intervals, T-flasks containing cells cultured under the four different conditions were used for the following measurements described below.

### 2.4.2 Culture Viabilities

The four different cultures displayed distinct viability profiles (Figure 2-2).  $\gamma$ -CHO cells cultured in 5% serum with regular medium exchange maintained viabilities exceeding 95% throughout the 14-day culture. The 5% serum batch culture showed similarly high viabilities for 6 days, before falling slightly below the 90% mark thereafter. The cell death observed in the later part of serum batch culture is a typical feature of batch cultures---it is attributed to nutrient limitation and metabolic waste accumulation, and it can be avoided with regular medium replacement. The phenol-red colored medium progressively lightened changed from its original red hue to orange, and finally to yellow by day 6. This color change is consistent with the lowering of the culture pH due to accumulation of metabolic wastes like carbon dioxide and lactate.

By contrast, viabilities of the serum-free cultures deteriorated progressively, in agreement with the demonstrated apoptosis-inducing ability of serum withdrawal in mammalian cell cultures (Chung et al., 1998; Mercille and Massie, 1994). The serum-free culture with regular fresh serum-free medium exchange showed initial high viabilities, but the viabilities proceeded to drop by 40% over the next 8 days. The sharpest decline in viability was observed in the serum-free batch culture---viabilities fell from over 95% to under 60% in 10 days. The phenol-red stained serum-free medium retained its color throughout the entire serum-free batch culture process, suggesting that metabolic waste accumulation and nutrient limitation are not significant.

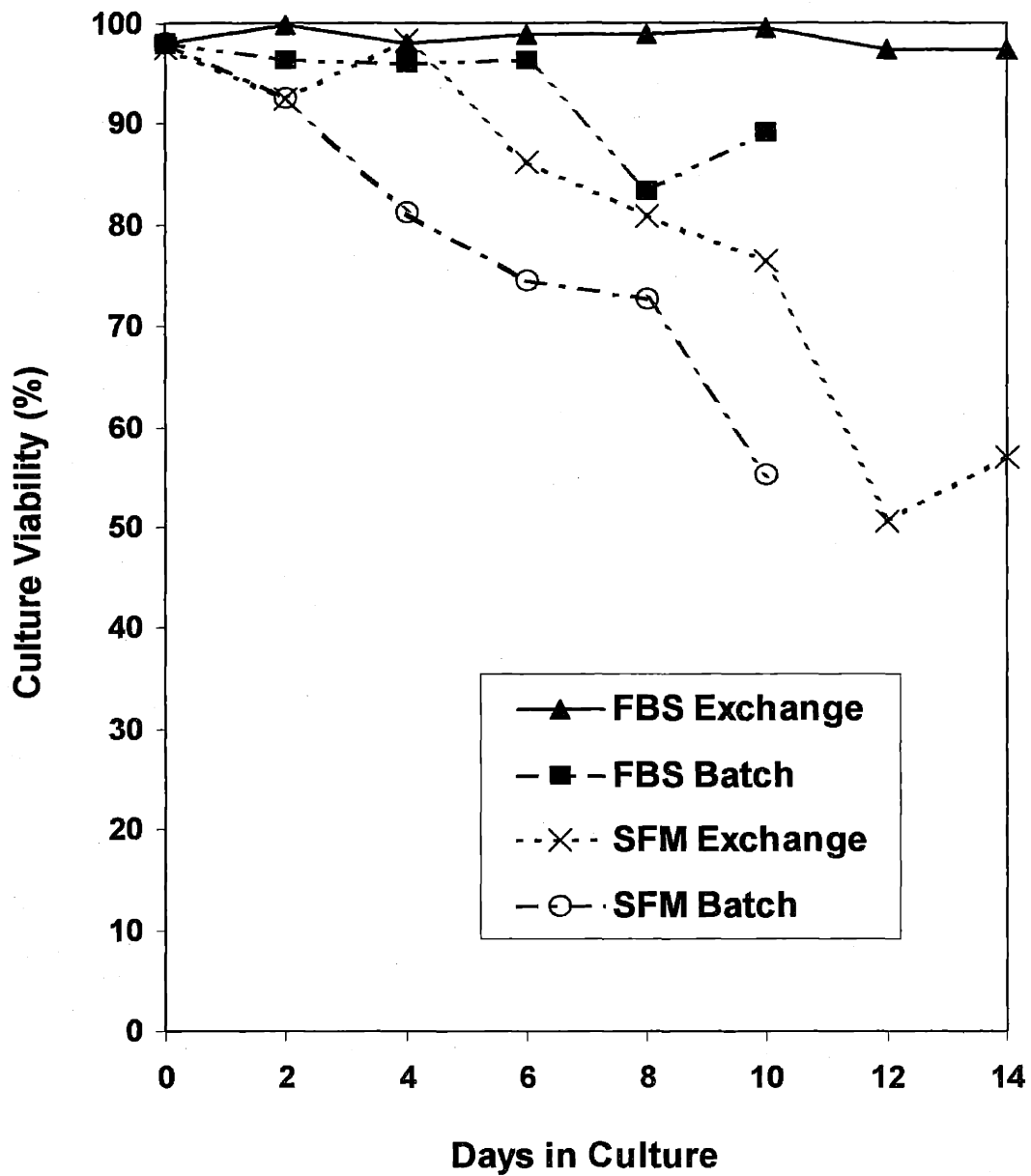


**Figure 2-2.** Viabilities of  $\gamma$ -CHO cells cultured under 4 different conditions are plotted over time. The cultures differed in the presence of fetal bovine serum (FBS) and in the application of fresh medium exchange every 48 hours. The various culture conditions were: serum-containing culture with regular fresh 5% FBS medium exchange ( $\blacktriangle$ ); serum-containing batch culture ( $\blacksquare$ ); serum-free culture with regular fresh serum-free medium exchange ( $\times$ ); serum-free batch culture ( $\circ$ ).

The difference in viability measurements between the two serum-free cultures is attributed to the removal of detached cells with each regular fresh medium exchange. In general, more than half of the detached cells were non-viable, whereas over 80% of attached cells were viable, as revealed by trypan blue dye exclusion assays (data not shown). Even if the detached cells were not stained by trypan blue, the fact that they were detached suggested that they were less robust than the attached cells, and were possibly in the process of undergoing cell death. Hence, regular medium replacement artificially raised cell viability measurements: each medium exchange enhanced the proportion of viable cells in the cultures by the removing the detached cells that were less robust. In the serum-free batch culture, all the detached cells were retained in the flasks; any subsequent deaths among them would be detected, and would contribute to the culture viability measurements.

### **2.4.3 Cell Densities**

Although all cultures were inoculated with identical numbers of viable cells, the four culture conditions yielded different final viable cell densities (Figure 2-3). The most notable difference was between the two 5% serum-containing cultures: the regular exchange of old medium for fresh 5% serum medium clearly boosted viable cell densities (Figure 2-3(A)). The medium replacement strategy engendered a 10-fold increase in viable cell density from  $1 \times 10^5$  cells/cm<sup>2</sup> to over  $1 \times 10^6$  cells/cm<sup>2</sup> after 14 days of culture. The high cell viabilities maintained in these high-density cultures (Figure 2-2) support the hypothesis that protective factors present in serum prevent cell density-dependent cell death. Apoptosis is commonly observed in high density cultures of

immortalized cell lines (Fiore and Degrassi, 1999). By contrast, viable cell densities in the 5% serum batch cultures declined steadily from the maximum of  $2.4 \times 10^5$  cells/cm<sup>2</sup> measured on day 4, to  $1.4 \times 10^5$  cells/cm<sup>2</sup> on day 10. This decline is attributed to the onset of cell death triggered by nutrient limitation and metabolic waste accumulation.

The serum-free cultures showed similar viable cell density profiles (Figure 2-3(B)). This supports the explanation proposed earlier for the observed difference in viabilities between the two serum-free cultures (Figure 2-2). Some of the detached cells in serum-free cultures were still viable as determined by the trypan blue dye exclusion assay. These cells contributed towards the viable cell count, and were fully accounted for in the serum-free batch cultures. However, viable detached cells were removed regularly from the culture with each medium exchange. Therefore, the use of medium replacement artificially and incrementally lowered the total number of cells (both viable and non-viable) counted for the culture over time.

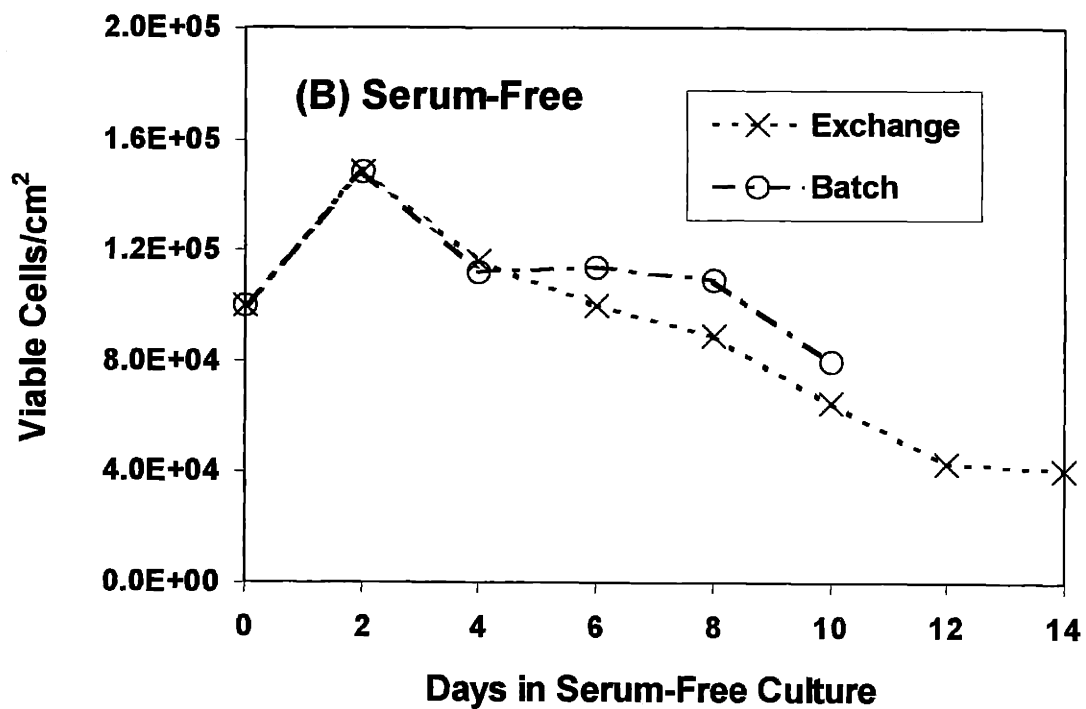
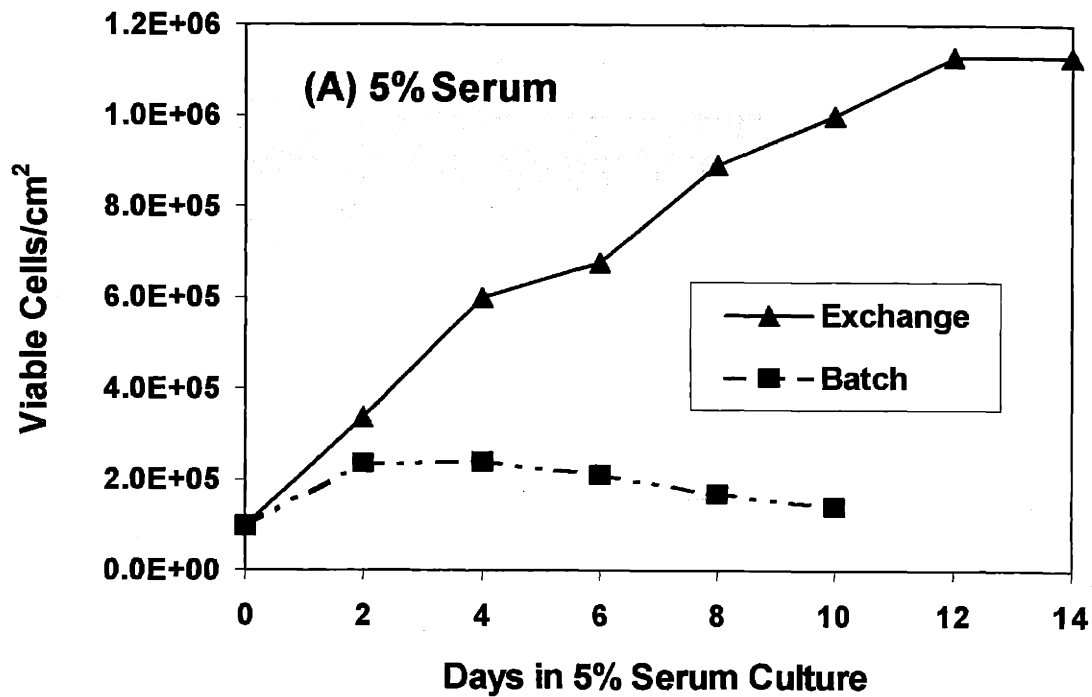


**Figure 2-3.** Viable cell densities of cultures in presence (A), and absence (B) of 5% serum. Four different culture conditions were used: serum-containing culture with regular fresh 5% FBS medium exchange (▲); serum-containing batch culture (■); serum-free culture with regular fresh serum-free medium exchange (×); serum-free batch culture (○).

Mitogens are polypeptide growth factors present in serum that provide extracellular signals required to activate cell proliferation in cultured mammalian cells. When mitogens are absent, cells withdraw from the cell cycle and enter the G0 quiescent phase. However, cells that have passed the restriction point in G1 phase are committed to enter the S phase, and these cells will complete S and G2 phases as well as mitosis in the absence of mitogens. For this reason, cell densities increased initially in the absence of serum; cells that had passed the restriction point at the time of serum withdrawal proceeded through the cell cycle to complete cell division before becoming growth-arrested in the G0 phase. Subsequently, viable cell densities in both serum-free cultures steadily declined from the peak of  $1.5 \times 10^5$  cells/cm<sup>2</sup> on day 2, to  $0.8 \times 10^5$  cells/cm<sup>2</sup> or less by day 10. Consistent with the known anti-proliferative and pro-apoptotic effects of serum withdrawal (Sanfeliu et al., 2000; Chung et al., 1998; Mercille and Massie, 1994), the serum-free cultures ended with overall net decreases in viable cell densities.

#### **2.4.4 Cell Cycle Analyses**

After staining the DNA with a fluorescent dye, the cells were analyzed by FACS. The amount of fluorescence measured in each cell was directly proportional to its cellular DNA content; G2/M phase cells would fluoresce twice as brightly as G0/G1 phase cells, since the former contained twice as much DNA as the latter. In this way, the cell cycle distribution within a cell population was readily determined.

For cells maintained in 5% serum, resolution of the G0/G1, S and G2/M phases revealed a gradual increase in the percent of cells in the G0/G1 phase during the first half of the culture, and a concurrent decrease in the proportion of S phase cells (Figure 2-4).



These changes leveled off halfway into the experiments; from day 6 onwards, more than 80% of the attached cells in both cultures were in the G0/G1 phase. The gradual accumulation of cells in the G0/G1 phase indicated the slowing down of cell proliferation in response to culture confluency. This incremental growth-arrest showed that the presence of serum and its associated growth factors could not completely override the growth-arresting effects of contact inhibition.

At the beginning of serum-free culture, less than 60% of the cells were in the G0/G1 phase (Figure 2-5). Within 2 days of serum-withdrawal, the proportion of cells in the quiescent phase had increased to 80% in both serum-free cultures. During the rest of serum-free culture, the fraction of G0/G1 phase cells increased marginally. The rapid, substantial and protracted enhancement in the fraction of G0/G1 phase cells illustrated the effectiveness of serum-withdrawal in inducing and sustaining growth-arrest.

#### **2.4.5 IFN- $\gamma$ Production**

Specific IFN- $\gamma$  productivity ( $q_{\text{IFN}}$ ) was calculated by dividing the amount of IFN- $\gamma$  secreted into the culture medium every 2 days by the integrated viable cell density measured over the same time period. Overall decline in  $q_{\text{IFN}}$  was observed in all the cultures, with the sharpest drop occurring between days 2 and 4 (Figure 2-6). By day 6,  $q_{\text{IFN}}$  had diminished to less than half of its peak value in all the cultures, and began to taper off. In the serum-containing cultures,  $q_{\text{IFN}}$  increased between days 0 and 2, before starting a steady decline thereafter. In the serum-free cultures,  $q_{\text{IFN}}$  declined consistently, yielding at least a 4-fold drop from its initial value by day 10.

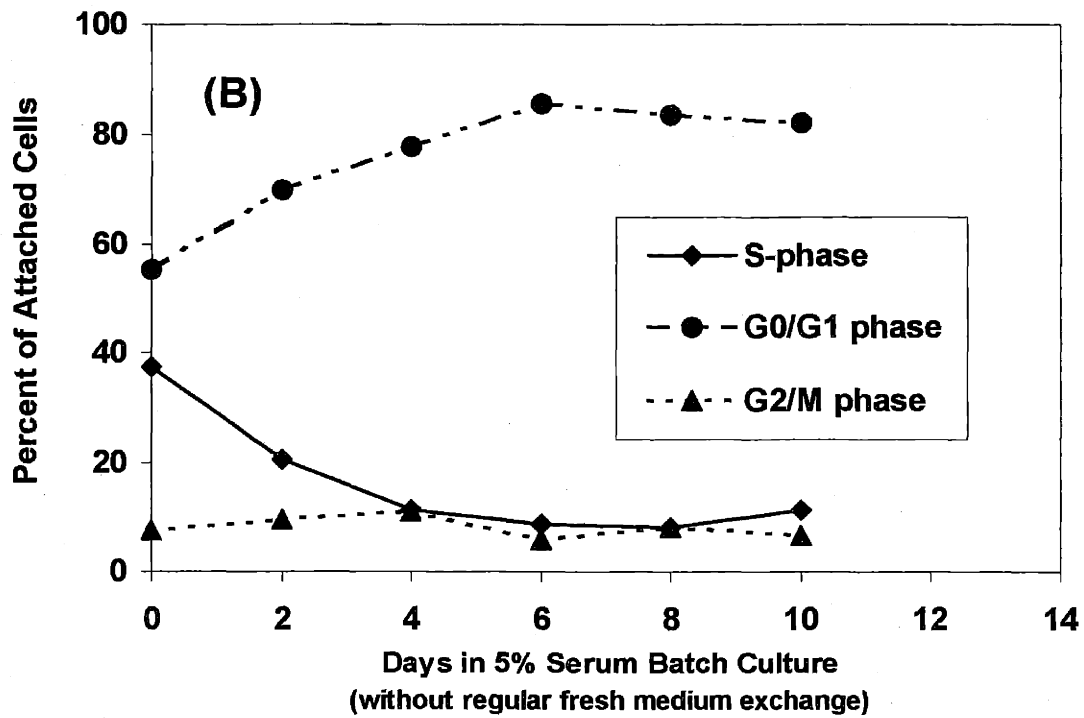
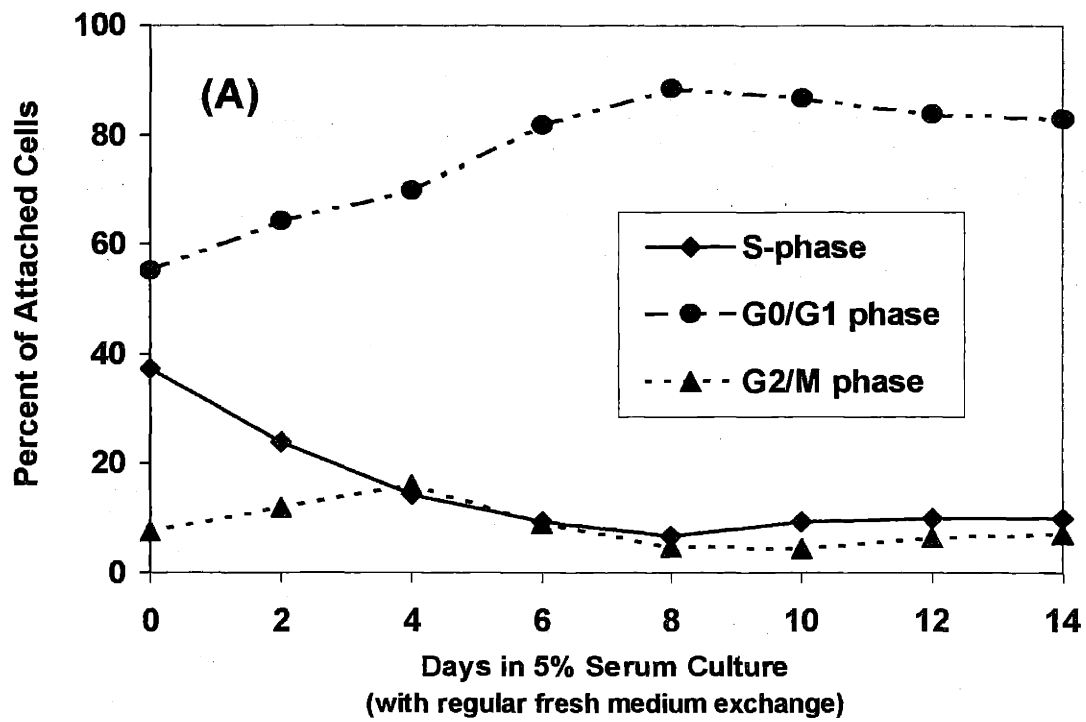


**Figure 2-4.** Cell cycle distribution of attached  $\gamma$ -CHO cells grown in 5% serum-containing culture with (A), and without (B) regular exchange of fresh serum medium.

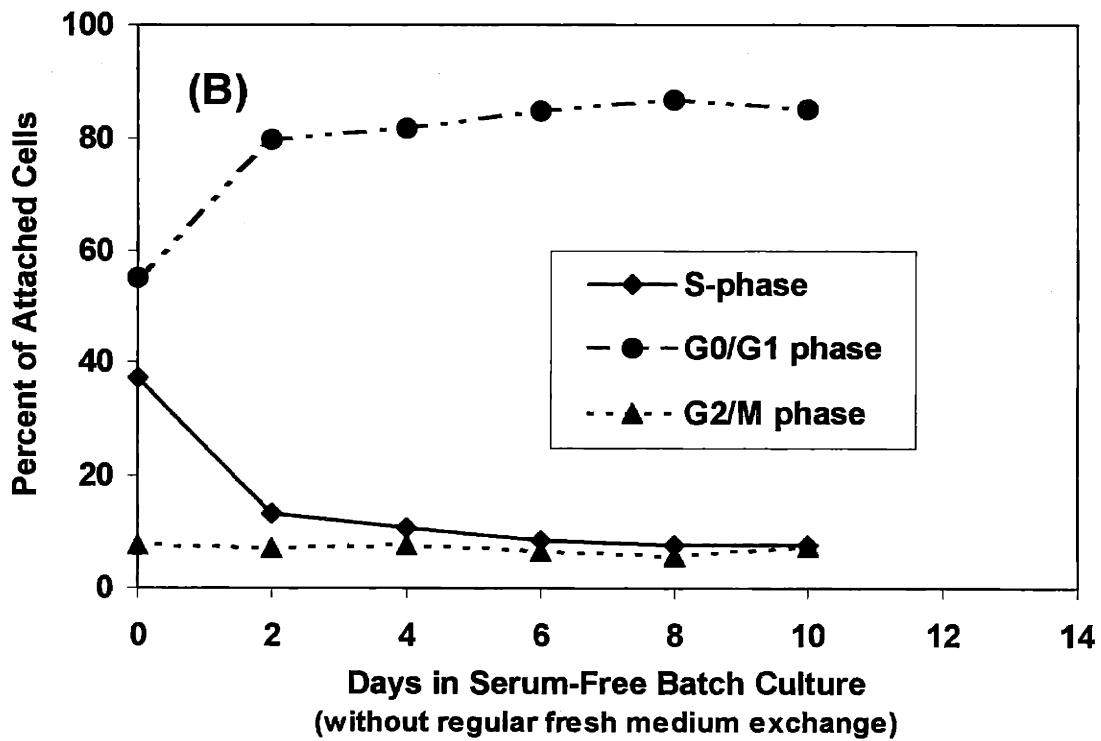
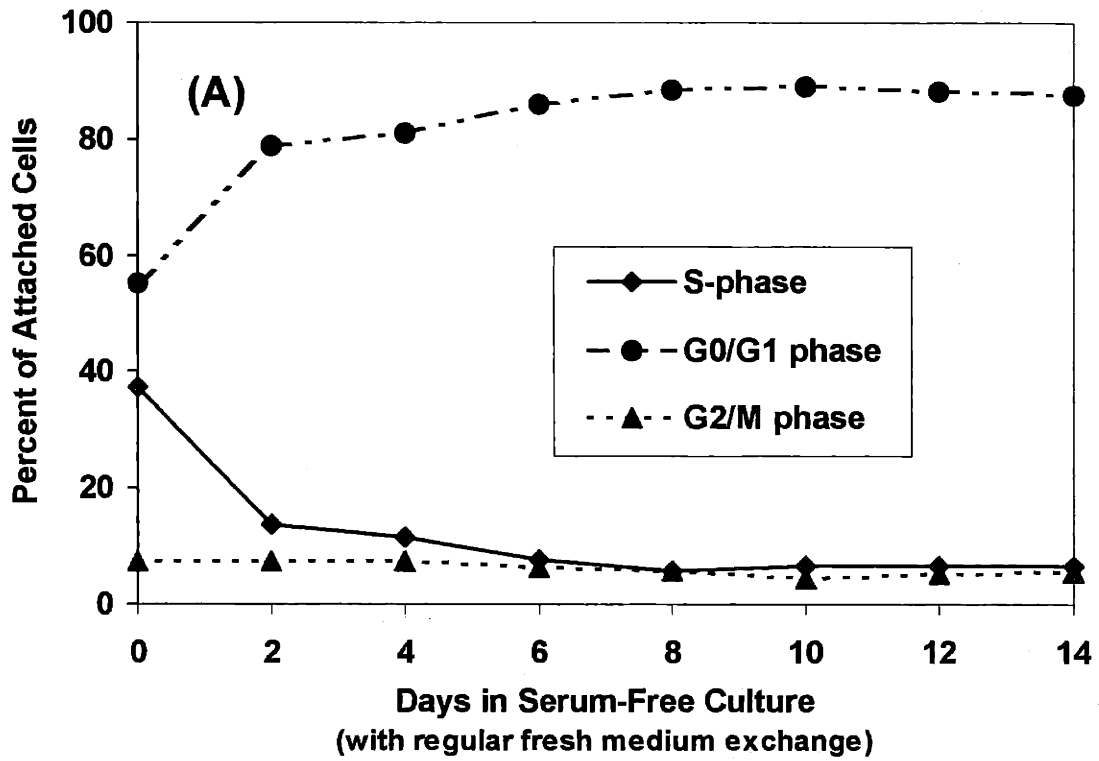


**Figure 2-5.** Cell cycle distribution of attached  $\gamma$ -CHO cells grown in serum-free culture with (A), and without (B) regular exchange of fresh serum-free medium.

#### 2.4.6 IFN- $\gamma$ Glycosylation Site Occupancy

The glycosylation site occupancy of IFN- $\gamma$  secreted by  $\gamma$ -CHO cells cultured in 5% serum under different modes showed negligible differences (Figure 2-7). With regular fresh serum-containing medium exchange, the percent of fully-glycosylated IFN- $\gamma$  appeared to marginally increase over 12 days (Figure 2-7(A)). In the absence of medium exchange, the fraction of fully-glycosylated IFN- $\gamma$  appeared to marginally decrease over time in the 5% serum batch culture (Figure 2-7(B)). In these batch cultures, rapid consumption of nutrients by the exponentially growing cells during the initial part of the culture process should have occurred. The resulting glucose and glutamine limitations would be expected to adversely impact glycosylation site occupancy. However, the results here show that glycosylation remains fairly constant over culture time, both in the absence and presence of regular medium exchange.

In both serum-free cultures, the percent of fully-glycosylated IFN- $\gamma$  remained fairly constant over culture time (Figure 2-8). Towards the end of the experiment, the amount of IFN- $\gamma$  secreted into the medium by the various cultures was so low that glycosylation site occupancy could not be determined accurately. Hence, data points were missing for the last 2-4 days of culture.

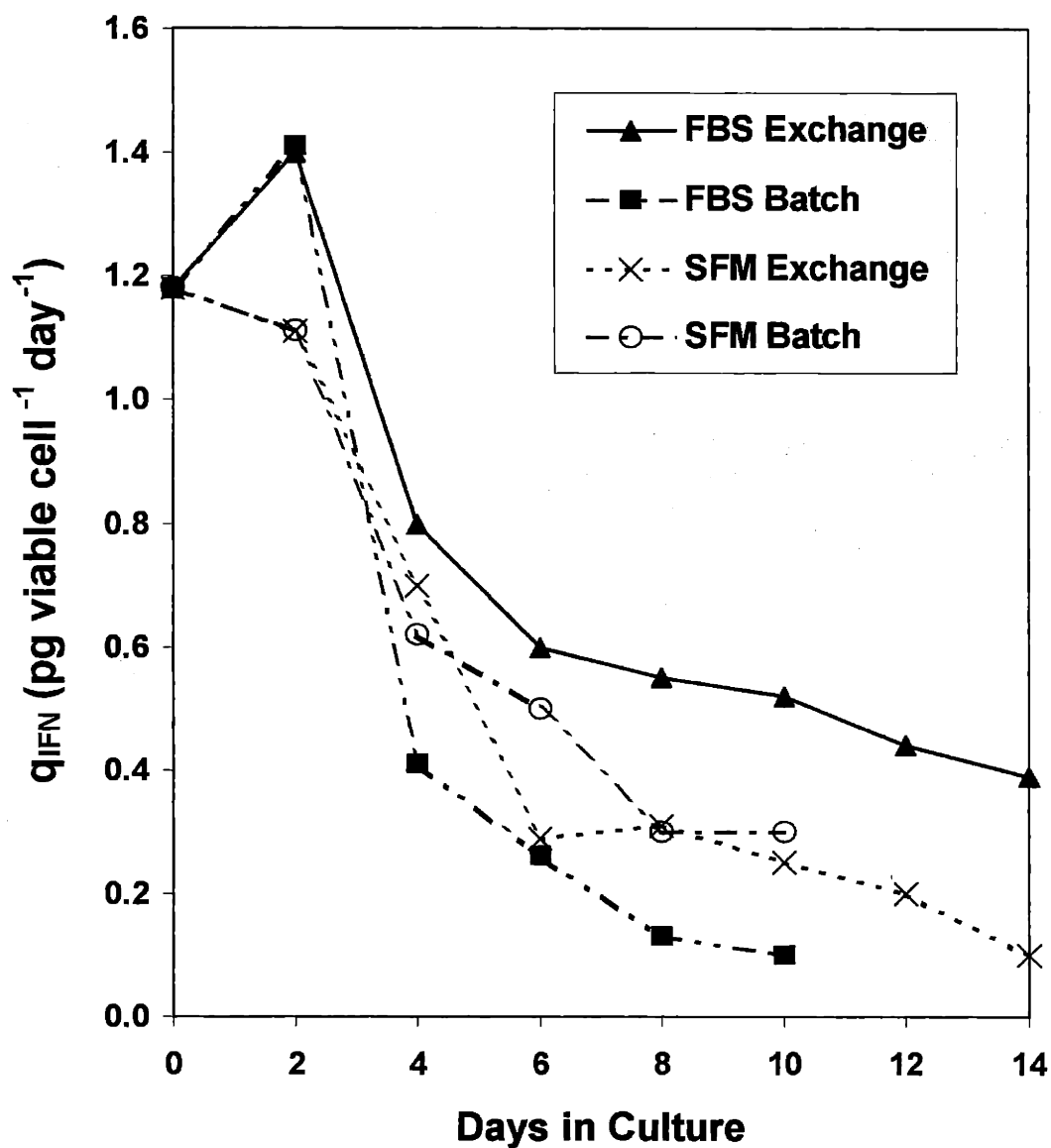


**Figure 2-6.** Specific IFN- $\gamma$  productivity of  $\gamma$ -CHO cells under the following culture conditions: serum-containing culture with regular fresh 5% serum medium exchange ( $\blacktriangle$ ); serum-containing batch culture ( $\blacksquare$ ); serum-free culture with regular fresh serum-free medium exchange ( $\times$ ); serum-free batch culture ( $\circ$ ).

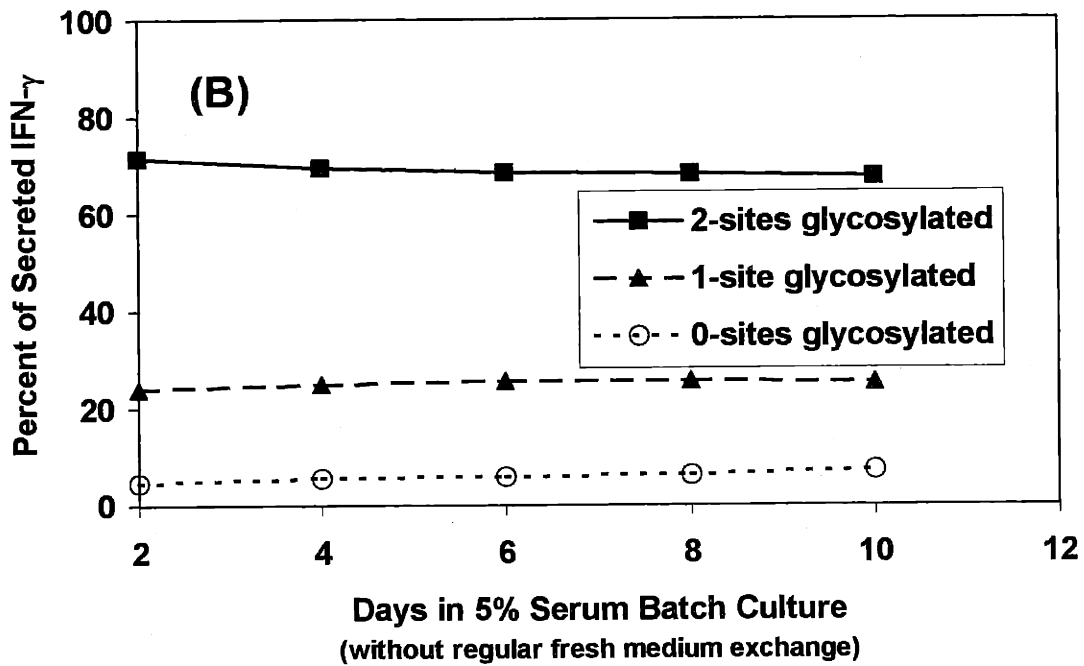
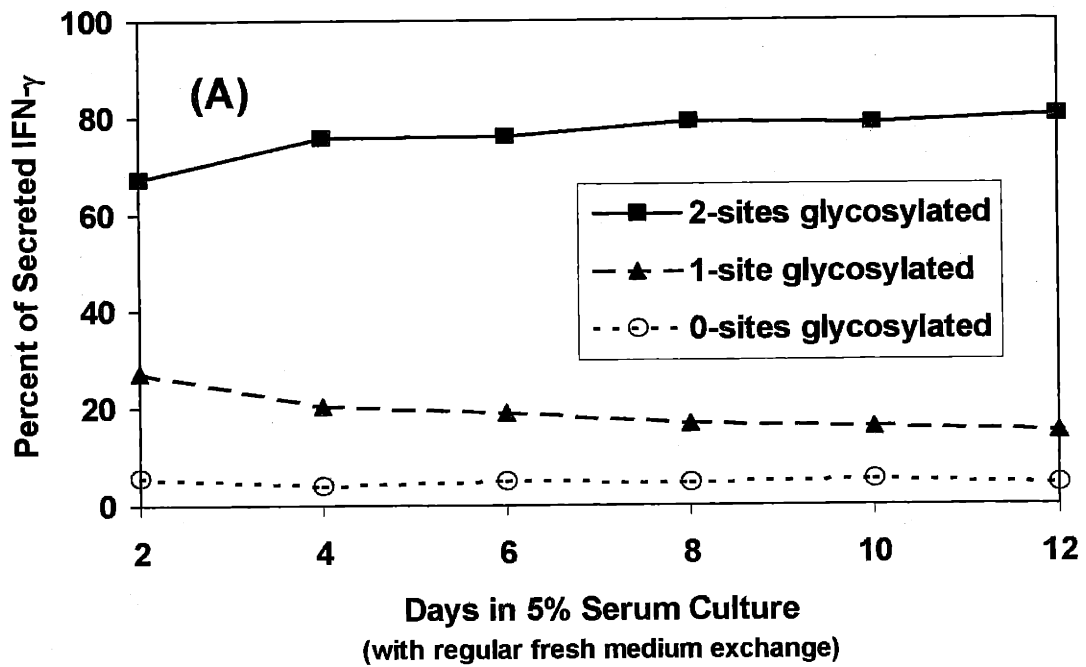


**Figure 2-7.** Glycosylation site occupancy distribution of IFN- $\gamma$  secreted by  $\gamma$ -CHO cells cultured in 5% serum-containing medium with (A), and without (B) regular exchange of fresh 5% FBS medium.

## 2.5 DISCUSSION

The CHO cell-line is the most widely-used mammalian cell line for the production of important recombinant therapeutic proteins such as thrombolytics, cytokines, blood-clotting factors, growth factors and immunoglobulins. Recombinant CHO cells are characterized by their anchorage- and serum-dependent growth properties. This work was undertaken to determine the applicability of using proliferation-controlled CHO cells for recombinant therapeutic protein production.

Serum consists of an ill-defined mixture of growth factors and other components beneficial to cultured cells. The growth factors regulate mammalian cell proliferation and differentiation through surface receptor binding and subsequent signal transduction cascades that lead to DNA synthesis and cell division. These signals are usually integrated by the D-type cyclins, and they stimulate the cells to transit rapidly from the G1 phase to the S phase of the cell cycle. Serum withdrawal from mammalian cell cultures results in cell cycle arrest in G1 phase, followed by entry into G0 phase (Zetterburg and Larson, 1985).

This work on CHO cells demonstrated the growth-arresting ability of serum withdrawal (Figure 2-5). However, it also implicated serum withdrawal as a key factor in inducing cell death. In cultures with regular fresh 5% serum medium exchange, the cells continued to proliferate and maintain viabilities exceeding 95% for over 2 weeks. By contrast, cell viabilities and viable cell numbers in serum-free cultures decreased by over 40% within 2 weeks of serum withdrawal.

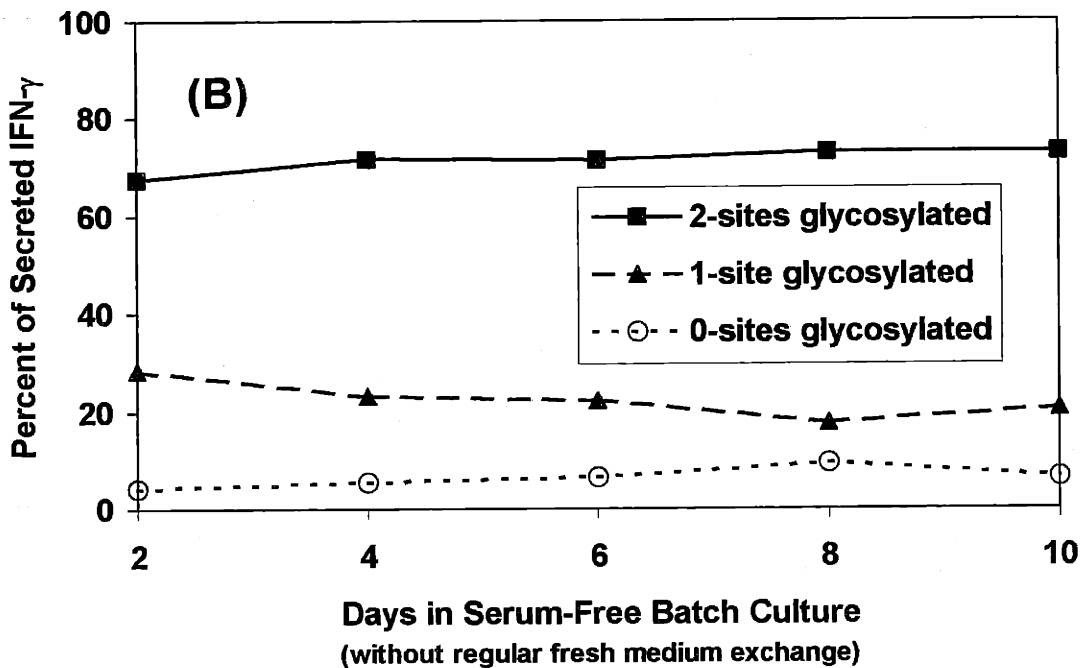
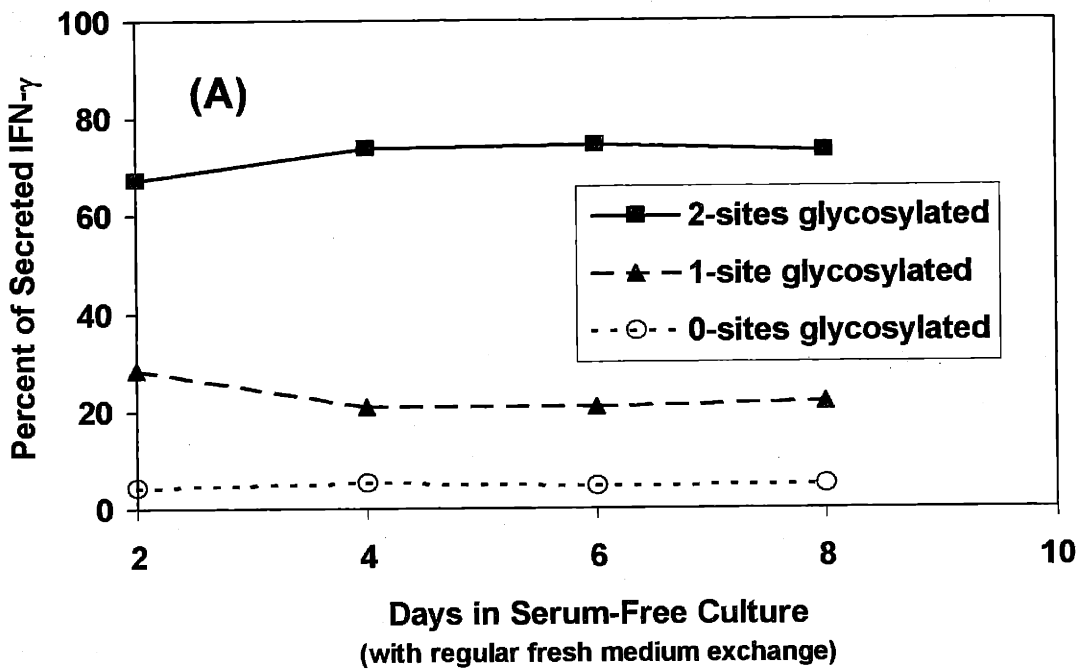


**Figure 2-8.** Glycosylation site occupancy distribution of IFN- $\gamma$  secreted by  $\gamma$ -CHO cells cultured in serum-free medium with (A), and without (B) regular exchange of fresh serum-free medium.



These results support the presence of both growth and survival factors in serum. The anti-apoptotic activity found in serum is well-documented, but the specific mechanisms involved remain unclear. In the absence of serum, many cell lines, including those of industrial importance, will undergo apoptosis (Al-Rubeai and Singh, 1998; Goswami et al., 1999). In particular, CHO cells grow well in virtually any serum-supplemented medium, but are susceptible to apoptosis in serum-free medium (Zanghi et al., 1999).

The onset of sustained growth-arrest in all the cultures preceded the decrease in IFN- $\gamma$  productivity. The drop in  $q_{\text{IFN}}$  (Figure 2-6) echoed the decline observed for the proportion of S-phase cells in each culture (Figures 2-4 and 2-5), suggesting a positive association between the two measurements in CHO cells. In a study on the role of the cell cycle in determining gene expression and productivity, similar trends were observed in suspension cultures of CHO cells expressing IFN- $\gamma$  under the control of the SV40 promoter (Lloyd et al., 1999).

Another study on suspension CHO cells established the cell cycle dependence of cellular dihydrofolate reductase (DHFR) content and tissue plasminogen activator (tPA) production and secretion (Kubbies and Stockinger, 1990). The researchers used a cell line obtained from the transfection of CHO DHFR-negative cells with a plasmid (pSVtPA.DHFR) carrying the tPA and DHFR genes, controlled by the SV40 early promoter and the major late promoter from the adenovirus 2 (Ad 2), respectively. The DHFR gene was used for gene amplification under selective pressure of 5  $\mu\text{M}$  methotrexate. In these plasmid-amplified cells, DHFR expression peaked in the G2/M phase. By contrast, tPA production and secretion increased continuously from the relative

value of 100% in G1, to 127% in early S phase, before reaching its maximum of 159% in late S phase, and then it decreased to 118% in G2/M phase. Since expression of the two proteins were driven by different promoters, disparate cell cycle-dependent regulation of promoter strength could account for the contrasting patterns of cell cycle-correlated DHFR accumulation and tPA secretion---the Ad 2 major late promoter could be G2/M phase dominant, while the SV40 promoter would be most active in the late S-phase. The proposed cell-cycle dependence of the SV40 promoter would explain the correlation between  $q_{IFN}$  and the proportion of S-phase cells observed in this work using CHO cells expressing SV40-driven IFN- $\gamma$ .

The decline in the proportion of S-phase cells (Figures 2-4 and 2-5) preceded the fall in  $q_{IFN}$  (Figure 2-6) by 2 days. The observed differences in tPA secretion between the early and late S-phases (Kubbies and Stockinger, 1990) could account for this observed 2-day lag phase. Although the percent of S-phase cells on day 2 was significantly lower than that measured on day 0, it is possible that the cultures contained a larger fraction of late S-phase cells between days 0 and 2, than on day 0. At the same time, a higher fraction of early S-phase cells existed on day 0, as compared to the fraction of early S-phase cells between days 0 and 2. In this way, the relatively higher proportion of cells in late S-phase between days 0 and 2 of culture would give rise to a correspondingly higher  $q_{IFN}$  calculated for that period.

Analyses of erythropoietin (EPO) secreted from BHK-21 cells revealed that the product glycosylation was similar, if not better, in proliferation-controlled cells than in actively growing cells (Mueller et al., 1999). Recent studies conducted on a DHFR negative CHO host stably transfected and amplified to express recombinant human tPA

showed a gradual increase in tPA glycosylation site occupancy over the course of batch and fed-batch cultures (Andersen et al., 2000). Culture conditions that lowered the growth rate improved the degree of tPA glycosylation. Subsequent experiments consistently demonstrated a positive correlation between tPA glycosylation site occupancy and the proportion of cells in the G0/G1 phase of the cell cycle. The percentage of a fully glycosylated form of tPA gradually increased by 15-20% when the percentage of G0/G1 phase cells in the fed-batch cultures increased from roughly 60% to 75%. In this work, as the percentage of G0/G1-phase cells gradually increased from approximately 60% to over 80%, glycosylation site occupancy of secreted IFN- $\gamma$  appeared to marginally increase over the same time period (Figure 2-7(A)). While the changes recorded here are minimal, they agree favorably with the reports for EPO (Mueller et al., 1999) and tPA (Andersen et al., 2000).

The detrimental effects of ammonia accumulation and glucose starvation on glycosylation site occupancy have been documented (Borys et al., 1994; Gershman and Robbins, 1981; Turco, 1980). Glycosylation site occupancy of secreted IFN- $\gamma$  in the 5% serum batch culture would be expected to show significant decline as a result of the corresponding deterioration in the culture conditions. However, glycosylation was negligibly impacted by the adverse culture conditions (Figure 2-7(B)). As suggested by Figure 2-8, growth arrest had no negative effects on IFN- $\gamma$  site occupancy in the serum-free cultures.

Collectively, these findings suggest that the growth state of the culture may exert slight but observable influences on glycosylation site occupancy. The cellular mechanisms governing these effects remain unknown. It is foreseeable that in viably

growth-arrested cells, the competition for the glycosylation machinery should decline in parallel with the overall protein synthesis, and thereby improve the glycosylation site occupancy of recombinant proteins. Ultimately, the effect of cell culture conditions such as growth rate on site occupancy cannot be properly interpreted without measuring parameters that directly influence the glycosylation reaction, such a glycosyl donor concentration.

In summary, serum-withdrawal was effective in growth-arresting the  $\gamma$ -CHO cells, but it also lead to decreased cell viabilities and specific IFN- $\gamma$  productivities. Although some robust  $\gamma$ -CHO cells remained at the end of two weeks in serum-free conditions, these cells collectively produced much less IFN- $\gamma$  when growth-arrested. Even if subpopulations that produce relatively higher amounts of IFN- $\gamma$  exist, there are no easy means of isolating them. Hence, the  $\gamma$ -CHO cells lacked the potential to be developed into an industrially relevant cell line for G0/G1 phase protein production.

### **3. An Effective Screen for Growth-arrested Recombinant Protein Producers**

#### **3.1 ABSTRACT**

Literature results have suggested that controlled cell proliferation bioprocesses can improve product yield and quality. Anchorage-dependent CHO cells become growth-arrested upon serum deprivation, and a significant portion of these cells remain viable for extended time periods in serum-free culture. This work presents a strategy to both rapidly generate a heterogeneous population of CHO cells as well as to select for subpopulations that remain robust and continue to produce recombinant protein when growth-arrested. Stable expression of recombinant proteins in mammalian cells is tedious and time-consuming since only a small percentage of transfected cells will express sufficient quantities of protein. To overcome the limitations associated with standard transformation and selection methods, bicistronic retroviral expression technology was employed. First, bicistronic constructs encoding for both IFN- $\gamma$ , the model therapeutic protein, and GFP, the quantitative selectable marker were generated. Next, recombinant viruses obtained from transient transfection of a helper cell-line were used to infect CHO-EcoR cells, a CHO cell-line susceptible to the viruses. Cells with the bicistronic expression module stably integrated into their genome would fluoresce green and could thereby be facily isolated by FACS. The large pool of successfully infected cells was subjected to serum withdrawal. The performance of the growth-arrested cultures deteriorated steadily with time---significant declines in cell viability and GFP expression occurred. After imposing this selection pressure on the cells for 8 days, GFP-producers were isolated from surviving cells by FACS. To verify the effectiveness of this selection strategy, the selected subpopulation was expanded and exposed to a second round of

serum-deprivation. Unlike the original cell population from which they were derived, the selected subpopulation remained robust and continued to stably express both GFP and IFN- $\gamma$  throughout the extended period of serum-free culture. Within 2 weeks, cells optimized for recombinant protein production under serum-free conditions were successfully generated and isolated. The applicability of this work and hypothesis to explain the enhanced performance of the selected cells are discussed.

### **3.2 INTRODUCTION**

Controlled cell proliferation offers an attractive alternative for recombinant protein production---the uncoupling of a production process into a growth phase for rapid cell growth to a desired high cell density, followed by a proliferation-inhibited phase in which cells can devote their metabolic capabilities to heterologous protein production should increase productivity. A 10-15 fold enhancement in the production of human secreted alkaline phosphatase (SEAP) was observed in cytostatic Chinese Hamster Ovary (CHO) cells (Mazur et al., 1998). The enhanced physiological stability associated with growth-arrested cells should lead to more consistent product quality. Analyses of erythropoietin (EPO) secreted from BHK-21 cells revealed that the product glycosylation was similar, if not better, in proliferation-controlled cells than in actively growing cells (Mueller et al., 1999).

However, most industrial mammalian cell lines, such as the widely used Chinese Hamster Ovary (CHO) cell line, were chosen partly for their ability to proliferate indefinitely. Robust cell growth is critical in cloning good producers and in propagating the cells to a high cell density in the production process. It seems unlikely that

industrially relevant cells would simultaneously exhibit the two principal characteristics desired in quiescent phase protein production cell lines---the ability to maintain both high recombinant protein productivities and prolonged viabilities upon growth arrest. Growth rate and product formation appear to be positively correlated; many researchers observed increased specific protein productivity in rapidly growing cells (Cockett et al., 1990; Hayter et al., 1991; Pendse et al., 1992; Robinson and Memmert, 1991; Smiley et al., 1989), whereas only a few investigators report the opposite effect (Bebbington et al., 1992; Tonouchi et al., 1992). In addition, the continuously cycling transformed cell lines used predominantly in biopharmaceutical production are susceptible to apoptotic cell death upon growth arrest (Al-Rubeai and Singh, 1998). Hence, conditions that control cell proliferation are likely to induce apoptosis. These concerns were confirmed by the initial investigation into protein production from growth-arrested  $\gamma$ -CHO cells described in the previous chapter: although serum withdrawal was effective in growth-arresting the cells, both the number of viable cells and the specific IFN- $\gamma$  production dropped by over 50% after 2 weeks of serum withdrawal (Figures 2-3(A) and 2-6).

However, the inherent heterogeneity observed within individual cell-lines (Coppen et al, 1994; Follstad et al., 2000; Pipeleers, 1992) leads to our premise that subpopulations adapted to continue to produce exogenous proteins when growth-arrested exist within each cell population. In this work, our goal is to test this hypothesis by first isolating these subpopulations and comparing the protein production and viabilities of the isolated cells to that of the original cell population under growth-arresting conditions.

The model system chosen for this study was an anchorage-dependent CHO cell-line expressing recombinant human Interferon-gamma (IFN- $\gamma$ ), a well-characterized

therapeutic protein. Research using two anchorage-dependent CHO cell lines showed that upon serum withdrawal, most of the cells became growth-arrested in the G0/G1 phase and a significant fraction of the cells remained viable (Sanfeliu et al., 2000). This supports the premise that some members of the original CHO cell population are better adapted to survive in the absence of serum than others. For this study, serum withdrawal was chosen as a simple and efficient means to control CHO cell proliferation. First, a large pool of CHO cells containing the human IFN- $\gamma$  gene had to be created. Next, an efficient and reliable method had to be established for selecting from among these newly-generated cells, subpopulations that are better adapted for IFN- $\gamma$  production under conditions that effect growth-arrest.

The generation of stable cell lines expressing recombinant therapeutic proteins is normally a lengthy process since only a small percentage of stable clones will express sufficient quantities of product. It generally begins with cotransfection of recombinant genes with drug resistant genes, followed by selection for increasing drug resistance in transformed cells. The need to repeat this procedure for the introduction of each new gene makes this process even more tedious and time-consuming. Moreover, standard transfection methods yield low rates of stable integration of the heterologous gene into the host cell genome. The stress of serum withdrawal, compounded with low transfection efficiencies, significantly reduces the chances of isolating robust subpopulations that stably produce recombinant protein when growth-arrested.

To overcome these limitations, a bicistronic retroviral expression system was employed. Retroviral gene transfer is known for its high efficiency. Bicistronic technology permits the coordinate expression of two genes from the same mRNA. While



the first cistron of the bicistronic mRNA is translated in a classical, cap-dependent manner, the internal ribosomal entry site (IRES) permits cap-independent translation of the second cistron containing a reporter gene (Jang et al, 1988). Strong correlation in expression levels of the gene of interest upstream of the IRES, and the downstream reporter has been demonstrated (Liu et al., 2000).

A modular system consisting of (i) bicistronic retroviral gene-expression constructs, (ii) a helper cell-line used for the production of helper-free viruses, and (iii) an infectable target cell-line was employed in this work.

First, bicistronic plasmids encoding for both the secreted model therapeutic protein IFN- $\gamma$ , and the cytosolic green fluorescent protein (GFP) were generated. In the bicistronic expression construct, the human IFN- $\gamma$  gene was placed upstream of an encephalomyocarditis virus IRES, as shown by the illustration in Figure 3-1. The GFP cDNA was immediately downstream of the IRES. Both ends of the heterologous gene sequences were flanked by long terminal repeats (LTRs), which provided ends for retroviral integration as well as transcriptional signals. GFP functioned as the quantitative selection marker; GFP fluorescence in successfully infected cells facilitated their facile identification by fluorescence activated cell-sorting (FACS).

Next, the Phoenix helper cell line was transiently transfected with the bicistronic plasmids. This human embryonic kidney 293T cell-derivative can generate high titers of helper-free recombinant murine ecotropic viruses for gene delivery (Pear et al., 1993). The bicistronic retroviruses thus obtained were used to infect CHO-EcoR cells. The expression of the murine ecotropic retrovirus receptor, a basic amino acid transporter, in this a CHO-K1 cell-line derivative made it susceptible to the murine ecotropic viruses

(Baker et al., 1992). The large pool of infected cells then underwent the two-step screening process to select for subpopulations that best satisfy the prerequisites for controlled proliferation protein production.

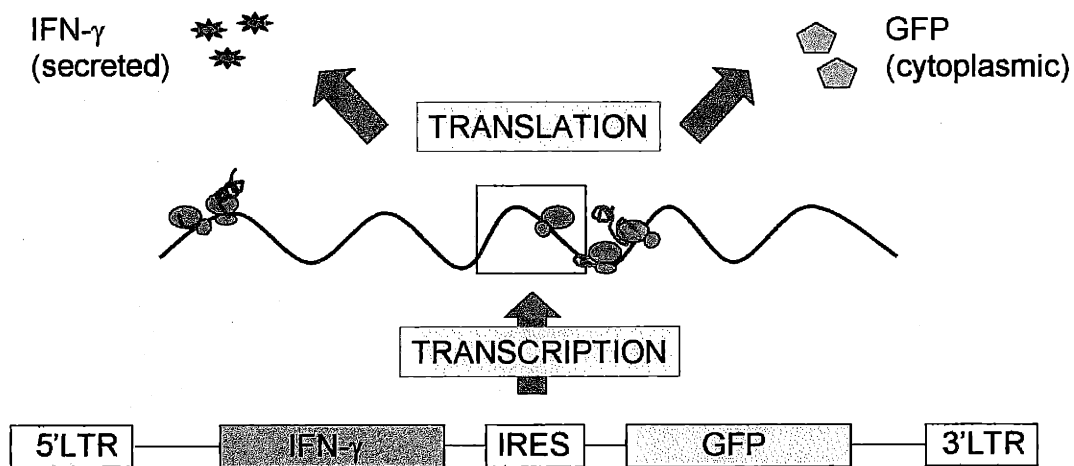


**Figure 3-1.** Cartoon illustrating the concept of bicistronic retroviral expression of both the secreted model therapeutic protein IFN- $\gamma$ , and the cytosolic green fluorescent protein (GFP). The human IFN- $\gamma$  gene was placed upstream of an encephalomyocarditis virus IRES in the bicistronic construct, while the GFP cDNA was immediately downstream of the IRES. Transcription of this retrovirus would generate a bicistronic mRNA. Subsequently, the first cistron (IFN- $\gamma$ ) would be translated in a classical, cap-dependent manner, while the presence of the internal ribosomal entry site (IRES) allowed the separate cap-independent translation of the second cistron (GFP). In this way, translation of a single bicistronic mRNA transcript could yield two different gene products.

### 3.3 MATERIALS AND METHODS

#### 3.3.1 Plasmid Constructions

DNA modifying enzymes were purchased from New England Biolabs Inc., unless otherwise stated. pMX-IRES-GFP, a generous gift from Harvey F. Lodish, Whitehead Institute of Biomedical Research, USA (Onishi *et al.*, 1996; Liu *et al.*, 2000), was digested with *EcoRI*. The resulting fragment was gel-purified and dephosphorylated with calf intestinal phosphatase in accordance to the manufacturer's recommendations.

Human IFN- $\gamma$  (gene bank accession number GI: 184638) was amplified from plasmid pHIIF-SV-GAMMA (ATCC Cat. No. 39046) using the 5' primer 5'-ATCGAATTCGCCGCCATGAAATATACAAGTTATATC-3' and the 3' primer 5'-ACTGAATTCTTACTGGGATGCTCTTCGACC-3'. These primers were chosen to introduce an *EcoRI* site at the 5'- and 3' end of the PCR product. The 5' end primer also contained a Kozak consensus sequence upstream of the AUG codon for more efficient translation (5'-GCCGCC-3'). The PCR product was digested with *EcoRI* and cloned into the *EcoRI* site in the pMX-IRES-GFP retroviral vector to make pMX-IFN- $\gamma$ -IRES-GFP (Figure 3-2). Ligation was verified by *EcoRI* digestion and the nucleotide sequence confirmed by di-deoxy sequencing.

#### 3.3.2 Cell Lines and Culture

CHO-*EcoRI* cells were kindly provided by H. Lodish, R. Lawrence and M. Krieger (M.I.T., USA). This line of CHO-K1 cells stably expressed the murine ecotropic retrovirus receptor (Baker *et al.*, 1992) and could be infected with high efficiency by murine ecotropic retroviruses. Cells were grown in T-flasks at 37°C/5-10%CO<sub>2</sub>/95%Rh

in Iscove's Modified Delbecco's Medium supplied with 10% FBS and 1% Penicillin-Streptomycin (PS), unless otherwise stated. Cells were transferred and media changed at 2-3 days interval using 0.1% trypsin in PBS.

HEK-293 (Phoenix-Ecotropic packaging cells, a gift from Garry P. Nolan, Stanford University, USA) were cultured at 37°C/5-10%CO<sub>2</sub>/95%Rh in Dulbecco's Modified Eagle Medium (DMEM/F-12) with 10% FBS and 1% Penicillin-Streptomycin (PS), unless otherwise stated. Cells were transferred and the medium was changed at 3-4 day intervals using 0.1% Trypsin in PBS. All materials for cell culture were purchased from Life Technologies Inc.

### **3.3.3 Retrovirus Production**

Murine ecotropic retroviruses were produced by modifying the protocol obtained from the webpage of the Nolan laboratory at Stanford University in California, USA ([http://www.stanford.edu/group/nolan/phx\\_helper\\_dep.html](http://www.stanford.edu/group/nolan/phx_helper_dep.html)). In six-well plates,  $6 \times 10^5$  HEK-293 cells were seeded in 2 ml of growth medium per well. After 24 hours of incubation, the spent medium was removed, the cells were washed with PBS and 1 ml of fresh serum-free growth medium was added to each well. Cells were transfected with 2 µg DNA that had been mixed with 6 µl FuGENE™6 (Roche Molecular Biochemicals) according to the manufacturer's protocol. After 5 hours of incubation, 1 ml DMEM/20%FBS/1%PS was added to the transfected cells. Twenty-four hours post-transfection, the spent medium was replaced with 1 ml fresh growth medium and the cells were transferred to 32°C/5-10%CO<sub>2</sub>/95%Rh. Forty-eight hours after transfection, the virus containing growth media was removed and stored in sterile tubes on ice while cells

were analysed by FACS. If more than 10% of the cells expressed GFP, the growth medium was centrifuged at  $200 \times g$  for 10 minutes, and the virus containing supernatant was transferred to a sterile tube, ready for infection.

### **3.3.4 Infection**

Twenty-four hours before infection, CHO-EcoRI cells were seeded in six well plates at  $1.5 \times 10^5$  cells/3 ml growth medium/well and incubated overnight. On the day of infection, 2 ml media was removed from each well and replaced by 1 ml of the virus-containing supernatant mixed with 2  $\mu$ l of 5 mg/ml polybrene. Cells were then moved to 32°C/5-10%CO<sub>2</sub>/95%Rh. Twenty-four hours after infection, the spent medium was replaced with fresh growth medium, and incubation was continued at 32°C/5-10%CO<sub>2</sub>/95%Rh. Seventy-two hours post-infection, the cells were suspended in DMEM/10%FBS/1%PS for FACS analysis.

### **3.3.5 GFP Fluorescence Measurements**

Cells were trypsinized and resuspended in growth media prior to analysis by Fluorescence Activated Cell Sorting (FACS) on a Becton Dickinson FACScan flow cytometer. Typically, 20,000 events per sample were measured. The data were processed using CELLQuest software. Calibrated FACS was accomplished using laminar flow fluorescent beads (Molecular Probes).

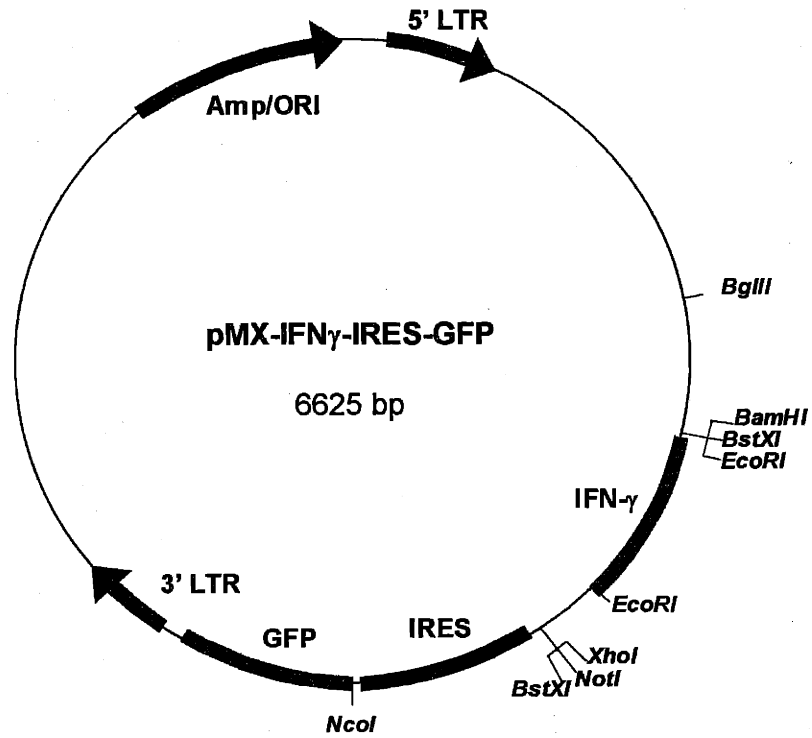


**Figure 3-2.** Schematic diagram of the pMX-IFN $\gamma$ -IRES-GFP retroviral expression vector. The solid arrows represent the viral LTR sequences, and indicate the direction of translation. The IRES sequence was placed between the model product IFN- $\gamma$  gene and the reporter GFP gene. Solid boxes represent the sequences encoding the heterologous proteins.

### **3.3.6 IFN- $\gamma$ Concentration Determination**

IFN- $\gamma$  concentrations were measured using a commercially available enzyme-linked immunosorbent assay (ELISA) kit (Biosource International Inc.).

### **3.3.7 Cell Density and Viability Measurements**

Attached cells were collected in suspension by trypsinization and subsequent addition of serum-containing growth medium. After staining the samples with trypan blue, cells were counted using hemacytometer. Since viable cells exclude the dye, while non-viable cells were stained blue due to their lack of membrane integrity, cell viability could be determined at the same time. At least 500 cells were counted for each measurement.

## **3.4 RESULTS**

### **3.4.1 Generation of Bicistronic Ecotropic Retroviruses**

The vector pMX-IFN- $\gamma$ -IRES-GFP was constructed to contain the Murine Moloney virus (MMV) long terminal repeats (LTRs) and a packaging signal; the encephalomyocarditis virus (EMCV) internal ribosomal entry site (IRES) was placed between the human IFN- $\gamma$  gene and the GFP cDNA (Figure 3-2). An RNA transcript containing an IRES is bicistronic---the EMCV IRES permits initiation of mRNA translation at an internal AUG sequence (Jang et al., 1988)---such that a single mRNA can yield two gene products.

Upon transfection of this plasmid into the ecotropic retroviral packaging cell line HEK-293, high titers of helper-free recombinant retroviruses that encode for both the secreted FN- $\gamma$  model protein and the cytosolic GFP were produced. These viruses can

stably infect murine cell lines as well as non-murine cells that express the recombinant ecotropic receptor, such as CHO-EcoRI cells.

### **3.4.2 Selection Strategy**

Two days after infecting anchorage-dependent CHO-EcoRI cells with the retroviruses, the 10% serum medium was replaced by serum-free medium. Subsequently, the old serum-free medium was replaced with fresh-serum free medium every 48 hours. By subjecting the cells to serum withdrawal, only cells strong enough to handle this imposed stress will survive. To assess the impact of serum starvation on these cells, culture parameters---cell density, culture viability and GFP fluorescence intensity---were measured every 48 hours throughout the course of serum-free culture.

After eight days of serum deprivation, the survivors of this initial screening step were analyzed by FACS. Since the model therapeutic protein IFN- $\gamma$  would be coordinately expressed from the same bicistronic unit as GFP, cells that produce IFN- $\gamma$  should also show intrinsic GFP fluorescence. Hence, GFP-producers were isolated from the non-fluorescent cells by FACS. The cells that satisfied this second screening criteria were considered to have met the requirements for a controlled proliferation protein production cell-line---the ability to survive serum-withdrawal and produce heterologous proteins upon growth arrest.

These selected cells were first expanded in 10% serum and then cultured for 2 weeks in the absence of serum. Every other day, the old serum-free medium was replaced with fresh serum-free medium. At the same time, cells from duplicate flasks were used to measure cell density and viability, and GFP expression levels. Culture supernatant from



identical flasks were retained to determine IFN- $\gamma$  levels by ELISA. The two-step selection process is illustrated in Figure 3-3.

### **3.4.3 Comparison of Serum-Free Culture Characteristics**

The serum-free culture performance of the selected subpopulation of cells with respect to viability, cell-density and heterologous protein production was compared with that of the original cell population. This served to test our hypothesis that the original cell population contained sufficient inherent diversity to permit the isolation of subpopulations endowed with the traits desired for protein production when growth-arrested. By highlighting differences between the cell populations, these comparisons also demonstrated the effectiveness of our selection process.

#### ***3.4.3.1 Cell Viabilities***

At the beginning of serum deprivation, over 95% of the original cell population was viable, as determined by Trypan blue assays (Figure 3-4). However, the culture viability steadily declined over time: at the end of 8 days in serum-free culture, approximately 60% of the attached cells were still viable. By contrast, viability of the selected subpopulation remained consistently over 90% throughout the 14 days of serum-free culture.

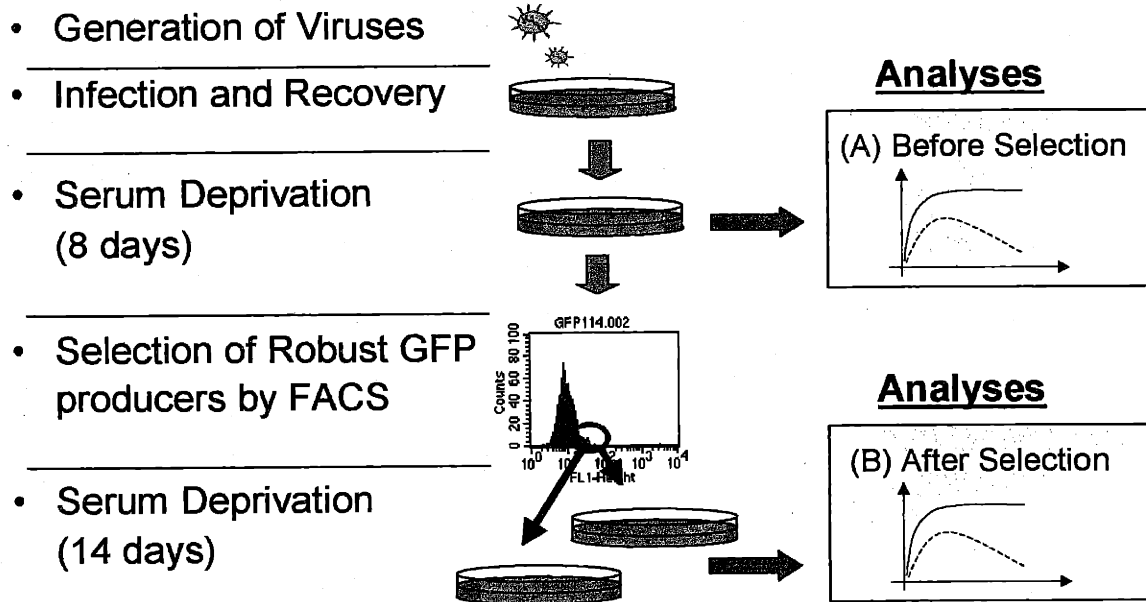


**Figure 3-3.** Flowchart of the experimental procedure. Helper cell-lines were transfected with plasmid pMX-IFN $\gamma$ -IRES-GFP (Figure 3-2). The target cell-line CHOecoR was infected with the recombinant virus. Cells were allowed to recover for 2 days before serum was removed. Subsequently, every other day, the spent medium was replaced by fresh serum-free medium, and the culture viability, cell density and GFP production were measured. After 8 days of serum deprivation, the surviving cells were sorted by FACS. GFP producers were selected and expanded. This subpopulation of cells was subjected to a second round of serum deprivation, lasting 14 days. The cells were treated and analyzed in the same manner as during the first round of serum deprivation.

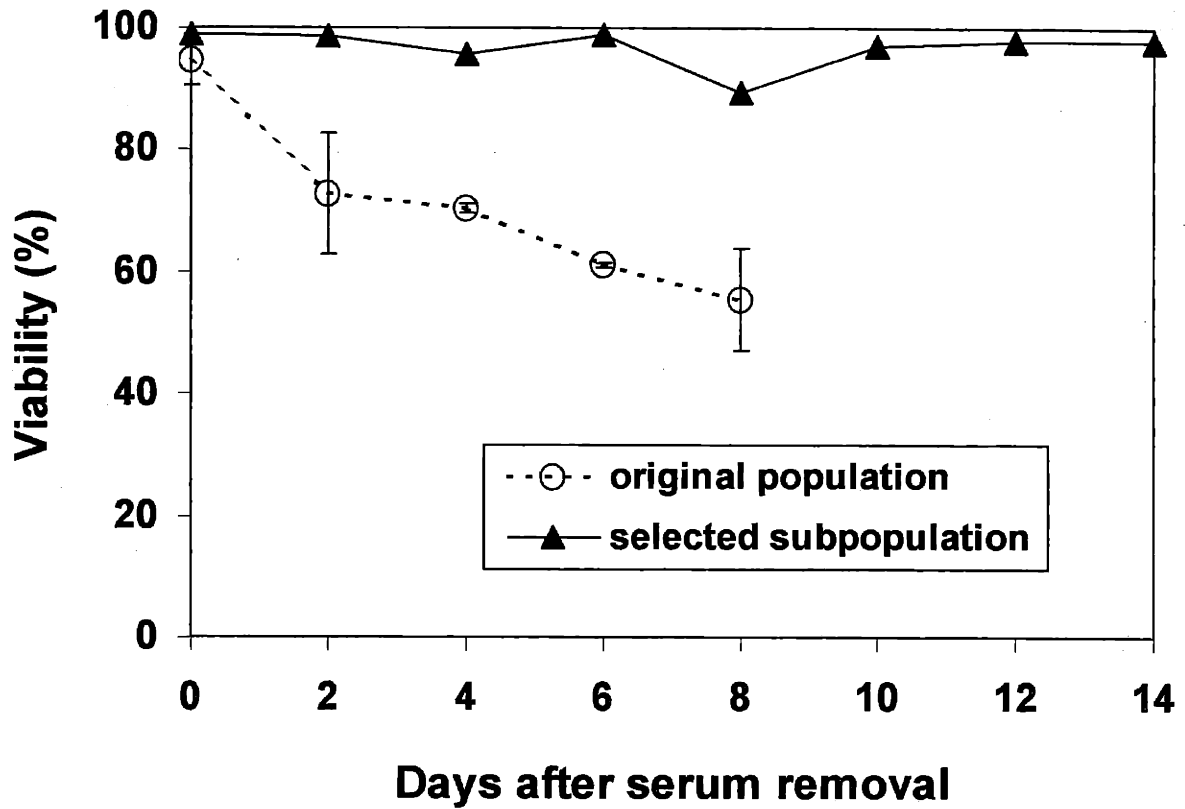


**Figure 3-4.** Cell viabilities over the course of serum-free culture were compared between the original population (O), and the selected subpopulation (▲) of cells. The selected subpopulation of cells was isolated from the original cell population after a two-step screening process. Error bars represent the range of measurements taken from duplicate cultures.

### ***3.4.3.2 Cell Densities***

The original cell population showed an initial increase in cell density immediately after serum removal (Figure 3-5). This was expected since residual growth factors had to be depleted and cells that had passed the restriction point at the time of serum removal would complete the cell cycle and thus divide before being growth-arrested in G0 phase. Thereafter, the cell density declined rapidly. At the end of 8 days of serum starvation, the cell density was only a quarter of the peak value.

In the selected subpopulation, cell density increased initially after serum removal, as expected, and subsequently remained fairly constant throughout the remaining culture time. The slight decline in cell density measured during the last few days of culture is attributed to the increasingly adherent behavior exhibited by the cells with time. On the eighth day after serum removal, in the effort to detach all the cells from the T-flasks for accurate cell counting, the trypsin treatment time was extended. Although this successfully suspended all the cells, the prolonged exposure to trypsin had a slight but noticeable adverse impact on cell viability: only 90% of the counted cells were viable on day eight, whereas on all other days, cell viability measurements consistently exceeded 95% (Figure 3-4). In view of this, the trypsin treatment time was not extended for subsequent cell counts. Consequently, towards the end of the culture, the cells became so strongly attached to the culture flasks that an estimated 10-20% of the cells remained adherent after the standard trypsinization process. Hence, the number of cells counted was less than the actual number of cells present in the flask.

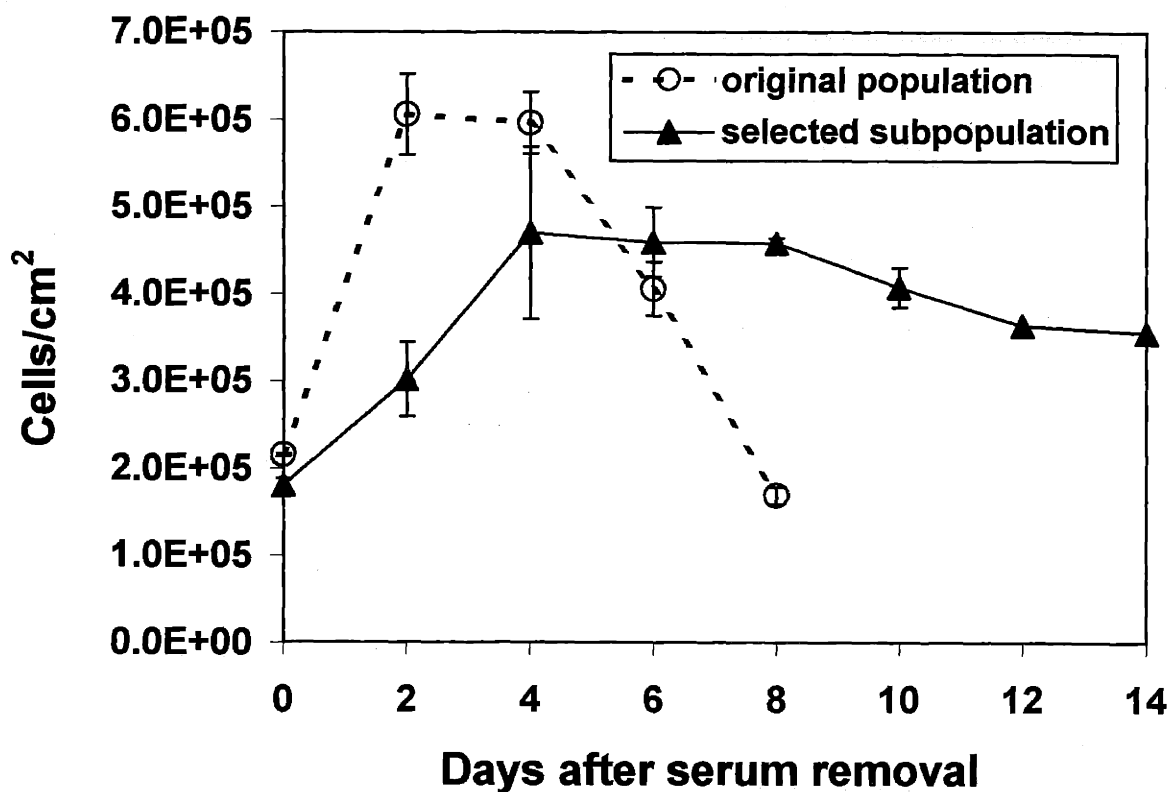


**Figure 3-5.** Cell densities over the course of serum-free culture were compared between the original population (O), and the selected subpopulation ( $\blacktriangle$ ) of cells. The selected subpopulation of cells was isolated from the original cell population after a two-step screening process. Error bars show the range of measurements obtained from identical parallel cultures.

#### ***3.4.3.3 Percent of Cells Producing GFP***

Of the original cell population that had been infected with the pMX-IFN $\gamma$ -IRES-GFP retrovirus, about 12 percent showed GFP fluorescence at the start of serum starvation (Figure 3-6). After 8 days under serum-free conditions, less than 2% of the attached cells produced GFP. A similar trend was concurrently observed in the viability of these cells (Figure 3-4). Intrinsic fluorescence should depend upon cell viability; only viable cells could continue to synthesize GFP and possessed the intact cell membranes needed to retain the cytosolic GFP. As cells entered the apoptotic cell death program, they lost their ability to produce and retain GFP. Since only viable cells could fluoresce, the steady decline in the percent of GFP producers in the original cell population was partly attributed to the corresponding drop in cell viability.

DNA methylation is known to silence the expression of retrovirally introduced genes (Cherry et al., 2000; Zentilin et al., 2000; Gram et al., 1998). It is possible that part of the decline in GFP expression in the original cell population arose from an increase in host cell silencing of the GFP genes through DNA methylation.

Throughout the 14 days of serum-free culture, approximately 80% of the selected subpopulation fluoresced. This finding is consistent with the corresponding high and stable culture viability (Figure 3-4), and it supports the proposed correlation between cell viability and GFP expression. Since the majority of the cells continued to express GFP, this observation also suggests that methylation of GFP genes was not spreading in these selected cells.

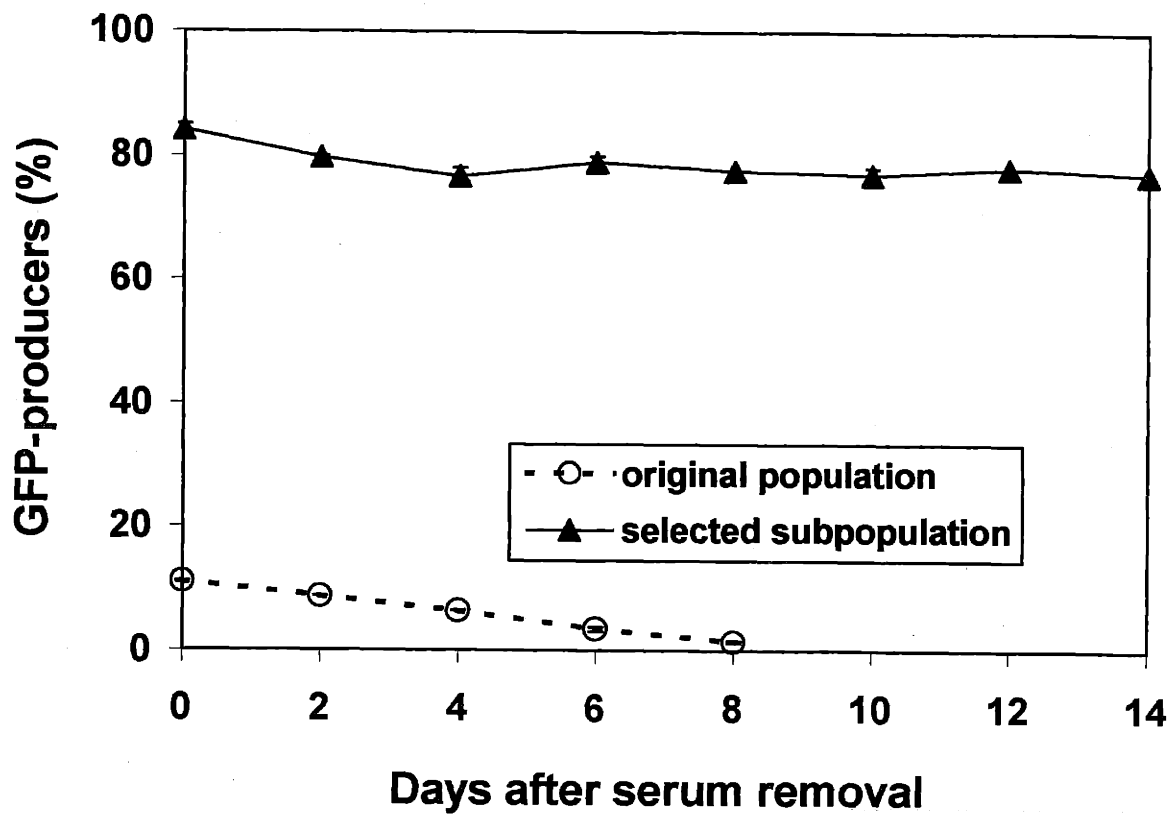


**Figure 3-6.** Percent of GFP-producing cells within the original population (O), and the selected subpopulation (▲) are compared over the course of serum-free culture. The selected subpopulation of cells was isolated from the original cell population after a two-step screening process.

#### ***3.4.3.4 Mean GFP Fluorescence Intensity***

The mean GFP fluorescent intensity among the GFP producers in the original cell population initially increased, but quickly declined steadily over time (Figure 3-7). This pattern mirrored the density time-profile of these unselected cells: the mean GFP fluorescence intensity increased with cell density. When cell growth stopped and cell death set in after the second day in serum-free culture, both the cell density and mean GFP fluorescence intensity declined. These observations support a positive correlation between GFP expression and cell viability. They also suggest a positive association between cell growth and the activity of the LTR promoter controlling expression.

The mean fluorescence intensity measured among GFP-producers in the selected subpopulation of cells increased with time. To account for this observed increase in GFP accumulated in the average GFP-producing cell over time, either the rate of GFP production increased, or the rate of GFP degradation decreased as the cells became progressively growth-arrested.



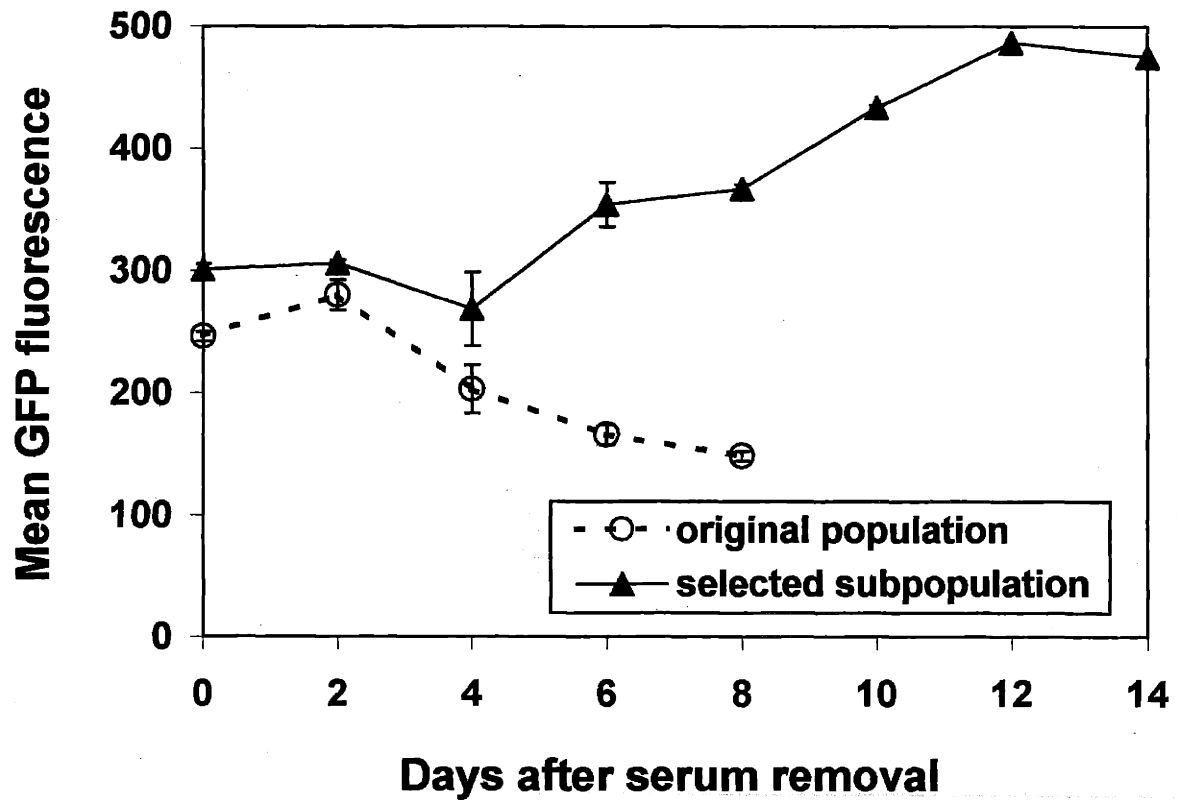


**Figure 3-7.** Mean GFP fluorescence intensities measured by FACS of the original population (O), and the selected subpopulation (▲) are compared over the course of serum-free culture. The selected subpopulation of cells was isolated from the original cell population after a two-step screening process. Error bars show the differences in data generated from identical parallel cultures.

#### ***3.4.3.5 Overlay of calibrated FACS data***

Calibrated FACS data of the selected subpopulation of cells taken at 0, 6 and 12 days after serum removal were overlaid onto a single plot (Figure 3-8). Using FACS analysis of non-infected CHO-EcoRI cells to determine the fluorescence range of non-GFP producing cells, the selected subpopulation of cells were sorted according to their fluorescence intensities into non-fluorescent cells (“negative cells”) and fluorescent cells (GFP-producers). Since an equal number of cells were used to generate each plot, we can conclude that the proportion of negative cells remained fairly small and constant, while the majority of the selected cells stably expressed GFP over the course of serum-free culture.

The peak GFP fluorescence shifted slightly to the right with time. This progressive increase in the GFP fluorescence mode with time in the selected cells is consistent with the rise in mean GFP fluorescence intensity observed in Figure 3-7. These results imply that the intrinsic GFP fluorescence measured in the average GFP-producing cell from the selected subpopulation increased with time in serum-free culture.

#### ***3.4.3.6 Coexpression of IFN- $\gamma$ and GFP***

Both IFN- $\gamma$  and GFP continued to be stably expressed over the extended period of serum-free culture (Figure 3-9). The expression levels of both proteins appeared to increase slightly with time under serum-free conditions. Coexpression of secreted IFN- $\gamma$  and cytosolic GFP was expected since the reading frames for both genes were located within the same bicistronic expression unit. Researchers have recently demonstrated a high correlation in the expression of genes in a similar bicistronic constructs (Liu et al., 2000).

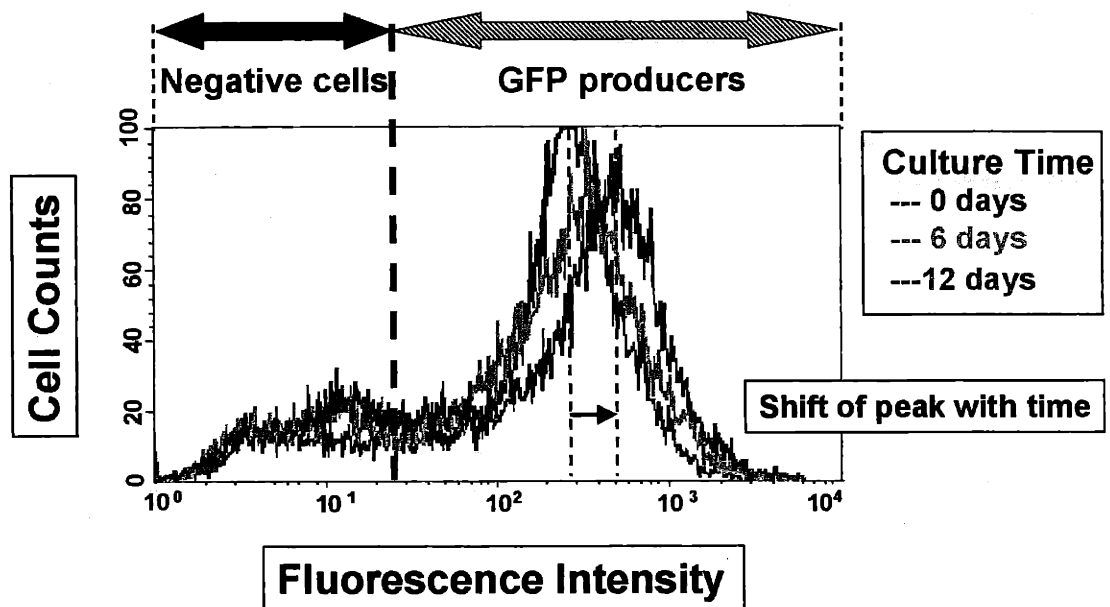


**Figure 3-8.** Calibrated FACS data of the selected subpopulation of cells taken at 0, 6 and 12 days after serum removal were overlaid onto a single plot. Equal numbers of cells were analyzed by FACS for each time point measurement. The vertical dotted line separated the non-fluorescent cells (negative cells) from the fluorescent cells (GFP-producers).

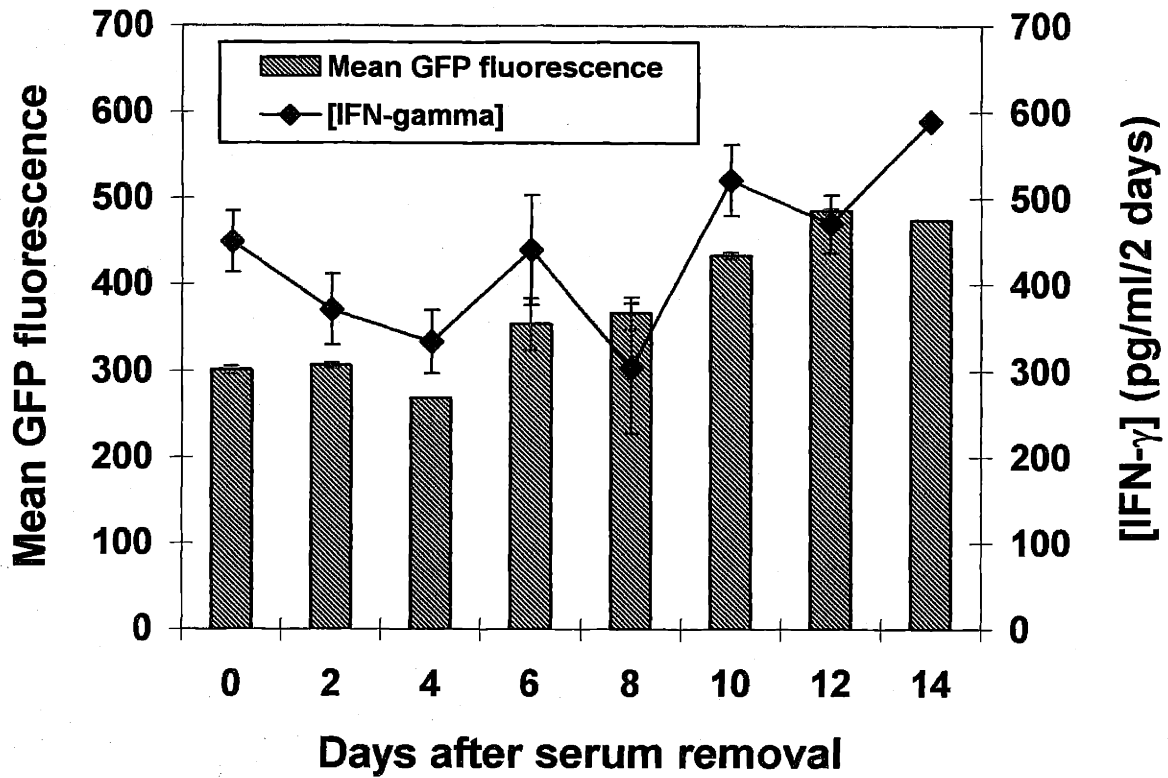


**Figure 3-9.** Coexpression of cytosolic reporter GFP (▨) and secreted model therapeutic protein IFN- $\gamma$  (◆) by the selected subpopulation of cells over the course of serum-free culture. Expression of cytosolic reporter GFP (▨) was shown as a function of the mean fluorescence intensity measured in the selected subpopulation. IFN- $\gamma$  (◆) production was calculated based on its accumulation in the medium. Error bars show the range in measurements obtained from identical parallel cultures.

### 3.5 DISCUSSION

Controlled cell proliferation technology offers an attractive means to improve recombinant protein production in mammalian cells. Actively proliferating cells are encumbered by demands for simultaneous production of cellular proteins and other cellular components. By contrast, growth-arrested cells can devote their protein synthesis and metabolic activities to the production of heterologous proteins. Despite extensive investigations into controlled proliferation bioprocesses, most growth regulation strategies suffer from various drawbacks.

Cell growth *in vitro* is dependent upon the presence of growth factors and cytokines, normally supplied in serum. Mitogens in serum activate cell proliferation in cultured cells. In the presence of these extracellular signals, cells in the G1 phase proceed in the cell cycle (Assoian, 1997). When mitogens are absent, cells withdraw from the cell cycle and enter the G0 quiescent phase. Although serum withdrawal is an effective means of achieving growth-arrest, it is implicated in inducing apoptosis. The anti-apoptotic activity found in serum is well-documented, but the specific mechanisms involved remain unclear. In the absence of serum, many cell lines, including those of industrial importance, will undergo apoptosis (Al-Rubeai and Singh, 1998). In particular, CHO cells grow well in virtually any serum-supplemented medium, but are susceptible to apoptosis in serum-free medium (Zanghi et al., 1999).

Sensitivity to apoptosis is therefore a key criterion in selecting an appropriate host cell line for biopharmaceutical production. Cellular robustness can be enhanced by transfecting cells with anti-apoptosis genes, such as Bcl-2 (Tey et al., 2000). Metabolic engineering approaches have been developed which address the need to simultaneously

suppress both growth and apoptosis. Fussenegger and coworkers (1998) demonstrated the use of multi-cistronic expression systems for the simultaneous expression of product (secreted alkaline phosphatase), growth-modifying gene (p27) and anti-apoptosis gene (Bcl-xl), resulting in cell cycle arrest and a multiple-fold improvement in protein productivity. However, it is time-consuming to establish such stable cell lines since only a small percentage of stable clones will express sufficient quantities of the heterologous proteins. Furthermore, tight regulation of this inducible system though necessary, can be difficult to achieve: growth arrest exerts an enormous selection pressure for cells that have evaded proliferation control through (i) mutation or loss of multi-cistronic units, (ii) mutation or loss of transcriptional activator, (iii) increased degradation of p27, (iv) activation of silent and redundant p27-insensitive cell-cycle control units, or (v) silencing of the multi-cistronic unit by methylation. The subpopulation of mutants that escape growth suppression can eventually overgrow the growth-arrested cells (Mazur et al., 1999).

Low cultivation temperatures can effect growth-arrest and prolong survival of mammalian cells, but the associated temperature shifts have varying effects on heterologous protein production, cell metabolism and post-translational protein modifications (Weidemann et al., 1994; Kaufmann et a., 1999). Detailed knowledge of the molecular mechanisms underlying the multiple effects of low temperature on mammalian cells remains lacking.

As opposed to the various tactics described above, the strategy employed here---to generate and isolate cells that exhibit potential for protein production under growth-arresting conditions---is simple and efficient. This bicistronic retroviral expression

system has many advantages. First, the generation of the “parental” cell lines is a one-time effort. Once the CHO-EcoR and Phoenix cells have been created, they can be used to generate stable recombinant CHO cells overexpressing any gene of interest in 4 days. Second, the high gene transfer efficiencies associated with retroviral infection permits the rapid generation of a large pool of recombinant cells. The use of different sites in the host genome for provirus integration guarantees considerable variability in the exogenous protein productivity among individual cells within an infected population. Additional cell-to-cell variability in heterologous protein expression can arise from multiple insertions of the provirus into the host genome. The large and varied pool of candidates significantly increases the probability of isolating cells with desired traits. Third, the coordinate expression of the GFP reporter gene and the model therapeutic gene in a single bicistronic expression vector allows the facile isolation of stably infected cells at predetermined GFP fluorescence levels by FACS. Fourth, the correlation in expression levels of both gene products facilitates the monitoring of gene-expression levels throughout the selection and subsequent production process.

This work established a straightforward and effective two-step process to isolate recombinant cells with enhanced potential for heterologous protein production when growth-arrested. In the first step, the original cell population was growth-arrested by serum withdrawal. The enormous selection pressure imposed by serum starvation ensured that only cells adapted to handle the stress survived. By eliminating the less robust cells, the likelihood of encountering viability problems in future controlled cell proliferation bioprocesses was reduced. The survivors of this first step were then subjected to FACS analyses. In this second step, GFP-producing cells were isolated, thereby enriching the

population with cells that actively synthesize heterologous proteins even when growth-arrested. Cells that satisfied both screening criteria were expanded. Subsequent comparison of the serum-free culture performance of the selected subpopulation with that of the original cell population demonstrated the success of the two-step screening process: the selected subpopulation displayed cellular robustness and stable heterologous protein production under conditions of growth-arrest effected by serum withdrawal.

As long as serum starvation prevailed, no escape from growth-arrest was detected in the selected subpopulation. However, when the cells were taken from day 14 of serum-free culture and cultured in serum-containing media, they immediately proliferated (data not shown). This demonstrates that the cells retained their clonogenic potential.

The concept that not all cells in a given culture are identical is supported by our results here and literature reports. NIH 3T3 cells showed a heterogeneous, adaptive response of competent cells to moderate constraints on cell growth, such as low serum concentration (Yao et al., 1990; Chow et al., 1994) and high cell densities (Yao and Rubin, 1993; Yao and Rubin, 1994). These authors espoused an epigenetic basis for the cellular transformation---their concept of "progressive state selection" assumed the existence of numerous metastable states within a cell population; unfavorable environments facilitated the selection of cells within a heterogeneous population that are in states better suited to handle the pressure. Studies on a cloned CHO cell line expressing IFN- $\gamma$  revealed heterogeneity in IFN- $\gamma$  production, number of mitotic spindles in dividing cells, and cellular environment (Coppen et al., 1995). Recent results from our laboratories demonstrated the existence of heterogeneity within mammalian cell populations with respect to mitochondrial physiology (Follstad et al., 2000). A hybridoma



cell population was separated into subpopulations of varying mitochondrial membrane potential (MMP). Cells with higher MMP exhibited dramatically higher resistance to apoptosis. The separate subpopulations continued to maintain their mean MMP difference after 20 generations, suggesting that the endogenous heterogeneity within the original cell population may be long-lived.

This work demonstrated that the intrinsic heterogeneity within a cell population can lead to enhancement of different phenotypes under different environmental conditions. However, the specific cellular pathways that were up-regulated or down-regulated to enhance survival in the selected subpopulation was not investigated. Although the adaptive changes that occurred in the metabolic machinery to facilitate survival upon serum-withdrawal are unknown, they are likely to be highly complex. In addition, the possibility that the robustness of the selected subpopulation resulted from disruption of a gene upon retroviral integration cannot be ruled out.

Literature results suggest that the variation in robustness observed within the original CHO cell population upon serum withdrawal may reflect differences in the expression profile of endogenous anti- and pro-apoptotic genes. Subpopulations of CHO 22H11 cells were found to express enhanced levels of endogenous Bcl-2 (Tey et al., 2000). In an NSO cell line, high-level expression of endogenous anti-apoptosis genes were observed (Murray et al., 1996). Research in an IL-3-dependent cell-line showed that the overexpression of endogenous pro-apoptotic proteins such as Bax resulted in increased susceptibility to apoptosis (Oltvai et al., 1993).

Interactions between cells and the extracellular matrix (ECM) are predominantly regulated by the integrins, a family of cell surface receptors composed of  $\alpha$  and  $\beta$

subunits. In addition to their role in mediating cell adhesion, these transmembrane proteins also regulate cellular functions such as cell growth and survival by eliciting intracellular signals upon adhesion. Many integrin signals converge on cell cycle regulation, directing cells to live or die, to proliferate, or to exit the cell cycle and differentiate. (Giancotti and Ruoslahti, 1999). Available models of anchorage-dependent cell growth imply that integrins and growth factors cooperate to activate the MAP kinase ERK, and thereby regulate progression through the G1 phase of the cell cycle (Assoian, 1997; Schwartz, 1997). The expression of the integrin  $\beta_{1C}$ , an alternatively spliced variant of the  $\beta_1$  subunit, inhibited cell proliferation in CHO cells (Fornaro et al., 1995).

Studies on the  $\alpha_5\beta_1$  integrin expressed in anchorage-dependent CHO cells provide a coherent and compelling explanation for the superior robustness demonstrated by subpopulations of CHO cells upon serum removal. The  $\alpha_5\beta_1$  integrin has also been identified as a suppressor of cell growth (Varner et al., 1995). Cell attachment mediated by the  $\alpha_5\beta_1$  integrin prevented cell death upon serum withdrawal (Zhang et al., 1995). Endogenous Bcl-2 was elevated in these CHO cells, suggesting that the  $\alpha_5\beta_1$  integrin suppressed apoptosis through the Bcl-2 pathway. In another study using anchorage-dependent CHO cells, increased  $\alpha_5\beta_1$  integrin-dependent cell-ECM adhesion and enhanced endogenous Bcl-2 expression were implicated in the prevention of high cell-density-dependent apoptosis in the presence of dimethyl sulfoxide (Fiore and Degraffi, 1999).

Anti-apoptotic phenomenon associated with integrin expression involves intracellular signaling pathways. Focal adhesion assembly and focal adhesion kinase (FAK), a kinase that regulates several intracellular processes such as tyrosine

phosphorylation, intracellular pH, and calcium levels, have been implicated in integrin-dependent cell survival (Frisch et al., 1996; Meredith et al., 1993). Other investigations identified a novel pathway linking integrin-mediated cell survival to activation of MAP kinase through integrin association to the adaptor protein Shc and activation of the Ras/Raf pathway (Wary et al., 1996; Price, 1997). The seemingly disconnected observation in this work---the selected subpopulation demonstrated increasing adherence to the T-flasks over time---corroborates the substantial body of evidence that links cellular robustness to integrin expression.

After the initial infection, the majority of cells in the original population rapidly lost their GFP expression. After 8 days in serum-free conditions, only 2% of the population still produced GFP (Figure 3-6). Loss of gene expression is a commonly observed problem with retroviral vectors (Gram et al., 1998; McInerney et al., 2000). Genes delivered by retroviruses can be transcriptionally silenced by chromatin modifications such as CpG methylation, histone deacetylation and H1 histone-mediated chromatin compaction (Tyler and Kadonaga, 1999). The degree of gene silencing can vary, depending on factors such as the site of chromosomal integration, as well as the presence of cis-acting elements that oppose the forces of silencing, such as enhancers, locus control regions, matrix attachment sites, and insulators (Bird and Wolffe, 1999). As a result of nearly random integration of the virus into host genome (Shih et al., 1988), some retroviruses may have integrated into loci that remained transcriptionally active over long time periods. By escaping down-regulation by DNA methylation or other chromatin modifications, these transgenes can maintain stable expression. In accordance with this proposition, gene silencing and age-dependent extinction of expression were

avoided by engrafting mice with ex vivo preselected stem cells infected with a retrovirus containing the human  $\beta$ -globulin and GFP genes, (Kalberer et al, 2000).

In the original pre-selection cell-line, the mean GFP fluorescence intensities (Figure 3-7) and cell densities (Figure 3-5) declined in unison upon serum withdrawal, suggesting a correlation between GFP production and growth rate. By contrast, serum withdrawal did not trigger a decrease in the level of GFP expression in the selected cells. To account for these differences, the screening criteria might have favored cells in which retroviral integration had occurred at loci that remained transcriptionally active in the absence of cell proliferation and/or serum. It is possible that the LTR in these selected cells had mutated and plasmid expression became driven by an endogenous promoter active in the absence of growth and/or growth factors instead of the retroviral LTR. This scenario bears a resemblance to the technique commonly applied in the detection of promoters/enhancers. Referred to as promoter/enhancer trapping, this approach uses reporter genes that have been engineered---these genes can only be expressed when they lie close to or within another gene after insertion into a genome (von Melchner et al., 1990; Bellen, 1999).

By modifying the screen developed in this work, different retroviral plasmid designs and gene amplification strategies can be conveniently evaluated. For instance, retroviral vectors containing the amplifiable selectable marker dihydrofolate reductase (DHFR) have been developed (Allay et al., 1998). The screen could be used to gauge the effectiveness of these vectors in increasing protein expression. In addition, this screen can be used to identify specific promoters and internal ribosomal entry sites that optimize protein expression in growth-arrested cells.

The model therapeutic protein IFN- $\gamma$  is associated with many properties (Farrar and Schreiber, 1993); it may even confer robustness to cells under serum withdrawal conditions. To address this possibility, the experiment was repeated with a simple modification---a retroviral vector pMX-IRES-GFP lacking the IFN- $\gamma$  insert was used in place of the bicistronic vector. The results obtained were consistent (data not shown): the selection process was successful in isolating subpopulations of recombinant CHO cells that remained robust and continued to fluoresce stably over an extended period in serum-free culture.



#### **4. Relative LLO and Glycosylation Levels in CHO cells over the Course of Batch Culture**

##### **4.1 ABSTRACT**

N-linked glycosylation is a key determinant in favoring the expression of recombinant protein therapeutics in mammalian cells. Although it imparts important features to proteins, N-linked glycosylation also introduces heterogeneity into the product: otherwise identical protein molecules that differ only in their N-linked glycosylation patterns can exhibit significantly different pharmacokinetic properties. For this reason, approval of drugs often requires therapeutic glycoproteins to demonstrate consistent glycosylation. An essential step in N-linked glycosylation is the *en bloc* transfer of an oligosaccharide species from the membrane lipid dolichol phosphate (Dol-P) to a potential glycosylation site. Variability in the success of this transfer step in the dolichol pathway results in glycosylation site occupancy heterogeneity. Glycosylation of recombinant proteins is not always constant during the culture of animal cells. Various researchers observed a decline in IFN- $\gamma$  glycosylation site occupancy over the course of batch and fed-batch cultures of recombinant CHO cells, but their investigations have so far failed to elucidate the reasons for this decline. Since lipid-linked oligosaccharides (LLOs) serve as donors in N-linked glycosylation, their availability is postulated to influence the extent of glycosylation site occupancy; a decreasing intracellular supply of LLOs should lower the extent of protein glycosylation. To test this hypothesis, LLO and glycosylation levels in CHO cells were monitored over time to determine if they exhibit corresponding changes. Despite significant changes in medium concentrations of glucose and lactate concentrations over the course of batch culture, radiolabeling studies showed that intracellular LLO levels

remained within a two-fold range. By contrast to the site occupancy trends observed for IFN- $\gamma$ , the overall protein glycosylation by the CHO cells improved slightly over time, prior to the onset of massive cell death. This 15-25% improvement in overall protein glycosylation is in agreement with that recently reported for recombinant tissue plasminogen activator (tPA) produced in fed-batch cultures of CHO cells; the pattern and extent of the tPA site occupancy increase were similar to the overall glycosylation enhancement in total CHO cell proteins observed in this work. The implications of these results, and various hypotheses to explain the findings are discussed.

## 4.2 INTRODUCTION

As record numbers of recombinant protein therapeutics enter clinical trials, it is evident that biopharmaceutical manufacturers are increasingly aware that considerations of product quality and consistency are of comparable significance to product yield. These criteria become more important as mammalian cell culture-derived recombinant products progressively dominate the therapeutic protein market. Despite the perceived economic advantages of using faster-growing, more productive and easier-to-manipulate organisms such as bacteria and yeast for recombinant protein production, mammalian cells are often chosen as the expression system on account of their ability to affect human-like post-translational modifications (Datar et al., 1993).

Glycosylation is often a desired feature in a recombinant protein; it can mediate the efficacy of a human therapeutic glycoprotein to a significant extent (reviewed by Goochee et al., 1991). The precise role of the sugar chains varies in each glycoprotein; however, their influences on antigenicity, *in vivo* half-life, and secretion rate are well-



documented in several proteins (reviewed by Cumming, 1991). The presence of oligosaccharides on proteins is often known to enhance solubility, promote resistance to protease attack, and protect against irreversible thermal inactivation. Partial or complete removal of oligosaccharides can affect the specific activity of a protein.

Non-human glycosylation patterns are potentially immunoreactive (reviewed in Goochee et al., 1991). Among established mammalian cell lines, Chinese Hamster Ovary (CHO) cells generate recombinant proteins with glycosylation patterns that most closely resemble the naturally occurring human forms (Utsumi et al., 1989). The oligosaccharide structures from human urinary erythropoietin (EPO) and recombinant CHO-derived EPO were essentially identical (Takeuchi et al., 1988). Detailed analyses of CHO-produced tissue-plasminogen activator (Spellman et al., 1989), interferon- $\beta$  (Kagawa et al., 1988) and interleukin-2 (Conradt et al., 1989) have also revealed glycosylation patterns similar to those found on their native human glycoprotein counterparts. This possession of a human-like glycosylation machinery has contributed to the widespread use of CHO cells in the commercial production of recombinant human protein therapeutics.

Asparagine-linked (N-linked) glycosylation is the most common and extensive of all post-translational modifications made to eukaryotic proteins (reviewed in Kornfeld and Kornfeld, 1985). It involves a polyisoprenoid lipid carrier, dolichol phosphate (Dol-P), and approximately 60 enzyme-catalyzed reactions. This complex intracellular process begins with the dolichol pathway in the endoplasmic reticulum (ER). It involves the enzyme-catalyzed sequential addition of the sugars N-acetylglucosamine (GlcNAc), mannose, and glucose from either their nucleoside diphosphate sugar derivatives or dolichol-linked sugar derivatives to the lipid carrier dolichol phosphate (Dol-P). The

product of the dolichol pathway is a lipid-linked oligosaccharide (LLO) composed of 14 monosaccharides (Glc<sub>3</sub>Man<sub>9</sub>GlcNAc<sub>2</sub>) linked via pyrophosphate bonds to dolichol. This lipid-linked oligosaccharide (LLO) species subsequently functions as the oligosaccharide donor in protein glycosylation.

During the crucial step in N-linked glycoprotein formation, the oligosaccharide moiety (Glc<sub>3</sub>Man<sub>9</sub>GlcNAc<sub>2</sub>) is transferred *en bloc* from dolichol pyrophosphate to an asparagine residue in the Asn-Xaa-Ser/Thr consensus sequence (where Xaa can be any amino acid except proline) of a nascent protein. However, the presence of this consensus sequence does not automatically ensure that an oligosaccharide will be attached to the side chain of the asparagine residue. It is often the case, both in cultured cells and *in vivo*, that at a specific Asn-Xaa-Ser/Thr consensus sequence in a particular protein, this glycosylation step would occur at some molecules, but not at other molecules of the same protein. Therefore, a given protein can be produced as a set of glycoforms---identical polypeptides that differ in the number of attached oligosaccharide chains (Rudd and Dwek, 1997).

After oligosaccharides are attached to proteins, they undergo a series of sugar trimming and addition reactions in the ER and Golgi (Figure 4-1). Each of these reactions is catalyzed by a specific enzyme, and does not always proceed to completion, thereby creating a variety of products. This probabilistic list of outcomes is further lengthened by the fact that different enzymes sometimes compete for the same glycoprotein substrate. Proteins ultimately exit the glycosylation pathway through secretory vesicles originating from the Golgi.

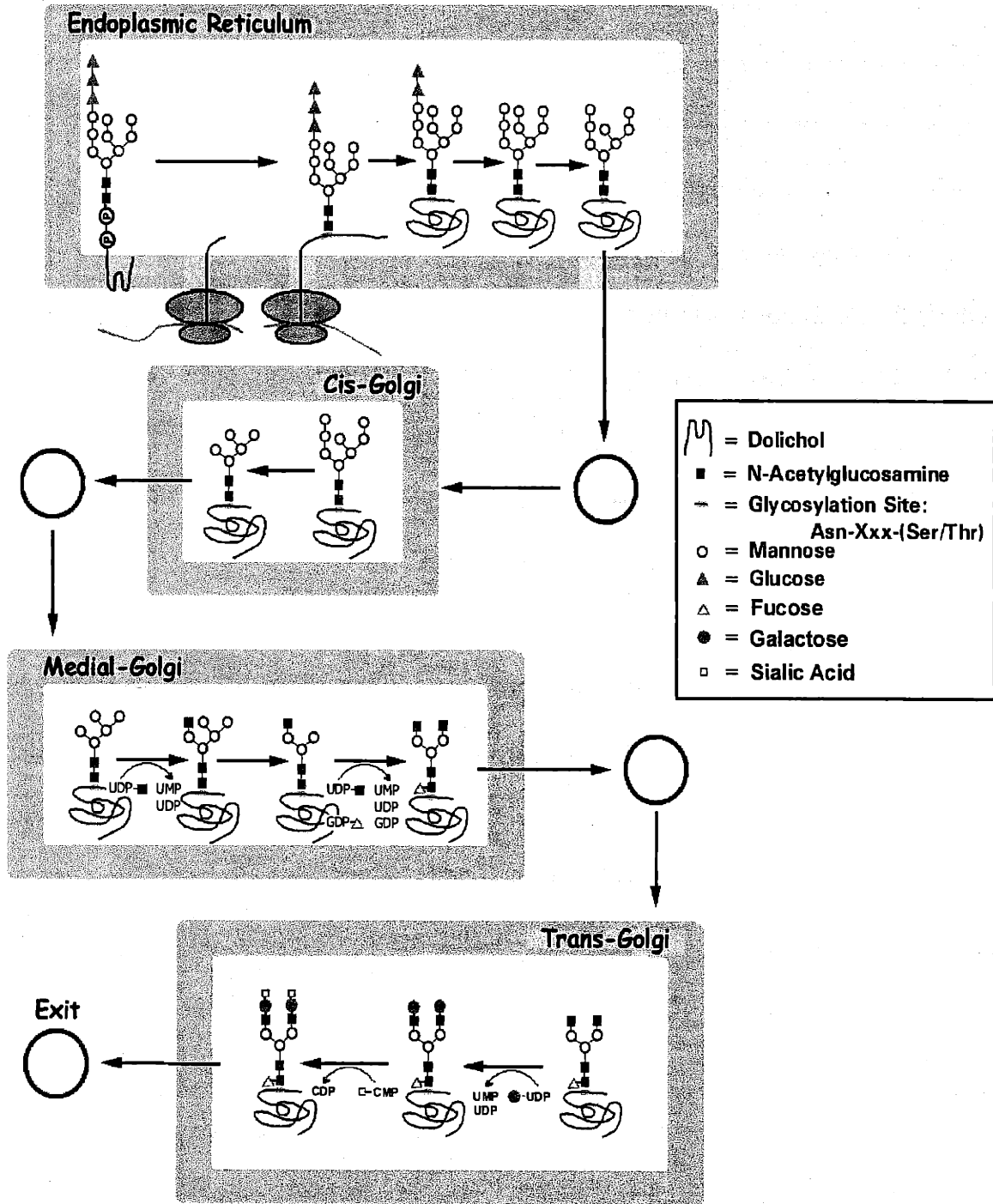


**Figure 4-1.** Schematic of the N-linked oligosaccharide processing pathway in the endoplasmic reticulum and Golgi compartments.

Variability in the presence of oligosaccharide within different molecules of the same protein is simply called “glycosylation site occupancy heterogeneity” or “glycosylation macroheterogeneity.” It is conceptually and physically distinct from “glycosylation microheterogeneity,” which addresses variations in the oligosaccharide structures at each glycosylation site. Different glycosylation patterns are often associated with different features and functions; molecules of the same protein can manifest distinct biological properties when glycosylated differently (Rademacher et al., 1988). For instance, plasma clearance rates of CHO cell-derived recombinant tPA in rabbits were significantly altered by the presence of an oligosaccharide at Asn 184 (Beebe and Aronson, 1988).

Heterogeneity in protein glycosylation presents special challenges to the development and production of a candidate therapeutic with consistent properties. Drug regulatory authorities recognize that glycosylation is an inherently heterogeneous phenomenon, but they also expect it to be specific and reproducible under defined culture conditions. Current regulatory practice thus defines a recombinant glycoprotein product by its respective process; product heterogeneity is permitted as long as efficacy, safety and consistency can be demonstrated (Liu, 1992).

In view of the inevitable occurrence and significance of glycosylation heterogeneity in glycoprotein therapeutics, much research has focused on understanding bioprocess factors that influence glycosylation heterogeneity (reviewed in Goochee et al., 1991). The host cell type and the specific amino acid sequence have the strongest impact on the presence and range of oligosaccharide structures at a particular glycosylation site. Although the N-linked glycosylation process possesses numerous stochastic elements, the

overall outcome can be consistent for a specified cell culture process---i.e., the distribution of glycoforms is reproducible for a particular glycoprotein produced and purified under identical conditions. However, an intentional or unintentional change in bioprocess conditions can lead to altered sets of glycoforms. Within a specific cell culture process, glycosylation heterogeneity is affected primarily by cell culture conditions, such as dissolved oxygen tension (Kunkel et al., 2000), pH (Borys et al., 1993), ammonia (Borys et al., 1994), glucose starvation (Elbein, 1987) and culture length (Hooker et al., 1995). Potential mechanisms that could explain these cell culture effects include the following: (1) depletion of the cellular energy state, (2) disruption of the local ER and Golgi environment, (3) interference with vesicle trafficking, and (4) modulation of glycosidase and glycosyltransferase activities (reviewed in Goochee et al., 1991).

N-linked glycosylation site occupancy of recombinant human interferon-gamma (IFN- $\gamma$ ) secreted by CHO cells has been particularly well-studied. This human antiviral therapeutic protein contains potential N-linked glycosylation sites at Asn 25 and Asn 97. As a result of variable occupancy at both potential glycosylation sites, IFN- $\gamma$  can exist in three forms differing in N-linked glycosylation status: doubly glycosylated at Asn 25 and Asn 97, singly glycosylated almost exclusively at Asn 25, or non-glycosylated. Various researchers, including Nyberg from this laboratory, observed a reproducible gradual decline in IFN- $\gamma$  N-linked glycosylation site occupancy over the course of batch and fed-batch cultures of recombinant CHO cells: the proportion of doubly glycosylated IFN- $\gamma$  decreased by 9-25% during the exponential growth phase (Castro et al., 1995; Curling et al., 1990; Goldman et al., 1998; Hooker et al., 1995, Nyberg, 1998). This deterioration in glycosylation did not arise from extracellular degradation of product (Curling, et al.,

1990), nor could it be overcome by supplementation of the cultures with extra nutrients, such as glucose and glutamine (Curling, et al., 1990; Hayter et al., 1991). Research from this laboratory demonstrated that this phenomenon was not caused by the depletion of nucleotide sugars since intracellular nucleotide sugar pools increased concomitant with the decline in IFN- $\gamma$  glycosylation (Nyberg, 1998). Certain lipid supplements could minimize the glycosylation changes, but the underlying mode of action was not understood (Jenkins et al., 1994).

The effect of cell culture conditions, such as glucose concentration or growth rate on site occupancy cannot be properly interpreted without measuring parameters that directly influence the glycosylation reaction. Since lipid-linked oligosaccharides (LLOs) serve as oligosaccharide donors in N-linked glycosylation, their availability should be a key regulatory mechanism for controlling the extent of glycosylation site occupancy. A structured kinetic model of N-linked glycosylation demonstrated the dependence of site occupancy on LLO availability (Shelikoff et al., 1996). Inadequate formation or excessive degradation of LLOs can result in LLO shortages and consequently limit the cellular glycosylation capacity (Spiro and Spiro, 1991). Under subsaturating LLO levels, a gradual decrease in the intracellular pool of LLOs would lead to a corresponding decrease in protein glycosylation. This scenario can account for the decline in IFN- $\gamma$  glycosylation observed in CHO cells. This work was conducted to test this hypothesis, and to acquire knowledge that can be applied towards the development of strategies for producing recombinant glycoproteins with consistent glycosylation.

## **4.3 MATERIALS AND METHODS**

### **4.3.1 Cell Line**

The recombinant CHO cell line used in this work was the same cell line described in previous studies on N-linked glycosylation by this laboratory (Gu et al., 1997; Nyberg et al., 1999). Referred to as the  $\gamma$ -CHO cell line for its ability to produce the recombinant human antiviral protein IFN- $\gamma$ , the cell line was obtained from Dr. Walter Fiers of the University of Ghent, Belgium (Scahill et al., 1983). The  $\gamma$ -CHO cells were created from a dihydrofolate reductase (DHFR) deficient CHO cell line by co-transfection with genes for DHFR and IFN- $\gamma$ . The IFN- $\gamma$  gene copy number was co-amplified using the DHFR system and the selection agent methotrexate. The  $\gamma$ -CHO cell line was originally anchorage-dependent, and cultured in the presence of serum. It was slowly adapted, in this laboratory, to suspension growth in two different serum-free media, either CHO-S-SFM II (Gu et al., 1997), or RPMI SFM (Nyberg et al., 1999).

### **4.3.2 Cell Culture**

All cultures were maintained in glass shake flasks agitated at 70 rpm on orbital shakers in a 37°C incubator with 95% humidity and 5-10% carbon dioxide overlay. In preparation for each experiment, a vial of frozen  $\gamma$ -CHO cells was taken from a working cell bank and the cells were inoculated at  $3 \times 10^5$  cells/ml in the serum-free medium they had been adapted to grow in (either CHO-S-SFM II or RPMI-SFM). The cells were subsequently resuspended 2-4 times into progressively larger amounts of the fresh serum-free medium until enough cells were obtained to start the experiment. In this way, all the cells used within any particular study had the same culture history. The cells were maintained at

densities of  $(3-10) \times 10^5$  cells/ml with viabilities exceeding 95% prior to the initiation of any experiment.

#### **4.3.3 Serum-Free Media: RPMI-SFM and CHO-S-SFM II**

The first set of experiments was conducted using a line of  $\gamma$ -CHO cells adapted to grow in a serum-free medium developed in this laboratory (Nyberg, 1998). As indicated by its designated name of RPMI-SFM, this serum-free medium was primarily composed of RPMI-1640 (Sigma), with the following supplements: 2.5 g/l Primatone RL (Quest International), 1 g/l Pluronic F-68, 0.4 g/l 2-hydroxypropyl- $\beta$ -cyclodextrin, 11 mg/l choline chloride, 10 mg/l streptomycin, 6.3 mg/l EDTA, 5 mg/l insulin, 5 mg/l transferrin, 1 mM sodium pyruvate, 100  $\mu$ M ethanolamine, 1.5  $\mu$ M linoleic acid, 1  $\mu$ M putrescine, 0.25  $\mu$ M methotrexate, 10,000 units/l penicillin, and trace minerals (5  $\mu$ M ferric citrate, 3  $\mu$ M zinc sulfate, 10 nM ammonium metavanadate, 10 nM cupric sulfate, 10 nM sodium selenite, 10 nM molybdic acid, and 1 nM manganese sulfate).

The second set of experiments was performed using  $\gamma$ -CHO cells that had been adapted to grow in CHO-S-SFM II (Gibco). This commercially available medium has been specially formulated for the serum-free culture of suspension CHO cells. Unlike RPMI-SFM, CHO-S-SFM II does not have defined components. The  $\gamma$ -CHO cultures using CHO-S-SFM II were supplemented with 0.25  $\mu$ M methotrexate, 10,000 units/l penicillin, and 10 mg/l streptomycin to maintain methotrexate selective pressure and eliminate bacterial contamination.



#### **4.3.4 Radiolabeled RPMI-SFM Batch Cultures**

At the start of this experiment,  $\gamma$ -CHO cells that had been cultured in unlabeled RPMI-SFM were collected by centrifugation (5 min,  $200 \times g$ ). The cell pellet was resuspended in fresh RPMI-SFM containing 12.3  $\mu\text{Ci/ml}$  D-[ $U$ - $^{14}\text{C}$ ] glucose (American Radiolabeled Chemicals) and 3.2  $\mu\text{Ci/ml}$  L- $^3\text{H}$  leucine (Amersham Pharmacia Biotech). The cells suspended at  $3.8 \times 10^5$  cells/ml in the radiolabeled medium were divided equally into two identical shake flasks. Throughout the course of batch culture, samples were taken from the duplicate flasks at regular time points. The cells were separated from the culture supernatant and used for cell enumeration as well as extraction of both LLOs and intracellular proteins. The supernatant was filtered and stored at  $-20^\circ\text{C}$  until it was used for future metabolite analyses and secretory protein extraction. After 100 hours of culture, no cells were viable and the experiment was ended.

#### **4.3.5 Radiolabeled CHO-S-SFM II Batch Cultures**

CHO-S-SFM II containing 6.7  $\mu\text{Ci/ml}$  D-[ $U$ - $^{14}\text{C}$ ] glucose (American Radiolabeled Chemicals) and 2.6  $\mu\text{Ci/ml}$  L- $^3\text{H}$  leucine (Amersham Pharmacia Biotech) was the labeling medium used in the cultures here. Prior to the start of the experiment,  $\gamma$ -CHO cells were incubated in the labeling medium for 26 hours. At the beginning of the experiment, the conditioned radiolabeled medium was separated from the cells by centrifugation (5 min,  $200 \times g$ ) and discarded. The prelabeled  $\gamma$ -CHO cells were resuspended in a larger volume of fresh labeling medium, and divided into duplicate shake flasks. Samples were taken from the parallel batch cultures every 12 hours throughout the length of the experiment for various measurements. The culture samples

were centrifuged at  $200 \times g$  for 5 minutes to sediment the cells. The cells were used for cell enumeration, cell cycle analyses, and for the extraction of LLOs and cellular proteins. The supernatant was filtered and then stored at  $-20^{\circ}\text{C}$  for future glucose and lactate measurements and extraction of secreted proteins.

#### **4.3.6 Determination of Cell Numbers and Viability**

Cell culture samples were diluted with an isotonic solution of 0.4% w/v trypan blue. Cells were then counted with a hemacytometer and microscope. Viable cells excluded trypan blue by virtue of their intact cell membranes; non-viable cells were stained blue due to loss of membrane integrity. In this way, viable cells were distinguished from their non-viable counterparts and cell viability was determined. To minimize random errors, at least 500 cells were counted for each culture sample.

#### **4.3.7 Determination of Glucose and Lactate Concentrations**

Filtered samples of cell culture supernatants were frozen at  $-20^{\circ}\text{C}$  until ready for metabolite analyses. Glucose and lactate concentrations in the thawed samples were measured directly by the YSI 23000 STAT Plus Glucose & Lactate Analyzer (YSI Life Sciences).

#### **4.3.8 Isolation of Lipid-linked Oligosaccharides (LLOs) and Cellular Proteins**

At regular time intervals, samples containing 5-10 million cells were taken from each culture. After centrifugation at  $200 \times g$  for 5 minutes, the supernatant was filtered and stored at  $-20^{\circ}\text{C}$  for metabolic and extracellular protein analyses. LLOs and intracellular

proteins were isolated from the cells using a well-established sequential extraction procedure (Bhat and Waechter, 1988; Hubbard and Robbins, 1979; Lucas et al., 1975). The cell pellets were quickly resuspended in 12 ml of ice-cold PBS, centrifuged at 0°C for 3 minutes at 300 × g, and the supernatant was discarded. The cells were subsequently washed 3 more times with fresh ice-cold PBS. After the final rinse, the cell pellet was resuspended in 7 ml of CHCl<sub>3</sub>/CH<sub>3</sub>OH (2:1) with the aid of vigorous vortex mixing. The cell material was allowed to stand at room temperature for at least 15 minutes, and clumps were dispersed with occasional vortex mixing or brief sonication. The suspension was centrifuged (4 min, 1200 × g), and the pellet was re-extracted with 2 × 6 ml CHCl<sub>3</sub>/CH<sub>3</sub>OH (2:1). The pellet was dried and then resuspended by sonication in 0.5 ml water, before 7 ml of water was added. This fine white suspension was centrifuged (4 min, 1200 × g), and the aqueous wash was discarded. The pellet was subjected to two more rinses with 7 ml water. LLOs were solubilized from the washed pellet using three 7 ml extractions with CHCl<sub>3</sub>/CH<sub>3</sub>OH/H<sub>2</sub>O (10:10:3). The three LLO extracts from each pellet were pooled together into a glass scintillation vial. After the extraction solvent was evaporated to dryness in a fume hood, 20 ml of Ultima Gold LSC cocktail (Packard Bioscience) was added to each scintillation vial to redissolve the LLOs in preparation for liquid scintillation counting. The residue remaining after lipid extraction contained cellular proteins. After the protein-containing pellet was air dried, it was dispersed in 1 ml 10% w/v trichloroacetic acid (TCA) by sonication. The mixture was allowed to stand for a few minutes at 4°C after 7 ml of ice-cold 10% TCA was added. Protein precipitated by the acid was sedimented by centrifugation (4 min, 1200 × g). The pellet was subsequently washed with 10 ml ice-cold 10% TCA and 10 ml ice cold water. The final

protein precipitate was first digested with 0.5 ml hot 1N NaOH to give a clear colorless solution before being dissolved in 20 ml Ultima Gold LSC cocktail and transferred to a scintillation vial for radioactivity measurements.

#### **4.3.9 Extraction of Secreted Proteins**

Samples of filtered cell culture supernatants (3-5 ml) that had been frozen at -20°C were thawed at room temperature. An equal volume of ice-cold 20% w/v TCA was added to each sample to precipitate the protein. The solutions were mixed and allowed to sit at 4°C for 1 hour prior to centrifugation (4°C, 5 min, 1200 × g). The TCA soluble wash was discarded and the TCA-precipitable material was rinsed twice with 8 ml ice-cold 10% w/v TCA. To prepare the final residue for liquid scintillation counting, it was first solubilized in 0.5 ml hot 1N NaOH and then mixed with 20 ml Ultima Gold LSC cocktail in a scintillation vial.

#### **4.3.10 Determination of Radioactivity**

Radioactivities were quantified using a LS 6500 Liquid Scintillation Counter (Beckman Instruments). The counting efficiency of  $^{14}\text{C}$  in single label measurements of LLO extracts was typically 95%, while the counting efficiencies of  $^{14}\text{C}$  and  $^3\text{H}$  in dual label measurements of TCA-precipitated proteins were approximately 75% and 46% respectively.

#### **4.3.11 Cell Cycle Analyses**

Every 12 hours, roughly one million cells were taken from each of the parallel CHO-S-SFM II batch cultures. After centrifugation for 5 minutes at  $200 \times g$ , the labeled supernatant was removed. Following one rinse with PBS, the cell pellet was resuspended in 0.5 ml stain solution containing 1.5% polyethylene glycol-4000 (PEG-4000), 1.5% PEG-8000, 50  $\mu\text{g/ml}$  propidium iodide, 180 units/ml RNAase, 0.1% Triton-X-1000, and 4 mM sodium citrate (final pH of solution was adjusted to 7.2). After incubating the cell suspension for 20 minutes in a  $37^\circ\text{C}$  water bath, 0.5 ml salt solution containing 1.5% PEG-4000, 1.5% PEG-8000, 50 mg/ml propidium iodide, 0.1% Triton-X-1000, and 0.4 M sodium chloride (final pH of solution was adjusted to 7.2) was added. Prior to cell cycle analyses, the sample was stored in the dark at  $4^\circ\text{C}$  for 12 to 24 hours. The propidium iodide-stained cells were sorted with a FACScan flow cytometer (Becton Dickinson). 30,000 events per sample were collected. Raw data was processed with ModFit Lt. v.2 analysis software (Verity Software House) to determine the cell cycle distribution within each sample.

## **4.4 RESULTS**

### **4.4.1 Radiolabeled RPMI-SFM Batch Cultures**

RPMI-SFM normally contained approximately 2.0 g/l D-glucose and 0.05 g/l L-leucine. The RPMI-SFM used in duplicate batch cultures of  $\gamma$ -CHO cells was spiked with  $^{14}\text{C}$  D-glucose and  $^3\text{H}$  L-leucine, such 0.5% of the total glucose was  $^{14}\text{C}$  labeled, and 0.005% of the overall leucine present was  $^3\text{H}$  labeled. These radioactive supplements should have negligible impacts on the culture performance since their amounts were minute relative to

the quantities of their unlabeled counterparts normally found in RPMI-SFM. The radioactive and cold versions of either nutrient should be indistinguishable to the cells. In this way, the radiolabels functioned as tracers to conveniently monitor the cellular uptake and metabolism of glucose and leucine in  $\gamma$ -CHO cells. Since glucose was the only external source of sugar for the cells growing in RPMI-SFM, it should be the primary metabolic precursor for generating nucleotide sugars used in LLO synthesis.  $^{14}\text{C}$  radioactivity originating from supplemental  $^{14}\text{C}$  glucose would therefore be detected in intermediates and products of the glycosylation pathway, such as LLOs and glycoproteins. By following incorporation of the  $^{14}\text{C}$  label into LLO and glycoprotein throughout the course of batch culture, corresponding changes in the relative levels of LLO and glycosylation could be determined.

#### ***4.4.1.1 Cell Density and Viability***

Total cell densities and viabilities in the parallel batch cultures of  $\gamma$ -CHO cells in RPMI-SFM demonstrated corresponding declines (Figure 4-2). After peaking at 60 hours, the total cell density rapidly dropped (Figure 4-2(A)). Culture viabilities remained consistently over 95% up to 60 hours of culture, but quickly fell to zero less than 40 hours later (Figure 4-2(B)). Even though cells were still present at 100 hours of culture, all the cells were dead, as determined by the trypan blue dye exclusion assay.

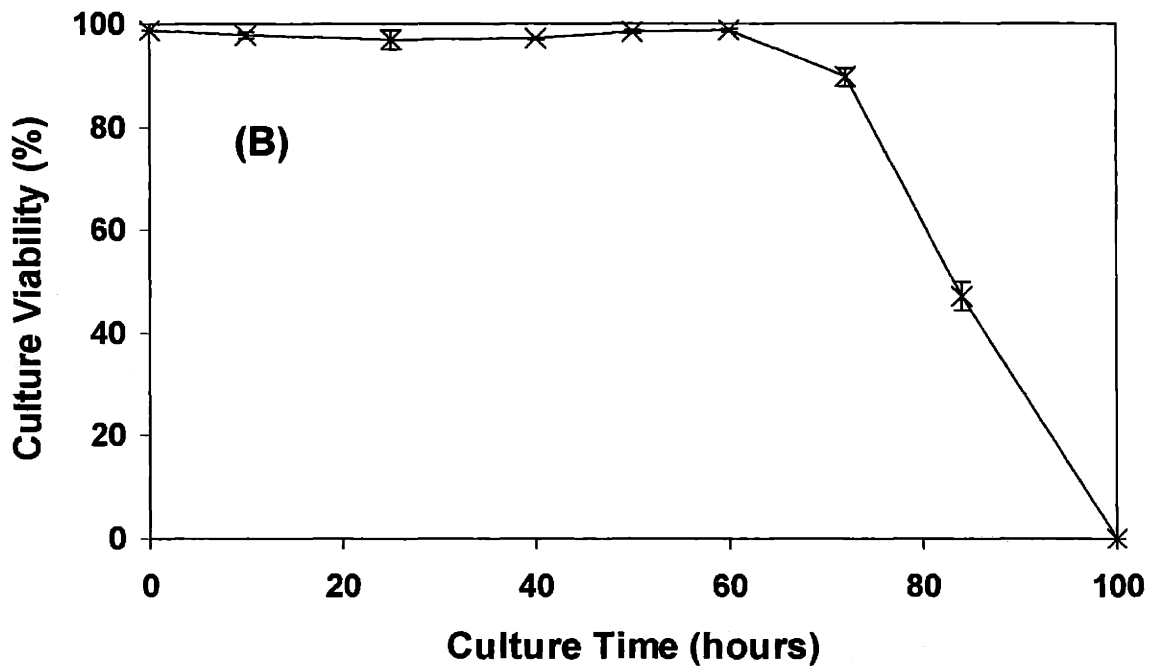
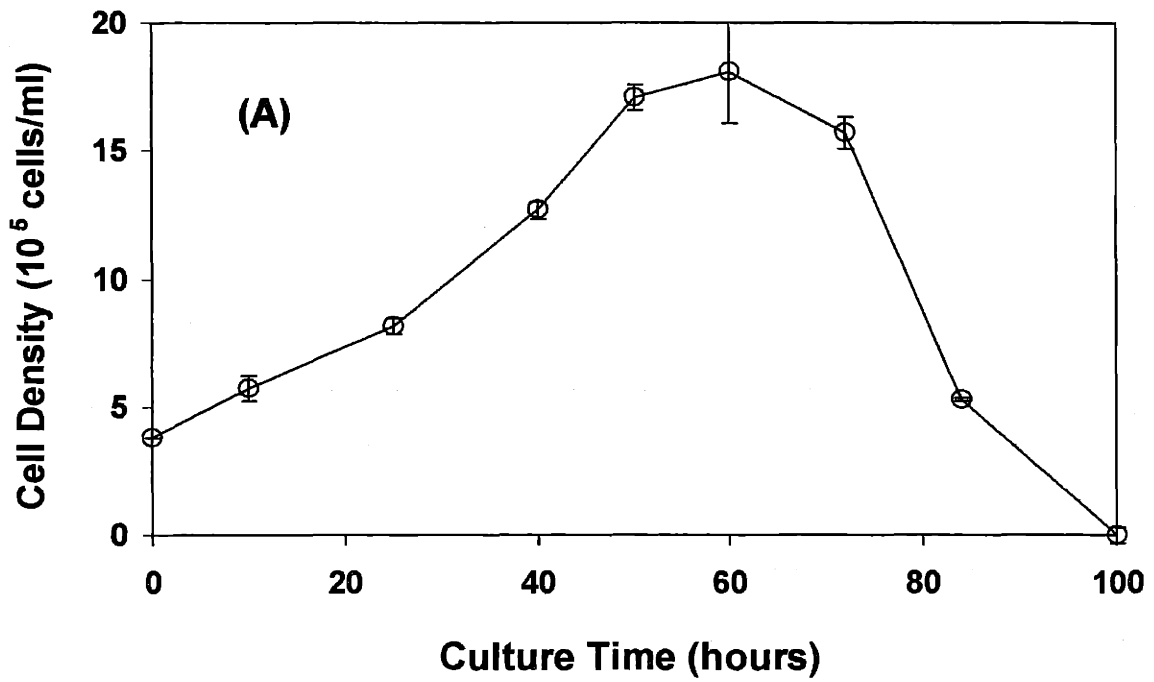


**Figure 4-2.** Cell densities (A) and viabilities (B) measured in parallel RPMI-SFM batch cultures. Error bars indicate the differences in measurements between the duplicate cultures.

#### ***4.4.1.2 Glucose and Lactate Concentrations***

Concentrations of glucose and lactate in the RPMI-SFM were monitored over time in the duplicate  $\gamma$ -CHO cultures (Figure 4-3). Within the first 40 hours of culture, glucose concentrations in the culture medium fell from about 2 g/l to under 0.1 g/l (Figure 4-3(A)). During this time period, lactate concentrations in the medium increased from about 0 g/l to over 1.5 g/l (Figure 4-3(B)). Research on CHO batch cultures had demonstrated that cell growth was not inhibited at these lactate concentrations (Hayter et al., 1991).

#### ***4.4.1.3 Relative LLO Levels over Culture Time***

Radiolabeling of the saccharide moiety of LLOs was achieved by incubating the cells in  $^{14}\text{C}$  glucose-spiked medium. An isolation procedure based on the fact that LLO is insoluble in  $\text{CHCl}_3/\text{CH}_3\text{OH}$  (2:1) and water, but soluble in  $\text{CHCl}_3/\text{CH}_3\text{OH}/\text{H}_2\text{O}$  (10:10:3) was used to extract LLO from the cells (Lucas et al., 1975). The molecules extracted into the  $\text{CHCl}_3/\text{CH}_3\text{OH}/\text{H}_2\text{O}$  (10:10:3) phase using this well-established method had been shown to be chiefly LLOs (Li and Kornfeld, 1979).

Normalization of LLO measurements to total cell number or cellular protein gave similar results (Figure 4-4). The level of  $^{14}\text{C}$  radioactivity in LLO extracts per million cells showed less than two-fold variations throughout most of the culture period (Figure 4-4(A)). The ratio of  $^{14}\text{C}$  radioactivity in LLO extracts to the  $^3\text{H}$  leucine radioactivity in the cellular protein extracts also remained fairly consistent with culture time (Figure 4-4(B)); this ratio gives an indication of the LLO levels relative to the amount of cellular protein. The unusually high values observed at the end of culture (100 hours) coincided with the measured 0% culture viability (Figure 4-2). Since this implied that all the LLOs



extracted for the  $^{14}\text{C}$  measurements at 100 hours originated from dead cells, the set of measurements at 100 hours was justifiably regarded as unreliable.

#### ***4.4.1.4 Relative Glycosylation Levels over Culture Time***

In this work, the radioactive TCA-precipitable materials in the cell culture supernatant were categorized as secreted proteins, while the radiolabeled TCA-insoluble residue left after lipid extractions were classified as cellular proteins. Proteins were labeled by incubating the cells in RPMI-SFM supplemented with a radioactive form of the essential amino acid, L-leucine, and isolated by TCA precipitation.  $^{14}\text{C}$  radioactivities on the oligosaccharide moieties of glycoproteins originated from the cellular uptake and metabolism of  $^{14}\text{C}$  D-glucose from the medium. The ratio of  $^{14}\text{C}$  disintegrations per minute (DPM) to  $^3\text{H}$  DPM in both intracellular and extracellular materials precipitated by TCA was determined at regular time intervals over the course of batch culture. Since this ratio compared overall  $^{14}\text{C}$  D-glucose incorporation into glycoproteins to total  $^3\text{H}$  L-leucine incorporation into proteins, it represented the relative extents of protein glycosylation in the duplicate cultures: the larger the ratio, the higher the overall degree of protein glycosylation.

The  $^{14}\text{C}$  to  $^3\text{H}$  ratios in both cellular and secreted proteins displayed similar trends (Figure 4-5). Their patterns followed that observed in the growth curve (Figure 4-2(A)): the values increased during the first half of the culture (growth phase), plateaued in the middle (stationary phase), and then decreased towards the end (decline phase).

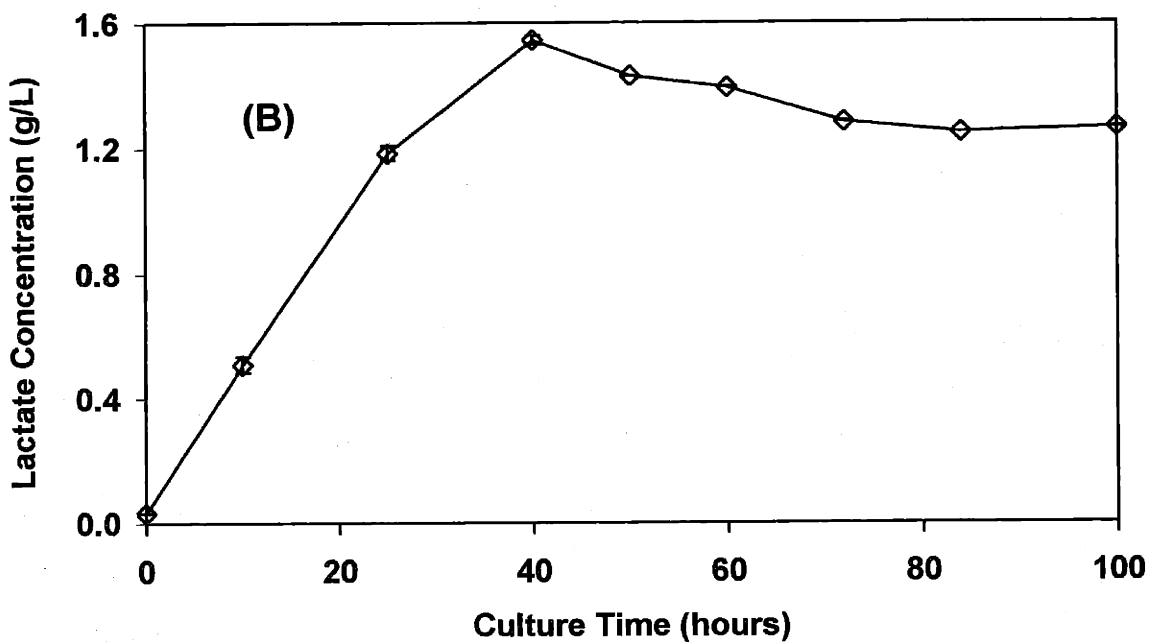
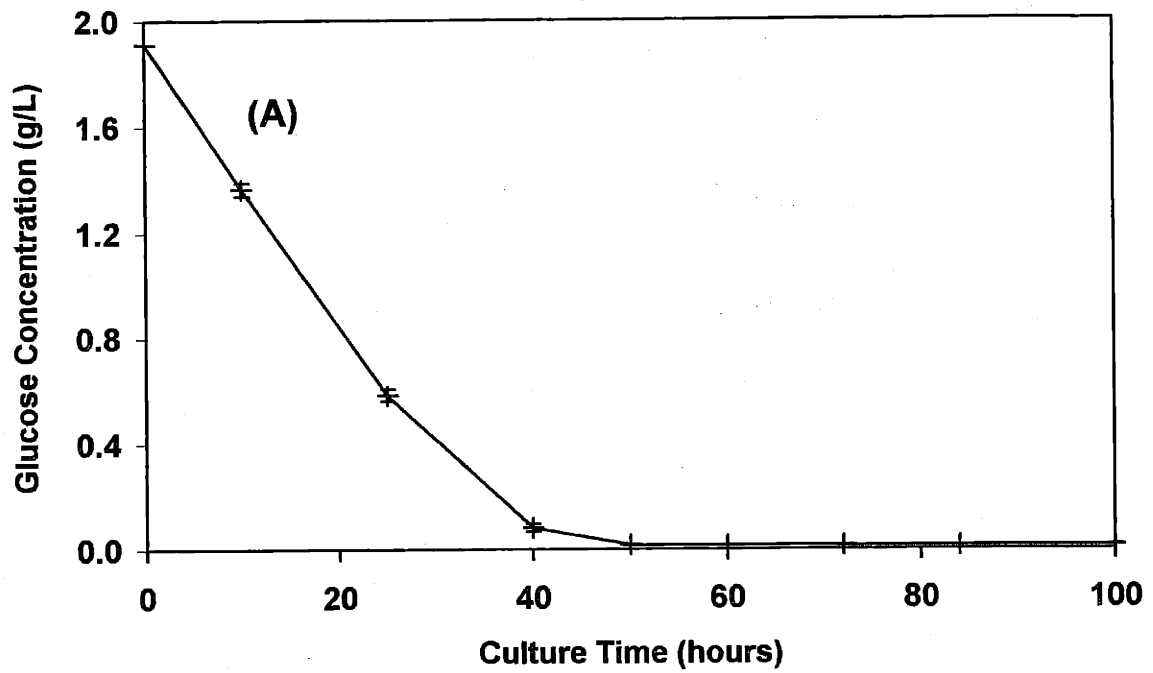


**Figure 4-3.** Concentrations of glucose (A) and lactate (B) in RPMI-SFM over culture time. Each data point was generated from measurements of filtered supernatants obtained from duplicate batch cultures.

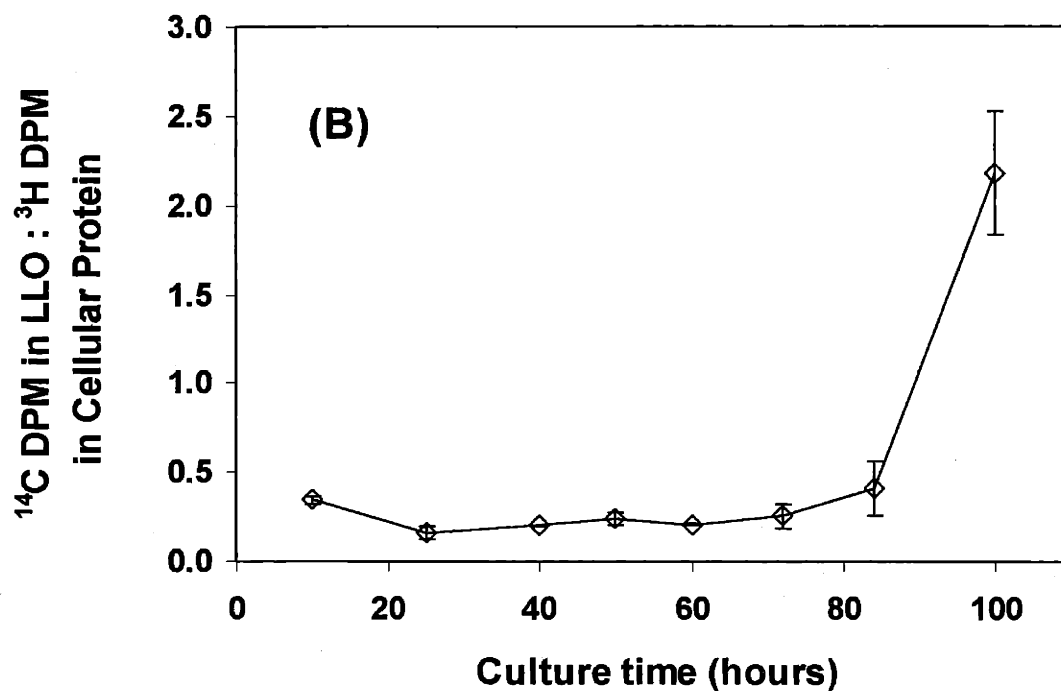
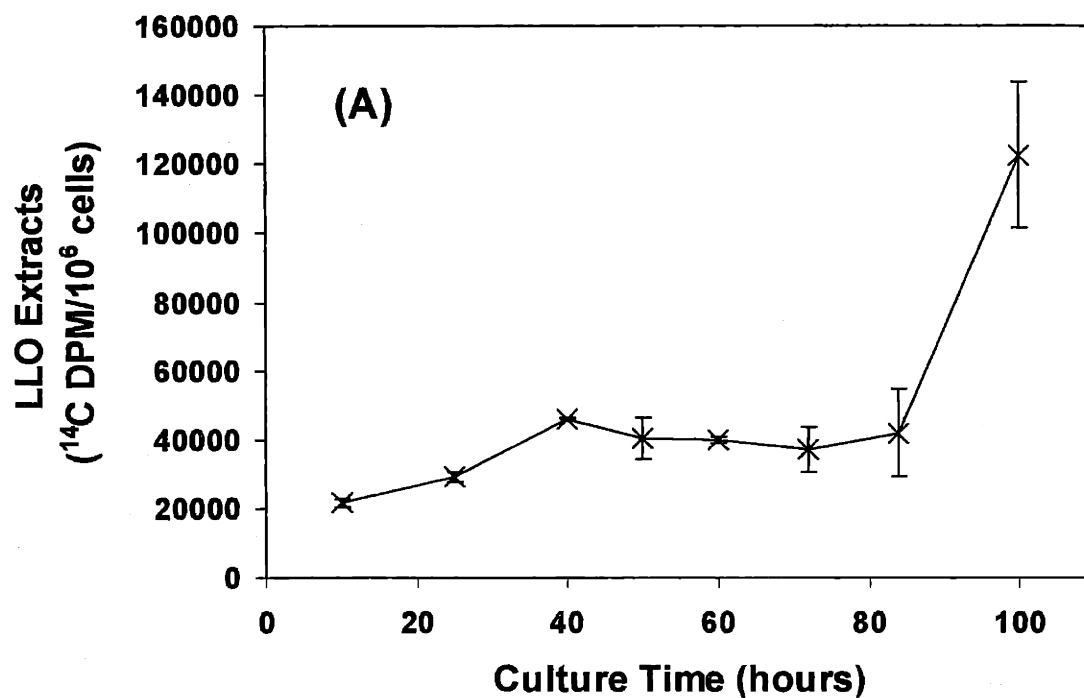


**Figure 4-4.**  $^{14}\text{C}$  radioactivity measured in LLO extracts divided by total cell number (A), or by  $^3\text{H}$  leucine radioactivity detected in cellular protein extracts (B). Error bars represent differences between duplicate RPMI-SFM CHO batch cultures supplemented with  $^{14}\text{C}$  glucose and  $^3\text{H}$  leucine. Radioactivity was counted in disintegrations per minute (DPM).

The  $^{14}\text{C}$  to  $^3\text{H}$  ratios measured during the early part of the culture may have been significantly affected by differences in the rates of  $^{14}\text{C}$  incorporation into glycoproteins and  $^3\text{H}$  leucine incorporation into proteins. If it took much longer for the pool of  $^{14}\text{C}$ -labeled LLOs to reach maximum steady-state levels whereas intracellular pool of  $^3\text{H}$  leucine reached equilibrium almost instantaneously, the  $^{14}\text{C}$  to  $^3\text{H}$  ratios measured in the TCA-precipitated proteins would be much lower at the beginning of the culture. Subsequently, the ratio would gradually rise as the prevalence of  $^{14}\text{C}$ -label within the intracellular pool of LLOs increased to steady-state levels. This possibility must be minimized before any conclusions can be drawn about the apparent correlation between glycosylation and growth state.

At each time point in batch culture, the  $^{14}\text{C}$  to  $^3\text{H}$  ratios were always higher in the secreted proteins than in the cellular proteins (Figure 4-5). This observation is attributed to the differences between secreted and cytosolic proteins in terms of exposure to glycosylation. Prior to the onset of massive cell death, radiolabeled TCA-precipitable materials in the cell culture supernatant would comprise mostly of secreted proteins; upon cell death, intracellular proteins released by cell lyses would contribute to the pool of labeled secreted proteins. Secreted proteins generally proceed through the glycosylation pathways in the ER and Golgi prior to secretion, and were thus likely to be glycosylated. By contrast, many intracellular proteins such as cytosolic and nuclear proteins remain unglycosylated in their fully processed native states. Such naturally unglycosylated proteins were synthesized on non-membrane bound ("free") cytosolic ribosomes, and released into the cytosol without any exposure to glycosylation enzymes in the ER and Golgi.

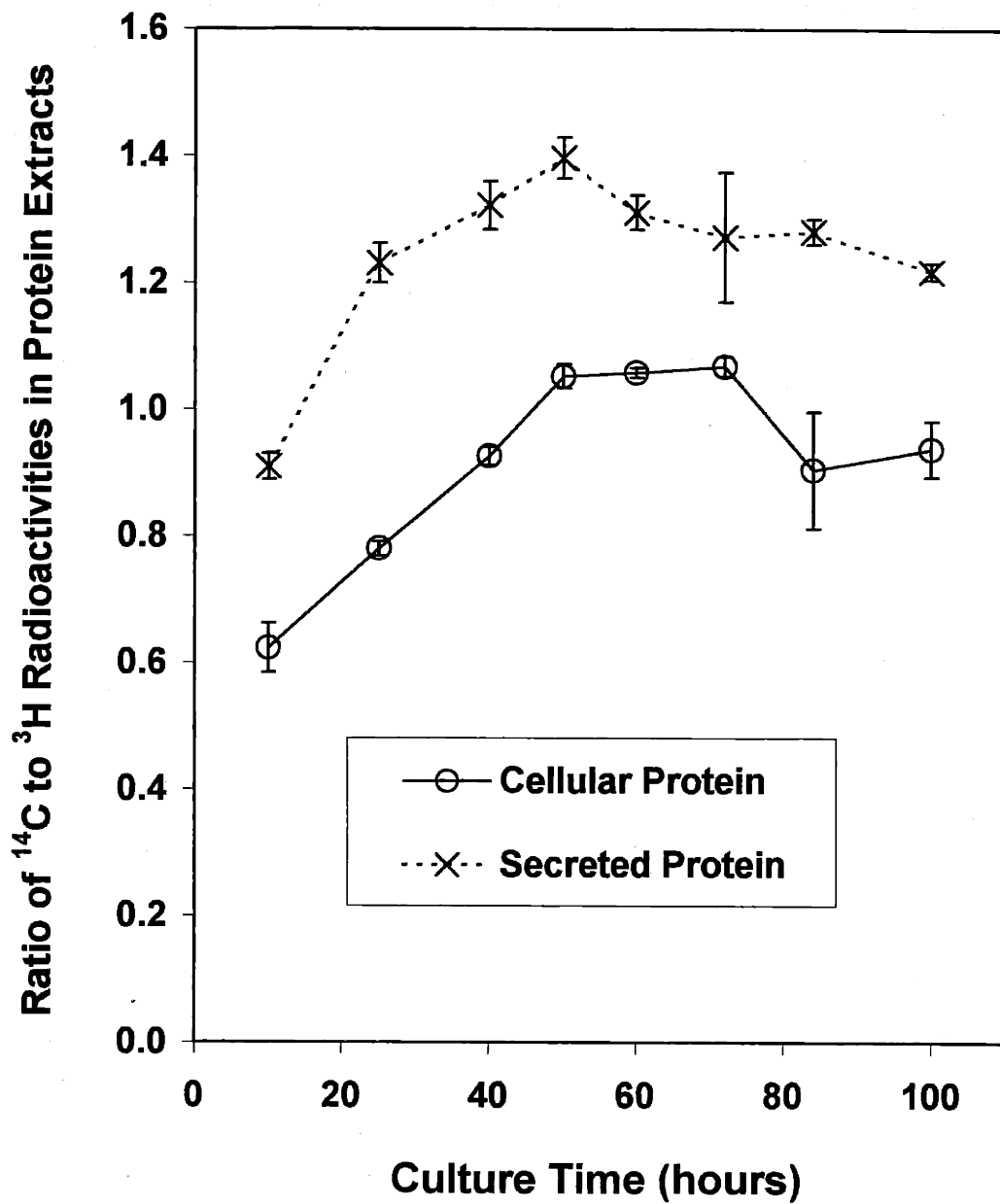


**Figure 4-5.** Ratio of  $^{14}\text{C}$  to  $^3\text{H}$  radioactivities measured in cellular and secreted proteins over the course of CHO batch culture. The RPMI-SFM cultures were supplemented with  $^{14}\text{C}$  D-glucose and  $^3\text{H}$  L-leucine. Proteins were extracted by TCA precipitation at regular time intervals and assessed for the incorporation of  $^{14}\text{C}$  radiolabel into glycoproteins and  $^3\text{H}$  leucine into proteins.

#### 4.4.2 Radiolabeled CHO-S-SFM II Batch Cultures

Various issues were raised in the previous time-course study in CHO RPMI-SFM batch cultures. This experiment was designed to address these issues and thereby determine with greater certainty and precision the changes in the relative LLO and glycosylation levels in CHO cells over time in batch cultures.

Glucose was rapidly depleted from the RPMI-SFM medium used in the previous study. The concentration of this primary source of carbon for the cells fell from about 2 g/l to below 0.1 g/l (0.6 mM) within 40 hours of culture (Figure 4-3(A)). Since glucose is an important substrate for LLO synthesis, glucose starvation will adversely affect LLO and glycosylation levels. To prevent glucose availability from becoming a limiting factor in CHO cell culture, CHO-S-SFM II, a high glucose medium---containing over 3.5 g/l glucose---was chosen for this experiment. In this way, the possibility that LLO and glycosylation levels were negatively impacted by low glucose concentration was eliminated.

Incubations of thyroid slices with radioactive glucose showed that over 3 hours were required for both the glucose and mannose residues of the LLO to be maximally labeled (Spiro et al., 1976). Studies in mice uteri tissues indicated that the incorporation of radiolabeled sugars into LLOs reached maximal levels only after 4 hours of incubation (Carson et al., 1987). These results suggest that the length of time required for LLO levels to be labeled to metabolic equilibrium with radioactive sugars is on the order of hours in mammalian cells. This is not surprising given the various saccharide interconversions and nucleotide sugar syntheses required to label the different sugar residues on LLO. Forseeably, the uptake of radioactive glucose by CHO cells and its

incorporation into LLO may be rapid, but the size of the LLO pools was large enough that its  $^{14}\text{C}$  glucose-derived radioactivity took a significantly longer time to increase to steady state levels. By comparison, the intracellular  $^3\text{H}$  leucine pool should take less time to rise to equilibrium levels. Therefore, the ratio of  $^{14}\text{C}$  to  $^3\text{H}$  radioactivity in the TCA precipitated proteins from the previous experiment using RPMI-SFM would be expected to be lower at the beginning of culture. With progression in time, the  $^{14}\text{C}$  glucose-derived radioactivity in LLOs should gradually increase to equilibrium levels, and thereby result in a corresponding increase in the  $^{14}\text{C}$  to  $^3\text{H}$  ratios in the proteins.

This experiment was designed to accomplish steady state labeling of both LLOs and proteins. CHO cells were first pre-incubated in the labeling medium for 26 hours before they were transferred into fresh labeling medium at the start of the time-course study. By pre-incubating the cells in the labeling medium for over a day, the intracellular LLOs and cellular proteins should be metabolically labeled to equilibrium in the continuously growing CHO cells. In fact, this incubation period of 26 hours should be long enough to label the various forms of glucose and leucine (such as metabolites, products and derivatives) to steady state levels. For instance, a consistent percentage of LLOs, say 0.5%, should contain  $^{14}\text{C}$  radioactivity throughout the course of culture.

The previous experiment suggested a connection between glycosylation and growth state. To further investigate this apparent association, FACS analyses of the cells were taken at regular time points to determine the cell cycle distribution of the cultures in this experiment.

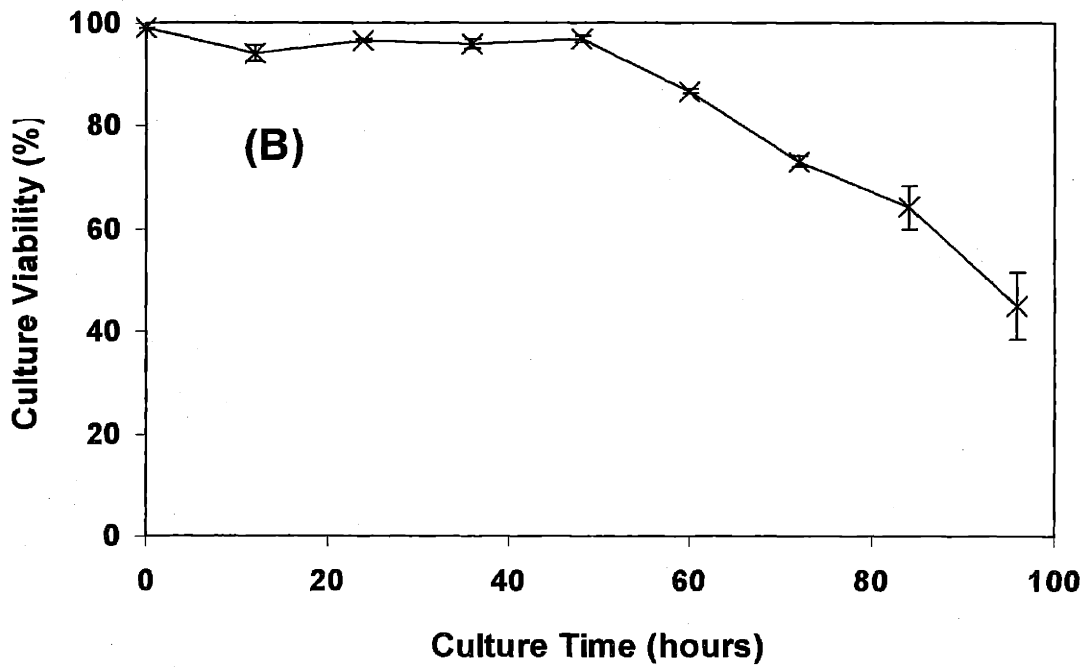
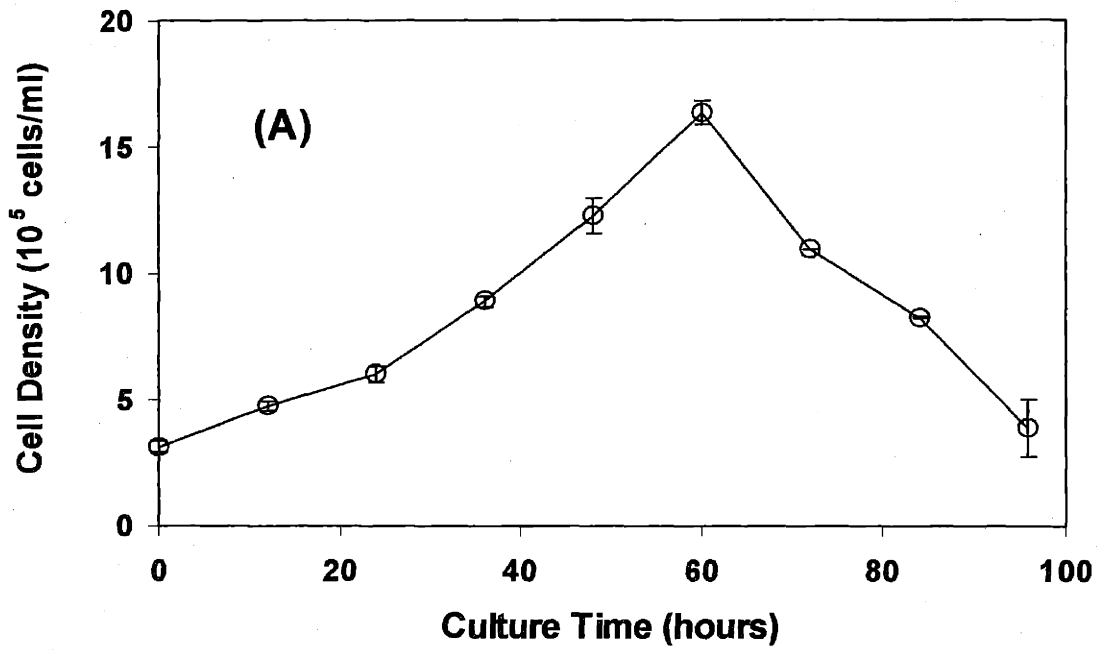


**Figure 4-6.** Cell densities (A) and viabilities (B) measured in parallel CH0-S-SFM II batch cultures. Error bars indicate the differences in measurements between the duplicate cultures.



#### ***4.4.2.1 Cell Density and Viability***

The duplicate batch cultures of  $\gamma$ -CHO cells in CHO-S-SFM II demonstrated corresponding declines in total cell densities and viabilities (Figure 4-6). Total cell densities peaked at 60 hours, and rapidly declined thereafter (Figure 4-6(A)). Culture viabilities started to fall below 95% after 48 hours of culture (Figure 4-6(B)). The experiment was ended when the culture viabilities dropped to 50% at 96 hours.

#### ***4.4.2.2 Glucose and Lactate Concentrations***

Glucose and lactate concentrations in the CHO-S-SFM II medium were monitored over time in the parallel  $\gamma$ -CHO batch cultures (Figure 4-7). In this high glucose medium, the glucose concentration in the medium never fell below 1.3 g/l throughout the entire course of culture (Figure 4-7(A)). During this time period, lactate concentrations in the medium increased from about 0 g/l to over 2.5 g/l (Figure 4-7(B)). By contrast to the RPMI-SFM cultures (Figure 4-3), glucose availability was not limiting in these CHO-S-SFM II cultures, although the higher initial glucose concentrations also led to a correspondingly higher lactate accumulation.

#### ***4.4.2.3 Cell Cycle Distributions***

The cell cycle distributions of  $\gamma$ -CHO batch cultures were measurable up to 72 hours of culture time (Figure 4-8). After 72 hours in batch culture, a considerable portion of the cells was nonviable (Figure 4-6(B)). The resulting accumulation of cell debris prevented accurate determination of cell cycle distributions in samples taken after 72 hours of batch culture.

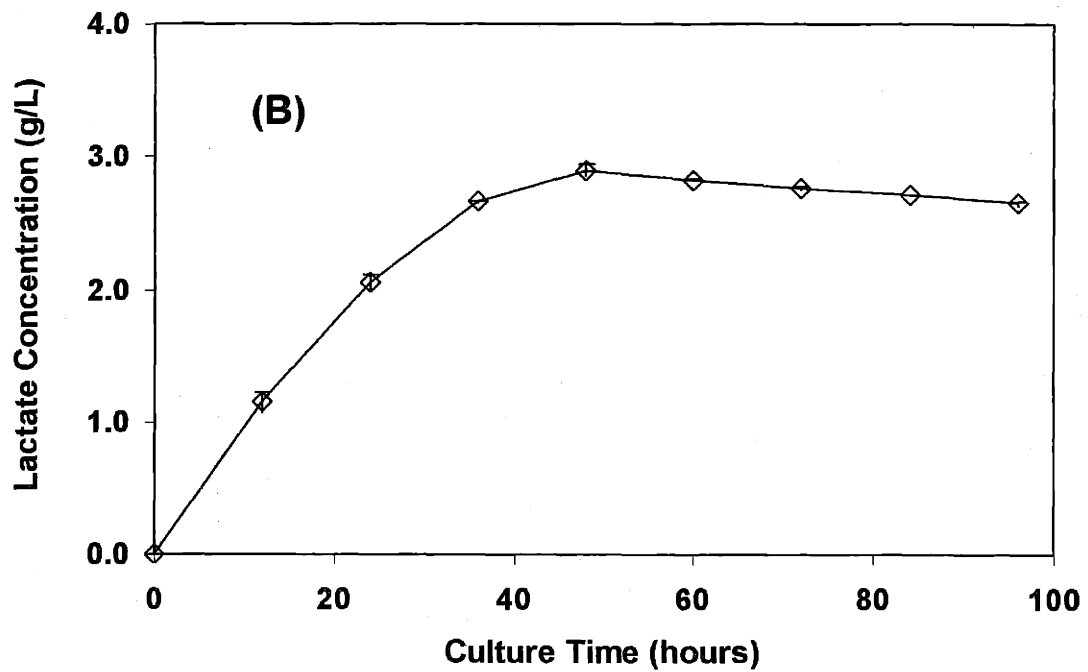
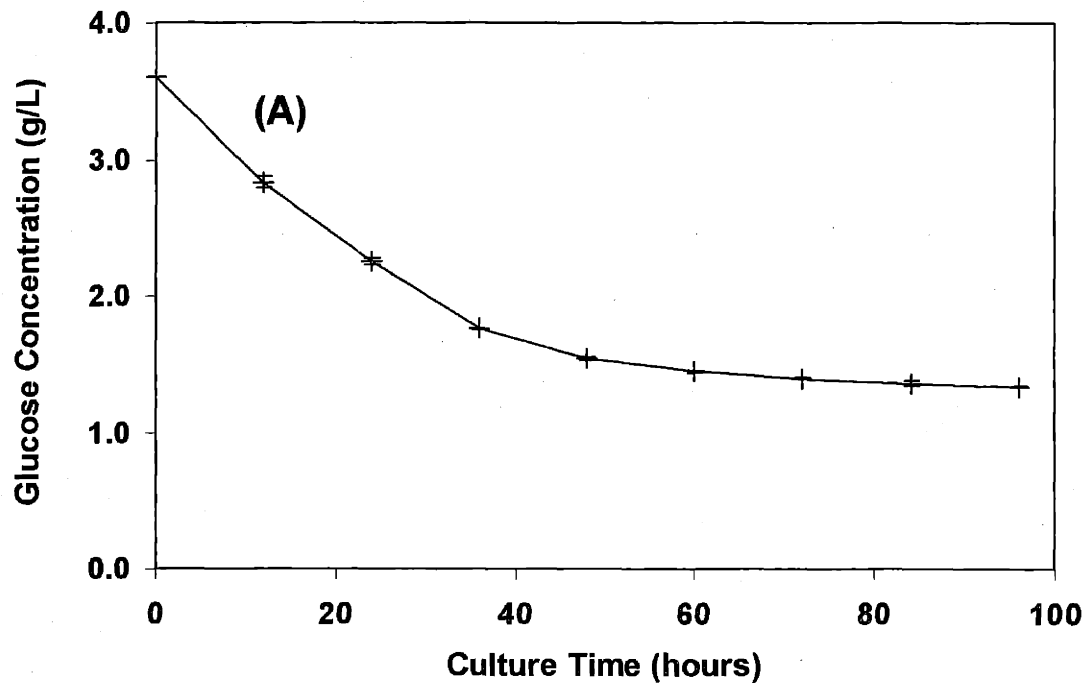


**Figure 4-7.** Glucose (A) and lactate (B) concentrations in CHO-S-SFM II over culture time. Each data point represents measurements of filtered supernatants obtained from duplicate batch cultures.

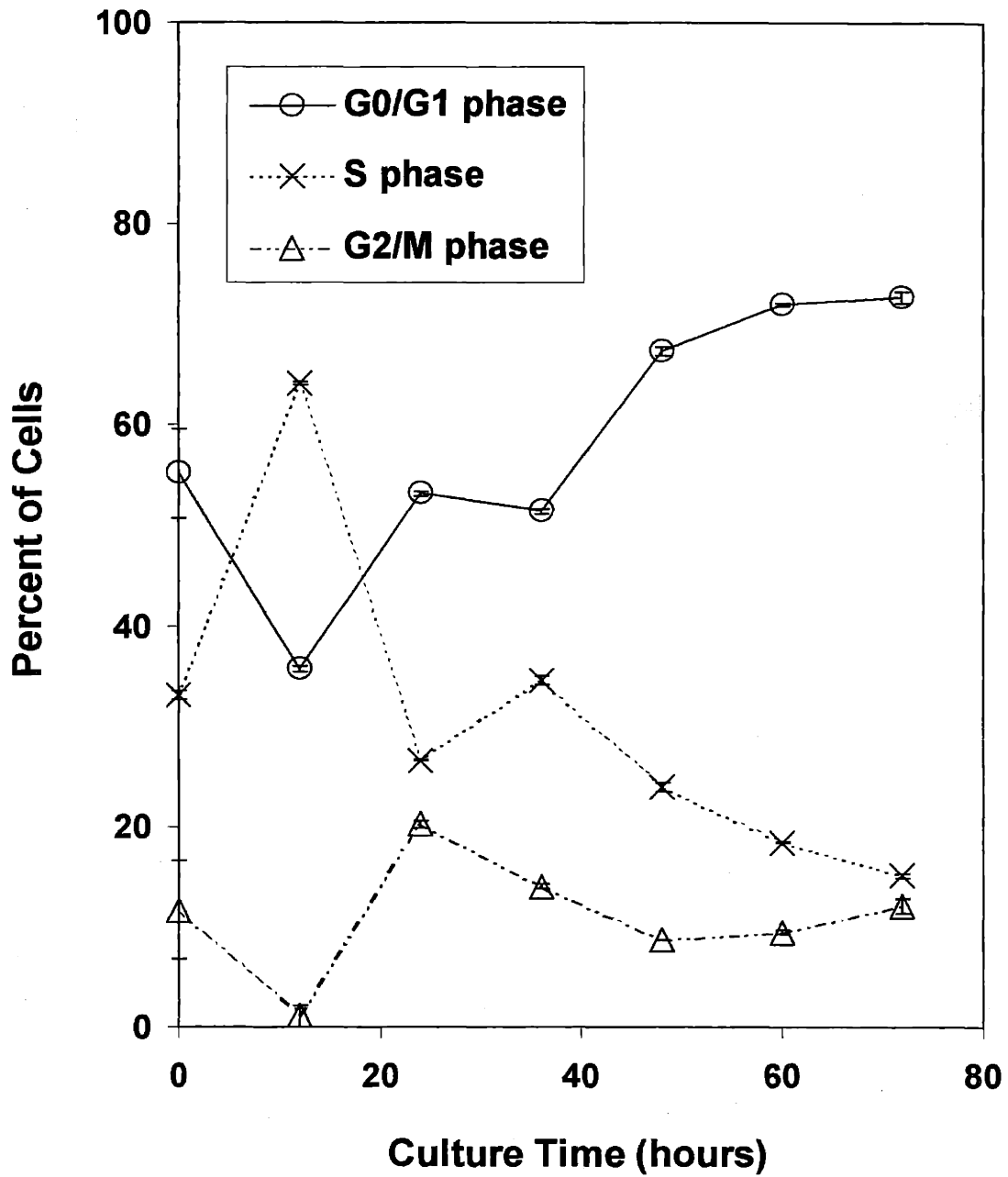


**Figure 4-8.** Cell cycle distributions of  $\gamma$ -CHO batch cultures in CHO-S-SFM II. Error bars show the differences in measurements between identical parallel cultures.

The first data point used for cell cycle analyses (taken at 0 hours) was obtained from  $\gamma$ -CHO cells that had been growing for 26 hours. At the start of this experiment (0 hours), these cells were transferred into fresh medium. It is not surprising that the cell cycle distributions measured at 0 hours were similar to those recorded at 24 and 36 hours, since all three sets of data were generated from cells that had been growing in fresh medium for approximately one day. The exposure to fresh medium stimulated growth in the cells, as confirmed by the highest percentage of S phase cells measured at 12 hours. Subsequently, the percentage of G0/G1 phase cells gradually increased at the expense of the percentage of S-phase cells.

#### ***4.4.2.4 Relative LLO Levels over Culture Time***

Normalization of LLO measurements to total cell number or cellular protein produced similar results (Figure 4-9). The level of  $^{14}\text{C}$  radioactivity in LLO extracts per million cells gradually decreased by about 50% over the course of culture (Figure 4-9(A)). The ratio of  $^{14}\text{C}$  radioactivity in LLO extracts to the  $^3\text{H}$  leucine radioactivity in the cellular protein extracts also showed a similar decline with culture time (Figure 4-9(B)). However, normalization of LLO  $^{14}\text{C}$  radioactivity to viable cell number showed that the relative LLO level per viable cell remained fairly constant over the length of culture (Figure 4-10). This suggested that the gradual decline in LLO levels relative to total cell numbers or cell protein can be attributed to the corresponding decline in viable cell density. Taken together, these results indicate that LLO levels did not vary by more than two-fold throughout the course of culture.

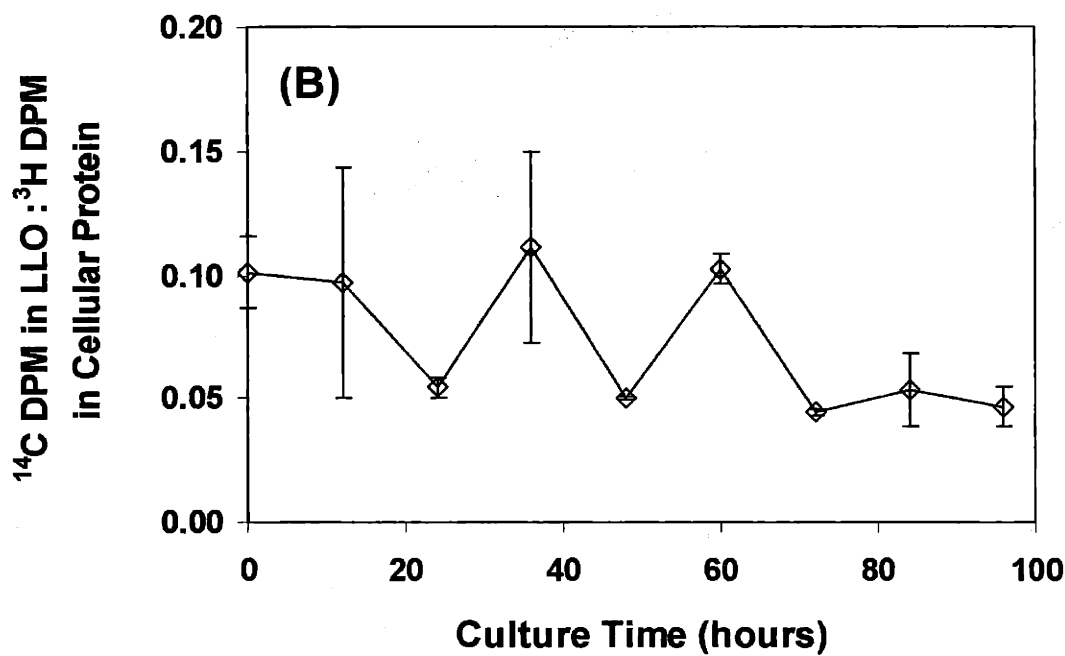
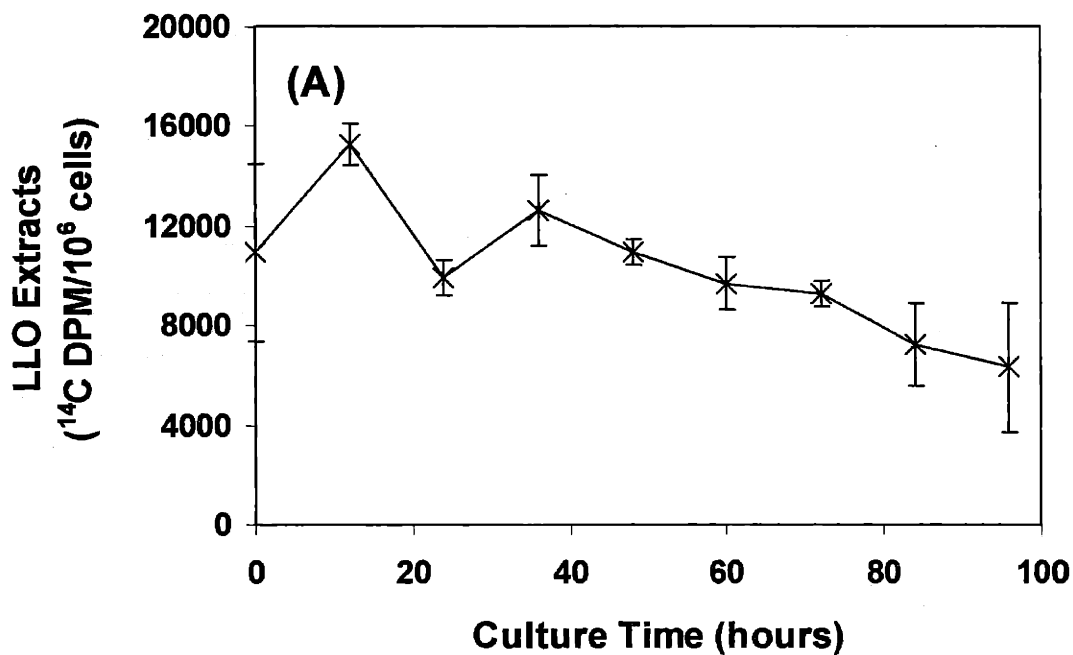


**Figure 4-9.**  $^{14}\text{C}$  radioactivity measured in LLO extracts divided by total cell number (A), or by  $^3\text{H}$  leucine radioactivity detected in cellular protein extracts (B). Radioactivity was counted in disintegrations per minute (DPM). Error bars show the differences in measurements obtained from duplicate CHO-S-SFM II cultures supplemented with  $^{14}\text{C}$  glucose and  $^3\text{H}$  leucine.

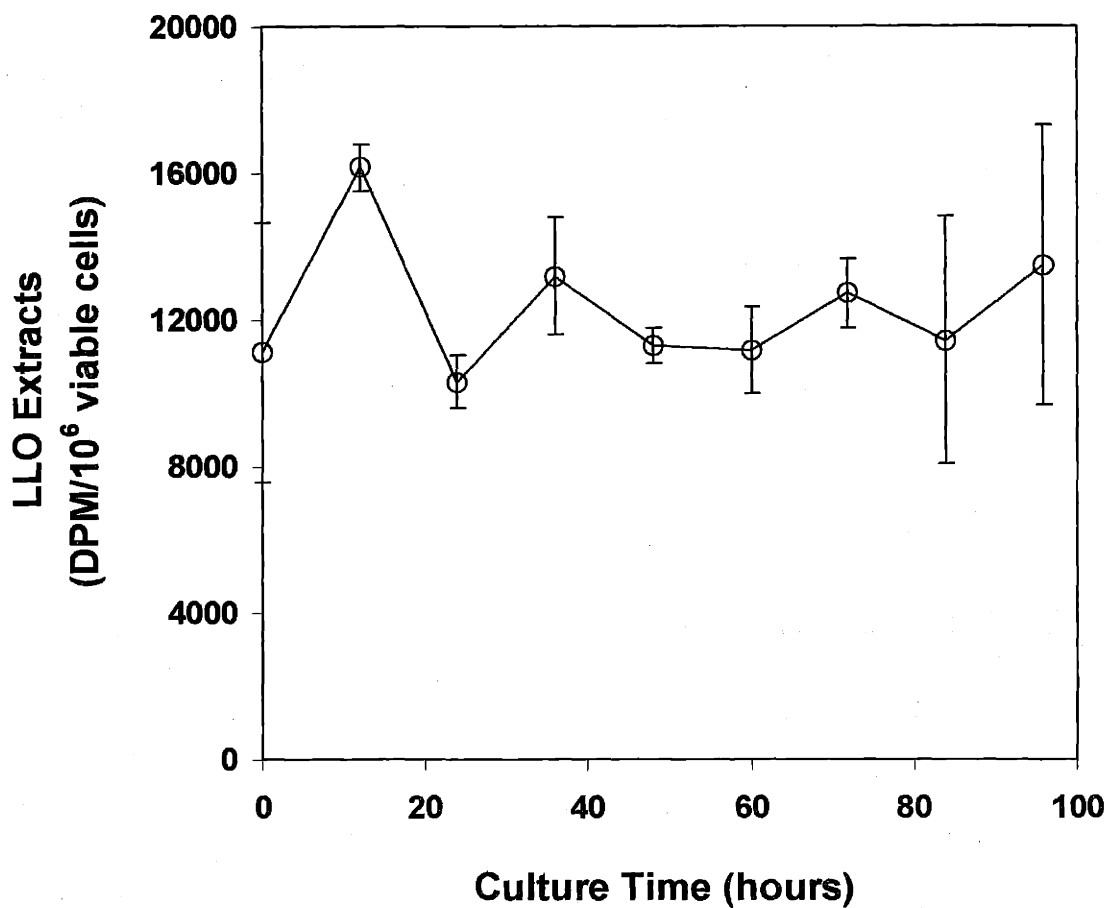


**Figure 4-10.** <sup>14</sup>C radioactivity measured in LLO extracts divided by viable cell number. Radioactivity was counted in disintegrations per minute (DPM). Each data point was generated from a set of identical parallel CHO batch cultures in CHO-S-SFM II supplemented with <sup>14</sup>C glucose and <sup>3</sup>H leucine. Error bars show the differences in measurements between the duplicate cultures.

#### ***4.4.2.5 Relative Glycosylation Levels over Culture Time***

The incorporation of  $^{14}\text{C}$  and  $^3\text{H}$  labels into TCA-insoluble material was assayed to determine relative glycosylation levels. The  $^{14}\text{C}$  to  $^3\text{H}$  ratios in both cellular and secreted proteins changed over the course of batch culture (Figure 4-11). Their changes reflected that observed in the percentage of G0/G1 phase cells in the culture (Figure 4-8). The values initially decreased, but the subsequent increase in the proportion of G0/G1 phase cells was followed by a corresponding elevation in the  $^{14}\text{C}$  to  $^3\text{H}$  ratios for both cellular and secreted proteins. Prior to the decline in cell viability around 60 hours (Figure 4-6(B)), the  $^{14}\text{C}$  to  $^3\text{H}$  ratios measured at each time point were always higher in secreted proteins than in cellular proteins, in accord with the higher likelihood for secreted proteins to be glycosylated. Upon the onset of massive cell death, the  $^{14}\text{C}$  to  $^3\text{H}$  ratios began to descend from their maximum values, consistent with the expectation that dying cells have impaired glycosylation machinery. Towards the end of culture, the  $^{14}\text{C}$  to  $^3\text{H}$  ratio in the secreted proteins approached the values measured in the cellular proteins (Figure 4-11). This is attributed to the release of intracellular proteins by cell lyses. The addition of nonglycosylated intracellular proteins such as cytosolic and nuclear proteins to the pool of extracellular proteins upon cell lysis is expected to lower the  $^{14}\text{C}$  to  $^3\text{H}$  ratio measured in the secreted proteins.

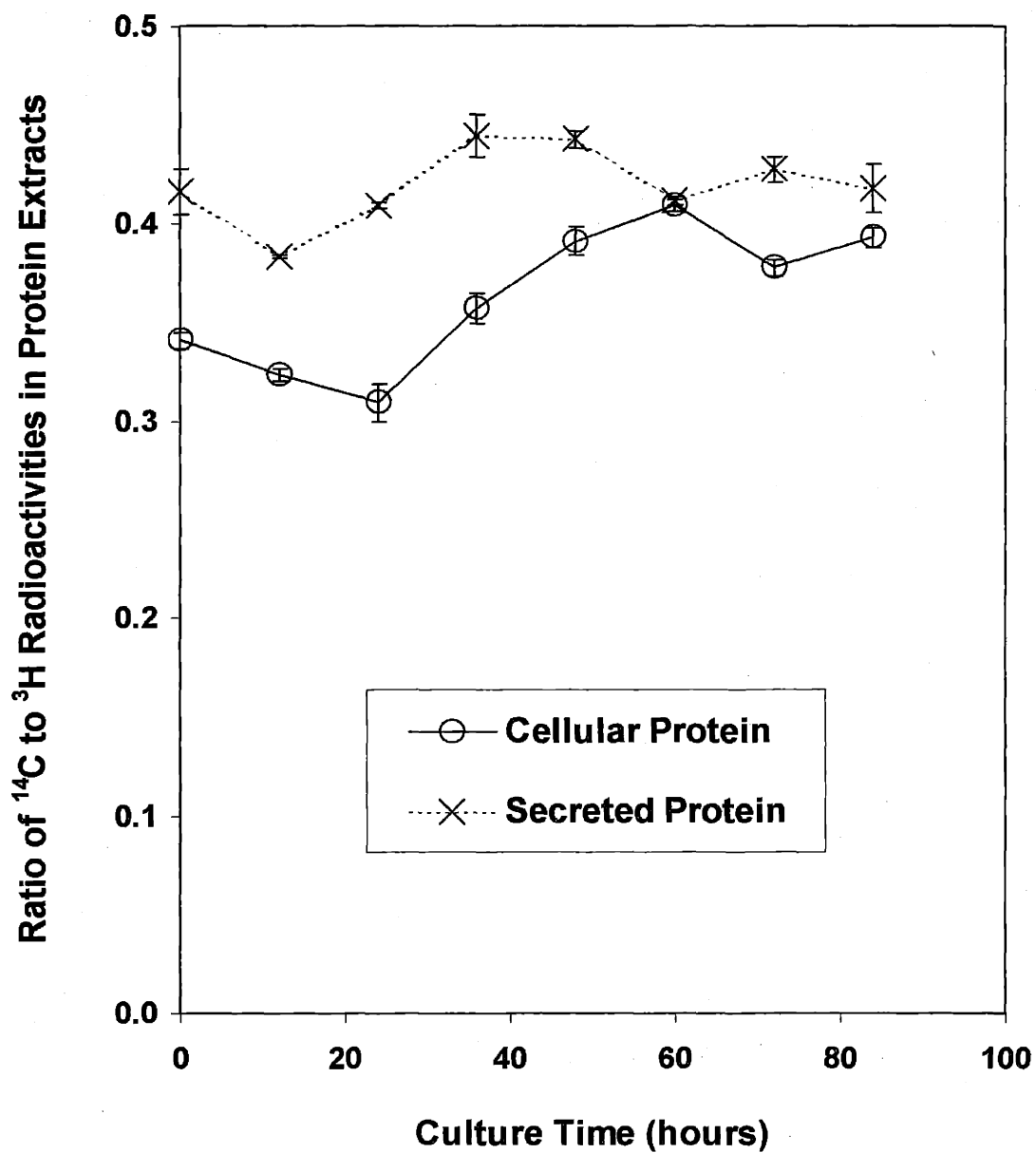


**Figure 4-11.** Ratio of  $^{14}\text{C}$  to  $^3\text{H}$  radioactivities measured in cellular and secreted proteins over the course of CHO-S-SFM II batch culture. The  $\gamma$ -CHO cells were preincubated in labeling medium containing  $^{14}\text{C}$  D-glucose and  $^3\text{H}$  L-leucine. Proteins were extracted by TCA precipitation at regular time intervals and assessed for the incorporation of  $^{14}\text{C}$  radiolabel into glycoproteins and  $^3\text{H}$  leucine into proteins.



## 4.5 DISCUSSION

The effect of cell culture conditions, such as glucose concentration or growth rate on site occupancy cannot be properly interpreted without measuring parameters that directly influence the glycosylation reaction, such as LLO availability. This work was conducted to investigate the intracellular changes responsible for the gradual decline in IFN- $\gamma$  N-linked glycosylation site occupancy over the course of CHO batch culture. Since LLOs are the oligosaccharide donors in N-linked glycosylation, their availability was postulated to limit the extent of site occupancy. To test this hypothesis, LLO and glycosylation levels in CHO cells were monitored over time in batch cultures to determine if they exhibit corresponding changes.

It is difficult to measure the absolute amount of LLO in CHO cells, since their total intracellular concentrations are very small---at least  $4 \times 10^8$  CHO cells were required to supply enough LLO (0.2-0.5 nmol) for quantification by direct sugar analysis (Li et al., 1978). Therefore, LLOs have typically been studied by radiolabeling their sugar or lipid components (Rosenwald et al., 1990). Most studies of the dolichol pathway have used radioactive sugar precursors to trace LLO metabolism. For instance, incubation of thyroid slices with  $^{14}\text{C}$  monosaccharides yielded LLOs labeled in the saccharide moieties; the neutral sugar components became labeled throughout the oligosaccharide portion of LLO (Spiro et al., 1976). The labeling of individual monosaccharides was qualitatively quite similar whether  $^{14}\text{C}$  glucose,  $^{14}\text{C}$  galactose or  $^{14}\text{C}$  mannose was used as the substrate, although the absolute conversions were different, presumably due to the variations in pool sizes and activity of enzymes involved in the saccharide interconversions. A

substantial amount of  $^{14}\text{C}$  radioactivity was also incorporated into the sugar components on glycoproteins, through the glycosylation process.

In this work,  $^{14}\text{C}$  glucose and  $^3\text{H}$  leucine were chosen as the radioactive supplements because their unlabeled forms were normal components of the cell culture media. By keeping the amounts of radiolabeled nutrients minute relative to the quantities of their unlabeled counterparts in the media, possible perturbations introduced to the cultures by radiolabeling were minimized. Since glucose was the only sugar source in the cell culture media, it became the major metabolic precursor of nucleotide sugars used in LLO synthesis. In this way, LLOs and glycoproteins became  $^{14}\text{C}$ -labeled. At the same time, proteins were labeled with  $^3\text{H}$  leucine. By labeling the LLOs to equilibrium with  $^{14}\text{C}$ , the  $^{14}\text{C}$  radioactivity in lipid extracts measured the amount of radiolabeled sugar present in LLOs. The ratio of  $^{14}\text{C}$  to  $^3\text{H}$  radioactivity in protein samples measured the abundance of sugars relative to amino acids, and thereby represented the extent to which proteins were glycosylated.

The radiolabeling studies showed that no dramatic changes in the intracellular levels of LLO occurred over the course of batch culture; CHO cells reproducibly maintained their LLO levels to within a two-fold range (Figures 4-4, 4-9 and 4-10). However, the possibility that smaller changes may have occurred could not be ruled out since the multi-step sequential process required to extract the lipids generated relatively large error margins. Hence, the measurements here were not sensitive enough to quantify 10-20% variations in LLO levels reliably.

Studies have identified a cell-cycle dependence of LLO biosynthesis in rat 3Y1 cells (Fukushima et al., 1997) and human fibroblasts (Ohkura et al., 1997). In these cells,

LLO levels were at least ten times higher during the S phase than during other phases of the cell cycle. Although results here demonstrate conclusively that LLO pools were constant to within an order of magnitude throughout the course of CHO cell culture, they do not convincingly argue for or against an association between LLO levels and the cell cycle.

The ratio of radiolabeled sugar to radiolabeled amino acid in both the cellular and secreted proteins displayed overall increases (Figures 4-5 and 4-11). The error margins associated with the duplicate batch cultures were small enough to support the validity of the observed trend. These results suggest that these IFN- $\gamma$  producing CHO cells glycosylate their proteins more extensively with progression in culture time, until the onset of massive cell death. This 15-25% improvement in overall protein glycosylation is in agreement with that reported for CHO-derived recombinant tissue plasminogen activator (tPA) (Andersen et al., 2000). Andersen and coworkers showed that the glycosylation site occupancy of tPA produced by fed-batch cultures of CHO cells increased by 15-25% over culture time. The pattern and extent of the tPA site occupancy enhancement were similar to that observed here with the overall protein glycosylation in the  $\gamma$ -CHO cells. However, these glycosylation trends contradict those observed specifically in IFN- $\gamma$  produced by CHO batch and fed-batch cultures (Castro et al., 1995; Curling et al., 1990; Goldman et al., 1998; Hooker et al., 1995, Nyberg, 1998). An explanation that can reconcile these divergent findings in CHO cells is as follows: although the net glycosylation efficiency in CHO cells improved with progression in culture time, the glycosylation site occupancy of different proteins can undergo different changes. This hypothesis has strong implications for recombinant protein production

using CHO cells---the glycosylation pattern of each individual glycoprotein product needs to be tracked over the course of culture because different proteins can exhibit different glycosylation variations with time, even if the same culture method is used.

The lack of obvious change in LLO and glycosylation levels in CHO cells despite the dramatic declines in glucose concentration in the medium suggests that the glucose supply can vary over a wide range without having major impact on LLO and glycosylation levels. This is supported by chemostat studies showing that a 40% reduction in UDP-GNAc resulted in only a relatively modest change of 10-15% in the percent of fully glycosylated IFN- $\gamma$  (Nyberg et al., 1999).

Prior to the significant loss of cell viability in the CHO cultures, changes in  $^{14}\text{C}$  to  $^3\text{H}$  ratios in both cellular and secreted proteins reflected those observed in the percentage of G0/G1 phase cells in the cultures, in support of a positive association between glycosylation and percent of G0/G1 phase cells in the culture. These results corroborate with previously observed correlations between tPA glycosylation site occupancy and fraction of cells in the G0/G1 phase of the cell cycle (Andersen et al., 2000). It is plausible that the slowing down of cell growth---suggested by the increase in the percentage of G0/G1 phase cells, the concomitant decrease in percentage of S phase cells, and the lack of amplification in cell density---could lead to a coordinate decline in net protein productivity. If intracellular LLO levels remained constant during this time, more LLOs would be available per protein for oligosaccharide transfer, and thereby result in an overall improvement in protein glycosylation.

The critical role of protein elongation rate in controlling glycosylation site occupancy suggests that another mechanism may be possible (Shelikoff et al., 1994).

This alternative hypothesis assumes that the protein elongation rate during translation would slow down under conditions of reduced growth. The resulting increase in contact time between the protein and oligosaccharide substrate would enhance the success rate of the enzyme-catalyzed glycosyl transfer reaction and thereby improve the extent of glycosylation.



## **5. Effects of Dolichol Phosphate Supplementation on CHO Batch Cultures**

### **5.1 ABSTRACT**

Asparagine-linked glycosylation is an important feature of many protein therapeutics. An essential step in this complex intracellular process is the transfer of oligosaccharide from dolichol monophosphate (Dol-P) to a potential glycosylation site. Variability in the success of this transfer results in glycosylation site occupancy heterogeneity. Given the critical role of Dol-P in this process, its availability was postulated to limit glycosylation by controlling the pool of lipid-linked oligosaccharides (LLOs), the oligosaccharide donor in glycosylation. To test this hypothesis, the impact of Dol-P supplementation on protein glycosylation in Chinese Hamster Ovary (CHO) cells was investigated. Although exogenous Dol-P was incorporated by CHO cells and processed into LLO in a dose-dependent manner, Dol-P supplementation had no marked effect on LLO or overall cellular glycosylation levels. Dosing studies showed that concentration of exogenous Dol-P exceeding 100 µg/ml were detrimental to CHO cell growth and viability. Analyses of recombinant interferon-gamma (IFN-γ) secreted by batch cultures of CHO cells revealed that maximum supplemental doses of Dol-P resulted in no more than a marginal increase in glycosylation of IFN-γ harvested after the mid-exponential growth phase. These results show that glycosylation in CHO cells cannot be readily manipulated by Dol-P feeding under normal culture conditions, and suggest that N-linked glycoprotein biosynthesis is tightly regulated in these cells. The implications of these findings, and a possible mechanism to explain the results are discussed.

## 5.2 INTRODUCTION

Asparagine-linked (N-linked) glycosylation is the most common and extensive modification made to recombinant proteins by eukaryotic cells. This complex intracellular process involves covalent attachment of oligosaccharides to newly synthesized polypeptides and subsequent modifications to these carbohydrate structures through the addition and removal of sugars. Glycosylation confers important features to proteins, such as protease resistance, thermal stability and solubility (reviewed by Varki, 1993). The biopharmaceutical industry is particularly interested in glycosylation because it can influence the blood plasma clearance rate, antigenicity and other biological activities of their glycoprotein products (reviewed by Lis and Sharon, 1993). The ability of mammalian cells to impart favorable glycosylation patterns to proteins is often cited as the primary reason for choosing mammalian cells over other expression systems for the commercial production of recombinant human protein therapeutics.

The dolichol pathway in the endoplasmic reticulum (ER) initiates biosynthesis of N-linked glycoproteins (Hirschberg and Snider, 1987). As illustrated schematically in Figure 5-1, oligosaccharides used in N-glycosylation are first assembled on dolichol monophosphate (Dol-P), a long-chain polyisoprenoid lipid in the ER membrane. By serving as the ER anchor to which sugars can be enzymatically attached by ER-bound glycosyltransferases, Dol-P is of crucial importance in the dolichol pathway. The assembly of the Dol-P bound oligosaccharide begins with the synthesis of N-acetylglucosaminylpyrophosphoryl dolichol (GlcNAc-P-P-Dol) catalyzed by the ER enzyme GPT. This reaction is subsequently followed by the addition of one equivalent of GlcNAc from uridine diphospho-N-acetylglucosamine (UDP-GlcNAc), five equivalents



of mannose from GDP-mannose, four equivalents of mannose from mannose-P-dolichol, and three equivalents of glucose from glucose-P-dolichol to the GlcNAc-P-P-Dol. The final product of the dolichol pathway is a lipid-linked oligosaccharide (LLO) composed of 14 monosaccharides ( $\text{Glc}_3\text{Man}_9\text{GlcNAc}_2$ ) linked via pyrophosphate bonds to dolichol. The lipid-linked oligosaccharide (LLO) subsequently functions as the oligosaccharide donor in protein glycosylation.

During the critical step in N-linked glycoprotein formation, the oligosaccharide moiety ( $\text{Glc}_3\text{Man}_9\text{GlcNAc}_2$ ) is transferred *en bloc* from dolichol pyrophosphate to an asparagine residue in the Asn-Xaa-Ser/Thr consensus sequence (where Xaa can be any amino acid except proline) of a nascent protein. However, the presence of this consensus sequence does not automatically ensure that an oligosaccharide will be attached to the side chain of the asparagine residue. It is often the case, both in cultured cells and *in vivo*, that at a specific Asn-Xaa-Ser/Thr consensus sequence in a particular protein, this glycosylation reaction would occur for some molecules, but not for other molecules of the same protein. In this way, identical potential glycosylation sites on different molecules of the same protein are often utilized to variable extents. Therefore, a given protein is often produced as a set of glycoforms---identical polypeptides that differ in the number of attached oligosaccharide chains (Rudd and Dwek, 1997). This variability in glycosylation site occupancy is referred to as “macroheterogeneity,” or simply “site occupancy heterogeneity.”

After oligosaccharides are attached to proteins, they undergo a series of sugar trimming and addition reactions in the ER and Golgi. Since each reaction is catalyzed by a specific enzyme, and does not always proceed to completion, the variety of

glycosylation variants incrementally increases with each step along the glycosylation pathway. In addition, different enzymes sometimes compete for the same glycoprotein substrate, thereby further extending the number of probable outcomes. The resulting variations in oligosaccharide structures at each glycosylation site is known as “microheterogeneity.” By the time proteins exit the glycosylation pathway through secretory vesicles originating from the Golgi, they may have encountered about 60 different glycosylation reactions.

An additional degree of complexity is introduced to the glycosylation process by differences in the availability and activity of glycosidases and glycosyltransferases among various host cell-types (reviewed by Jenkins et al., 1996). The same recombinant protein can differ significantly in glycosylation when expressed in yeast, insect and mouse cells since different expression systems often impart different glycosylation patterns to the same protein. Among established mammalian cell lines, Chinese Hamster Ovary (CHO) cells generate recombinant proteins with glycosylation patterns that most closely resemble the naturally occurring human forms (Utsumi et al., 1989). Since non-human glycosylation patterns are potentially immunoreactive (reviewed in Goochee et al., 1991), the ability of CHO cells to impart human-type glycosylation structures to their proteins has contributed to the preeminence of the CHO cell line in the recombinant human therapeutic protein industry.

Although the N-linked glycosylation process possesses numerous stochastic elements, the overall outcome can be consistent for a specified cell culture process----i.e., the distribution of glycoforms is reproducible for a particular glycoprotein produced and purified under identical conditions. However, an intentional or unintentional change in

bioprocess conditions can lead to altered sets of glycoforms. Within a specific cell culture process, glycosylation heterogeneity is affected primarily by cell culture conditions, such as dissolved oxygen tension (Kunkel et al., 2000), pH (Borys et al., 1993), ammonia (Borys et al., 1994), glucose starvation (Elbein, 1987) and culture length (Hooker et al., 1995).

Information regarding the control of the glycosylation pathway remains inconclusive even though the individual glycosylation reactions and the function of Dol-P have been characterized in detail. In particular, the biosynthesis of LLO in the dolichol pathway has been the subject of numerous studies. Since LLOs are the oligosaccharide donors in the critical glycosyl transfer step in N-linked glycosylation, their availability should be a key regulatory mechanism for controlling the extent of glycosylation site occupancy. A structured kinetic model of N-linked glycosylation demonstrated the dependence of site occupancy on LLO availability (Shelikoff et al., 1996). Inadequate formation or excessive degradation of LLOs can result in LLO shortages and consequently limit the cellular glycosylation capacity (Spiro and Spiro, 1991). At the minimum, active synthesis of LLO in mammalian cells requires sufficient cytosolic pools of the pertinent sugar nucleotides, adequate ER pools of Dol-P, and 16 glycosyltransferases. It remains unclear which elements in the intricate dolichol pathway are rate-controlling for LLO synthesis.

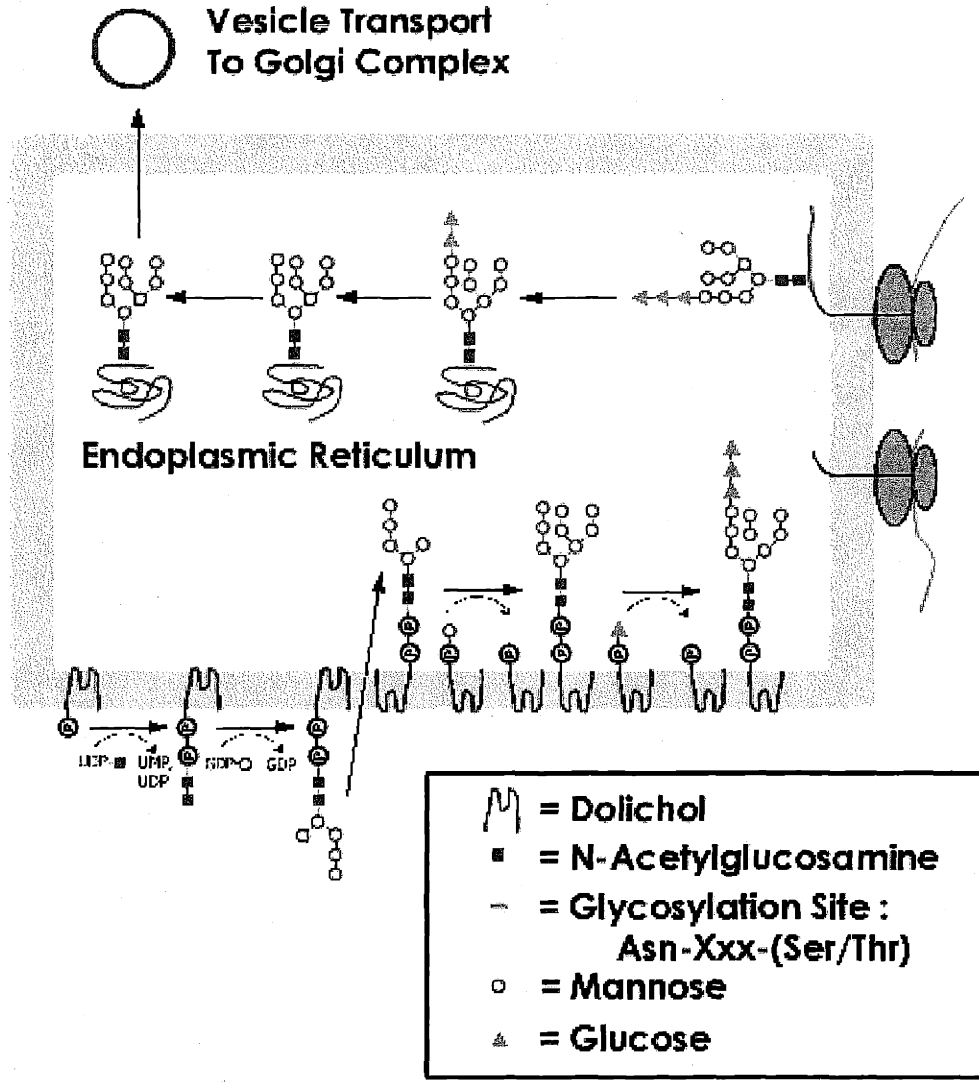


**Figure 5-1.** Schematic of the N-linked glycosylation pathway in the endoplasmic reticulum. The sequential addition of monosaccharides to dolichol phosphate (Dol-P) in the dolichol pathway generates a lipid-linked oligosaccharide (LLO). During the initial step in N-linked glycosylation, the oligosaccharide is transferred from Dol-P to a potential glycosylation site on a newly synthesized polypeptide.

The essential role Dol-P plays as a glycosyl carrier in the lipid intermediate pathway for glycoprotein synthesis suggests that the intracellular amount of Dol-P may determine the flux through the glycosylation pathway by controlling LLO availability. Support for this hypothesis has come from many different lines of investigations. Correlations between Dol-P levels and glycoprotein synthesis were clearly shown in studies on the developmental changes in oviducts of hormone-treated chicks (Lucas and Levin, 1977) and embryos of sea urchins (Carson and Lennarz, 1979).

Studies on the impact of exogenous Dol-P supplementation on mammalian cultures provided the most direct evidence for the regulatory role of Dol-P in lipid intermediate and N-linked glycoprotein biosynthesis. Preincubation of mouse LM cells with Dol-P (5  $\mu\text{g/ml}$ ) resulted in a three-fold stimulation of LLO synthesis (Grant and Lennarz, 1983), indicating that Dol-P is one limiting factor for LLO synthesis *in vivo*. Supplementation of culture medium with 20  $\mu\text{g/ml}$  Dol-P enhanced protein glycosylation in hen oviduct and bovine pancreas tissue slices, without any effects on protein synthesis (Carson et al., 1981). This exogenous supply of Dol-P (20  $\mu\text{g/ml}$ ) resulted in an approximately two-fold increase in the overall incorporation of labeled sugar into TCA-precipitated glycoproteins by hen oviduct tissues and a four-fold elevation in the sugar content of ribonuclease secreted by bovine pancreatic tissues. Similar findings were observed in dispersed rat parotid gland acinar cells (Kousvelari et al., 1983). Incubation of cells with exogenously supplied Dol-P had no impact of protein secretion, but led to dose-dependent increases in protein glycosylation; incorporation of radiolabeled mannose into total TCA-precipitated glycoproteins was increased by three-fold at Dol-P concentrations of 10  $\mu\text{g/ml}$ , and five-fold at the maximum Dol-P concentration of 100

$\mu\text{g/ml}$  in the culture medium. Supplementation of Madin-Darby canine kidney (MDCK) cell cultures with exogenous Dol-P stimulated mannose incorporation into both LLOs and glycoproteins by over 150% at 2.5  $\mu\text{g/ml}$ , and 250% at 10  $\mu\text{g/ml}$  (Pan and Elbein, 1990).

Despite the overwhelming literature evidences indicating that cellular levels of Dol-P in mammalian cells are subsaturating, the role of Dol-P in controlling glycosylation in CHO cells under normal culture conditions has not been investigated. This work was conducted to determine if glycosylation in typical CHO batch cultures is limited by Dol-P availability.

The model system used in this study was a recombinant CHO cell line transfected with the human interferon-gamma (IFN- $\gamma$ ) gene. N-linked glycosylation patterns in recombinant IFN- $\gamma$  secreted by these cells was previously characterized by other members of this laboratory (Nyberg, 1998; Gu et al., 1997). This human antiviral therapeutic protein contains potential N-linked glycosylation sites at Asn 25 and Asn 97. As a result of variable occupancy at both potential glycosylation sites, IFN- $\gamma$  can exist in three forms differing in N-linked glycosylation status: doubly glycosylated at Asn 25 and Asn 97, singly glycosylated almost exclusively at Asn 25, or non-glycosylated. Various researchers, including Nyberg from this laboratory, observed a reproducible gradual decline in IFN- $\gamma$  N-linked glycosylation site occupancy over the course of batch and fed-batch cultures of recombinant CHO cells: the proportion of doubly glycosylated IFN- $\gamma$  decreased by 9-25% during the exponential growth phase (Castro et al., 1995; Curling et al., 1990; Goldman et al., 1998; Hooker et al., 1995, Nyberg, 1998). This deterioration in glycosylation did not arise from extracellular degradation of product (Curling, et al.,

1990), nor could it be overcome by supplementation of the cultures with extra nutrients, such as glucose and glutamine (Curling, et al., 1990; Hayter et al., 1991). Certain lipid supplements could minimize the glycosylation changes, but the underlying mode of action was not understood (Jenkins et al., 1994). Research from this laboratory demonstrated that this phenomenon was not caused by the depletion of nucleotide sugars since intracellular nucleotide sugar pools increased concomitant with the decline in IFN- $\gamma$  glycosylation (Nyberg, 1998).

To test the hypothesis that glycosylation in batch cultures of CHO cells is regulated by Dol-P availability, the impact of exogenous Dol-P supplementation was studied in CHO cells. First, the uptake and incorporation of exogenous Dol-P into LLO by CHO cells was verified. Next, the impact of increasing concentrations of Dol-P on the cultures was examined to establish the maximum non-toxic doses of exogenous Dol-P that the cells could tolerate, and thereby determine the amounts of Dol-P that should be for feeding studies. Third, the effects of Dol-P on LLO and overall cellular glycosylation levels in CHO cells were determined. Fourth, the dependence of IFN- $\gamma$  glycosylation macro- and micro-heterogeneity on exogenous Dol-P levels was investigated. The knowledge acquired in this work will establish the applicability of using Dol-P supplementation to control glycosylation in CHO cells, and guide the development of strategies for producing recombinant glycoproteins from CHO cultures with consistent glycosylation.

## **5.3 MATERIALS AND METHODS**

### **5.3.1 CHO Cell Line and Culture**

Recombinant human IFN- $\gamma$  was produced by a CHO cell line obtained from Dr. Walter Fiers of the University of Ghent, Belgium (Scahill et al., 1983). These cells, referred to as  $\gamma$ -CHO cells, were adapted to suspension growth in two serum-free media, either CHO-S-SFM II (Gu et al., 1997) or RPMI-SFM (Nyberg et al., 1999). All cultures were performed in batch mode in shake flasks agitated at 70 rpm in a 37°C incubator with 5-10% CO<sub>2</sub> overlay. For each separate experiment, a vial of frozen  $\gamma$ -CHO cells was taken from a working cell bank and inoculated in serum-free medium. The cells were subsequently passaged 2-4 times and maintained at greater than 95% viability until enough cells were obtained to start the experiment. In this way, all cells used within an experiment had the same culture history.

### **5.3.2 Dol-P Supplementation**

Unlabeled Dol-P was obtained from a commercial source (Sigma) dissolved in chloroform/methanol (2:1). Prior to use, the organic solvents were removed on a high vacuum line. The remaining yellow oil was redissolved in dimethylsulfoxide (DMSO) before insertion into the culture medium. Serial dilution of Dol-P with DMSO was subsequently performed to obtain different concentrations of Dol-P in DMSO. To trace the uptake and incorporation of Dol-P by CHO cells, <sup>3</sup>H Dol-P (American Radiolabeled Chemicals, Inc.) was used; it was purchased dissolved in DMSO. The shake flask containing the medium was always agitated vigorously when Dol-P (dissolved in DMSO) was added directly into it in order to enhance dispersion of Dol-P in the culture medium.



The medium in control flasks contained 0.5% (v/v) DMSO, while medium in test flasks contained 0.5% (v/v) DMSO mixed with Dol-P of various amounts, depending on the experiment. The flasks were always agitated at 70 rpm in a 37°C incubator with 10% CO<sub>2</sub> overlay for one hour prior to starting each experiment.

#### **5.3.4 Determination of Cell Density, Viability and Mode of Cell Death**

Cells were counted with a hemacytometer and microscope, and a Coulter electronic particle counter (Coulter Electronics, Hialeah, FL). Cell viabilities were determined by staining samples with trypan blue: viable cells exclude the dye, whereas non-viable cells lose their membrane integrity and were stained blue. The mode of cell death was studied by morphological examination of cells stained with acridine orange/ethidium bromide (AO/EB) dye (Mercille and Massie, 1994). By determining the integrity of both the membrane and DNA of cells, this assay is able to distinguish between the four different types of cells---viable cells, necrotic cells, early and late apoptotic cells.

#### **5.3.4 Analyses of IFN- $\gamma$ Glycosylation and Concentration**

Glycosylation macroheterogeneity of accumulated IFN- $\gamma$  was determined by the immunoprecipitation of IFN- $\gamma$  from culture supernatants and analysis of the purified protein by means of micellar electrokinetic capillary chromatography (MECC), as described in detail by Nyberg et. al. (1999). Following the method previously developed in this laboratory, a combination of immunoaffinity, reversed-phase and neutral reversed-phase high performance liquid chromatography was employed to analyze glycosylation

microheterogeneity (Gu et al., 1997). Concentrations of IFN- $\gamma$  were measured with an ELISA kit (Biosource International, Camarillo, CA).

### **5.3.5 Cell Cycle Analyses**

Cell cycle distributions were determined by following the procedure below. A total of  $1 \times 10^6$  cells from a culture flask was centrifuged and resuspended in 0.5 ml stain solution. This solution contained 1.5% polyethylene glycol-4000 (PEG-4000), 1.5% PEG-8000, 50  $\mu$ g/ml propidium iodide, 180 units/ml RNAase, 0.1% Triton-X-1000, and 4 mM sodium citrate; the final pH of solution was adjusted to 7.2. After a 20-minute incubation at 37°C, 0.5 ml salt solution was added (1.5% PEG-4000, 1.5% PEG-8000, 50 mg/ml propidium iodide, 0.1% Triton-X-1000, 0.4 M sodium chloride, and final pH of solution was adjusted to 7.2). For the next 12 to 36 hours, the sample was stored in the dark at 4°C. Cell sorting was performed on a FACScan flow cytometer (Becton Dickinson, San Jose, CA). Raw data was processed with ModFit Lt. v.2 analysis software (Verity Software House, Topsham, ME) to determine cell cycle distributions.

### **5.3.6 Determination of Glucose and Lactate Concentrations**

Filtered samples of cell culture supernatants were frozen at -20°C until ready for metabolite analyses. Glucose and lactate concentrations in the thawed samples were measured directly by the YSI 23000 STAT Plus Glucose & Lactate Analyzer (YSI Life Sciences).

### **5.3.7 LLO and Cellular Protein Extractions**

Between 5-10 million cells were taken from each culture for extraction of LLO and cellular protein based on a well-established sequential extraction procedure (Bhat and Waechter, 1988; Hubbard and Robbins, 1979; Lucas et al., 1975). Briefly, the cells were first rinsed with ice-cold PBS. Next, the cell pellet was soaked three times in  $\text{CHCl}_3/\text{CH}_3\text{OH}$  (2:1), and then washed with water. Finally, LLOs were extracted from the partially delipidated cell pellet by  $\text{CHCl}_3/\text{CH}_3\text{OH}/\text{H}_2\text{O}$  (10:10:3). The residue remaining after lipid extraction contained cellular proteins. After precipitating the proteins with cold 10% w/v trichloroacetic acid (TCA), 0.5 ml hot 1N NaOH was added to dissolve the proteins.

### **5.3.8 Radioactivity Measurements**

Radioactivity was measured in disintegrations per minutes (DPM) with an LS 6500 Liquid Scintillation Counter (Beckman Instruments, Fullerton, CA). Organic solvents were removed from radiolabeled LLO extracts by drying in a fume hood prior to liquid scintillation counting. Unless otherwise stated, 20 ml of the scintillation cocktail Ultima Gold (Packard Instrument Company) was used to dissolve the radiolabeled samples.

### **5.3.9 Uptake and Incorporation of exogenous $^3\text{H}$ Dol-P into LLO by CHO cells**

Prior to starting the time-course experiment, labeled and unlabeled forms of Dol-P were mixed and then serially diluted with DMSO such that varying Dol-P concentrations were generated. This method made it possible to supply different concentrations of Dol-P to the culture medium while keeping the total amount of DMSO added to the medium

constant at 0.5% v/v. By spiking cold Dol-P with  $^3\text{H}$  Dol-P (20 Ci/mmol) such that 0.4% of the total lipid supplied to each culture was  $^3\text{H}$  Dol-P, the radiolabeled tracer provided an easy means of monitoring the cellular uptake and metabolism of Dol-P. In this experiment, four CHO cultures were run simultaneously. All flasks contained 0.5% v/v DMSO in CHO-S-SFM II medium. The first flask served as the control, while other three flasks contained increasing concentrations of Dol-P (of which 0.4% was radiolabeled). Varying concentrations of Dol-P in DMSO were added to these three flasks and incubated with shaking for 2 hours prior to starting the experiment. At the start of the experiment,  $\gamma$ -CHO cells growing exponentially in a single flask of CHO-S-SFM II medium were divided into four centrifuge tubes, spun down and resuspended at approximately  $3.8 \times 10^5$  cells/ml into each of the four separate flasks. One hour into the experiment, three samples (50  $\mu\text{l}$  each) were drawn at random from each culture flask and assayed for  $^3\text{H}$  Dol-P radioactivity by liquid scintillation counting. The random sampling served to ascertain even distribution of the exogenous lipid in the aqueous medium, and to verify the actual amount of  $^3\text{H}$  Dol-P supplied to the medium. The amount of Dol-P present in each flask was calculated from the corresponding  $^3\text{H}$  Dol-P radioactivities measured, using the assumption that 0.4% of the supplemental lipid in the medium was radioactive. Subsequently, samples were taken from each flask for cell counting and LLO extraction at 24-hour intervals.

#### **5.3.10 Distribution of $^3\text{H}$ Dol-P in CHO cells and Impact of Dol-P on IFN- $\gamma$ Glycosylation**

Suspension CHO cells cultured in CHO-S-SFM II medium were divided into four flasks (each containing  $3.0 \times 10^5$  cells/ml) for radiolabeling studies. One flask served as the

control, while the other three test flasks contained 60 µg/ml, 100 µg/ml and 180 µg/ml Dol-P. In the test flasks, cold Dol-P was spiked with 0.07% <sup>3</sup>H Dol-P (15 Ci/mmmole) such that the flasks contained 4 µCi, 7 µCi and 12 µCi, respectively, of radiolabel in 10 ml of medium. After 62 hours of incubation at 37°C, the cells were separated from the medium by centrifugation. The cell pellet from each flask was washed four times with PBS and then divided into three fractions. The cell pellet in the first fraction was used to measure bulk cellular radioactivity. It was first incubated at 37°C for 3 hours with 0.5 ml tissue solubilizer (BTS-450, Beckman Coulter, Inc., Fullerton, CA). A drop of glacial acetic acid and 6 ml of Ready Organic scintillation fluid (Beckman Coulter, Inc., Fullerton, CA) were then added to the cell digest, after which the sample was ready for scintillation counting. The second fraction was used to determine radioactivity incorporated into microsomes by employing a standardized procedure to extract microsomes from the cell pellet (Kamath and Narayan, 1972). The cell pellet was first resuspended in ice-cold 0.25 M sucrose and homogenized by sonication. It was then transferred to a microcentrifuge tube for centrifugation (10,800 rpm; 2 × 10 minutes). The supernatant was collected, mixed with 1 ml 0.25 M sucrose containing 16 mM CaCl<sub>2</sub>, and allowed to sit at room temperature for 5 minutes. After centrifugation for 3 minutes at 10,800 rpm, the supernatant was removed and the microsomal pellet was dissolved in 6 ml Universol ES Scintillation Cocktail (ICN Radiochemicals) in preparation for scintillation counting. The third fraction was assayed for [<sup>3</sup>H]Dol-P that had been incorporated into LLO by the CHO cells. The LLO was extracted as described above. Culture supernatant was filtered and frozen at -20°C until it was thawed for IFN-γ glycosylation and concentration analyses.

### **5.3.11 Effects of Dol-P supplementation on Cell Cycle, Growth and Viability of CHO cells**

Cells cultured in CHO-S-SFM II were seeded at  $3.5 \times 10^5$  cells/ml into 3 different flasks containing 0  $\mu\text{g/ml}$  (control), 140  $\mu\text{g/ml}$  and 240  $\mu\text{g/ml}$  Dol-P, respectively. Samples were taken from the flasks daily for (i) cell counting, (ii) determination of cell viability and mode of cell death, and (iii) cell cycle analysis.

### **5.3.12 Impact of Dol-P Supplementation on LLO and Cellular Glycosylation Levels**

#### **5.3.12.1 RPMI-SFM Cultures**

Fresh RPMI-SFM containing 5.9  $\mu\text{Ci/ml}$  D-[ $U\text{-}^{14}\text{C}$ ] glucose (American Radiolabeled Chemicals) and 1.3  $\mu\text{Ci/ml}$  L- $^3\text{H}$  leucine (Amersham Pharmacia Biotech) was transferred into 3 identical shake flasks. One flask served as the control, and the other two flasks were supplemented with 20  $\mu\text{g/ml}$  and 40  $\mu\text{g/ml}$  unlabeled Dol-P respectively. The flasks were then incubated at 37°C with shaking (70 rpm) for one hour before starting the experiment. At the beginning of the experiment,  $\gamma$ -CHO cells that had been growing exponentially in a shake flask containing unlabeled RPMI-SFM were equally divided into three centrifuge tubes and collected by centrifugation (5 min,  $200 \times g$ ). Each cell pellet was resuspended at  $2.7 \times 10^5$  cells/ml in one of the three flasks containing labeled RPMI-SFM and varying amounts of Dol-P. Samples were subsequently taken from each of the three flasks at regular time points for cell enumeration as well as extraction of LLOs and cellular proteins. The experiment was ended after 90 hours of culture when culture viabilities were below 50%.

### **5.3.12.2 CHO-S-SFM II Cultures**

Fresh CHO-S-SFM II containing 10.4  $\mu\text{Ci/ml}$  D-[U- $^{14}\text{C}$ ] glucose (American Radiolabeled Chemicals) and 4.3  $\mu\text{Ci/ml}$  L- $^3\text{H}$  leucine (Amersham Pharmacia Biotech) was transferred into 4 identical shake flasks. One flask served as the control, and the other three flasks were supplemented with increasing amounts of unlabeled Dol-P to give final concentrations of 20  $\mu\text{g/ml}$ , 50  $\mu\text{g/ml}$ , and 100  $\mu\text{g/ml}$  Dol-P respectively. The flasks were then incubated at 37°C with shaking (70 rpm) for one hour before starting the experiment. At the beginning of the experiment,  $\gamma$ -CHO cells that had been growing exponentially for 21 hours in a shake flask of labeled CHO-S-SFM II containing 10.4  $\mu\text{Ci/ml}$  D-[U- $^{14}\text{C}$ ] glucose and 4.3  $\mu\text{Ci/ml}$  L- $^3\text{H}$  leucine were equally divided into three centrifuge tubes and collected by centrifugation (5 min, 200  $\times$  g). Each cell pellet was resuspended at  $(3-4) \times 10^5$  cells/ml into one of the four flasks containing fresh CHO-S-SFM II supplemented with 10.4  $\mu\text{Ci/ml}$  D-[U- $^{14}\text{C}$ ] glucose, 4.3  $\mu\text{Ci/ml}$  L- $^3\text{H}$  leucine and varying amounts of Dol-P. Samples were subsequently taken from each of the four flasks at regular time points for various measurements. The cells were separated from the culture supernatant and used for cell enumeration in addition to the extraction of LLOs and cellular proteins. The supernatant was filtered and stored at -20°C until it was used for future metabolite analyses.

### **5.3.13 IFN- $\gamma$ Glycosylation Time Profile Studies**

Fresh CHO-S-SFM II was mixed with varying amounts of Dol-P to yield final concentrations of 0  $\mu\text{g/ml}$  (control), 20  $\mu\text{g/ml}$ , 50  $\mu\text{g/ml}$  and 100  $\mu\text{g/ml}$ , respectively, of

Dol-P in four separate flasks. These flasks were then preincubated at 37°C with shaking (70 rpm) for one hour. To start the experiment, cells from a CHO-S-SFM II batch culture were inoculated at  $3.5 \times 10^5$  cells/ml into the four separate flasks. Samples were taken daily from the flasks for cell counting, IFN- $\gamma$  concentration and glycosylation determination. The last measurements were taken at 100 hours, when viabilities of all the cultures were less than 10%.

## 5.4 RESULTS

### 5.4.1 Uptake and Incorporation of Exogenous $^3\text{H}$ Dol-P into LLO by CHO cells

The uptake of exogenous Dol-P had been demonstrated in several types of mammalian cells and tissues, but not in CHO cells (Carson et al., 1981; Grant and Lennarz, 1983; Kousvelari et al., 1983; Pan and Elbein, 1990). This experiment was conducted to determine the ability of CHO cells to incorporate exogenous Dol-P supplied in the manner described. To this end, cold Dol-P was spiked with  $^3\text{H}$  Dol-P, such that 0.4% of total Dol-P used was tritium-labeled. The radioactivity in  $^3\text{H}$  Dol-P provided a convenient means of monitoring the uptake and metabolism of exogenous Dol-P by CHO cells.

To ascertain the effectiveness of the method used here in evenly distributing the exogenous lipid throughout the aqueous culture medium, three samples were drawn at random from each culture flask and assayed for  $^3\text{H}$  Dol-P radioactivity. The random samplings confirmed that the treatment used in this work was successful in dispersing supplemental Dol-P throughout the culture;  $^3\text{H}$  DPM measured in the three samples from each flask varied by less than 10% (data not shown). The radioactivity measurements of the culture flasks showed that they contained 0  $\mu\text{Ci/ml}$ , 0.59  $\mu\text{Ci/ml}$ , 0.85  $\mu\text{Ci/ml}$  and



1.74  $\mu\text{Ci/ml}$  [ $^3\text{H}$ ]Dol-P, which corresponded to 0  $\mu\text{g/ml}$ , 12  $\mu\text{g/ml}$ , 17  $\mu\text{g/ml}$  and 35  $\mu\text{g/ml}$  respectively, of Dol-P.

Radioactivities in the LLO extracts increased in proportion to the exogenous concentration of supplemental  $^3\text{H}$  Dol-P and Dol-P (Figure 5-2). This shows that exogenous Dol-P was taken up by CHO cells and processed into LLOs, the oligosaccharide donor in N-linked glycosylation, in a dose-dependent manner. Since LLOs were formed in the ER by the sequential addition of monosaccharides to Dol-P catalyzed by ER enzymes, these results indicate that the cells were able to transport exogenous Dol-P from the cell surface to ER membranes.

Cell density and viability profiles show that at the range of Dol-P concentrations used in this experiment, exogenous Dol-P had negligible impact on CHO cell growth and survival (Figure 5-3).

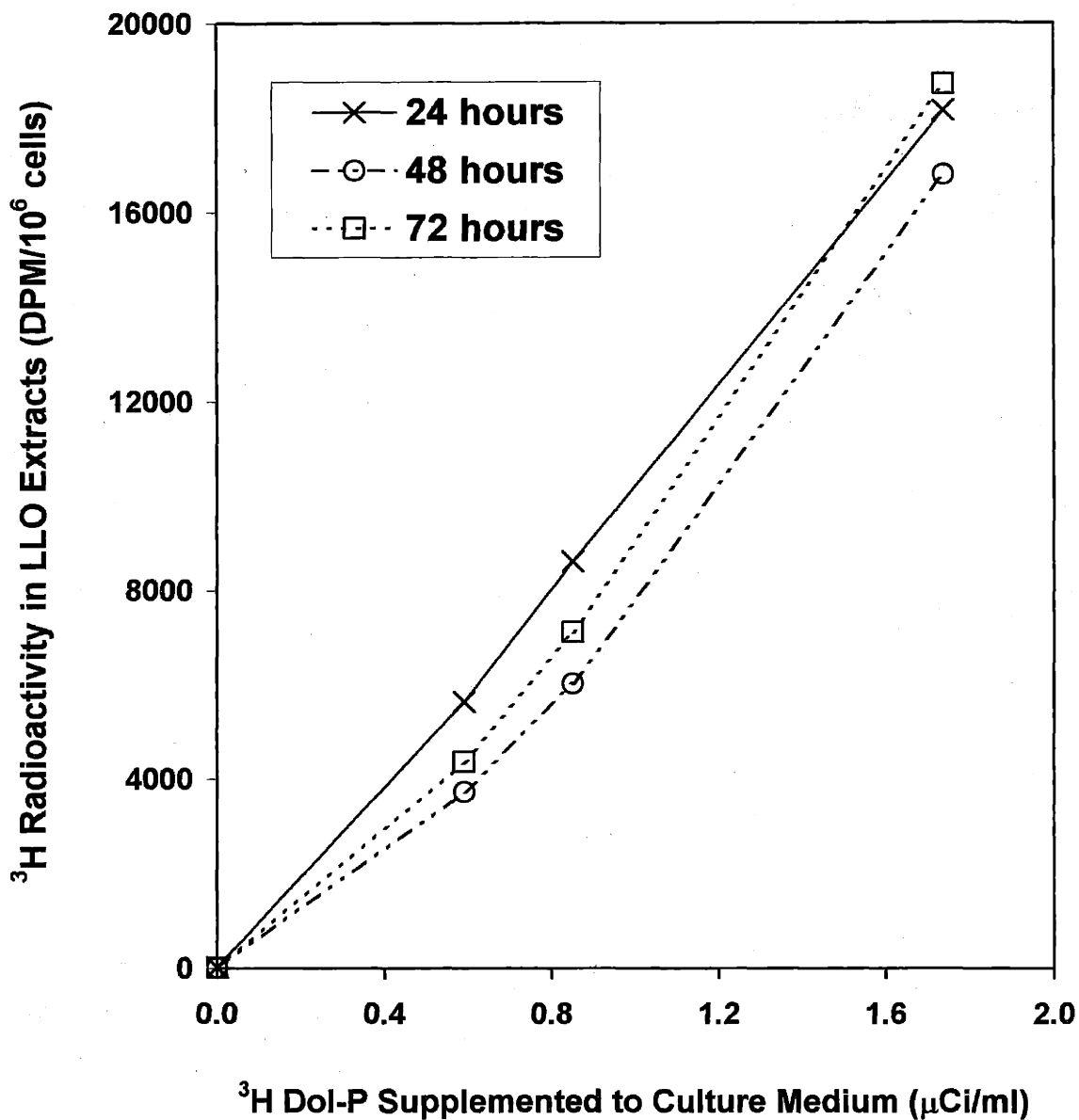


**Figure 5-2.** Uptake and incorporation of <sup>3</sup>H Dol-P into LLO by CHO cells. Four batch cultures of  $\gamma$ -CHO cells in CHO-S-SFM II cultures supplemented with varying amounts of exogenous Dol-P were run simultaneously. The concentrations of supplemental Dol-P in the culture medium were 0  $\mu$ g/ml, 12  $\mu$ g/ml, 17  $\mu$ g/ml and 35  $\mu$ g/ml, of which 0.4% was in the form of <sup>3</sup>H Dol-P. The corresponding amounts of <sup>3</sup>H Dol-P added to each culture were 0  $\mu$ Ci/ml, 0.59  $\mu$ Ci/ml, 0.85  $\mu$ Ci/ml and 1.74  $\mu$ Ci/ml.

#### 5.4.2 Distribution of $^3\text{H}$ Dol-P in CHO cells and Impact of Dol-P on IFN- $\gamma$ Glycosylation

Incubations of mammalian cells and tissues with exogenous Dol-P typically involved less than 20  $\mu\text{g/ml}$  Dol-P (Carson et al., 1981; Grant and Lennarz, 1983; Pan and Elbein, 1990). The highest concentration of exogenous Dol-P used for *in vivo* studies was 100  $\mu\text{g/ml}$  Dol-P (Kousvelari et al., 1983). Kousvelari and coworkers showed that incorporation of radiolabeled mannose into total TCA-precipitated glycoproteins in dispersed rat parotid gland acinar cells was increased three-fold by 10  $\mu\text{g/ml}$  Dol-P, and five-fold at the maximum Dol-P concentration of 100  $\mu\text{g/ml}$  in the culture medium. However, none of the studies investigated the distribution of supplemental Dol-P in the cells, or the impact of high doses of Dol-P on culture viability and recombinant protein glycosylation. This study was conducted to address these issues.

To trace the cellular distribution of exogenously supplied Dol-P, 0.07% of the lipid supplemented to the cultures was tritium-labeled. The four parallel cultures contained 0  $\mu\text{g/ml}$ , 60  $\mu\text{g/ml}$ , 100  $\mu\text{g/ml}$  and 180  $\mu\text{g/ml}$  supplemental Dol-P, corresponding to 0  $\mu\text{Ci/ml}$ , 0.4  $\mu\text{Ci/ml}$ , 0.7  $\mu\text{Ci/ml}$  and 1.2  $\mu\text{Ci/ml}$   $^3\text{H}$  radioactivity. Liquid scintillation counting of whole cell digests showed that bulk cellular radioactivity increased in proportion to the amount of supplemental  $^3\text{H}$  Dol-P (Figure 5-4(A)). Figure 5-4(B) shows the radioactivity measured in microsomes extracted from the cells. For cultures supplemented with 0.4  $\mu\text{Ci/ml}$  and 0.7  $\mu\text{Ci/ml}$   $^3\text{H}$  Dol-P, microsomal radioactivity increased with the amounts of exogenous radiolabel. However, the radioactivity found in microsomes extracted from the culture with 1.2  $\mu\text{Ci/ml}$  of  $^3\text{H}$  Dol-P was less than half of that measured in the culture to which 0.7  $\mu\text{Ci/ml}$   $^3\text{H}$  Dol-P had

been added. To the naked eye, the microsome pellet extracted from the 1.2  $\mu\text{Ci/ml}$   $^3\text{H}$  Dol-P culture was significantly smaller than the microsome pellets extracted from the other three cultures. In agreement with earlier results demonstrating the dose-dependent incorporation of  $^3\text{H}$  Dol-P into precursors for N-linked glycosylation (Figure 5-2), radioactivity in the LLO extracts increased with the amount of supplemental  $^3\text{H}$  Dol-P (Figure 5-4(C)).

Viabilities of cultures were monitored over time by the trypan blue assay (Figure 5-5). After 2 days in culture, cell viability in the presence of 180  $\mu\text{g/ml}$  Dol-P began to drop sharply. At this highest Dol-P concentration, less than 50% of the cells were viable after 62 hours of culture. By contrast, the other three cultures consistently maintained viabilities exceeding 90%. The mode of cell death caused by 180  $\mu\text{g/ml}$  of exogenous Dol-P could not be determined in this experiment since trypan blue staining does not differentiate between apoptotic and necrotic cells.

While the addition of 60  $\mu\text{g/ml}$  and 100  $\mu\text{g/mL}$  of Dol-P to the culture medium appeared to marginally improve the glycosylation of IFN- $\gamma$  accumulated after 60 hours of culture, the highest Dol-P supplementation (180  $\mu\text{g/ml}$ ) had an opposite effect (Figure 5-6). In comparison to the control sample, the percentage of doubly glycosylated IFN- $\gamma$  was approximately 10% higher in the 100  $\mu\text{g/ml}$  Dol-P sample, but it was slightly lower in the 180  $\mu\text{g/ml}$  Dol-P sample.

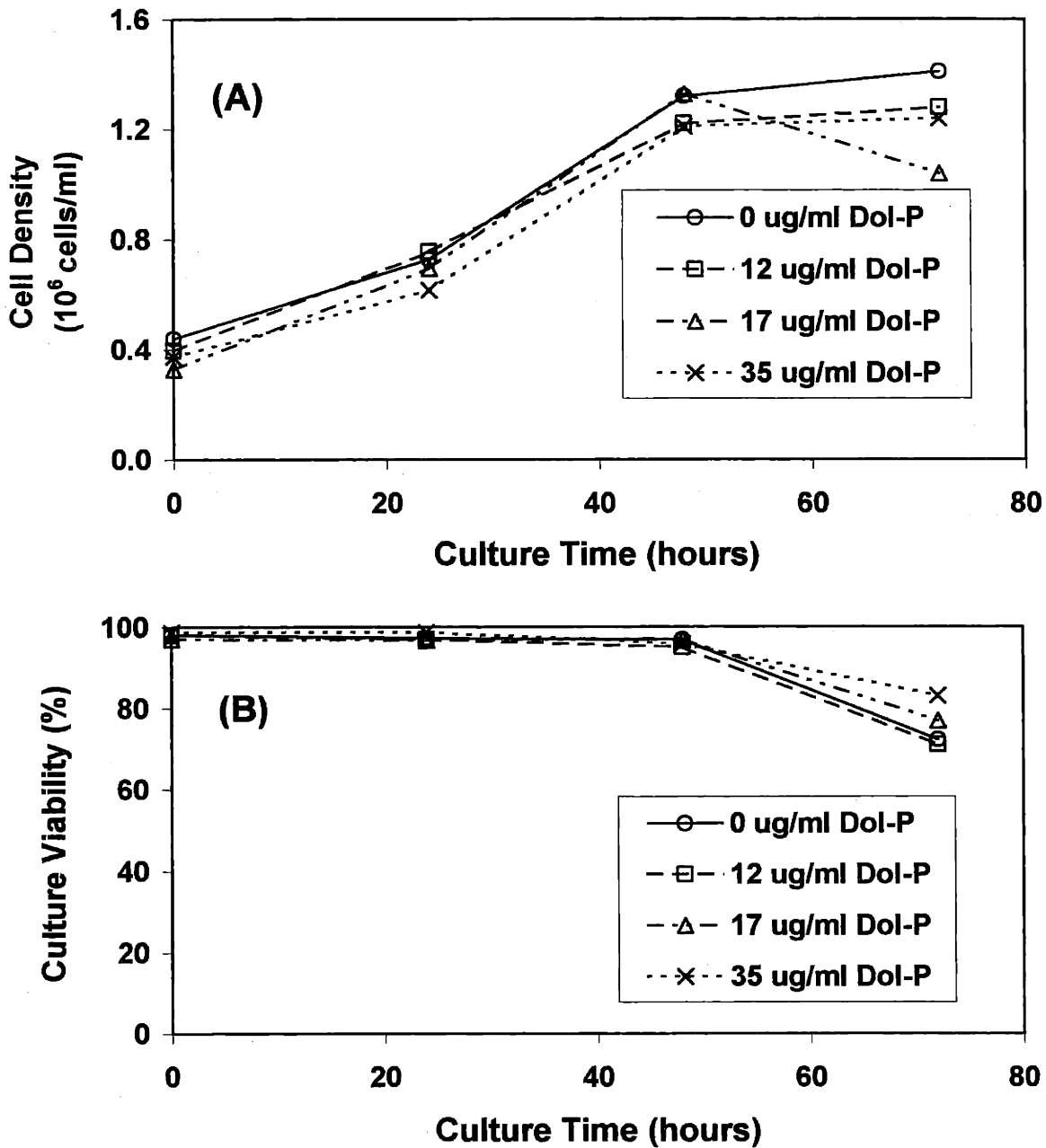


**Figure 5-3.** Total cell density (A), and viability (B) of four parallel batch cultures supplemented with 0  $\mu\text{g/ml}$ , 12  $\mu\text{g/ml}$ , 17  $\mu\text{g/ml}$  and 35  $\mu\text{g/ml}$  Dol-P, respectively. Of the supplemental Dol-P, 0.4% was tritium-labeled. The corresponding concentrations of supplemental  $^3\text{H}$  Dol-P in each culture were 0  $\mu\text{Ci/ml}$ , 0.59  $\mu\text{Ci/ml}$ , 0.85  $\mu\text{Ci/ml}$  and 1.74  $\mu\text{Ci/ml}$ .

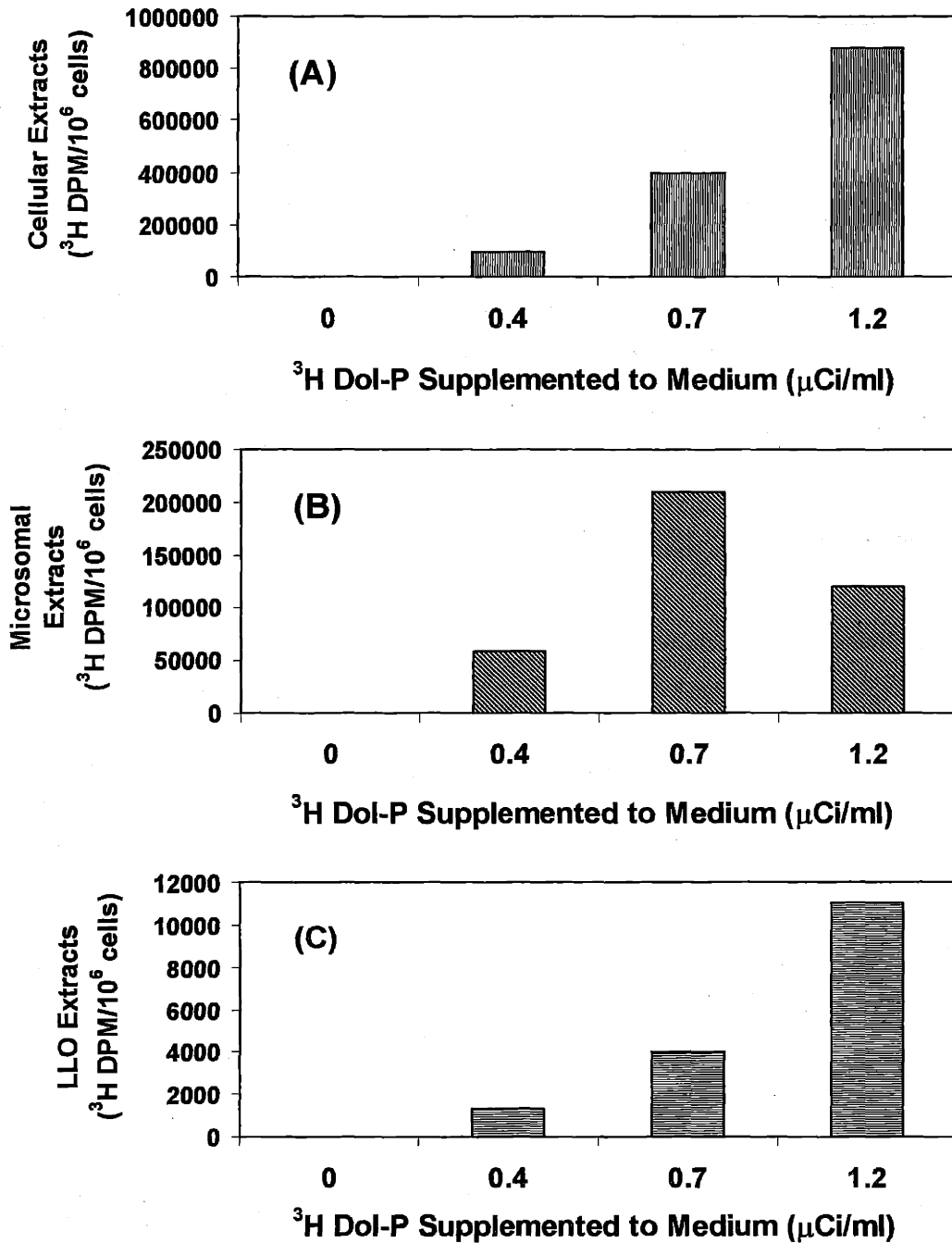


**Figure 5-4.** Distribution of  $^3\text{H Dol-P}$  in cells (A), microsomes (B), and LLO (C) obtained from  $\gamma\text{-CHO}$  batch cultures supplemented with varying amounts of Dol-P. Amounts of supplemental Dol-P ranged from 0  $\mu\text{g/ml}$ , 60  $\mu\text{g/ml}$ , 100  $\mu\text{g/ml}$ , to 180  $\mu\text{g/ml}$ . The exogenous Dol-P was spiked with 0.07%  $^3\text{H Dol-P}$ , such that the corresponding supplemental  $^3\text{H Dol-P}$  concentrations in the cultures were 0  $\mu\text{Ci/ml}$ , 0.4  $\mu\text{Ci/ml}$ , 0.7  $\mu\text{Ci/ml}$ , and 1.2  $\mu\text{Ci/ml}$ .

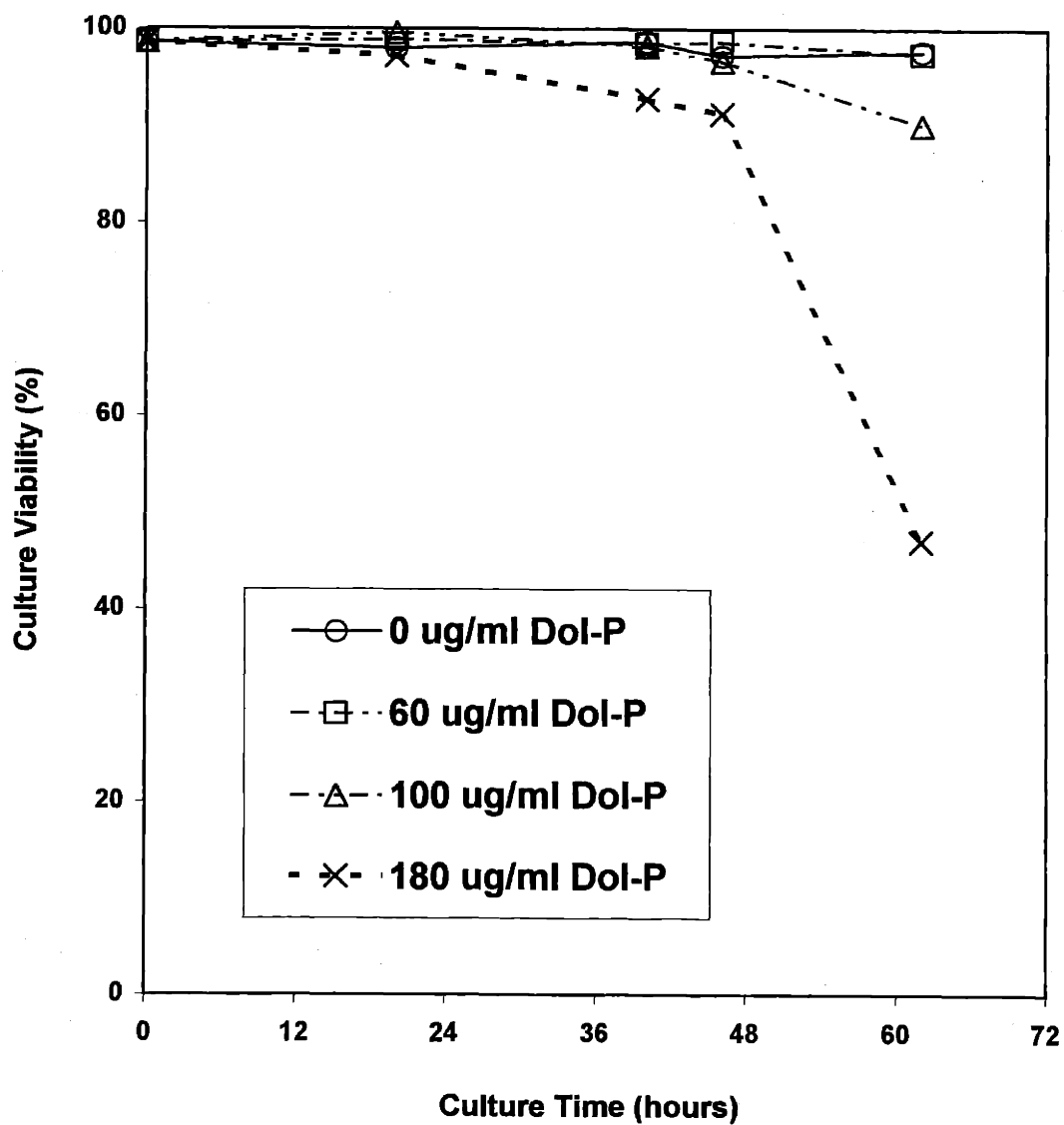


**Figure 5-5.** Viabilities of CHO batch cultures supplemented with varying amounts of Dol-P. The four cultures were run simultaneously and contained 0  $\mu\text{g/ml}$  ( $\circ$ ), 60  $\mu\text{g/ml}$  ( $\square$ ), 100  $\mu\text{g/ml}$  ( $\triangle$ ), and 180  $\mu\text{g/ml}$  ( $\times$ ) supplemental Dol-P. Culture viabilities were determined by trypan blue dye exclusion assay.

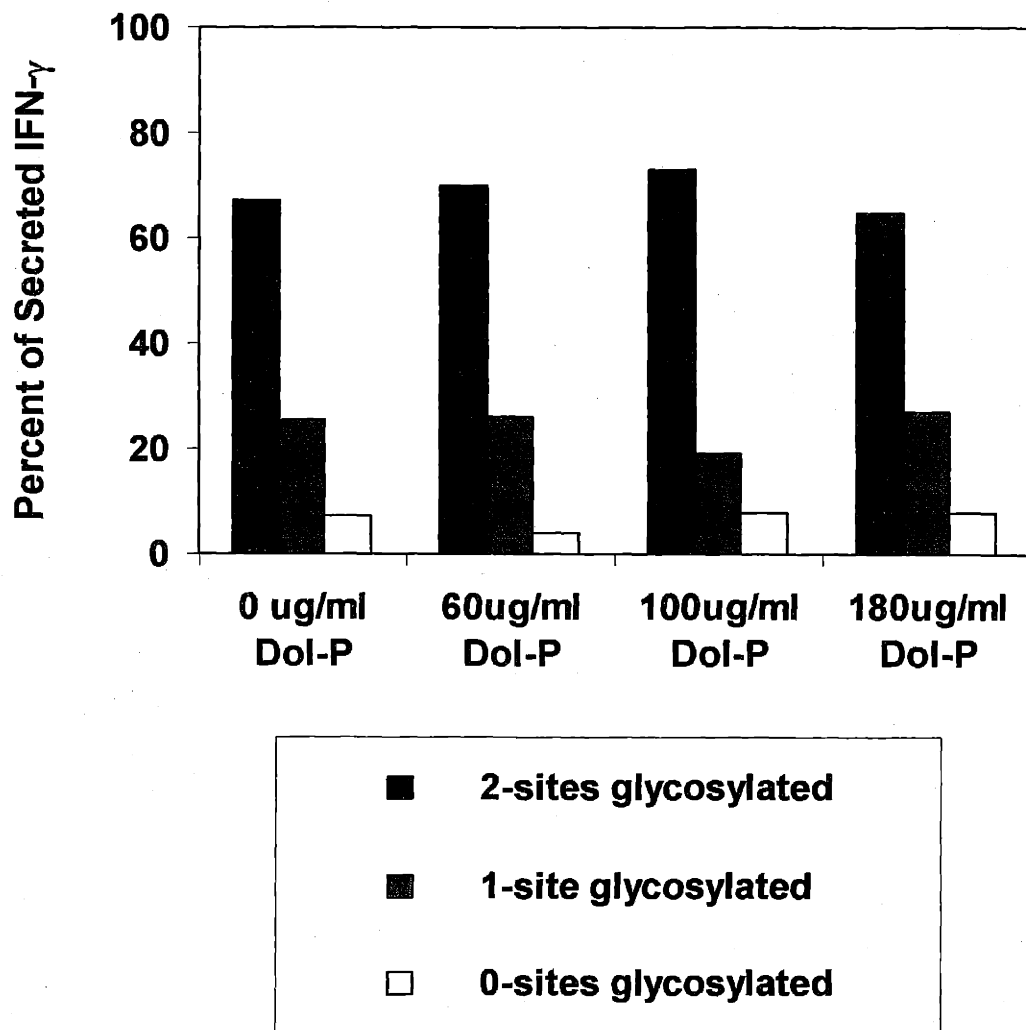


**Figure 5-6.** Glycosylation site occupancy of IFN- $\gamma$  accumulated in medium after 62 hours of batch culture. CHO cells were grown in the presence of 0  $\mu\text{g/ml}$ , 60  $\mu\text{g/ml}$ , 100  $\mu\text{g/ml}$ , and 180  $\mu\text{g/ml}$  supplemental Dol-P. Three forms of recombinant human IFN- $\gamma$  were secreted by the CHO cells, as determined by capillary electrophoresis: 2-sites glycosylated (■), 1-site glycosylated (▣), and 0-sites glycosylated (□).



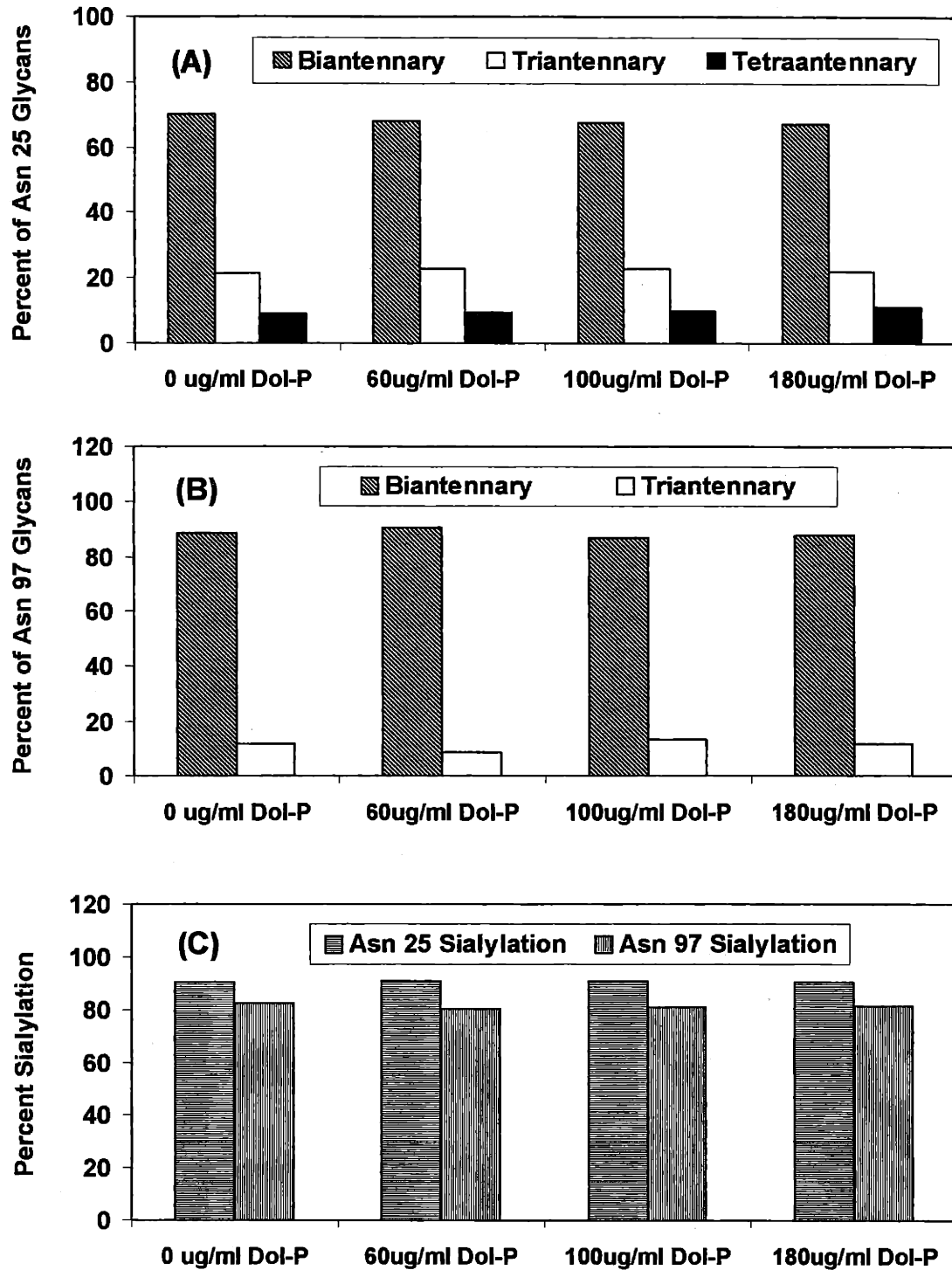


**Figure 5-7.** Glycosylation microheterogeneity of IFN- $\gamma$  secreted by CHO cells after 62 hours of culture in the presence of varying amounts of supplemental Dol-P. The antennarity distribution of the glycans at Asn 25 (A), and Asn 97 (B), as well as the sialylation percentage of biantennary glycans at both glycosylation sites (C) were determined according to the method described in detail by Gu et al. (1997).

Consistent with the fact that Dol-P is not involved in the subsequent branching and sugar trimming and addition reactions that lead to glycosylation microheterogeneity, Dol-P supplementation had no obvious impact on IFN- $\gamma$  microheterogeneity (Figure 5-7). The branching pattern (antennarity) of IFN- $\gamma$  glycans at both Asn 25 and Asn 97 glycosylation sites (Figures 5-7(A) and 5-7(B)), as well as the sialylation of IFN- $\gamma$  biantennary glycans (Figure 5-7(C)) (calculated using the definition by Gu et al. (1997)), were unaffected by Dol-P feeding.

#### **5.4.3 Effects of Dol-P supplementation on Cell Cycle, Growth and Viability of CHO cells**

The previous study indicated that high concentrations of exogenous Dol-P (180  $\mu\text{g/ml}$ ) were detrimental to CHO cell viability. This study was performed to investigate the impact of high doses of supplemental Dol-P on CHO cell cycle distribution, growth and the mode of cell death.

At the highest Dol-P concentration (250  $\mu\text{g/ml}$ ), cell densities were significantly lower than in the other cultures (Figure 5-8(A)). This negative impact of high doses of exogenous Dol-P was especially apparent with progression in time. AO/EB assays revealed a consistently higher proportion of cells undergoing necrosis in the culture supplemented with 250  $\mu\text{g/ml}$  Dol-P (Figure 5-8(B)). Compared to the control culture, the 120  $\mu\text{g/ml}$  Dol-P supplemented culture only showed a marginally higher proportion of necrotic cells after 70 hours of culture. At the end of the experiment, the percentage of

cells undergoing necrosis was 14% in the control culture, 26% in the 120 µg/ml Dol-P culture, and 44% in the 250 µg/ml Dol-P culture.

High doses of Dol-P did not have a noticeable effect on cell cycle distributions (data not shown), indicating that the adverse impact of high doses of exogenous Dol-P on cell growth did not arise from growth-arrest, but rather from the increase in necrotic cell death.

#### **5.4.4 Impact of Dol-P Supplementation on LLO and Cellular Glycosylation Levels**

Dol-P supplementation has been shown to significantly enhance glycosylation levels in non-CHO mammalian systems (Carson et al., 1981; Grant and Lennarz, 1983; Kousvelari et al., 1983). For example, 10 µg/ml exogenous Dol-P stimulated mannose incorporation into LLOs and glycoproteins by over 250% in MDCK cells (Pan and Elbein, 1990). These findings support the hypothesis that the subsaturating levels of endogenous Dol-P limit protein glycosylation in mammalian cells by constraining LLO levels.

To test the applicability of this hypothesis to the CHO glycosylation system, CHO cells were cultured in the presence of varied amounts of cold Dol-P in either RPMI-SFM or CHO-S-SFM II. Cellular incorporation of supplemental <sup>14</sup>C glucose and <sup>3</sup>H leucine was monitored over the course of culture to determine the impact of Dol-P supplementation on the relative levels of LLO and protein glycosylation. The level of <sup>14</sup>C radioactivity measured in LLO extracts indicated the relative amount of LLO, while the ratio of <sup>14</sup>C to <sup>3</sup>H radioactivities detected in cellular proteins precipitated by 10% TCA represented the relative glycosylation level in the cells.

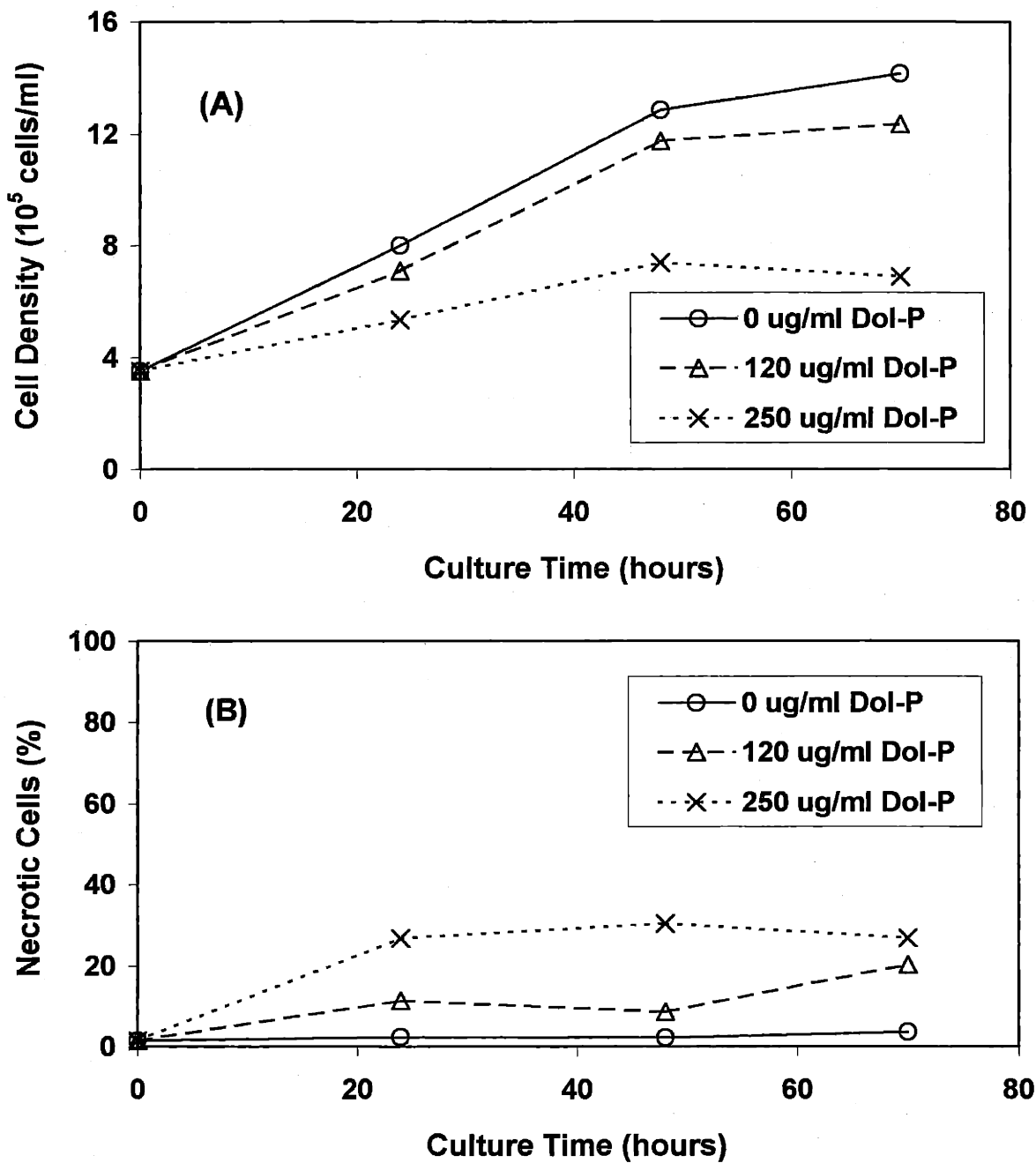


**Figure 5-8.** Cell density (A) and percent of necrotic cells (B) in CHO batch cultures supplemented with varying amounts of Dol-P. Cultures containing 0  $\mu\text{g/ml}$  ( $\circ$ ), 120  $\mu\text{g/ml}$  ( $\Delta$ ), and 250  $\mu\text{g/ml}$  ( $\times$ ) Dol-P were run simultaneously. Distribution of necrotic cells in cultures was determined by AO/EB assay.

#### **5.4.4.1 RPMI-SFM Cultures**

Since Dol-P supplementations at 20  $\mu\text{g/ml}$  or less have been observed to elevate glycosylation levels in other mammalian systems by over 200% (Carson et al., 1981; Grant and Lennarz, 1983; Kousvelari et al., 1983; Pan and Elbein, 1990), and earlier experiments showed that exogenous Dol-P concentrations of up to 35  $\mu\text{g/ml}$  had negligible impact on CHO cell growth and survival, CHO cultures were supplemented with 20  $\mu\text{g/ml}$  and 40  $\mu\text{g/ml}$  Dol-P in this experiment.

All the cultures showed similar cell density and viability profiles over the length of culture (data not shown).

The  $^{14}\text{C}$  radioactivities measured in the LLO extracts were normalized to either cell number (Figure 5-9(A)), or to  $^3\text{H}$  leucine radioactivity detected in cellular proteins (Figure 5-9(B)). The former values represent relative LLO levels per cell, and the latter values represent relative LLO levels per unit cellular protein. Cells in Dol-P supplemented medium appeared to have slightly enhanced LLO levels in RPMI-SFM cultures of CHO cells (Figure 5-9). However, results from the previous chapter in this thesis (Chapter 4) showed that the multiple-step LLO extraction process introduced significant random errors that limited confidence in LLO measurements to within a two-fold range. Taking this into consideration, the only conclusion that can be drawn here is that Dol-P supplementation did not lead to multiple-fold elevations in intracellular LLO levels in CHO cells. The impact of Dol-P supplementation on the ratio of  $^{14}\text{C}$  sugar to  $^3\text{H}$  amino acid in cellular proteins was negligible (Figure 5-10).

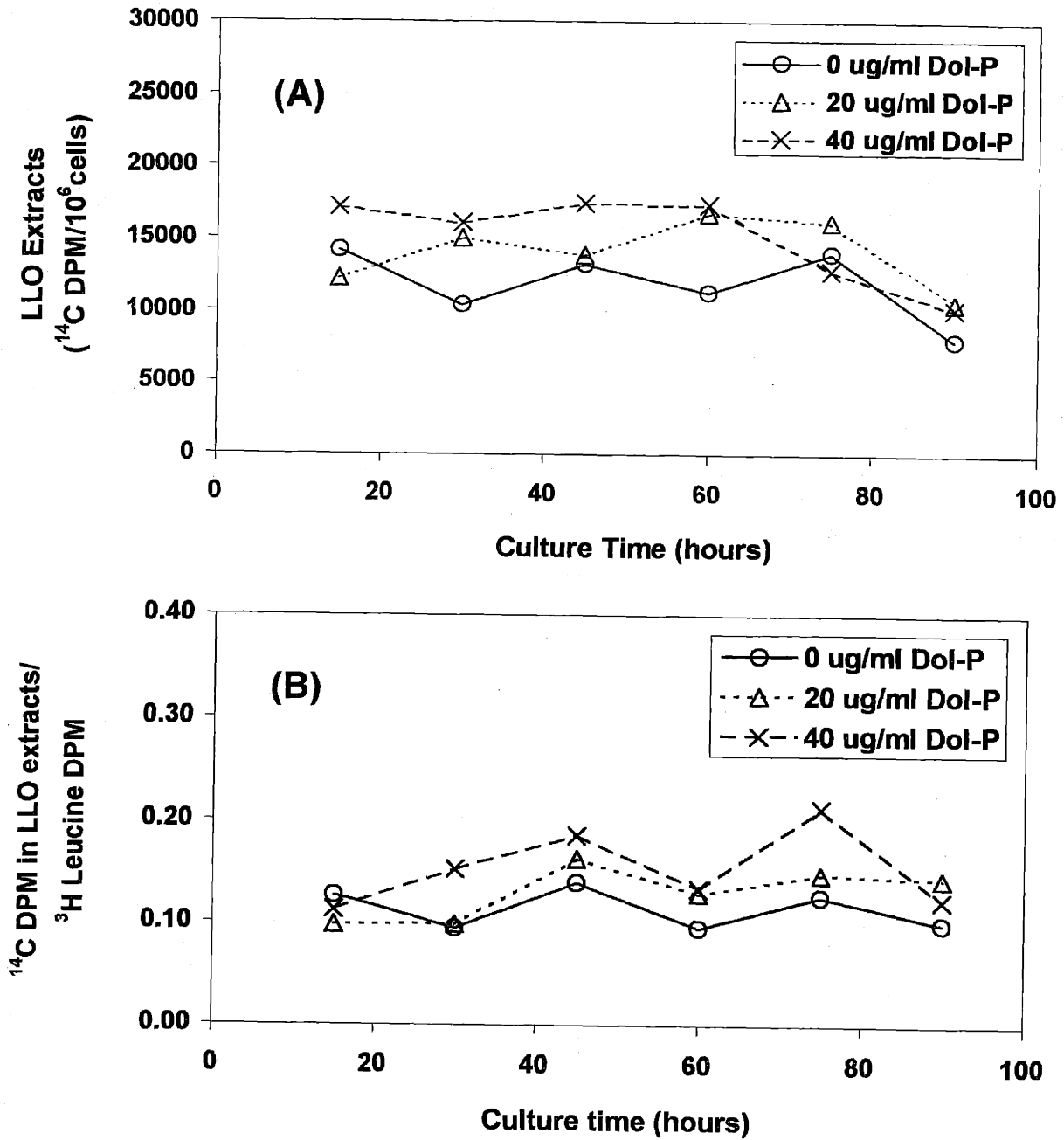


**Figure 5-9.** Impact of Dol-P supplementation on relative LLO levels normalized to cell number (A) and  $^3\text{H}$  radioactivity in cellular proteins (B). RPMI-SFM culture medium contained  $^{14}\text{C}$  glucose and  $^3\text{H}$  leucine, as well as supplemental Dol-P at either 0  $\mu\text{g}/\text{ml}$ , 20  $\mu\text{g}/\text{ml}$ , or 40  $\mu\text{g}/\text{ml}$ . LLOs and cellular proteins were extracted from the CHO batch cultures at regular time intervals.

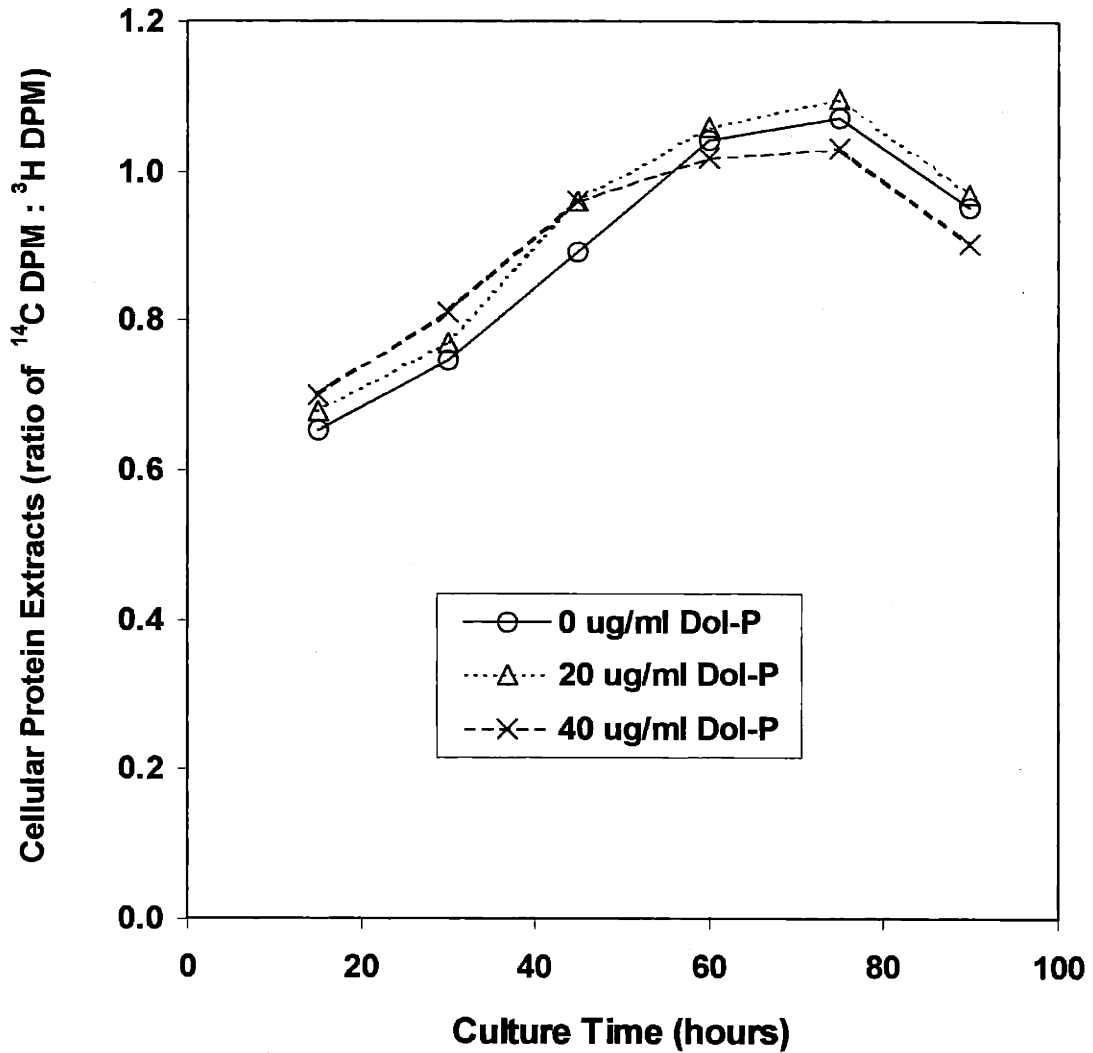


**Figure 5-10.** Impact of Dol-P supplementation on cellular proteins extracted at regular time intervals from RPMI-SFM CHO batch cultures. Culture medium contained  $^{14}\text{C}$  glucose and  $^3\text{H}$  leucine, as well as supplemental Dol-P at either 0  $\mu\text{g}/\text{ml}$ , 20  $\mu\text{g}/\text{ml}$ , or 40  $\mu\text{g}/\text{ml}$ . The ratio of  $^{14}\text{C}$  to  $^3\text{H}$  radioactivities in cellular proteins extracted by 10% TCA precipitation indicated the relative cellular glycosylation levels.

#### **5.4.4.2 CHO-S-SFM II Cultures**

Results from the previous experiment demonstrated inconclusively the impact of Dol-P supplementation on LLO levels in CHO cells. To further investigate this possibility, this experiment was performed. This experiment is essentially a repeat of the previous experiment using different serum-free medium (CHO-S-SFM II). However, the major difference in this experiment lay in the highest exogenous Dol-P concentration used. To maximize any positive impact Dol-P feeding may have on glycosylation, and simultaneously avoid the adverse effects of high doses of Dol-P on cell viability, the maximum dose of Dol-P used in this experiment was 100 µg/ml.

Both LLO and glycosylation levels were not noticeably affected by Dol-P supplementation, even at the maximum dose of Dol-P used (Figures 5-11 and 5-12). While Dol-P supplementation clearly did not stimulate LLO and glycoprotein synthesis, the possibility that small changes in LLO levels (e.g., 10-20% increase) resulting from Dol-P feeding cannot be excluded. Cell density and viability time profiles of the cultures showed the adverse impact of high doses of Dol-P on CHO cell growth (Figure 5-13). All cultures showed similar glucose and lactate concentrations in the medium over time (Figure 5-14).

#### **5.4.5 IFN- $\gamma$ Glycosylation Time Profile Studies**

The previous experiments demonstrated that Dol-P supplementation had minimal impact on overall glycosylation of proteins in CHO cell cultures, but they did not show how individual proteins were affected. An earlier experiment suggested that exogenous Dol-P might be able to marginally increase the fully glycosylated form of recombinant human



IFN- $\gamma$  accumulated in the culture medium after 60 hours of batch culture (Figure 5-6). This experiment was conducted to determine the impact of Dol-P supplementation on the glycosylation of IFN- $\gamma$  secreted by CHO cells throughout the course of culture.

In the control culture, glycosylation site occupancy of IFN- $\gamma$  accumulated in the medium declined marginally over time (Figure 5-15). This slight trend appeared to be minimized in those cultures supplemented with Dol-P. It is important to note that Dol-P supplementation did not noticeably increase glycosylation of IFN- $\gamma$  when it was secreted prior to the mid-exponential growth phase. The viable cell density and concentration of IFN- $\gamma$  secreted into the culture medium did not vary significantly among cultures with Dol-P supplementation, although the culture containing 100  $\mu\text{g/ml}$  exogenous Dol-P showed slightly lower viable cell density and IFN- $\gamma$  accumulation (Figure 5-16).

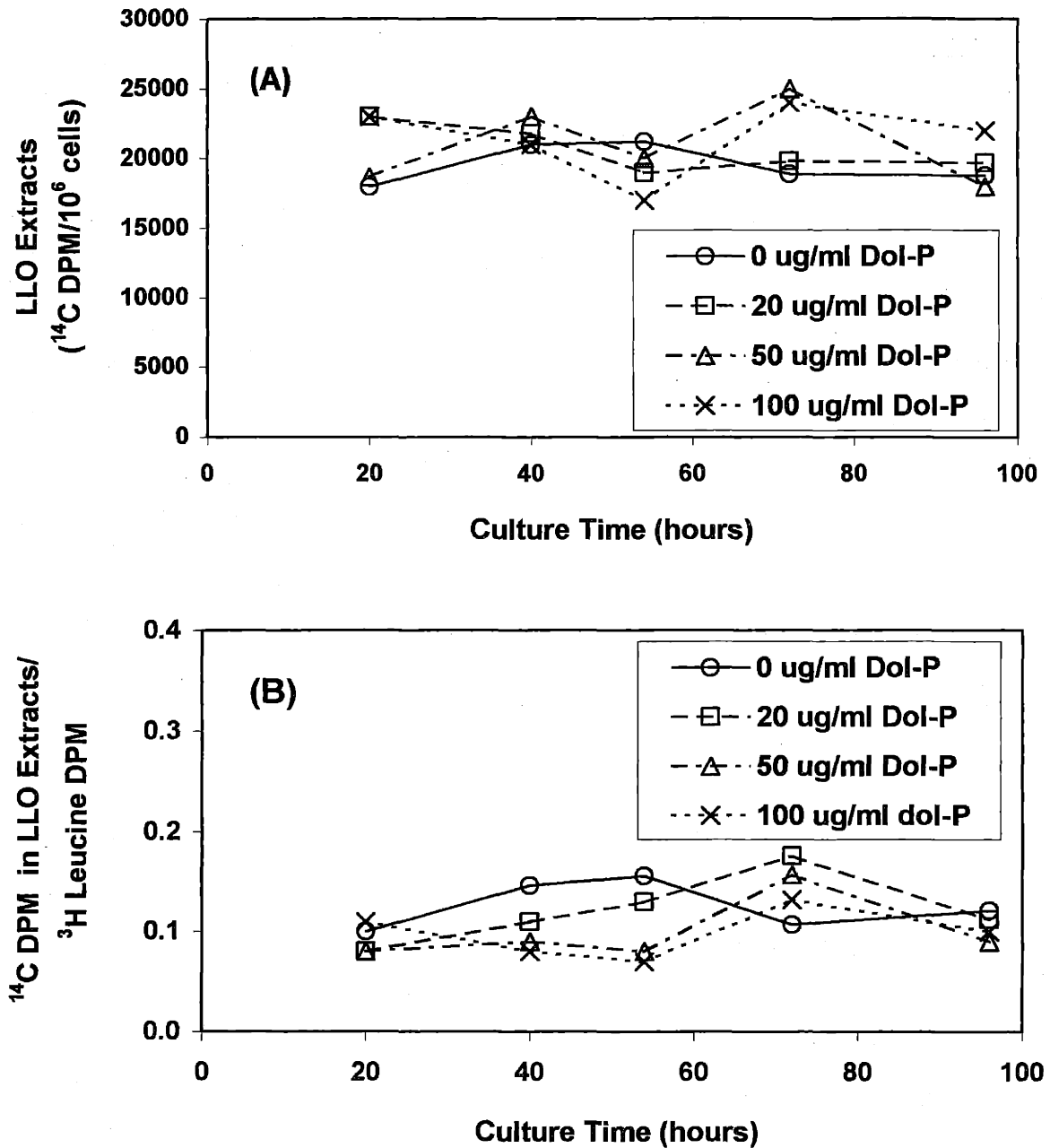


**Figure 5-11.** Impact of Dol-P supplementation on relative LLO levels normalized to cell number (A) and <sup>3</sup>H radioactivity in cellular proteins (B). CHO-S-SFM II culture medium contained <sup>14</sup>C glucose and <sup>3</sup>H leucine, as well as supplemental Dol-P at either 0 μg/ml, 20 μg/ml, 50 μg/ml or 100 μg/ml. LLOs and cellular proteins were extracted from the CHO batch cultures at regular time intervals.

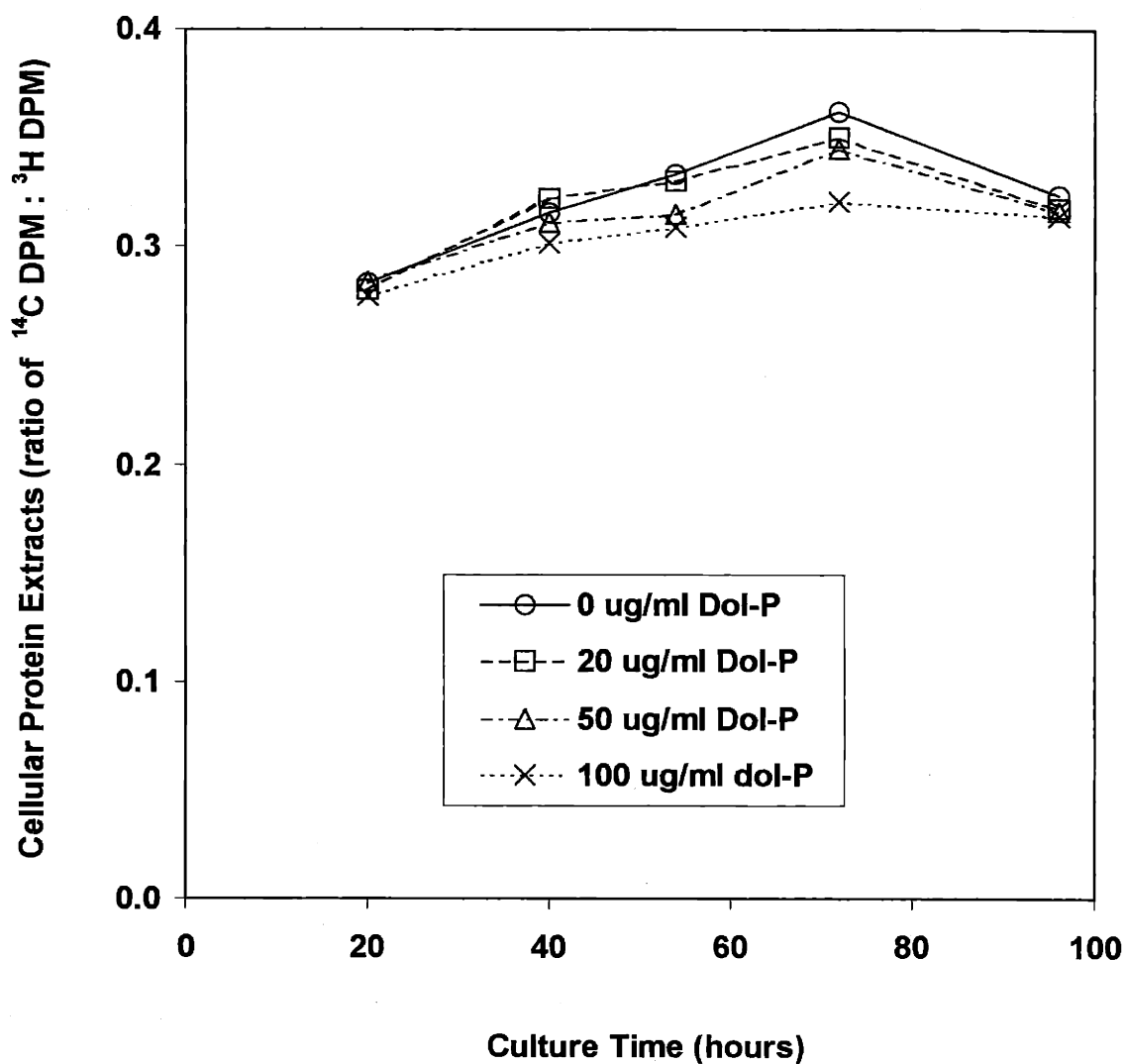


**Figure 5-12.** Impact of Dol-P supplementation on cellular proteins extracted at regular time intervals from CHO-S-SFM II CHO batch cultures. Culture medium contained  $^{14}\text{C}$  glucose and  $^3\text{H}$  leucine, as well as supplemental Dol-P at either 0  $\mu\text{g/ml}$ , 20  $\mu\text{g/ml}$ , 50  $\mu\text{g/ml}$  or 100  $\mu\text{g/ml}$ . The ratio of  $^{14}\text{C}$  to  $^3\text{H}$  radioactivities in cellular proteins extracted by 10% TCA precipitation indicated the relative cellular glycosylation levels.

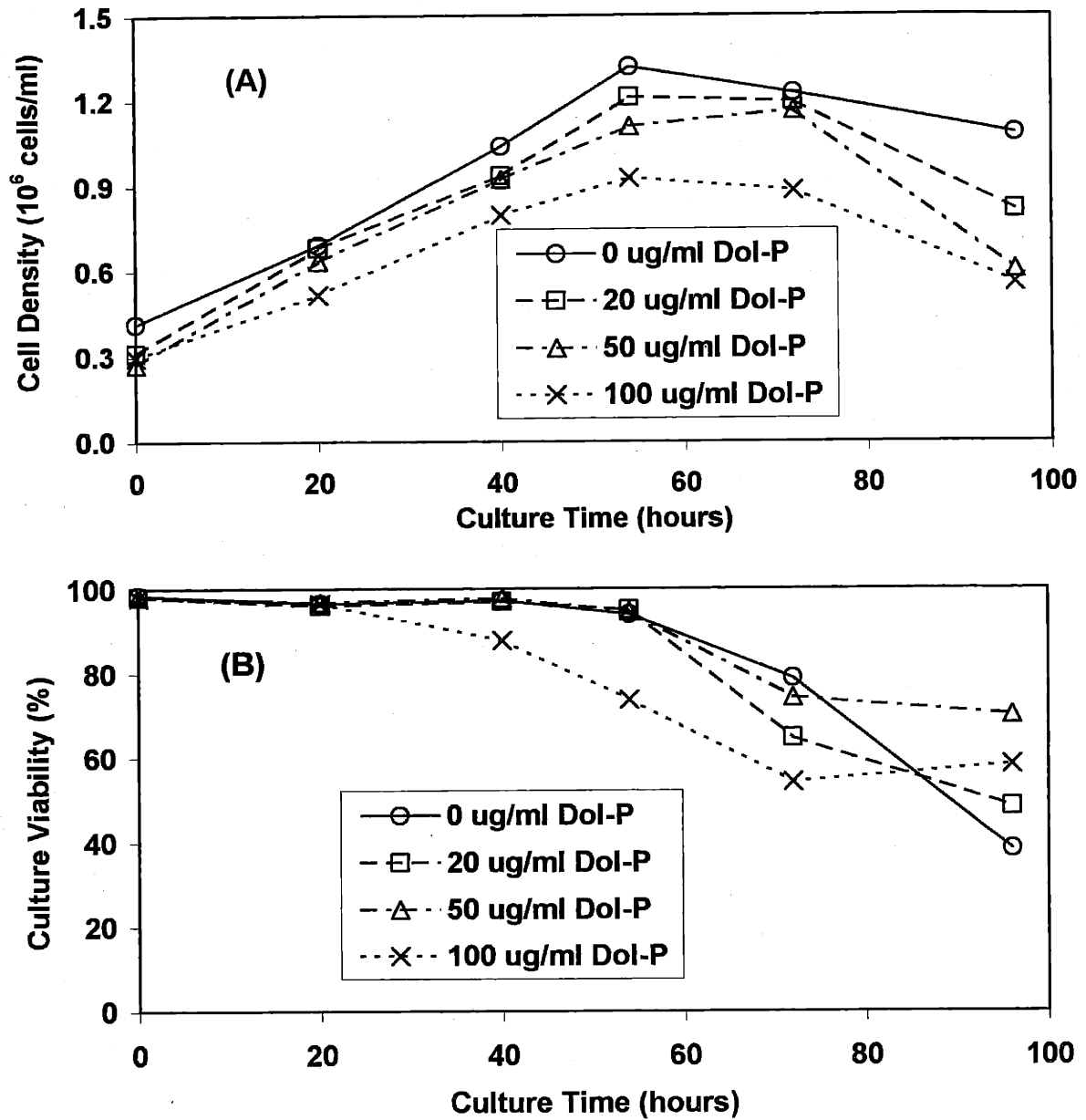


**Figure 5-13.** Cell density (A) and culture viability (B) profiles of four CHO-S-SFM II batch cultures supplemented with varying amounts of Dol-P. Culture medium contained  $^{14}\text{C}$  glucose and  $^3\text{H}$  leucine, as well as supplemental Dol-P at either 0  $\mu\text{g/ml}$ , 20  $\mu\text{g/ml}$ , 50  $\mu\text{g/ml}$ , or 100  $\mu\text{g/ml}$ .

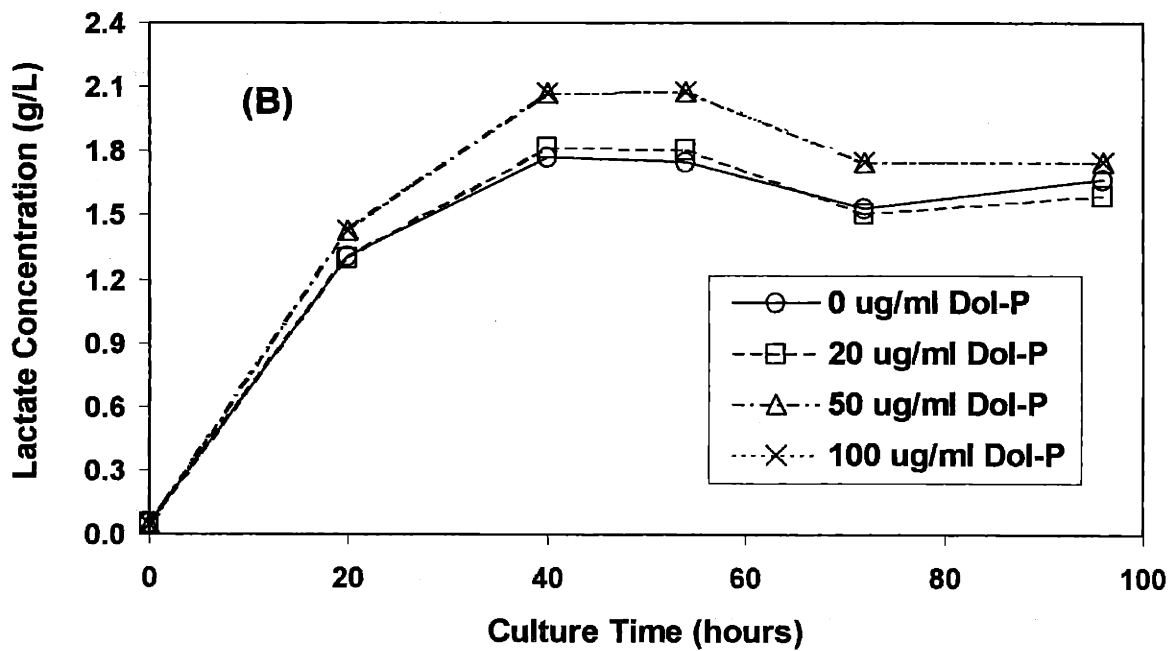
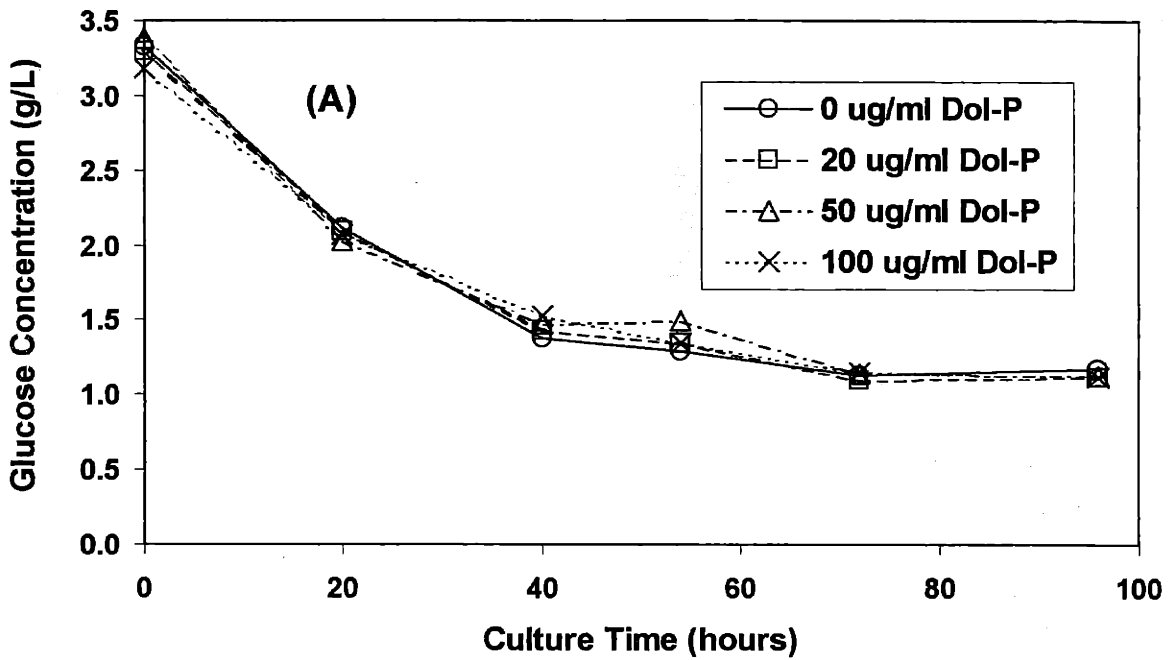


**Figure 5-14.** Glucose (A) and lactate (B) concentrations in CHO-S-SFM II culture medium supplemented with varying amounts of Dol-P. Four CHO batch cultures containing  $^{14}\text{C}$  glucose and  $^3\text{H}$  leucine, as well as supplemental Dol-P at either 0  $\mu\text{g/ml}$ , 20  $\mu\text{g/ml}$ , 50  $\mu\text{g/ml}$ , or 100  $\mu\text{g/ml}$ , were run simultaneously.

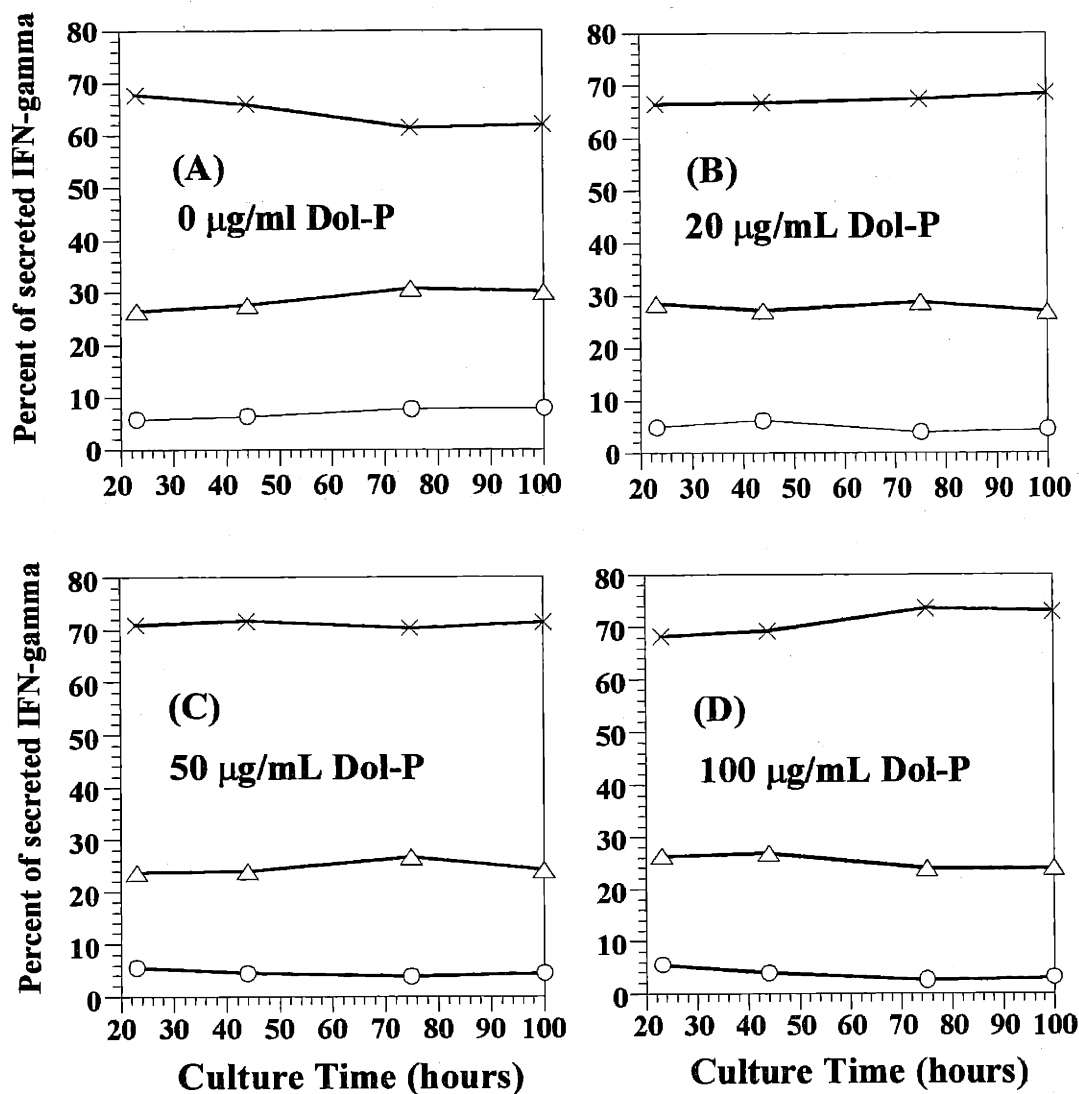


**Figure 5-15.** Glycosylation site occupancy of IFN- $\gamma$  secreted by CHO cells over time. Four CHO batch cultures containing supplemental Dol-P at either 0  $\mu\text{g/ml}$  (A), 20  $\mu\text{g/ml}$  (B), 50  $\mu\text{g/ml}$  (C), or 100  $\mu\text{g/ml}$  (D) were run simultaneously. Recombinant human IFN- $\gamma$  accumulated in the culture medium was collected at regular time intervals for glycosylation site occupancy analyses. Three forms of recombinant human IFN- $\gamma$  were secreted by the CHO cells, as determined by capillary electrophoresis: 2-sites glycosylated ( $\times$ ), 1-site glycosylated ( $\Delta$ ), and 0-sites glycosylated ( $\circ$ ).

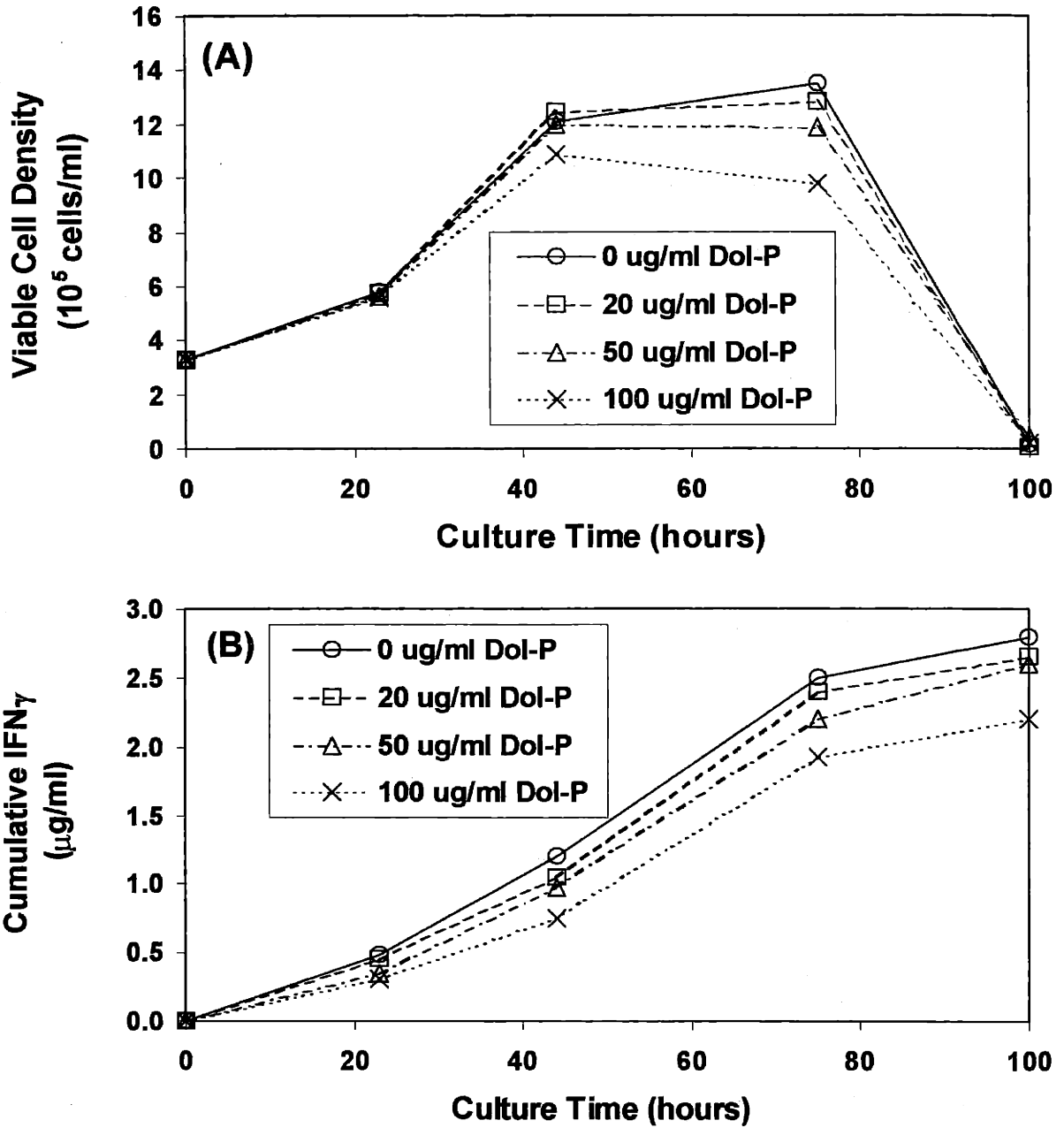


**Figure 5-16.** Time profiles of viable cell density (A) and concentration of IFN- $\gamma$  accumulated in culture medium (B). Four CHO batch cultures containing supplemental Dol-P at either 0  $\mu\text{g/ml}$ , 20  $\mu\text{g/ml}$ , 50  $\mu\text{g/ml}$ , or 100  $\mu\text{g/ml}$ , were run simultaneously.

## 5.5 DISCUSSION

Heterogeneity in protein glycosylation presents special challenges to the development and production of a candidate therapeutic with consistent properties. For unknown reasons, glycosylation site occupancy of recombinant proteins have been found to vary throughout the course of CHO cell culture (Andersen et al., 2000; Goldman et al., 1998). Since proteins that differ in glycosylation can have different biological properties, much pharmaceutical research is devoted to maintaining consistent glycosylation patterns in glycoprotein therapeutics.

A major locus of control for N-linked glycosylation has been postulated to be the level of Dol-P in ER membranes; subsaturating levels of can limit LLO availability and consequently the cellular glycosylation capacity. Support for this hypothesis has been observed in multiple *in vivo* and *in vitro* investigations. Some of the most compelling evidence demonstrated the ability of exogenous Dol-P, at concentrations of 20  $\mu\text{g/ml}$  or less, to elevate glycosylation levels in mammalian cultures by over 200% (Carson et al., 1981; Grant and Lennarz, 1983; Kousvelari et al., 1983; Pan and Elbein, 1990).

Despite the wealth of evidence supporting the regulatory role of Dol-P in mammalian glycosylation, contrary findings have suggested that availability of endogenous Dol-P is not always limiting. Studies in mouse L-1210 cells showed that glycoprotein synthesis remained constant despite two-fold variations in Dol-P levels during the cell cycle (Adair and Cafmeyer, 1987). When calf thyroid microsomes were given Dol-P directly, or agents that allowed Dol-P to recycle, the LLO levels doubled, but protein glycosylation remained unchanged (Spiro and Spiro, 1986).



This extensive study on the effects of Dol-P feeding on CHO batch cultures concurs with the findings in mouse L-1210 cells and calf thyroid microsomes. Extraction of CHO cells with chloroform/methanol/water (10:10:3) has been shown to yield primarily LLOs (Li and Kornfeld, 1979; Li et al., 1978). Enzymes that catalyze the sequential addition of sugars to Dol-P to generate these LLOs are found exclusively in the ER (Hirschberg and Snider, 1987). Therefore, the detection of  $^3\text{H}$  radioactivity in chloroform/methanol/water (10:10:3) extracts in the  $^3\text{H}$  Dol-P single label experiment demonstrates the ability of CHO cells to transport some of the exogenous Dol-P to the ER, where carbohydrate moieties were subsequently attached by glycosyltransferases to generate LLO. The results in Figure 5-2 illustrate a dose-dependent uptake and incorporation of exogenous Dol-P by CHO cells:  $^3\text{H}$  radioactivity measured in LLO extracts increased with the amounts of supplemental  $^3\text{H}$  Dol-P in the culture medium. However, subsequent experiments showed that Dol-P feeding did not lead to corresponding increases in endogenous LLO levels (Figures 5-9 and 5-11) and had negligible impact on glycosylation (Figures 5-10 and 5-12). This work therefore demonstrates conclusively that the ability of exogenous Dol-P supplementation to stimulate glycosylation is not universal for all mammalian systems, and should be examined on a case-by-case basis.

The following mechanisms could explain cellular control of protein glycosylation site occupancy: (1) the cellular concentration of nascent polypeptide chains might be subsaturating with respect to glycosylation capacity; (2) the activity of an enzyme in the dolichol pathway could be rate-limiting. Recent literature results have suggested that the latter possibility is operative: metabolic regulation of the first reaction of the dolichol

pathway, and thus of glycoprotein biosynthesis, was demonstrated in mammalian microsomal preparations (Kean et al., 1999).

The dolichol pathway in the ER initiates the biosynthesis of N-linked glycoproteins. The first step involves the addition of N-acetylglucosamine (GlcNAc) to Dol-P in the ER membrane to form N-acetylglucosaminylpyrophosphoryl dolichol (GlcNAc-P-P-Dol). This reaction, known to be the first committed step in a complex series of enzyme-mediated events, is catalyzed by the ALG7 gene product, N-acetylglucosamine-1-P-transferase (GPT). Regulation of GlcNAc-P-P-Dol formation should influence the steady-state concentration of the final product of the pathway, the 14-sugared LLO species that functions as the donor in N-glycosylation. In accord with the sensitive site in metabolism that this reaction may occupy, down-regulation of GPT has been shown to inhibit the glycosylation and secretion of proteins by *Xenopus* oocytes, and cause defects in the life cycle of yeast (Kukuruzinska and Lennon, 1998).

Recent research using microsomes prepared from the retinas of embryonic chicks revealed various regulatory influences on this reaction, such as feedback inhibition by the second intermediate of the pathway (GlcNAc<sub>2</sub>-P-P-Dol), and product inhibition by GlcNAc-P-P-Dol itself (Kean et al., 1999). The findings by Kean and coworkers are summarized schematically in Figure 5-17. Besides being regulated by the pools of metabolic precursors, the dolichol pathway is also controlled by the level of expression of the ALG genes. Regulatory controls over ALG7 transcript abundance include transcriptional repression/derepression, alternative poly(A) site selection, and changes in transcript stability (Kukuruzinska and Lennon, 1998). The presence of such numerous regulatory mechanisms corroborates with the critical role of ALG7 mRNA levels in N-

linked glycosylation. The network of inhibitory and stimulatory influences on GlcNAc-P-P-Dol formation demonstrates a powerful means by which cells can exert metabolic control over the dolichol pathway, and consequently, glycoprotein biosynthesis.

These recent findings support the following hypothesis: throughout the course of culture, CHO cells exert tight regulation over the formation of GlcNAc-P-P-Dol; the pool of GlcNAc-P-P-Dol cannot be easily perturbed by changes in precursor concentrations. This hypothesis suggests that in Dol-P supplemented CHO cells, feedback inhibition prevents significant elevations in the levels of LLO and LLO precursors by limiting GlcNAc-P-P-Dol formation.

The amount of glycosylation may not be dependent on a single rate-limiting step, but rather on the interplay of a number of enzymes and substrates. The large number of intermediates, substrates and enzymes required to generate the final LLO species used for glycosyl transfer to protein indicate that the formation of the LLO may be regulated at a number of different steps in the dolichol pathway. Hence, GlcNAc-P-P-Dol formation may be one of several reactions that are regulated the dolichol pathway.

This study also uncovered deleterious effects of high doses of Dol-P on CHO cell viability. Cell death *in vivo* can result from necrosis or apoptosis. Necrosis occurs in response to physical or chemical trauma to the cell, and it leads to the disruption of the cell membrane. Unlike necrosis, apoptosis is regulated by events within the cell. Also known as “programmed cell death”, apoptosis is characterized by visible morphological features that distinguish it from necrosis (Fesus and Davies, 1991).

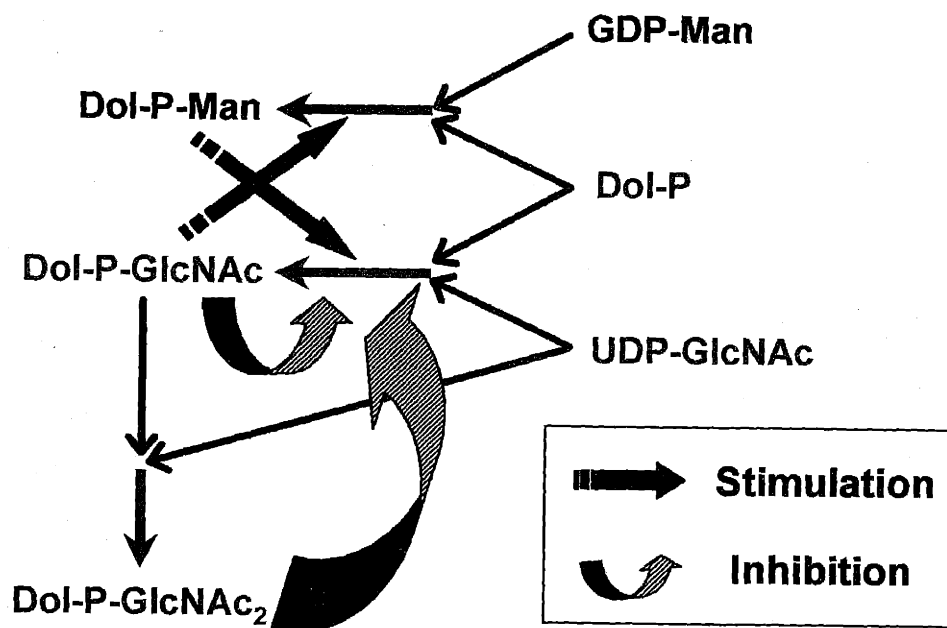


**Figure 5-15.** Regulatory influences on the first step in the dolichol pathway (adapted from Kean et al., 1999). Studies conducted by Kean and coworkers on microsomes prepared from embryonic chick retinas indicated that the first step in the dolichol pathway, involving the addition of N-acetylglucosamine to Dol-P, was tightly regulated. As shown by the arrows, this reaction can be stimulated by Dol-P-Man, and inhibited by both its product and downstream product.

Since the amount of bulk cellular radioactivity increases in proportion to the amount of supplemental [<sup>3</sup>H]Dol-P, increasing the amounts of exogenous Dol-P should elevate the presence of Dol-P in cell membranes. Consistent with the phospholipid bilayer-destabilizing character of Dol-P (Schutzbach and Jensen, 1989; Valtersson et al., 1985), cell membranes with richer Dol-P content would predictably have lower stability. Taking into consideration the enhanced shear sensitivities of cells with higher plasma membrane fluidity (Ramirez and Mutharasan, 1992), higher Dol-P concentrations could increase the susceptibility of cells to shear-induced necrotic death. Results from AO/EB assays (Figure 5-8(B)), which showed that high concentrations of Dol-P promoted cell death primarily through necrosis, support this hypothesis. As the Dol-P dosage rose above 100 µg/ml, its deleterious effects were manifested more quickly and forcefully (Figure 5-5). By contrast, lower concentrations of Dol-P exerted negligible impact on cell viability (Figure 5-3).

Flow cytometry data showed that the regulation of the CHO cell cycle was not affected by Dol-P supplemented. Since cell density correlated positively with cell viability, and since high doses of Dol-P increased necrotic cell death without affecting cell cycle distribution, it is reasonable to conclude that the low cell densities observed at high Dol-P levels resulted from decreased cell viability rather than growth arrest.

Inhibition of Dol-P synthesis can hinder glycoprotein production and cell growth (Kabakoff et al., 1990). However, this does not imply that increased availability of Dol-P under normal culture conditions generates an opposite effect. Compared to the control, cultures that were supplemented with Dol-P showed slightly lower cell density and IFN-γ product titer (Figure 5-16). Hence, Dol-P supplementation did not increase the average

amount of IFN- $\gamma$  secreted by each cell. These results suggest that Dol-P availability does not normally limit CHO cell growth or IFN- $\gamma$  production. Incubation of hen oviduct and bovine pancreas tissue slices with exogenous Dol-P elevated glycosylation of all N-linked glycoproteins but did not stimulate protein synthesis (Carson et al., 1981). Glycosylation and protein production may be independently regulated in CHO cells under the experimental conditions studied here. This hypothesis is consistent with findings that glycosylation of tissue-type plasminogen activator occurs independently of its production rate *in vitro* (Bulleid et al., 1992) and *in vivo* (Lin et al., 1993).

The well-regulated N-linked glycosylation of pertinent sites on numerous glycoproteins is indispensable for proper functioning of various secreted and membrane-bound glycoproteins. Three well-known examples are listed: (1) if the human transferrin receptor lacks one of its three N-linked sugar chains, it cannot form a dimer and is readily degraded by proteases in the ER (Hoe and Hunt, 1992); (2) carbohydrate-deficient glycoprotein (CDG) syndrome type I is characterized by partial deficiency of N-linked sugar chain transfer (Yamashita et al., 1993); (3) normal human microtubule-associated protein tau is nonglycosylated, while N-linked glycosylated tau appears in Alzheimer's disease (Wang et al., 1996). In view of these examples, it is not surprising for N-linked glycosylation to be tightly-regulated in CHO cells.

## **6. Summary and Recommendations for Future Work**

### **6.1 SUMMARY**

Major goals in optimizing mammalian cell culture production processes include increasing specific recombinant protein productivities, extending culture viabilities, and improving protein quality. Using CHO cells expressing recombinant human IFN- $\gamma$  as the model system, this thesis investigated strategies that can potentially enhance heterologous protein expression or control the extent of protein glycosylation.

The major goals of this thesis were to: (1) evaluate the feasibility of using proliferation-controlled bioprocesses for recombinant protein production, (2) develop an effective method for rapidly generating and isolating cells that are better adapted for heterologous protein production under growth-arresting conditions, (3) determine the relative abundance of lipid-linked oligosaccharides (LLOs) and the extent of glycosylation over the course of batch culture, and (4) test the hypothesis that dolichol phosphate (Dol-P) availability is a bottleneck in the glycosylation pathway.

#### **6.1.1 Protein Expression in CHO cells**

An initial investigation into proliferation-controlled bioprocesses for recombinant protein production employed a line of serum-dependent attached recombinant CHO cells expressing IFN- $\gamma$  under the control of the SV40 early promoter. Growth arrest was observed to have a negligible to slightly positive effect on IFN- $\gamma$  glycosylation site occupancy. Although serum-withdrawal proved to be a simple and effective means of arresting cell growth, it adversely impacted culture performance. After two weeks of serum deprivation, both culture viabilities and specific IFN- $\gamma$  productivities declined by

over 40%. Some CHO cells remained robust after two weeks in serum-free conditions, but the average IFN- $\gamma$  production in these cells declined upon growth-arrest. Even if subpopulations that produce relatively larger amounts of IFN- $\gamma$  exist, they cannot be conveniently isolated. Therefore, this particular line of CHO cells did not have the potential to be developed for use in controlled proliferation bioprocesses. These results showed how that under normal growth conditions, established mammalian cell lines can meet the two major requirements for a production cell line, namely high viabilities and productivities, but they may not satisfy these criteria under proliferation-inhibited environments.

The initial study demonstrated the existence of CHO cell subpopulations that can survive serum-starvation, and suggest that that subpopulations that are productive as well upon serum withdrawal may also exist. In the following study, a method to rapidly generate and isolate subpopulations of CHO cells that exhibit enhanced potential for use in proliferation-controlled bioprocesses was developed. To overcome the limitations associated with standard transformation and selection methods, bicistronic retroviral technology was employed to generate a large pool of recombinant cells. First, bicistronic constructs encoding for both IFN- $\gamma$ , the model therapeutic protein, and GFP, the fluorescent reporter protein were generated. Next, recombinant viruses containing these bicistronic constructs were used to infect susceptible CHO cells. Successfully infected cells were readily identified by their green fluorescence. To isolate cells optimized for recombinant protein production under growth-arresting conditions, the original heterogeneous cell population was first subjected to the selection pressure of serum withdrawal. After 8 days in serum-free culture, a substantial fraction of the cells died.



GFP-producers were isolated from the survivors by FACS. To evaluate the effectiveness of this screening process, the selected subpopulation of cells was put through a second round of serum-starvation. The serum-free culture performance of the selected subpopulation demonstrated significant improvements over the original heterogeneous population; the selected cells maintained high viabilities and continued to stably coexpress GFP and IFN- $\gamma$  for two weeks in serum-free conditions. Hence, the screening process was successful in selecting for cells with enhanced potential for development into recombinant protein production cell lines used in proliferation-controlled bioprocesses.

#### **6.1.2 Protein Glycosylation in CHO batch cultures**

An essential step in asparagine-linked (N-linked) glycosylation is the transfer of oligosaccharide from dolichol phosphate (Dol-P) to a potential glycosylation site on a polypeptide. Despite the importance of N-linked glycosylation to proteins, this transfer reaction can have variable success rates at identical potential glycosylation sites on different molecules of the same protein. The glycosylation site occupancy heterogeneity that results has been found to change with culture time in CHO cells. Since lipid-linked oligosaccharides (LLOs) function as glycosyl donors, their availability is expected to impact glycosylation. To better understand the relationship between LLO availability and the extent of glycosylation, radiolabeling studies were conducted to monitor relative LLO and glycosylation levels in CHO cells over the course of batch culture. Despite considerable changes in glucose and lactate concentrations in the medium over culture time, intracellular LLO levels remained within a two-fold range. Prior to the onset of massive cell death, a gradual 15-25% improvement in overall protein glycosylation with

culture time was measured. These results are in agreement with recent observations for recombinant tissue-plasminogen activator (tPA) produced in fed-batch cultures of CHO cells: the pattern and extent of the tPA glycosylation site occupancy increase were similar to the findings for overall CHO cellular protein glycosylation in this work. However, these results contradict the decline in IFN- $\gamma$  glycosylation site occupancy observed by various researchers over the course of CHO batch and fed-batch cultures.

Given the critical role of Dol-P in this process, its availability was postulated to limit glycosylation site occupancy by controlling the abundance of LLOs. To test this hypothesis, the impact of Dol-P supplementation on protein glycosylation in CHO cells was studied. Although exogenous Dol-P was incorporated by CHO cells and processed into LLOs in a dose-dependent manner, Dol-P feeding had no marked effect on LLO or overall cellular glycosylation levels. Dosing studies revealed that at concentrations exceeding 100  $\mu\text{g/ml}$  in the culture medium, exogenous Dol-P was detrimental to CHO cell growth and viability. Even when the maximum doses of supplemental Dol-P that the CHO cells could tolerate were used, glycosylation site occupancy of recombinant IFN- $\gamma$  secreted by the cells was at best, marginally enhanced. These results showed that Dol-P supplementation had essentially no positive effects on CHO cell viability, growth and glycosylation, and demonstrated that glycosylation in CHO cells cannot be readily manipulated by Dol-P supplementation under normal culture conditions. N-linked glycoprotein biosynthesis appears to be regulated in CHO cells.

## 6.2 RECOMMENDATIONS FOR FUTURE WORK

### 6.2.1 Protein Expression in CHO cells

The bicistronic retroviral system is a powerful means of rapidly introducing exogenous genes into mammalian cells. Since expression from the two reading frames in these bicistronic vectors should be correlated, this system allows functional selection for the gene cloned upstream of the IRES to be detected by a proportionate increase in the expression of a fluorescent marker encoded by the gene downstream of the IRES. This bicistronic system is especially useful for preliminary *in vivo* studies of heterologous proteins whose expression levels are difficult or impossible to quantify directly. For instance, by using FACS to select for GFP producers varying in GFP fluorescence intensities, the *in vivo* effects of different levels of overexpression of the gene of interest can be studied. Furthermore, by superinfecting the cells with multiple bicistronic retroviral vectors, each expressing a unique set of fluorescent markers and exogenous gene of interest, cells that simultaneously express several heterologous proteins can be rapidly generated.

The bicistronic technology can be used to compare the impact of different culture conditions and cultivation methods on recombinant protein production. For instance, the effects of different medium additives on GFP productivity can be assessed.

By making the appropriate alterations to the bicistronic constructs, different retroviral vector designs and gene amplification strategies can be conveniently evaluated using the heterologous protein production screening process developed in this work. For instance, the screen can be used to compare the effectiveness of the dihydrofolate reductase and glutamine synthetase selectable markers in amplifying GFP expression. In

addition, this screen can also be used to identify specific promoters and internal ribosomal entry sites (IRES) that optimize protein expression under various culture and growth conditions. For example, by inserting the SV40 and CMV promoters into the retroviral constructs, the promoter strengths can be qualitatively assessed by contrasting the abilities of the SV40 and CMV promoters to drive GFP expression in growth-arrested cells. In this way, the combinations of promoters and selectable markers that optimize exogenous protein production under desired culture conditions can be determined. In facilitating the comparison of various amplifiable expression systems and promoters, this screening process will guide the development of producer cell lines used for proliferation-controlled bioprocesses.

The heterogeneity within a cell population observed in this work indicates that subpopulations that are better adapted for different environments exist. This intrinsic heterogeneity should be exploited in the early stages of selecting for robust industrial production cell lines. For instance, enhancing the proportion of robust cells in the culture can be enhanced by exposing the cells to slightly exaggerated forms of stresses that are expected to arise in the course of the culture process, since the imposed selection pressure will eliminate the weaker subpopulations. Investigations into the cellular mechanisms that led to enhanced robustness and sustained recombinant protein expression in the selected subpopulation of cells may yield interesting results. For instance, endogenous expression of well-known anti-apoptotic genes may differ between the control population and the robust selected subpopulation. The findings here will guide efforts by the biopharmaceutical manufacturing industry to create more robust strains of mammalian cells.

### **6.2.2 Protein Glycosylation in CHO batch cultures**

Results in this work showed that prior to the onset of massive cell death, the overall glycosylation improved with time in CHO cell cultures. Researchers at Genentech observed similar glycosylation trends in their CHO-derived recombinant tPA. Various studies report an opposite trend for IFN- $\gamma$  produced by batch and fed-batch cultures of CHO cells. To reconcile these divergent observations in the CHO system, the extent of glycosylation in different CHO proteins was proposed to undergo unique changes over the course of culture. However, this explanation raises more questions than it answers. For instance, CHO cells seem to be able to selectively enhance glycosylation site occupancy of tPA, and concurrently reduce glycosylation of IFN- $\gamma$ . What are the mechanisms that enable CHO cells to differentiate between different proteins in order to bring about this apparent effect? Before even beginning to address these issues, more data points on the variation of glycosylation site occupancy of CHO-derived proteins over the course of batch culture are needed. The glycosylation of various individual proteins produced simultaneously by the same CHO batch cultures should first be investigated.

Results from the work here support a previously observed positive association between glycosylation site occupancy and the proportion of cells in the G0/G1 phase of the cell cycle. This relationship also deserves further investigation.

The cellular mechanisms that control changes in protein glycosylation in CHO cells remain unclear, and should be investigated. One starting point could be at the first step in the dolichol pathway. Studies conducted in microsomes derived from embryonic chick retinas showed that this reaction, catalyzed by the ER enzyme known as GPT, is

regulated tightly by various stimulatory and inhibitory influences. To test the applicability of these findings to the CHO glycosylation system, similar experiments should be conducted using CHO cells. Ultimately, the extent of glycosylation may not be dependent on a single rate-limiting step, but rather on the interplay of a number of enzymes and substrates. This is highly probable since the large number of intermediates, substrates and enzymes required to generate the final LLO species used for glycosyl transfer to protein allows for the formation of LLO to be regulated at a number of different steps in the dolichol pathway.

## ABBREVIATIONS

BHK	Baby Hamster Kidney
CHO	Chinese Hamster Ovary
DHFR	dihydrofolate reductase
Dol-P	dolichol phosphate
DPM	disintegrations per minute
ECM	extracellular matrix
EPO	Erythropoietin
ER	endoplasmic reticulum
FACS	fluorescence activated cell sorting
FBS	fetal bovine serum
GFP	green fluorescent protein
GlcNAc	N-acetylglucosamine
GPT	N-acetylglucosamine-1-P-transferase
IFN- $\gamma$	Interferon-gamma
IRES	internal ribosomal entry site
LLO	lipid-linked oligosaccharide
LSC	liquid scintillation counting
LTR	long terminal repeat
MECC	micellar electrokinetic capillary chromatography
N-linked	asparagine-linked
PBS	phosphate-buffered saline
qIFN	specific Interferon-gamma productivity
SFM	serum-free medium
SV40	simian virus 40
TCA	trichloroacetic acid
tPA	tissue plasminogen activator





## REFERENCES

- Adair, W. L., Jr. & Cafmeyer, N. (1987) Cell-cycle dependence of dolichyl phosphate biosynthesis, *Arch Biochem Biophys.* 258, 491-497.
- Allay, J. A., Galipeau, J., Blakley, R. L. & Sorrentino, B. P. (1998) Retroviral vectors containing a variant dihydrofolate reductase gene for drug protection and in vivo selection of hematopoietic cells, *Stem Cells.* 16, 223-233.
- al-Rubeai, M., Emery, A. N., Chalder, S. & Jan, D. C. (1992) Specific monoclonal antibody productivity and the cell cycle-comparisons of batch, continuous and perfusion cultures, *Cytotechnology.* 9, 85-97.
- al-Rubeai, M. & Singh, R. P. (1998) Apoptosis in cell culture, *Curr Opin Biotechnol.* 9, 152-156.
- Andersen, D. C., Bridges, T., Gawlitzek, M. & Hoy, C. (2000) Multiple cell culture factors can affect the glycosylation of Asn-184 in CHO-produced tissue-type plasminogen activator, *Biotechnol Bioeng.* 70, 25-31.
- Arakawa, T., Alton, N. K. & Hsu, Y. R. (1985) Preparation and characterization of recombinant DNA-derived human interferon-gamma, *J Biol Chem.* 260, 14435-14439.
- Ashwell, G. & Harford, J. (1982) Carbohydrate-specific receptors of the liver, *Annu Rev Biochem.* 51, 531-554.
- Assoian, R. K. (1997) Anchorage-dependent cell cycle progression, *J Cell Biol.* 136, 1-4.
- Avgerinos, G. C., Drapeau, D., Socolow, J. S., Mao, J. I., Hsiao, K. & Broeze, R. J. (1990) Spin filter perfusion system for high density cell culture: production of recombinant urinary type plasminogen activator in CHO cells, *Biotechnology (N Y).* 8, 54-58.
- Baker, B. W., Boettiger, D., Spooner, E. & Norton, J. D. (1992) Efficient retroviral-mediated gene transfer into human B lymphoblastoid cells expressing mouse ecotropic viral receptor, *Nucleic Acids Res.* 20, 5234.
- Batt, B. C., Davis, R. H. & Kompala, D. S. (1990) Inclined sedimentation for selective retention of viable hybridomas in a continuous suspension bioreactor, *Biotechnol Prog.* 6, 458-464.
- Bebbington, C. R., Renner, G., Thomson, S., King, D., Abrams, D. & Yarranton, G. T. (1992) High-level expression of a recombinant antibody from myeloma cells using a glutamine synthetase gene as an amplifiable selectable marker, *Biotechnology (N Y).* 10, 169-175.

- Beebe, D. P. & Aronson, D. L. (1988) Turnover of tPA in rabbits: influence of carbohydrate moieties, *Thromb Res.* 51, 11-22.
- Bellen, H. J. (1999) Ten years of enhancer detection: lessons from the fly, *Plant Cell.* 11, 2271-2281.
- Bhat, N. R. & Waechter, C. J. (1988) Induction of N-glycosylation activity in cultured embryonic rat brain cells, *J Neurochem.* 50, 375-381.
- Bird, A. P. & Wolffe, A. P. (1999) Methylation-induced repression--belts, braces, and chromatin, *Cell.* 99, 451-454.
- Borys, M. C., Linzer, D. I. & Papoutsakis, E. T. (1993) Culture pH affects expression rates and glycosylation of recombinant mouse placental lactogen proteins by Chinese hamster ovary (CHO) cells, *Biotechnology (N Y).* 11, 720-724.
- Borys, M. C., Linzer, D. I. & Papoutsakis, E. T. (1994) Ammonia affects the glycosylation patterns of recombinant mouse placental lactogen-I by Chinese hamster ovary Cells in a pH-dependent manner, *Biotechnol Bioeng.* 43, 505-514.
- Bulleid, N. J., Bassel-Duby, R. S., Freedman, R. B., Sambrook, J. F. & Gething, M. J. (1992) Cell-free synthesis of enzymically active tissue-type plasminogen activator. Protein folding determines the extent of N-linked glycosylation, *Biochem J.* 286, 275-280.
- Carlberg, M., Dricu, A., Blegen, H., Wang, M., Hjertman, M., Zickert, P., Hoog, A. & Larsson, O. (1996) Mevalonic acid is limiting for N-linked glycosylation and translocation of the insulin-like growth factor-1 receptor to the cell surface. Evidence for a new link between 3-hydroxy-3-methylglutaryl-coenzyme a reductase and cell growth, *J Biol Chem.* 271, 17453-17462.
- Carson, D. D., Earles, B. J. & Lennarz, W. J. (1981) Enhancement of protein glycosylation in tissue slices by dolichylphosphate, *J Biol Chem.* 256, 11552-11557.
- Carson, D. D. & Lennarz, W. J. (1979) Inhibition of polyisoprenoid and glycoprotein biosynthesis causes abnormal embryonic development, *Proc Natl Acad Sci U S A.* 76, 5709-5713.
- Carson, D. D., Tang, J. P. & Hu, G. (1987) Estrogen influences dolichyl phosphate distribution among glycolipid pools in mouse uteri, *Biochemistry.* 26, 1598-1606.
- Castro, P. M., Ison, A. P., Hayter, P. M. & Bull, A. T. (1995) The macroheterogeneity of recombinant human interferon-gamma produced by Chinese hamster ovary cells is affected by the protein and lipid content of the culture medium, *Biotechnol Appl Biochem.* 21, 87-100.

- Cherry, S. R., Biniszkiwicz, D., van Parijs, L., Baltimore, D. & Jaenisch, R. (2000) Retroviral expression in embryonic stem cells and hematopoietic stem cells, *Mol Cell Biol.* 20, 7419-7426.
- Chow, M., Yao, A. & Rubin, H. (1994) Cellular epigenetics: topochronology of progressive "spontaneous" transformation of cells under growth constraint, *Proc Natl Acad Sci U S A.* 91, 599-603.
- Chung, J. D., Sinskey, A. J. & Stephanopoulos, G. (1998) Growth factor and bcl-2 mediated survival during abortive proliferation of hybridoma cell line, *Biotechnol Bioeng.* 57, 164-171.
- Chung, J. D. & Stephanopoulos, G. (1996) On physiological multiplicity and population heterogeneity of biological systems, *Chem Eng Sci.* 51, 1509-1521.
- Cockett, M. I., Bebbington, C. R. & Yarranton, G. T. (1990) High level expression of tissue inhibitor of metalloproteinases in Chinese hamster ovary cells using glutamine synthetase gene amplification, *Biotechnology (N Y).* 8, 662-667.
- Conradt, H. S., Nimtz, M., Dittmar, K. E., Lindenmaier, W., Hoppe, J. & Hauser, H. (1989) Expression of human interleukin-2 in recombinant baby hamster kidney, Ltk-, and Chinese hamster ovary cells. Structure of O-linked carbohydrate chains and their location within the polypeptide, *J Biol Chem.* 264, 17368-17373.
- Coppen, S. R., Newsam, R., Bull, A. T. & Baines, A. J. (1995) Heterogeneity within populations of recombinant Chinese hamster ovary cells expressing human interferon-gamma, *Biotechnol Bioeng.* 46, 147-158.
- Cotter, T. G. & al-Rubeai, M. (1995) Cell death (apoptosis) in cell culture systems, *Trends Biotechnol.* 13, 150-155.
- Crick, D. C. & Waechter, C. J. (1994) Long-chain cis-isoprenyltransferase activity is induced early in the developmental program for protein N-glycosylation in embryonic rat brain cells, *J Neurochem.* 62, 247-256.
- Crow, J. F. (1983) Genetic notes, *An introduction to genetics (New York, NY: Macmillan Publishing Co.)*.
- Cumming, D. A. (1991) Glycosylation of recombinant protein therapeutics: control and functional implications, *Glycobiology.* 1, 115-130.
- Curling, E. M., Hayter, P. M., Baines, A. J., Bull, A. T., Gull, K., Strange, P. G. & Jenkins, N. (1990) Recombinant human interferon-gamma. Differences in glycosylation and proteolytic processing lead to heterogeneity in batch culture, *Biochem J.* 272, 333-337.
- Dahms, N. M., Lobel, P. & Kornfeld, S. (1989) Mannose 6-phosphate receptors and lysosomal enzyme targeting, *J Biol Chem.* 264, 12115-12118.

- Datar, R. V., Cartwright, T. & Rosen, C. G. (1993) Process economics of animal cell and bacterial fermentations: a case study analysis of tissue plasminogen activator, *Biotechnology (N Y)*. 11, 349-357.
- Devos, R., Cheroutre, H., Taya, Y., Degrave, W., Van Heuverswyn, H. & Fiers, W. (1982) Molecular cloning of human immune interferon cDNA and its expression in eukaryotic cells, *Nucleic Acids Res.* 10, 2487-2501.
- Doyle, J. W., Ward-Bailey, P. F. & Kandutsch, A. A. (1993) Effects of growth factors on cell cycle arrest in dolichyl phosphate-depleted cultures, *J Cell Physiology*. 155, 171-178.
- Dricu, A., Wang, M., Hjertman, M., Malec, M., Blegen, H., Wejde, J., Carlberg, M. & Larsson, O. (1997) Mevalonate-regulated mechanisms in cell growth control: role of dolichyl phosphate in expression of the insulin-like growth factor-1 receptor (IGF-1R) in comparison to Ras prenylation and expression of c-myc, *Glycobiology*. 7, 625-633.
- Dykhuisen, D. E. & Hartl, D. L. (1983) Selection in chemostats, *Microbiol Rev.* 47, 150-168.
- Elbein, A. D. (1987) Inhibitors of the biosynthesis and processing of N-linked oligosaccharide chains, *Annu Rev Biochem.* 56, 497-534.
- Farrar, M. A. & Schreiber, R. D. (1993) The molecular cell biology of interferon-gamma and its receptor, *Annu Rev Immunol.* 11, 571-611.
- Fesus, L., Davies, P. J. & Piacentini, M. (1991) Apoptosis: molecular mechanisms in programmed cell death, *Eur J Cell Biol.* 56, 170-177.
- Fiore, M. & Degrassi, F. (1999) Dimethyl sulfoxide restores contact inhibition-induced growth arrest and inhibits cell density-dependent apoptosis in hamster cells, *Exp Cell Res.* 251, 102-110.
- Follstad, B. D., Wang, D. I. & Stephanopoulos, G. (2000) Mitochondrial membrane potential differentiates cells resistant to apoptosis in hybridoma cultures, *Eur J Biochem.* 267, 6534-6540.
- Fornaro, M., Zheng, D. Q. & Languino, L. R. (1995) The novel structural motif Gln795-Gln802 in the integrin beta 1C cytoplasmic domain regulates cell proliferation, *J Biol Chem.* 270, 24666-24669.
- Frisch, S. M., Vuori, K., Ruoslahti, E. & Chan-Hui, P. Y. (1996) Control of adhesion-dependent cell survival by focal adhesion kinase, *J Cell Biol.* 134, 793-799.
- Fukushima, K., Ohkura, T. & Yamashita, K. (1997) Synthesis of lipid-linked oligosaccharides is dependent on the cell cycle in rat 3Y1 cells, *J Biochem (Tokyo)*. 121, 415-418.

- Fussenegger, M., Mazur, X. & Bailey, J. E. (1997) A novel cytostatic process enhances the productivity of Chinese hamster ovary cells, *Biotechnol Bioeng.* 55, 927-939.
- Fussenegger, M., Schlatter, S., Datwyler, D., Mazur, X. & Bailey, J. E. (1998) Controlled proliferation by multigene metabolic engineering enhances the productivity of Chinese hamster ovary cells, *Nat Biotechnol.* 16, 468-472.
- Gawlitzeck, M., Valley, U., Nimtz, M., Wagner, R. & Conradt, H. S. (1995) Characterization of changes in the glycosylation pattern of recombinant proteins from BHK-21 cells due to different culture conditions, *J Biotechnol.* 42, 117-131.
- Gershman, H. & Robbins, P. W. (1981) Transitory effects of glucose starvation on the synthesis of dolichol-linked oligosaccharides in mammalian cells, *J Biol Chem.* 256, 7774-7780.
- Giancotti, F. G. & Ruoslahti, E. (1999) Integrin signaling, *Science.* 285, 1028-1032.
- Glacken, M. W., Fleischaker, R. J. & Sinskey, A. J. (1986) Reduction of waste product excretion via nutrient control: possible strategies for maximizing product and cell yields on serum in cultures of mammalian cells, *Biotechnol Bioeng.* 28, 1376-1389.
- Goldman, M. H., James, D. C., Rendall, M., Ison, A. P., Hoare, M. & Bull, A. T. (1998) Monitoring recombinant human interferon-gamma N-glycosylation during perfused fluidized-bed and stirred-tank batch culture of CHO cells, *Biotechnol Bioeng.* 60, 596-607.
- Goochee, C. F., Gramer, M. J., Andersen, D. C., Bahr, J. B. & Rasmussen, J. R. (1991) The oligosaccharides of glycoproteins: bioprocess factors affecting oligosaccharide structure and their effect on glycoprotein properties, *Biotechnology (N Y).* 9, 1347-1355.
- Goswami, J., Sinskey, A. J., Steller, H., Stephanopoulos, G. N. & Wang, D. I. (1999) Apoptosis in batch cultures of Chinese hamster ovary cells, *Biotechnol Bioeng.* 62, 632-640.
- Gram, G. J., Nielsen, S. D. & Hansen, J. E. (1998) Spontaneous silencing of humanized green fluorescent protein (hGFP) gene expression from a retroviral vector by DNA methylation, *J Hematother.* 7, 333-341.
- Gramer, M. J. & Goochee, C. F. (1993) Glycosidase activities in Chinese hamster ovary cell lysate and cell culture supernatant, *Biotechnol Prog.* 9, 366-373.
- Grant, S. R. & Lennarz, W. J. (1983) Relationship between oligosaccharide-lipid synthesis and protein synthesis in mouse LM cells, *Eur J Biochem.* 134, 575-583.
- Gu, M. B., Todd, P. & Kompala, D. S. (1994) Analysis of foreign protein overproduction in recombinant CHO cells. Effect of growth kinetics and cell cycle traverse, *Ann N Y Acad Sci.* 721, 194-207.

- Gu, X., Harmon, B. J. & Wang, D. I. C. (1997) Site- and branch-specific sialylation of recombinant human interferon-gamma in Chinese hamster ovary cell culture, *Biotechnol Bioeng.* 55, 390-398.
- Hayter, P. M., Curling, E. M., Baines, A. J., Jenkins, N., Salmon, I., Strange, P. G. & Bull, A. T. (1991) Chinese hamster ovary cell growth and interferon production kinetics in stirred batch culture, *Appl Microbiol Biotechnol.* 34, 559-564.
- Hirschberg, C. B. & Snider, M. D. (1987) Topography of glycosylation in the rough endoplasmic reticulum and Golgi apparatus, *Annu Rev Biochem.* 56, 63-87.
- Hoe, M. H. & Hunt, R. C. (1992) Loss of one asparagine-linked oligosaccharide from human transferrin receptors results in specific cleavage and association with the endoplasmic reticulum, *J Biol Chem.* 267, 4916-4923.
- Hooker, A. D., Goldman, M. H., Markham, N. H., James, D. C., Ison, A. P., Bull, A. T., Strange, P. G., Salmon, I., Baines, A. J. & Jenkins, N. (1995) N-Glycans of recombinant human interferon-gamma change during batch culture of Chinese hamster ovary cells, *Biotechnol Bioeng.* 48, 639-648.
- Horvitz, H. R. & Herskowitz, I. (1992) Mechanisms of asymmetric cell division: two Bs or not two Bs, that is the question, *Cell.* 68, 237-255.
- Hu, W. S. & Peshwa, M. V. (1991) Animal cell bioreactors---recent advances and challenges to scale-up, *Can J Chem Eng.* 69, 409-420.
- Hubbard, S. C. & Robbins, P. W. (1979) Synthesis and processing of protein-linked oligosaccharides in vivo, *J Biol Chem.* 254, 4568-4576.
- James, D. C., Freedman, R. B., Hoare, M. & Jenkins, N. (1994) High-resolution separation of recombinant human interferon-gamma glycoforms by micellar electrokinetic capillary chromatography, *Anal Biochem.* 222, 315-322.
- James, D. C., Freedman, R. B., Hoare, M., Ogonah, O. W., Rooney, B. C., Larionov, O. A., Dobrovolsky, V. N., Lagutin, O. V. & Jenkins, N. (1995) N-glycosylation of recombinant human interferon-gamma produced in different animal expression systems, *Biotechnology (N Y).* 13, 592-596.
- Jan, Y. N. & Jan, L. Y. (1998) Asymmetric cell division, *Nature.* 392, 775-778.
- Jang, S. K., Krausslich, H. G., Nicklin, M. J., Duke, G. M., Palmenberg, A. C. & Wimmer, E. (1988) A segment of the 5' nontranslated region of encephalomyocarditis virus RNA directs internal entry of ribosomes during in vitro translation, *J Virol.* 62, 2636-2643.
- Jenkins, N. (1996) Role of physiology in the determination of protein heterogeneity, *Curr Opin Biotechnol.* 7, 205-209.

- Jenkins, N., Castro, P., Menon, S., Ison, A. & Bull, A. (1994) Effect of lipid supplements on the production and glycosylation of recombinant interferon-gamma expressed in CHO cells, *Cytotechnology*. 15, 209-215.
- Jenkins, N. & Curling, E. M. (1994) Glycosylation of recombinant proteins: problems and prospects, *Enzyme Microb Technol*. 16, 354-364.
- Jenkins, N. & Hovey, A. (1993) Temperature control of growth and productivity in mutant Chinese hamster ovary cell synthesizing a recombinant protein, *Biotechnol Bioeng*. 42, 1029-1036.
- Jenkins, N., Parekh, R. B. & James, D. C. (1996) Getting the glycosylation right: implications for the biotechnology industry, *Nat Biotechnol*. 14, 975-981.
- Jo, E., Park, H., Kim, D. & Moon, H. M. (1993) Repeated fed-batch culture of hybridoma cells in nutrient-fortified high density medium, *Biotechnol Bioeng*. 42, 1229-1237.
- Kabakoff, B. D., Doyle, J. W. & Kandutsch, A. A. (1990) Relationships among dolichyl phosphate, glycoprotein synthesis, and cell culture growth, *Arch Biochem Biophys*. 276, 382-389.
- Kagawa, Y., Takasaki, S., Utsumi, J., Hosoi, K., Shimizu, H., Kochibe, N. & Kobata, A. (1988) Comparative study of the asparagine-linked sugar chains of natural human interferon-beta 1 and recombinant human interferon-beta 1 produced by three different mammalian cells, *J Biol Chem*. 263, 17508-17515.
- Kalberer, C. P., Pawliuk, R., Imren, S., Bachelot, T., Takekoshi, K. J., Fabry, M., Eaves, C. J., London, I. M., Humphries, R. K. & Leboulch, P. (2000) Preselection of retrovirally transduced bone marrow avoids subsequent stem cell gene silencing and age-dependent extinction of expression of human beta-globin in engrafted mice, *Proc Natl Acad Sci U S A*. 97, 5411-5415.
- Kamath, S. A. & Narayan, K. A. (1972) Interaction of Ca<sup>2+</sup> with endoplasmic reticulum of rat liver: a standardized procedure for the isolation of rat liver microsomes, *Anal Biochem*. 48, 53-61.
- Kaufmann, H., Mazur, X., Fussenegger, M. & Bailey, J. E. (1999) Influence of low temperature on productivity, proteome and protein phosphorylation of CHO cells, *Biotechnol Bioeng*. 63, 573-582.
- Kean, E. L., Wei, Z., Anderson, V. E., Zhang, N. & Sayre, L. M. (1999) Regulation of the biosynthesis of N-acetylglucosaminylpyrophosphoryldolichol, feedback and product inhibition, *J Biol Chem*. 274, 34072-34082.
- Konrad, M. & Merz, W. E. (1994) Regulation of N-glycosylation. Long term effect of cyclic AMP mediates enhanced synthesis of the dolichol pyrophosphate core oligosaccharide, *J Biol Chem*. 269, 8659-8666.

- Kornfeld, R. & Kornfeld, S. (1985) Assembly of asparagine-linked oligosaccharides, *Annu Rev Biochem.* 54, 631-664.
- Kousvelari, E. E., Grant, S. R. & Baum, B. J. (1983) Dolichol phosphate supplementation increases N-linked protein glycosylation in rat parotid acinar cells without increasing glycoprotein secretion, *Exp Cell Res.* 149, 271-276.
- Kubbies, M. & Stockinger, H. (1990) Cell cycle-dependent DHFR and t-PA production in cotransfected, MTX- amplified CHO cells revealed by dual-laser flow cytometry, *Exp Cell Res.* 188, 267-271.
- Kukuruzinska, M. A. & Lennon, K. (1998) Protein N-glycosylation: molecular genetics and functional significance, *Crit Rev Oral Biol Med.* 9, 415-448.
- Kunkel, J. P., Jan, D. C., Butler, M. & Jamieson, J. C. (2000) Comparisons of the glycosylation of a monoclonal antibody produced under nominally identical cell culture conditions in two different bioreactors, *Biotechnol Prog.* 16, 462-470.
- Li, E. & Kornfeld, S. (1979) Biosynthesis of lipid-linked oligosaccharides. Isolation and structure of a second lipid-linked oligosaccharide in Chinese hamster ovary cells, *J Biol Chem.* 254, 2754-2758.
- Li, E., Tabas, I. & Kornfeld, S. (1978) The synthesis of complex-type oligosaccharides. Structure of the lipid-linked oligosaccharide precursor of the complex-type oligosaccharides of the cesicular stomatitis virus G protein, *J Biol Chem.* 253, 7762-7770.
- Lin, A. A., Kimura, R. & Miller, W. M. (1993) Production of tPA in recombinant CHO cells under oxygen-limited conditions, *Biotechnol Bioeng.* 42, 339-350.
- Lis, H. & Sharon, N. (1993) Protein glycosylation. Structural and functional aspects, *Eur J Biochem.* 218, 1-27.
- Liu, D. T. (1992) Glycoprotein pharmaceuticals: scientific and regulatory considerations, and the US Orphan Drug Act, *Trends Biotechnol.* 10, 114-120.
- Liu, X., Constantinescu, S. N., Sun, Y., Bogan, J. S., Hirsch, D., Weinberg, R. A. & Lodish, H. F. (2000) Generation of mammalian cells stably expressing multiple genes at predetermined levels, *Anal Biochem.* 280, 20-28.
- Lloyd, D. R., Leelavatcharamas, V., Emery, A. N. & Al-Rubeai, M. (1999) The role of the cell cycle in determining gene expression and productivity in CHO cells, *Cytotechnology.* 30, 49-57.
- Lucas, B. K., Giere, L. M., DeMarco, R. A., Shen, A., Chisholm, V. & Crowley, C. W. (1996) High-level production of recombinant proteins in CHO cells using a dicistronic DHFR intron expression vector, *Nucleic Acids Res.* 24, 1774-1779.



- Lucas, J. J. & Levin, E. (1977) Increase in the lipid intermediate pathway of protein glycosylation during hen oviduct differentiation, *J Biol Chem.* 252, 4330-4336.
- Lucas, J. J., Waechter, J. & Lennarz, W. J. (1975) The participation of lipid-linked oligosaccharide in synthesis of membrane glycoproteins, *J Biol Chem.* 250, 1992-2002.
- Mastrangelo, A. J. & Betenbaugh, M. J. (1998) Overcoming apoptosis: new methods for improving protein-expression systems, *Trends Biotechnol.* 16, 88-95.
- Mazur, X., Eppenberger, H. M., Bailey, J. E. & Fussenegger, M. (1999) A novel autoregulated proliferation-controlled production process using recombinant CHO cells, *Biotechnol Bioeng.* 65, 144-150.
- Mazur, X., Fussenegger, M., Renner, W. A. & Bailey, J. E. (1998) Higher productivity of growth-arrested Chinese hamster ovary cells expressing the cyclin-dependent kinase inhibitor p27, *Biotechnol Prog.* 14, 705-713.
- McAdams, H. H. & Arkin, A. (1998) Simulation of prokaryotic genetic circuits, *Annu Rev Biophys Biomol Struct.* 27, 199-224.
- McAdams, H. H. & Arkin, A. (1999) It's a noisy business! Genetic regulation at the nanomolar scale, *Trends Genet.* 15, 65-69.
- McInerney, J. M., Nawrocki, J. R. & Lowrey, C. H. (2000) Long-term silencing of retroviral vectors is resistant to reversal by trichostatin A and 5-azacytidine, *Gene Ther.* 7, 653-663.
- Meier, S. J., Hatton, T. A. & Wang, D. I. (1999) Cell death from bursting bubbles: role of cell attachment to rising bubbles in sparged reactors, *Biotechnol Bioeng.* 62, 468-478.
- Mercille, S. & Massie, B. (1994) Induction of apoptosis in nutrient-deprived cultures of hybridoma and myeloma cells, *Biotechnol Bioeng.* 44, 1140-1154.
- Meredith, J. E., Jr., Kiesses, W. B., Takada, Y. & Schwartz, M. A. (1999) Mutational analysis of cell cycle inhibition by integrin beta1C, *J Biol Chem.* 274, 8111-8116.
- Miller, W. M., Blanch, H. W. & Wilke, C. R. (2000) A kinetic analysis of hybridoma growth and metabolism in batch and continuous suspension culture: effect of nutrient concentration, dilution rate, and pH. Reprinted from *Biotechnology and Bioengineering*, Vol. 32, Pp 947-965 (1988), *Biotechnol Bioeng.* 67, 853-871.
- Mueller, P. P., Schlenke, P., Nimtz, M., Conradt, H. S. & Hauser, H. (1999) Recombinant glycoprotein product quality in proliferation-controlled BHK-21 cells, *Biotechnol Bioeng.* 65, 529-536.

- Murray, K., Ang, C. E., Gull, K., Hickman, J. A. & Dickson, A. J. (1996) NSO myeloma cell death: influence of bcl-2 overexpression, *Biotechnol Bioeng.* 51, 298-304.
- Mutsaers, J. H., Kamerling, J. P., Devos, R., Guisez, Y., Fiers, W. & Vliegthart, J. F. (1986) Structural studies of the carbohydrate chains of human gamma-interferon, *Eur J Biochem.* 156, 651-654.
- Nyberg, G. B. (1998) Glycosylation site occupancy heterogeneity in Chinese hamster ovary cell culture, *Ph.D. thesis*, Massachusetts Institute of Technology.
- Nyberg, G. B., Balcarcel, R. R., Follstad, B. D., Stephanopoulos, G. & Wang, D. I. (1999) Metabolic effects on recombinant interferon-gamma glycosylation in continuous culture of Chinese hamster ovary cells, *Biotechnol Bioeng.* 62, 336-347.
- Ohkura, T., Fukushima, K., Kurisaki, A., Sagami, H., Ogura, K., Ohno, K., Hara-Kuge, S. & Yamashita, K. (1997) A partial deficiency of dehydrodolichol reduction is a cause of carbohydrate-deficient glycoprotein syndrome type I, *J Biol Chem.* 272, 6868-6875.
- Oltvai, Z. N., Milliman, C. L. & Korsmeyer, S. J. (1993) Bcl-2 heterodimerizes in vivo with a conserved homolog, Bax, that accelerates programmed cell death, *Cell.* 74, 609-619.
- Onishi, M., Kinoshita, S., Morikawa, Y., Shibuya, A., Phillips, J., Lanier, L. L., Gorman, D. M., Nolan, G. P., Miyajima, A. & Kitamura, T. (1996) Applications of retrovirus-mediated expression cloning, *Exp Hematol.* 24, 324-329.
- Ozturk, S. S. & Palsson, B. O. (1990) Effects of dissolved oxygen on hybridoma cell growth, metabolism, and antibody production kinetics in continuous culture, *Biotechnol Prog.* 6, 437-446.
- Pan, Y. T. & Elbein, A. D. (1990) Control of N-Linked oligosaccharide synthesis: cellular levels of dolichyl phosphate are not the only regulatory factor, *Biochemistry.* 29, 8077-8084.
- Papoutsakis, E. T. (1991) Media additives for protecting freely suspended animal cells against agitation and aeration damage, *Trends Biotechnol.* 9, 316-324.
- Patel, T. P., Parekh, R. B., Moellering, B. J. & Prior, C. P. (1992) Different culture methods lead to differences in glycosylation of a murine IgG monoclonal antibody, *Biochem J.* 285, 839-845.
- Peakman, T. C., Worden, J., Harris, R. H., Cooper, H., Tite, J., Page, M. J., Gewert, D. R., Bartholemew, M., Crowe, J. S. & Brett, S. (1994) Comparison of expression of a humanized monoclonal antibody in mouse NSO myeloma cells and Chinese hamster ovary cells, *Hum Antibodies Hybridomas.* 5, 65-74.

- Pear, W. S., Nolan, G. P., Scott, M. L. & Baltimore, D. (1993) Production of high-titer helper-free retroviruses by transient transfection, *Proc Natl Acad Sci U S A.* 90, 8392-8396.
- Pendse, G. J., Karkare, S. & Bailey, J. E. (1992) Effect of cloned gene dosage on cell growth and hepatitis B surface antigen in recombinant CHO cells, *Biotechnol Bioeng.* 40, 119-129.
- Pipeleers, D. G. (1992) Heterogeneity in pancreatic beta-cell population, *Diabetes.* 41, 777-781.
- Price, L. S. (1997) Morphological control of cell growth and viability, *Bioessays.* 19, 941-943.
- Rademacher, T. W., Parekh, R. B. & Dwek, R. A. (1988) Glycobiology, *Annu Rev Biochem.* 57, 785-838.
- Ramirez, O. T. & Mutharasan, R. (1992) Effect of serum on the plasma membrane fluidity of hybridomas: an insight into its shear protective mechanism, *Biotechnol Prog.* 8, 40-50.
- Rinderknecht, E., O'Connor, B. H. & Rodriguez, H. (1984) Natural human interferon-gamma. Complete amino acid sequence and determination of sites of glycosylation, *J Biol Chem.* 259, 6790-6797.
- Riske, F. J., Cullen, B. R. & Chizzonite, R. (1991) Characterization of human interferon-gamma and human interleukin-2 from recombinant mammalian cell lines and peripheral blood lymphocytes, *Lymphokine Cytokine Res.* 10, 213-218.
- Robinson, D. K. & Memmert, K. W. (1991) Kinetics of recombinant immunoglobulin production by mammalian cells in continuous culture, *Biotechnol Bioeng.* 38, 972-976.
- Rosenwald, A. G., Stoll, J. & Krag, S. S. (1990) Regulation of glycosylation. Three enzymes compete for a common pool of dolichyl phosphate in vivo, *J Biol Chem.* 265, 14544-14553.
- Rudd, P. M. & Dwek, R. A. (1997) Glycosylation: heterogeneity and the 3D structure of proteins, *Crit Rev Biochem Mol Biol.* 32, 1-100.
- Rush, J. S., Snow, E. C. & Waechter, C. J. (1987) Induction of glycoprotein biosynthesis in activated B lymphocytes, *Arch Biochem Biophys.* 259, 567-575.
- Sanfeliu, A., Chung, J. D. & Stephanopoulos, G. (2000) Effect of insulin stimulation on the proliferation and death of chinese hamster ovary cells, *Biotechnol Bioeng.* 70, 421-427.

- Sareneva, T., Cantell, K., Pyhala, L., Pirhonen, J. & Julkunen, I. (1993) Effect of carbohydrates on the pharmacokinetics of human interferon- gamma, *J Interferon Res.* 13, 267-269.
- Sareneva, T., Pirhonen, J., Cantell, K. & Julkunen, I. (1995) N-glycosylation of human interferon-gamma: glycans at Asn-25 are critical for protease resistance, *Biochem J.* 308, 9-14.
- Sareneva, T., Pirhonen, J., Cantell, K., Kalkkinen, N. & Julkunen, I. (1994) Role of N-glycosylation in the synthesis, dimerization and secretion of human interferon-gamma, *Biochem J.* 303, 831-840.
- Scahill, S. J., Devos, R., Van der Heyden, J. & Fiers, W. (1983) Expression and characterization of the product of a human immune interferon cDNA gene in Chinese hamster ovary cells, *Proc Natl Acad Sci U S A.* 80, 4654-4658.
- Schutzbach, J. S. & Jensen, J. W. (1989) Bilayer membrane destabilization induced by dolichylphosphate, *Chem Phys Lipids.* 51, 213-218.
- Schwartz, M. A. (1997) Integrins, oncogenes, and anchorage independence, *J Cell Biol.* 139, 575-578.
- Shelikoff, M., Sinskey, A. J. & Stephanopoulos, G. (1994) The effect of protein synthesis inhibitors on the glycosylation site occupancy of recombinant human prolactin, *Cytotechnology.* 15, 195-208.
- Shelikoff, M., Sinskey, A. J. & Stephanopoulos, G. (1996) A modeling framework for the study of protein glycosylation, *Biotechnol Bioeng.* 50, 73-90.
- Shih, C. C., Stoye, J. P. & Coffin, J. M. (1988) Highly preferred targets for retrovirus integration, *Cell.* 53, 531-537.
- Smiley, A. L., Hu, W. S. & Wang, D. I. C. (1989) Production of human immune interferon genes by recombinant mammalian cells cultivated on microcarriers, *Biotechnol Bioeng.* 33, 1182-1190.
- Spellman, M. W., Basa, L. J., Leonard, C. K., Chakel, J. A., O'Connor, J. V., Wilson, S. & van Halbeek, H. (1989) Carbohydrate structures of human tissue plasminogen activator expressed in Chinese hamster ovary cells, *J Biol Chem.* 264, 14100-14111.
- Spiro, M. J. & Spiro, R. G. (1986) Control of N-linked carbohydrate unit synthesis in thyroid endoplasmic reticulum by membrane organization and dolichyl phosphate availability, *J Biol Chem.* 261, 14725-14732.
- Spiro, M. J. & Spiro, R. G. (1991) Potential regulation of N-glycosylation precursor through oligosaccharide-lipid hydrolase action and glucosyltransferase- glucosidase shuttle, *J Biol Chem.* 266, 5311-5317.

- Spiro, R. G., Spiro, M. J. & Bhojroo, V. D. (1976) Lipid-saccharide intermediates in glycoprotein biosynthesis. II. Studies on the structure of an oligosaccharide-lipid from thyroid, *J Biol Chem.* 251, 6409-6419.
- Spudich, J. L. & Koshland, D. E., Jr. (1976) Non-genetic individuality: chance in the single cell, *Nature.* 262, 467-471.
- Takeuchi, M., Takasaki, S., Miyazaki, H., Kato, T., Hoshi, S., Kochibe, N. & Kobata, A. (1988) Comparative study of the asparagine-linked sugar chains of human erythropoietins purified from urine and the culture medium of recombinant Chinese hamster ovary cells, *J Biol Chem.* 263, 3657-3663.
- Tey, B. T., Singh, R. P., Piredda, L., Piacentini, M. & Al-Rubeai, M. (2000) Influence of bcl-2 on cell death during the cultivation of a Chinese hamster ovary cell line expressing a chimeric antibody, *Biotechnol Bioeng.* 68, 31-43.
- Tonouchi, N., Koyama, N. & Miwa, K. (1992) A CHO strain producing high-level human IL-6 with the 3' deletion construct, *J Biotechnol.* 22, 283-9.
- Turco, S. J. (1980) Modification of oligosaccharide-lipid synthesis and protein glycosylation in glucose-deprived cells, *Arch Biochem Biophys.* 205, 330-339.
- Tyler, J. K. & Kadonaga, J. T. (1999) The "dark side" of chromatin remodeling: repressive effects on transcription, *Cell.* 99, 443-446.
- Utsumi, J., Mizuno, Y., Hosoi, K., Okano, K., Sawada, R., Kajitani, M., Sakai, I., Naruto, M. & Shimizu, H. (1989) Characterization of four different mammalian-cell-derived recombinant human interferon-beta 1s. Identical polypeptides and non-identical carbohydrate moieties compared to natural ones, *Eur J Biochem.* 181, 545-553.
- Valtersson, C., van Duyn, G., Verkleij, A. J., Chojnacki, T., de Kruijff, B. & Dallner, G. (1985) The influence of dolichol, dolichol esters, and dolichyl phosphate on phospholipid polymorphism and fluidity in model membranes, *J Biol Chem.* 260, 2742-2751.
- van Duijn, G., Valtersson, C., Chojnacki, T., Verkleij, A. J., Dallner, G. & de Kruijff, B. (1986) Dolichyl phosphate induces non-bilayer structures, vesicle fusion and transbilayer movement of lipids: a model membrane study, *Biochim Biophys Acta.* 861, 211-223.
- van Schravendijk, C. F., Kiekens, R. & Pipeleers, D. G. (1992) Pancreatic beta cell heterogeneity in glucose-induced insulin secretion, *J Biol Chem.* 267, 21344-21348.
- Varki, A. (1993) Biological roles of oligosaccharides: all of the theories are correct, *Glycobiology.* 3, 97-130.

- Varner, J. A., Emerson, D. A. & Juliano, R. L. (1995) Integrin alpha 5 beta 1 expression negatively regulates cell growth: reversal by attachment to fibronectin, *Mol Biol Cell.* 6, 725-740.
- von Melchner, H., Reddy, S. & Ruley, H. E. (1990) Isolation of cellular promoters by using a retrovirus promoter trap, *Proc Natl Acad Sci U S A.* 87, 3733-3737.
- Wang, J. Z., Grundke-Iqbal, I. & Iqbal, K. (1996) Glycosylation of microtubule-associated protein tau: an abnormal posttranslational modification in Alzheimer's disease, *Nat Med.* 2, 871-875.
- Wary, K. K., Mainiero, F., Isakoff, S. J., Marcantonio, E. E. & Giancotti, F. G. (1996) The adaptor protein Shc couples a class of integrins to the control of cell cycle progression, *Cell.* 87, 733-743.
- Weidemann, R., Ludwig, A. & Kretzmer, G. (1994) Low temperature cultivation--a step towards process optimisation, *Cytotechnology.* 15, 111-116.
- Wyllie, A. H., Kerr, J. F. & Currie, A. R. (1980) Cell death: the significance of apoptosis, *Int Rev Cytol.* 68, 251-306.
- Xie, L. & Wang, D. I. (1994) Applications of improved stoichiometric model in medium design and fed- batch cultivation of animal cells in bioreactor, *Cytotechnology.* 15, 17-29.
- Yamashita, K., Hitoi, A., Taniguchi, N., Yokosawa, N., Tsukada, Y. & Kobata, A. (1983) Comparative study of the sugar chains of gamma-glutamyltranspeptidases purified from rat liver and rat AH-66 hepatoma cells, *Cancer Res.* 43, 5059-5063.
- Yamashita, K., Ideo, H., Ohkura, T., Fukushima, K., Yuasa, I., Ohno, K. & Takeshita, K. (1993) Sugar chains of serum transferrin from patients with carbohydrate deficient glycoprotein syndrome. Evidence of asparagine-N-linked oligosaccharide transfer deficiency, *J Biol Chem.* 268, 5783-5789.
- Yao, A., Rubin, A. L. & Rubin, H. (1990) Progressive state selection of cells in low serum promotes high density growth and neoplastic transformation in NIH 3T3 cells, *Cancer Res.* 50, 5171-5176.
- Yao, A. & Rubin, H. (1993) Automatic enumeration and characterization of heterogeneous clonal progression in cell transformation, *Proc Natl Acad Sci U S A.* 90, 10524-10528.
- Yao, A. & Rubin, H. (1994) A critical test of the role of population density in producing transformation, *Proc Natl Acad Sci U S A.* 91, 7712-7716.
- Yoshimi, M., Sekiguchi, T., Hara, N. & Nishimoto, T. (2000) Inhibition of N-linked glycosylation causes apoptosis in hamster BHK21 cells, *Biochem Biophys Res Commun.* 276, 965-969.

- Zanghi, J. A., Fussenegger, M. & Bailey, J. E. (1999) Serum protects protein-free competent Chinese hamster ovary cells against apoptosis induced by nutrient deprivation in batch culture, *Biotechnol Bioeng.* 64, 108-119.
- Zentilin, L., Qin, G., Tafuro, S., Dinauer, M. C., Baum, C. & Giacca, M. (2000) Variegation of retroviral vector gene expression in myeloid cells, *Gene Ther.* 7, 153-166.
- Zetterburg, A. & Larson, O. (1985) Kinetic analysis of regulatory events in G1 leading to proliferation or quiescence of Swiss 3T3 cells, *Proc Natl Acad Sci U S A.* 82, 5365-5369.
- Zhang, Z., Vuori, K., Reed, J. C. & Ruoslahti, E. (1995) The alpha 5 beta 1 integrin supports survival of cells on fibronectin and up-regulates Bcl-2 expression, *Proc Natl Acad Sci U S A.* 92, 6161-6165.